Loss of Hepatitis B virus HBeAg contributes to immune escape from CD8$^+$ T cells directed against the core-protein

Inaugural-Dissertation

zur Erlangung des Doktorgrades
der Mathematisch-Naturwissenschaftlichen Fakultät
der Heinrich-Heine-Universität Düsseldorf

vorgelegt von

Maximilian Paul Damagnez
aus Les Lilas (Frankreich)

Düsseldorf, August 2024

aus dem Institut für Virologie
der Heinrich-Heine-Universität Düsseldorf

Gedruckt mit der Genehmigung der
Mathematisch-Naturwissenschaftlichen Fakultät der
Heinrich-Heine-Universität Düsseldorf

Berichterstatter:

1. Prof. Dr. Jörg Timm (Heinrich-Heine-Universität Düsseldorf)
2. Prof. Dr. Rainer Kalscheuer (Heinrich-Heine-Universität Düsseldorf)

Tag der mündlichen Prüfung: 12. Dezember 2024

Danksagung

Zuallererst möchte ich mich herzlich bei dir, Jörg, bedanken. Unsere Unterhaltungen und Diskussionen habe ich aufrichtig geschätzt. Besonders hoch rechne ich dir an, dass du stets eine offene Tür und ein offenes Ohr für mich hattest und mich in jeder Lage unterstützt hast. Dank dir habe ich vieles gelernt, und ich bin froh, dich als meinen Doktorvater zu haben.
Ein Dankeschön geht auch an Rainer Kalscheuer für die Übernahme der Zweitbetreuung. Die jährlichen Supervisor-Meetings haben mir stets neue Ideen und Anregungen gebracht, wofür ich dankbar bin.
Mein Dank gilt auch dir, Andreas. Dein umfassendes Wissen über HBV, Excel, Molekularbiologie und so vieles mehr war von unschätzbarem Wert. Ich danke dir herzlich dafür, dass du dein Wissen so großzügig mit mir geteilt hast.
Christopher, dir danke ich für die vielen inspirierenden Gespräche und besonders für deine Unterstützung bei immunologischen Fragen und der Arbeit mit dem FACS. Deine Expertise und Hilfsbereitschaft haben mir sehr geholfen.
Ein Dankeschön geht an Mirjam Heemskerk für die warme Aufnahme in der Arbeitsgruppe in Leiden und die Ermöglichung eines bereichernden Auslandsaufenthalts, der meiner Forschung und mir sehr geholfen hat.
Ich möchte der Manchot Stiftung für die Finanzierung und Unterstützung meinen Dank aussprechen. Ohne diese Hilfe wäre meine Promotion in dieser Form nicht möglich gewesen.

Einen besonderen Dank richte ich an dich, Laura. Du hast mich über die gesamte Zeit hinweg unterstützt, an mich geglaubt und mir den Rücken freigehalten, sodass ich mich bestmöglich auf die Promotion konzentrieren konnte. Deine Geduld und dein Verständnis waren unbezahlbar.
Moritz und Emil, euch danke ich dafür, dass ihr trotz der vielen Tage, an denen ich keine Zeit hatte, um mit euch zu toben, bauen, malen oder durch Pfützen zu springen, es immer wieder geduldig probiert habt. Es hat mich ungemein aufgebaut, dass ihr euch jeden Abend aufs neue so sehr gefreut habt, mich nach dem langen Tag wiederzusehen.

Diese Promotion wäre ohne die Hilfe und den Rückhalt all der oben genannten Personen und vielen weiteren nicht möglich gewesen. Dafür bin ich allen zu großem Dank verpflichtet.

Table of contents

Zusammenfassung

Das Hepatitis-B-Virus (HBV) ist ein kleines, behülltes Virus mit einer zirkulären, überwiegend doppelsträngigen DNA. Eine Infektion mit dem Virus führt beim Patienten zu einer akuten oder auch chronischen Infektion der Leber. In der akuten Phase der Infektion spielen die körpereigenen CD8+ T-Lymphozyten eine entscheidende Rolle bei der Virusabwehr. Beim Übergang von einer akuten zu einer chronischen HBV-Infektion kommt es zu einem Versagen der zellulären Immunantwort gegen das Virus. Bei der Analyse von CD8+ T-Lymphozyten in chronisch infizierten Patienten dominieren T-Lymphozyten mit einem Phänotyp, der durch Merkmale charakterisiert ist, die auf Erschöpfung oder Gedächtniszellen hinweisen. Betrachtet man die Interaktion von CD8+ T-Lymphozyten mit infizierten Hepatozyten stellen Epitope aus der Core-Region des HBV Genoms ein bedeutendes Ziel dar.

Interessanterweise könnten zwei verschiedene virale Proteinquellen als Ursprung der präsentierten Epitope der Core-Region dienen: Zum einen könnten die Epitope vom Core-Protein stammen, das aus der prägenomischen mRNA (pgRNA) translatiert wird und das virale Nukleokapsid bildet. Zum anderen könnten die Epitope vom N-terminal verlängerten Precore-Protein stammen, das aus der precore-mRNA translatiert, anschließend prozessiert und als Hepatitis-B-Virus-e-Antigen (HBeAg) sezerniert wird.

Der HBeAg-Status des Patienten dient als wichtiger diagnostischer Marker für die Prognose und Klassifikation der chronischen Hepatitis-B-Erkrankung. Eine HBeAg-positive chronische Infektion ist durch eine hohe Viruslast und geringe bis nicht nachweisbare CD8+ T-Zell-Antworten gekennzeichnet. Im Gegensatz dazu ist der Übergang zu einer HBeAg-negativen chronischen Infektion (HBeAg-Serokonversion) mit einer verstärkten Aktivierung HBV-spezifischer CD8+ T-Lymphozyten assoziiert.

In HBeAg-negativen chronisch infizierten Patienten können häufig zwei Mutationen im Virus nachgewiesen werden, die mit einer verminderten oder fehlenden HBeAg-Sekretion assoziiert sind. Die erste Mutation befindet sich in der basalen Core-Promotor-Region (BCP) des Core-Promotors, welcher für die Transkription der pgRNA und der precore mRNA verantwortlich ist. Diese Mutation umfasst zwei Nukleotidaustausche an den Positionen A1762T und G1764A und wird als BCP-Doppelmutation (BCP mut.) bezeichnet. Die zweite Mutation führt durch den Austausch eines Guanins durch ein Adenin an Position 1896 (W28*) zu einem vorzeitigen Abbruch der Translation der precore mRNA.

Ziel dieser Arbeit war es, den Beitrag von Precore/HBeAg-Peptiden zu den auf der Zelloberfläche präsentierten Epitopen festzustellen und die Auswirkungen des Verlusts von HBeAg auf die CD8+ T-Lymphozyten-vermittelte Immunantwort zu untersuchen. Für diese Untersuchung musste zunächst ein HBV-Zellkulturmodell etabliert werden. Dabei diente in vitro generierte kovalent geschlossene zirkuläre DNA (cccDNA) als Grundlage, die in HepG2-hNTCP-Zellen eingebracht wurde.

Die Fragestellung sollte an Viren der Genotypen A und D untersucht werden, da diese den Großteil der in Deutschland und Europa zirkulierenden HBV-Stämme repräsentieren. Zusätzlich zu den von Patienten gewonnenen Virussequenzen wurden Konsensussequenzen der Genotypen A und D erstellt, um die genetische Diversität angemessen abzubilden. Die Analyse der Düsseldorfer HBV-Kohorte identifizierte, neben den bereits bekannten HBeAg-Mutationen (BCP-Mutation und W28*), eine vorwiegend im Genotyp A auftretende Mutation im Startcodon des Precore-Proteins (Startmutation). Zudem wurde nachgewiesen, dass sich die Genotypen in Bezug auf HBeAg-selektierende Mutationen unterscheiden. Genotyp A zeigte eine heterogene Verteilung, während Genotyp D eine homogenere Verteilung der HBeAg-Mutationen aufwies.
In den durchgeführten Experimenten führten alle Precore-Mutationen zu einer Reduktion der HBeAg-Sekretion, wobei quantitative Unterschiede zwischen den einzelnen Mutationen auftraten, jedoch unabhängig vom Genotyp. Die BCP-Mutation bewirkte eine Reduktion, jedoch keinen vollständigen Verlust von HBeAg, während die W28*-Mutation und die Startmutation zu einem vollständigen Verlust von HBeAg führten. Darüber hinaus wurden Zellen, die mit cccDNA transfiziert waren, als Zielzellen für CD8+ Reporterzellen verwendet, welche einen HBV Core- oder HBV Surface-spezifischen T-Zellrezeptor (TCR) exprimierten. Mittels dieser TCR-Reporterzellen konnte nachgewiesen werden, dass der Verlust von HBeAg mit einer Reduktion der Aktivierung der Core-spezifischen Reporterzellen korreliert.

Die Ergebnisse dieser Studie zeigen, dass, obwohl die Anwesenheit von HBeAg ein wichtiges Entwicklungskriterium für die Progression zu einer chronischen Infektion darstellt und zur Immuntoleranz beiträgt, von HBeAg abgeleitete Epitope dennoch maßgeblich zur Präsentation auf der Zelloberfläche beitragen. Diese Entdeckung stellt einen wichtigen Schritt zum Verständnis der viralen HBeAg-Serokonversion dar und könnte zur Entwicklung verbesserter Therapien beitragen, mit dem langfristigen Ziel einer funktionellen Heilung der HBV-Infektion.

Summary

The hepatitis B virus is a small, enveloped virus containing a relaxed circular DNA. The virus can cause an acute or chronic infection of the liver. During the acute infection, CD8+ T cells are essential in controlling the ongoing infection. The development of a chronic HBV infection is associated with a failure of the cellular immune response against the virus. During chronic infection, CD8+ T cells exhibit an exhausted or memory-like phenotype. Epitopes in the hepatitis B core region are an important target for HBV-specific CD8+ T cell-directed immune control. The epitopes in the hepatitis B core region could originate from two distinct viral proteins. The core protein, which is translated from the pregenomic mRNA (pgRNA) and forms the viral nucleocapsid, and the N-terminally elongated precore protein, which is translated from a different viral transcript (the precore mRNA) and further processed and secreted as the Hepatitis B virus e-antigen (HBeAg). The HBeAg status is used as an important serological diagnostic marker for disease prognosis and classification of the chronic disease stages. While an HBeAg-positive chronic infection is characterized by high viral loads and weak or even undetectable CD8+ T cell responses, the transition to HBeAg-negative chronic infection (HBeAg seroconversion) is associated with an increase in activation of HBV-specific CD8+ T cells. Upon HBeAg seroconversion, two types of mutations that are associated with decreased HBeAg secretion are frequently selected. The first mutation is located in the basal core promoter (BCP) region of the core promoter responsible for the transcription of the pgRNA and the precore mRNA. The mutation comprises two nucleotide exchanges at position A1762T and G1764A, called the BCP double mutation (BCP mut.). The other mutation associated with HBeAg seroconversion is a mutation in the N-terminal elongation of the precore at position G1896A which introduces a stop codon (W28*).

The project aimed to better understand how precore/HBeAg peptides contribute to the epitopes presented on the cell surface. The hypothesis of this work was that loss of HBeAg leads to a decrease in the abundance of epitopes for HBV-specific CD8 T cells, thereby contributing to a CD8+ T cell immune escape.

The HBeAg mutations in the Dusseldorf cohort were analyzed, and an HBV cell culture model that uses the covalently closed circular DNA (cccDNA) in HepG2-hNTCP cells as a starting point was established. Sequences from HBV genotype A and D infected patients and inferred consensus sequences were utilized in the HBV cell culture model to test the hypothesis. Furthermore, the cells transfected with the cccDNA were used as targets for CD8+ reporter cells carrying a core- or surface-specific T-cell receptor (TCR).

Analysis of the Düsseldorf HBV cohort indicated, besides the two known HBeAg-altering mutations, a predominantly in genotype A occurring third mutation in the start codon of the precore protein.

Further, it was shown that in genotype A, a more heterogenous, and in genotype D, a more homogenous distribution of HBeAg-altering mutations was found.

In the HBV cell culture assay, all precore mutations decreased HBeAg secretion with quantitative differences between mutations but independend of the HBV genotype. The BCP mutation resulted in a reduction but not a loss of HBeAg, whereas the G1896A stop mutation and the start codon mutation led to a loss of HBeAg.

Introducing the reporter cells containing the core-specific TCR into the HBV cell culture model could demonstrate that the loss of HBeAg correlated with a reduction in activation of the reporter cells, whereas this did not affect the reporter cell containing a surface-specific TCR.

The results of this project provide evidence that despite the contribution of HBeAg to an immune tolerant state at the beginning of a chronic infection, HBeAg-derived epitopes contribute to the presented peptide repertoire in the tested model system. This discovery is an important step in understanding the viral HBeAg seroconversion and could contribute to developing better therapies with the ultimate goal of a functional cure of HBV infection.

List of Abbrevations

Abbrevation	
°C	Celcius
BCP	Basal core promoter
BCP mut.	Basal core promoter double mutation
BP	Base pair
cccDNA	Covalently closed circular DNA
CD	Cluster of differentiation
CDR	Complementarity determining region
CTD	C-terminal domaine
CTG mut.	Precore start codon mutation
CTL	Cytotoxic T lymphocyte
DAA	directly acting antivirals
DMEM	Dulbecco's Modified Eagle Medium
DNA	Deoxyribonucleic acid
ER	Endoplasmatic reticulum
ESCRT	Endosomal sorting complex required for transport
FACS	Fluorescence activated cell sorting
FBS	Fetal Bovine Serum
FWD	forward
G1896A	Stop-mutation (W28*)
GALV	gibbon ape leukemia virus
HBc	Hepatitis B core-protein
HBeAg	Hepatitis B e-antigen
HBV	Hepatitis B virus
HBsAg	Hepatitis B surface-antigen
HBx	Hepatitis B x-protein
HCC	Hepatucellular carcinoma
HLA	Human leukocyte antigen
ICTV	International committee on Taxonomy of Viruses
IMDM	Iscove's Modified Dulbecco's Medium
J76	Jurkat 76
J76m	Jurkat 76 mono NFkB
mRNA	Messenger RNA

mTCRb	Murine T-cell receptor beta chain
NEAA	Non essential amini acids
NFkB	Nuclear factor `kappa-light-chain-enhancer´ of activated B-cells
NK cells	Natural killer cells
NTCP	Sodium-taurocholate cotransporting polypeptide
NTD	N-terminal domaine
NUC	nucleoside or nucleotide analogues
ORF	Open reading frame
PBS	Phosphate-buffered saline
PCR	Polymerase chain reaction
Pen	Penicillin
PES	polyethersulfone
PHH	Primary human hepatocytes
Pol	Hepatitis B virus polymerase
rcDNA	Relaexed circular DNA
RCF	Relative centrifugal force
REV	reverse
RNA	Ribonucleic acid
RPM	Rounds per minutes
RRID	Research Resource Identification
RT	Room temperature
Strep	Streptomycin
TBE	TRIS-borat-EDTA
TCR	T-cell receptor
W28*	Stop mutation (G1896A)
WHO	World health organisation

1 Introduction

1.1 Hepatitis B virus

The Hepatitis B virus (HBV) is an entity that has plagued humans since ancient times. The discovery of the deoxyribonucleic acid (DNA) of HBV in 2000-year-old Egyptian mummified individuals [1] and the remains of 10 thousand-year-old hunter-gatherers from the Mesolithic [2] is a testament to the long-standing connection between the virus and its human hosts. Further, it could be demonstrated that the most recent common ancestor of the known HBV lineages dates back approximately 21 thousand years [3], which only serves to underline the long relation.

The first sign of the causative agent responsible for viral hepatitis was the "Australia antigen" isolated from leukemia sera of Australian Aboriginals [4]. Subsequent studies established a link between the antigen and hepatitis [5,6]. The discovery of a virus-like particle (Dane particle) in antigen-positive sera via electron microscopy in 1970 was the first identification of the hepatitis B inducing virus [7]. The isolation of DNA from the Dane particle in 1974 was the next step in proving the viral characteristics [8] of the particle. The final proof that the found virus was the cause of hepatitis B came from the labs of Friedrich Deinhard and Heinz Schaller when the team demonstrated that injecting the cloned DNA (pSHH2.1) found in the Dane particle into the liver of chimpanzees led to detectable replication and an acute hepatitis [9].

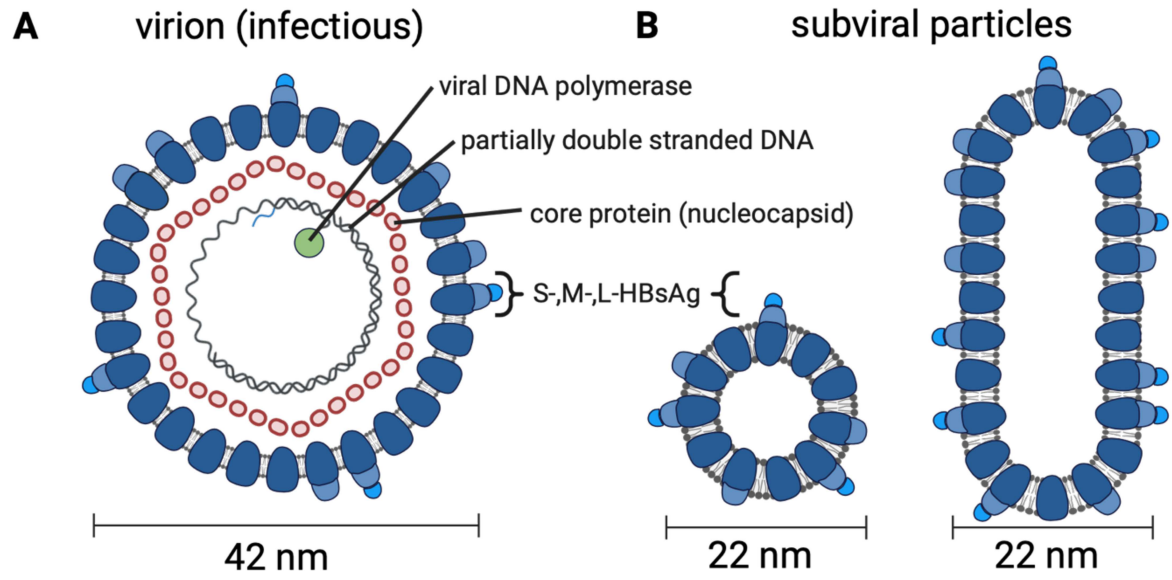

Figure 1 Graphical representation of the viral morphology: A) The infectious virion consisting of the lipid envelope with the different HBsAg anchored (blue). Inside the envelope is the viral nucleocapsid (red), comprised of core proteins, and holds the partially double-stranded DNA covalently bound to the viral DNA polymerase. B) Non-infectious subviral particles only consisting of the lipid envelope with the small (S), middle (M), and large (L) hepatitis B surface antigen (HBsAg). Graphical representation was adapted from [10] and created with BioRender.com.

The virion (Figure 1 A), previously known as the Dane particle, has a diameter of 42 nm and consists of a nucleocapsid enclosing the circular, partially double-stranded DNA bound to the DNA polymerase. A lipid envelope surrounds the nucleocapsid, carrying the embedded small (S), middle (M), and large (L) hepatitis B surface antigens (HBsAg) [11]. During replication, additionally rod (22 nm) and spherical (17- 25 nm) shaped subviral particles (Figure 1 B) are released from infected cells previously described as the "Australian antigen". These particles comprise the lipid envelope with the HBsAg present but without the nucleocapsid or viral DNA [12].

Today, viruses are classified taxonomically by the International Committee on Taxonomy of Viruses (ICTV). HBV belongs to the *Hepadnaviridae* family, which constitutes small enveloped viruses with partially double-stranded DNA and a narrow host range [13]. The *Hepadnaviridae* family includes five genera, with HBV belonging to the orthohepadnavirus genus. The orthohepadnavirus genus differs from the other genera in the *Hepadnaviridae* family by a 20% nucleotide sequence divergence and can only infect mammals [14]. The orthohepadnavirus genus comprises twelve known species, each with a highly conserved species and tissue specificity. The members of the Hepatitis B virus species infect Hominidae, whereas the other members of the genus infect rodents (woodchuck hepatitis virus, ground squirrel hepatitis virus), bats (Long-fingered bat hepatitis B virus), shrews, or artiodactyls [15].

1.2 Hepatitis B virus genome

The isolation of the viral DNA in 1974 by Robinson et al. made it possible to investigate the viral genome [8]. In the viral particle, the genome is present as a relatively small, partially double-stranded relaxed circular DNA (rcDNA) with an approximate size of 3200 base pairs (bp) [16] (Figure 2 A). The viral genome consists of a full-length minus DNA strand with the coding information and an incomplete plus DNA strand [17]. The minus strand displays an overlap at the 5' end where the viral DNA polymerase is covalently bound [18]. The positive DNA strand covers two-thirds of the viral genome of HBV and overlaps with the 5' and 3' ends of the minus DNA strand, ensuring the circular structure of the genome [19]. The coding information is organized in four overlapping open reading frames (ORF). The largest ORF encodes the viral polymerase (Pol). Inside the Pol ORF, the surface proteins are encoded in a +1 shifted ORF (S). The S ORFs feature three transcription initiation codons, pre-S1, pre-S2, and S, resulting in different subgenomic RNAs. The Core ORF (C) partially overlaps with the Pol ORF and contains two transcription initiation sites transcribing the precore RNA and the pregenomic (pg) RNA (Figure 2 B). The X ORF is the smallest and partially overlaps with the Pol ORF. It encodes for the X protein [20]. The viral transcripts of subgenomic and genomic RNAs differ with their 5' initiation site, but all have the same 3' terminus [21].

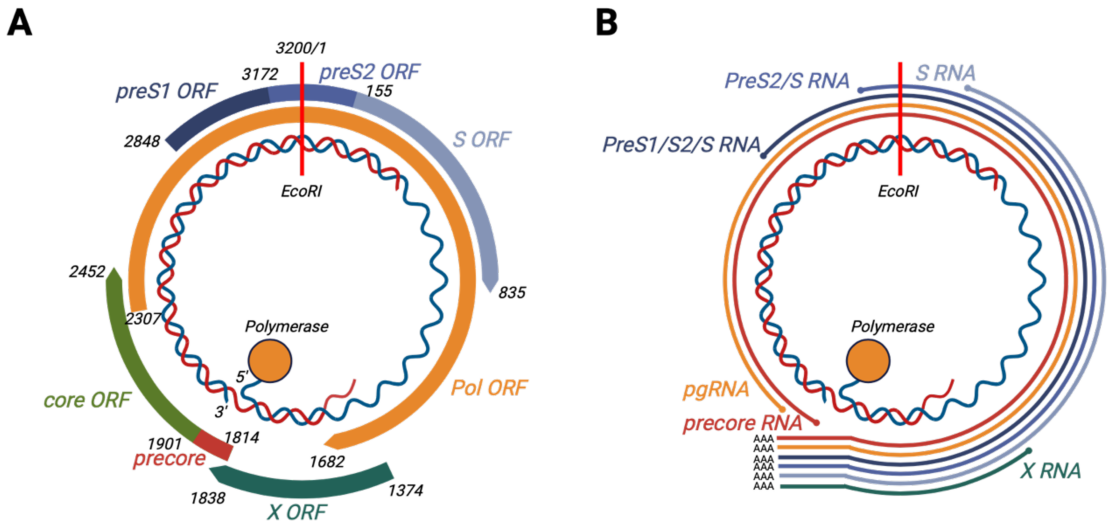

Figure 2 Graphical representation of the virus genome and transcription: A) HBV genome with relaxed circular DNA (rcDNA) bound to the viral polymerase. In red is the precore region, in green is the core open reading frame (ORF), in orange is the polymerase (pol) ORF, in blue are the different surface ORFs, and in dark green is the X ORF. The red line marks the EcoRI restriction site found in some genotypes and used as the starting point of the genome from which the nucleotide positions are counted. B) The different transcription products with their start position and poly-A tail. In red is the precore RNA display, and in orange is the pregenomic RNA (pgRNA) displayed. The different surface transcripts displayed are in blue. The X RNA is displayed in dark green. For orientation, the EcoRI site is displayed in red. Graphical representation was adapted from [22] and created with BioRender.com.

Since the project focuses on the HBeAg, the two genomic RNAs will be described here in more detail. The pgRNA and the precore mRNA are transcribed by the cellular RNA polymerase II and contain a 5' cap structure and 3' terminally poly-adenylated sites [23]. The core promoter initiates transcription of both RNAs. The pgRNA starts shortly after the precore transcription initiation site and contains the entire HBV genome. Via reverse transcription, it is used as the template for newly formed viral genomes bound to be incorporated into the virions [24]. Further, it serves as the mRNA for the viral core protein and the viral polymerase [25]. The precore RNA is a 5' terminal extended genomic RNA also comprising the entire HBV genome length. It serves as an mRNA for the viral precore precursor protein. Even though it has all the genetic information, the precore RNA cannot be used as a genomic template [26], nor is it efficient to initiate the translation of the core or polymerase proteins [27].

The four ORFs of the HBV genome translate to seven proteins. They are categorized into structure proteins with core, S-, M- and L-HBs responsible for the viral structure and the non-structure proteins precore, polymerase, and HBx.

1.2.1 Viral structural proteins

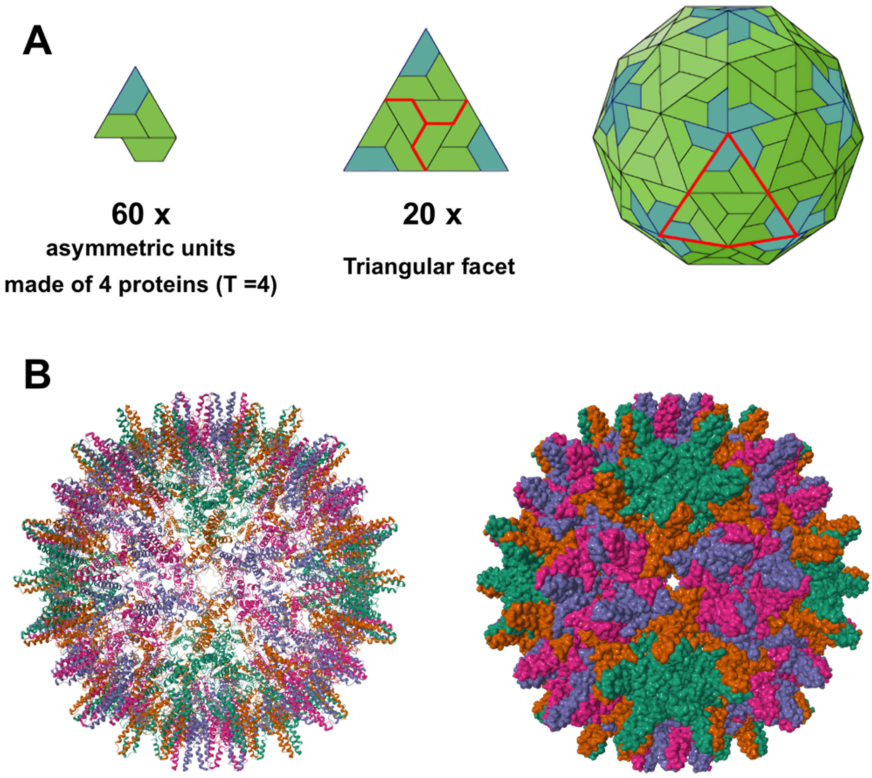

Figure 3 Hepatitis B capsid structure: A) Arrangement of a T = 4 icosahedral surface lattice applying Caspar-Klug Theory containing 60 asymmetrical subunits, each made of four proteins (T = 4) and organized in 20 triangles. B) Modeling the Hepatitis B virus capsid from Hepatitis B core proteins organization in a T =4 icosahedral derived from Caspar-Klug Theory. Graphical representation was taken from [28] for figure A and [29] for figure B.

Hepatitis B core protein (HBc) is a 183-185 amino acid (aa) long polypeptide chain with a weight of 21.5 kDa [30]. As a dimer, the protein is assembled to form the viral nucleocapsid with 120 dimers, resulting in a T = 4 icosahedral structure (figure 3) [31]. The protein consists of the N-terminal domain (NTD) from aa 1-149 and the C-terminal domain (CTD) from the last 34-36 aa depending on the genotype [32]. The NTD is responsible for the assembly of the viral nucleocapsid, and the CTD is responsible for the pgRNA encapsidation. Experiments with truncated C-terminal domain showed that the dimer still forms an icosahedral nucleocapsid [33], but could not encapsidate the pgRNA [34].

Besides HBc, the three closely related transmembrane proteins are responsible for the viral structure. They are the small (S), middle (M), and large (L) hepatitis B surface antigens (HBsAg), all expressed from the surface ORF. All three proteins have a 226 aa long CTD in common (S), where the M-HBsAg contains an N-terminal 55 aa extension (preS2+S), and the L-HBsAg contains a N-terminal 174 aa extension (preS1+preS2+S) [35]. With >80%, the S-HBsAg is the most abundant form on the viral envelope. It harbors important immunological determinants [36] and can be used in vaccines for induction of

neutralizing antibodies [37]. Besides functioning as a structural protein in the viral envelope, the function of the M-HBsAg is not well described. It functions as a transcriptional activator [38] and harbors a cell permeability motif [39]. The preS1 N-terminal extension in the L-HBsAg is essential for binding to entry receptor NTCP and entry into the host cell [40,41].

1.2.2 Viral non-structural proteins

The viral polymerase is a versatile multifunctional tool for the virus. The Pol ORF covers 80% of the viral genome and consists of three functional domains and a spacer. The so called terminal protein (TP) domain is located at the N-terminus. The domain functions as a linker-protein attached to the first nucleotides of the newly formed minus DNA strand [42,43]. A highly variable spacer region ties the terminal protein domain to the other two domains [44]. The other two domains are the polymerase/reverse transcriptase domain, which displays a DNA- and RNA-dependent polymerase function [45], and the C-terminal RNase H domain, which degrades the pgRNA template during reverse transcription [46].

Hepatitis B x-protein (HBx) is a regulatory protein with a wide variety of functions. The protein can interfere with cellular proliferation, DNA repair, transcription, and signalling [47–49] but is also involved in the transcriptional regulation of the viral genome [50].

The last non-structural protein is the hepatitis B e antigen (HBeAg) and its precore precursor protein (Figure 4). HBeAg was discovered in 1972 by Magnius when he studied HBsAg positive sera [51]. HBeAg is a secreted form of the core protein with completely different processing and functions [52,53]. It is transcribed as the precore RNA starting from a 29 aa N-terminal extension of the Core ORF [10]. HBeAg is found in all known orthohepadnaviruses [54] and derived from animal studies, the protein is not required for infection, replication, or assembly [55,56]. The precore N-terminal extension sequence contains a signal peptide that directs the translated precore protein from the cytosol into the endoplasmatic reticulum (ER). In the ER, the cellular signal peptidase cleaves 19 aa from the NTD [57]. The remaining 10 aa long extension mediates the formation of a disulfide bond between the cysteine at positions 7 and 61, preventing a multimerization of the protein [58]. The protein is further transported via the constitutive secretion pathway into the Golgi apparatus, where the C-terminal domain is cleaved by a furin-like protease [59], resulting in the mature secretory HBeAg. The role of HBeAg was not clear for a long time, but several studies over the years demonstrated immunotolerogenic and modulatory functions [60]. Further, in chronically infected patients, the loss of HBeAg from the serum can occur and is an important marker of disease progression.

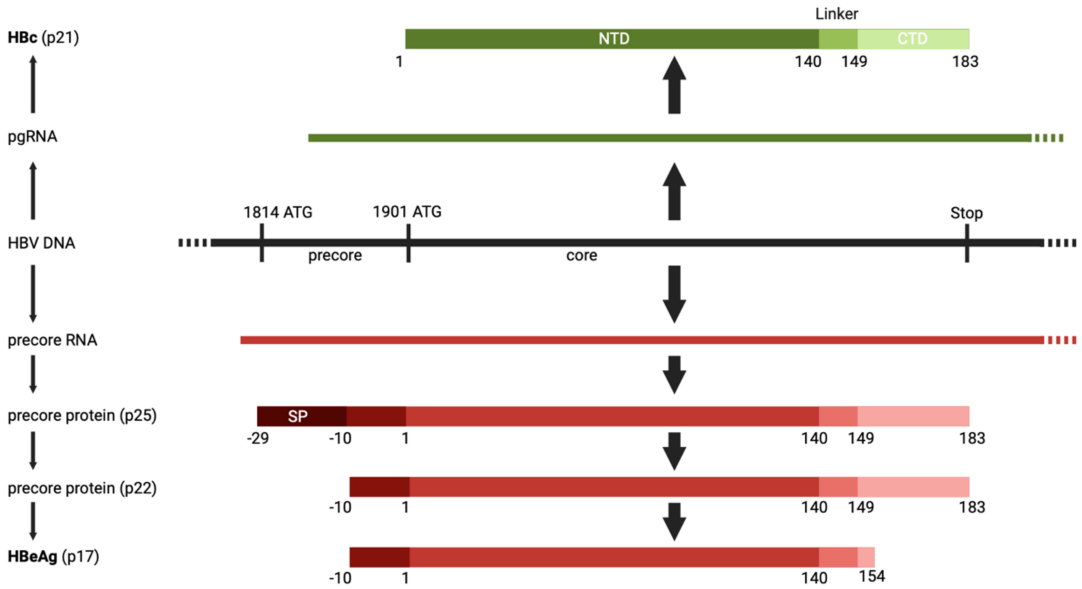

Figure 4 Graphical representation of the HBc and HBeAg processing: The pregenomic RNA (pgRNA) and the HBV core protein (HBc) are represented in green. HBc is translated from the pgRNA and forms the viral nucleocapsid. The precore RNA and the different processed precores and HBeAg proteins are represented in red. The precore protein (p25) is translated from the precore RNA. In the endoplasmatic reticulum (ER), the signal peptide (SP) is cleaved from the precore protein resulting in the precore protein p22. The p22 precore protein is further cleaved at the C terminal domain (CTD) by the furin-like protease resulting in the secreted HBeAg. HBc and HBeAg share, besides the N-terminal elongation, the same amino acid sequence. Graphical representation was adapted from [61] and created with BioRender.com

The immuntolerogenic and immunomodulatory role of HBeAg and the importance of the presence or absence from the serum will be discussed in length in a later section of this chapter.

1.2.3 HBV Genotypes

The error-prone reverse transcription and the long coevolution between the virus and hosts in different regions led to the emergence of nine distinct genotypes distributed across the globe. The genotypes are phylogenetically classified by genetic divergence of more than 7.5% over the complete genome labeled A to J [62–64]. Studies show that infections with different genotypes can vary in disease progression and treatment response [65,66]. A meta-analysis from Stoyan Velkov et al. tried to map the global HBV genotype appearance [64]. They found that genotypes A and D are the most common genotypes in Europe. Eastern Europe, Western, Central, and Northern Asia, and Northern Africa are dominated by genotype D. Genotype C is widespread in Eastern and Southeast Asia and Australia. In China genotypes C and B are highly prevalent. In the western part of sub-Saharan Africa, genotype E is the most prevailing genotype, whereas the eastern part is dominated by genotype A. The genotypes F, G, and H are prevalent in South America. As the frequency of the different HBV genotypes in a population is strongly influenced by migration history, it is no surprise that North America is one of the most diverse regions regarding HBV genotypes, with genotypes A, B, C, and D being similarly distributed.

1.3 Hepatitis B virus replication cycle

HBV not only displays a very narrow host tropism but is also only able to productively infect hepatocytes, the parenchymal tissue of the liver. The circulating virions reversibly attach via their surface proteins to heparin sulfacte proteoglycans (HSPGs) on the hepatocytes [67] (Figure 5). The attachment to the HSPGs is followed by an irreversible binding to the sodium taurocholate co-transporting polypeptide (NTCP) [68], a hepatocyte-specific acid bile transporter [69]. After binding, HBV is assumed to be internalized via clathrin-dependent endocytosis [70]. The virus is transported via the endosomal pathway, but it is still poorly understood how the HBV nucleocapsid is released into the cytoplasm [71,72]. In the cytoplasm, the nucleocapsid containing the relaxed circular partially double-stranded DNA (rcDNA) is transported along microtubules to the cell nucleus [24]. The rcDNA attached to the viral polymerase is released into the nucleoplasma [73]. In the nucleus the rcDNA is “repaired” to form the covalently closed circular DNA (cccDNA), but the exact mechanisms and enzymes involved are not clear yet [74]. The cccDNA binds to cellular histones to form some sort of mini-chromosome [75] and functions as the transcriptional template for the six viral RNAs. The precore RNA and the pregenomic RNA (pgRNA) transcription is coordinated from the core promoter. The preS1 RNA transcription is directed from the PreS promoter. The S promoter is responsible for the initation of the preS2 and S RNAs. At last the X RNA is controlled by the X promoter [76]. The capped and polyadenylated RNAs are transported via host factors in an unspliced form out of the nucleus into the cytoplasma [74].

The X-proten (HBx) is translated from the X RNA. It is believed that the X-protein is one of the first expressed proteins as it seems to play an important role in the transcription regulation of the cccDNA [50]. The large hepatitis B surface antigen (L-HBsAg), the middle (M)-HBsAg and the small (S)-HBsAg are translated from the preS1 RNA, preS2 RNA and S RNA. The different HBsAgs are transported to the lumen of the endoplasmatic reticulum (ER) where they play part of the envelopment of the viral nucleocapsid. The hepatitis B e-antigen (HBeAg) is translated as the precore protein from the precore RNA. The precore protein is processed as explained in detail on page 5 (section 1.2.2) and secreted via the ER as HBeAg from the cell.

The core protein (HBc) and the polymerase (pol) are translated from the pgRNA. Both proteins and the pgRNA are further involved in the complex formation. The viral polymerase binds the packaging signal ε near the 5’ end of the pgRNA initating the encapsidation by the core protein dimers [42]. After the formation of the nucleocapsid the reverse transcription of the pgRNA is initiated. The pgRNA is covalently linked to the polymerase and the complete minus DNA strand is synthesised followed by the plus strand resulting in the rcDNA [23]. The mature nucleocapsid containing the rcDNA and polymerase can now be transported in two directions. It is assumed that early on in the infection the nucleocapsid is transported back into the cell nucleus leading to aggregation of up to 50 cccDNA copies for an

enhanced viral protein expression [77]. The other route is the envelopment by the lipid bilayer containing the surface proteins and the release of virions via formation of multivesicular bodies accociated with proteins from the endosomal sorting complex required for transport (ESCRT) [78]. Similarly it was found that the subviral particles are released by the formation of multivescular bodies [79].

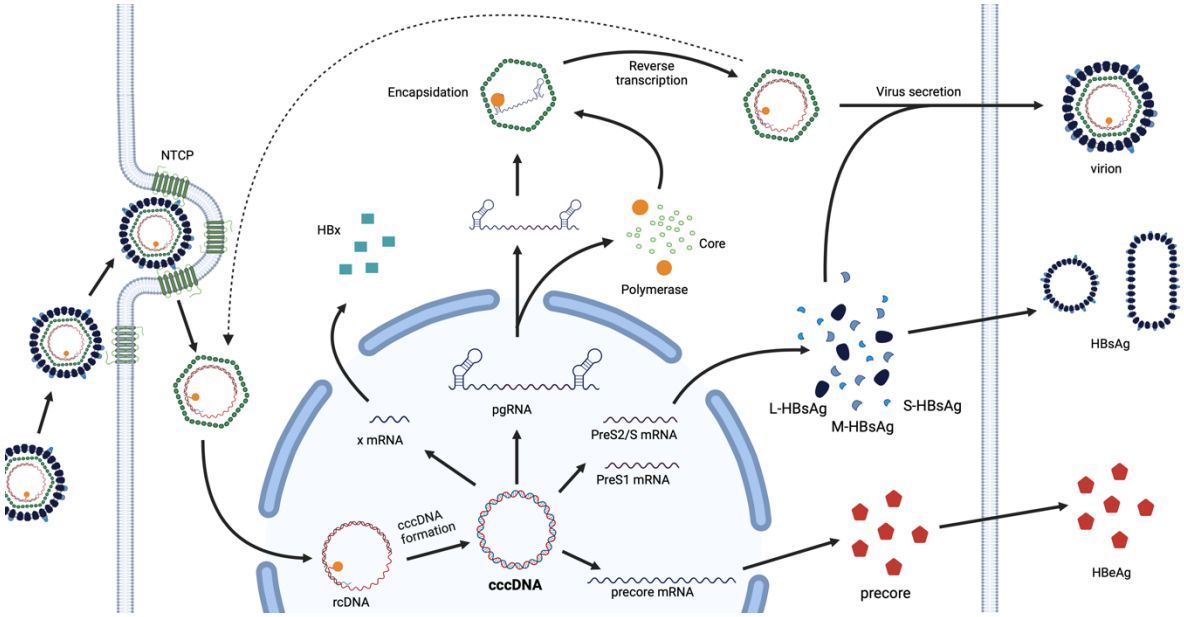

Figure 5 Hepatitis B virus replication cycle: HBV binds the NTCP receptor on the surface of the hepatocyte. The virion is transported into the cytoplasm. The nucleocapsid containing the relaxed circular DNA (rcDNA) is transported to the cell nucleus. The rcDNA is transported into the nucleus, forming the covalently closed circular DNA (cccDNA). The cccDNA is the basis for all viral transcripts. The different viral RNAs and the pregenomic RNA (pgRNA) are transcribed. The pgRNA translates the core protein (HBc) and the polymerase. Further, the pgRNA and the polymerase are encapsidated by the HBc. During encapsidation, the pgRNA is reverse-transcribed into rcDNA by the viral polymerase. Especially in the early phase of the infection, the nucleocapsid can be transported back into the nucleus, but is mainly further processed to be released as a virion. The PreS2/S and PreS1 mRNAs are translated into the L-HBsAg, M-HBsAg, and S-HBsAg. The encapsidated rcDNA is enveloped in cell lipids containing the HBsAg and released as the mature virion. The HBsAg is further also released in high concentrations without nucleocapsid or DNA. From the precore mRNA, the precore protein is translated. The precore protein is processed and released from the hepatocyte as the HBeAg. The X mRNA is translated into the X protein.
Graphical representation was adapted from [80] and created with BioRender.com.

1.3.1 Animal and cell culture models

In virology, models are essential for studying the replication cycle, drug targets, and immunological aspects of viral infection. Infection studies in apes were crucial in early findings regarding HBV [9,81]. They are still influential in exploring fibrosis, cirrhosis, or hepatocellular carcinoma (HCC) but have some apparent disadvantages, making them not the ideal and versatile replication model needed. The use of other viruses from the hepadnaviridae family, such as the woodchuck hepatitis B virus (WHV), in combination with the animal host, was essential for studying virus-host interactions [82]. Nevertheless, they had the problem of requiring expensive facilities and high-level animal maintenance and care. Therefore, many animal experiments involving HBV were conducted in mouse models, even

though they are not able to sustain viral infection without significant modification. Liver Humanized Mouse Models allow HBV infection but are highly immunodeficient, lacking T-cells, B-cells, and NK cells [83].

Compared to animal models, cell culture models have many advantages, from handling to cost. Unfortunately, for HBV, no good cell culture model is available to address all diverse scientific questions. Each cell system has its advantages and disadvantages. Primary human hepatocytes (PHH) are naturally permissive to an HBV infection and allow the study of many aspects of the viral life cycle [84]. Unfortunately, the cells are often difficult to obtain, and a potential lack of reproducibility between donors can be a disadvantage. Furthermore, PHHs can not be subcultured and rapidly lose their permissiveness for HBV infections [85]. HepRG cells isolated from an HCV-positive patient's liver tumor tissue allow the differentiation into hepatocyte-like cells that can partially sustain an HBV infection [86]. However, the HBV infection efficiency is low, and the differentiation into hepatocyte-like cells takes at least four weeks, making the cell line labor-intensive [87].

With the discovery of NTCP as the specific receptor for HBV entry [68], it became possible to work with the hepatoma cell lines Huh7 and HepG2. NTCP is expressed only in low quantities on those cell lines, but artificially expressing NTCP in high quantities makes the two cell lines susceptible to HBV infection [68]. Compared to PHH and HepRG, the two hepatoma cell lines still need a high initial viral titer for infection. The introduction of Polyethylene glycol 8000 (PEG 8000) to facilitate the HBV attachment and Dimethylsulfoxide (DMSO) to slow down cell proliferation enhanced the efficiency of an HBV infection in the cell lines but not nearly to levels similar to PHH [88].

Another problem with in vitro infection systems is to generate viral stocks. That is done with the help of stable integrated HBV cell lines. Generating viral particles is fine when looking at replication mechanisms but introduces an inflexibility when differences between mutations must be analyzed. Historically, plasmids containing overlength HBV genomes were used for transfecting cell lines or transduction via adenovirus. The overlength is needed to incorporate an additional core promoter, which is needed to generate the pgRNA [87]. As the HBV replication cycle involves the cccDNA resembling a mini plasmid, the idea emerged to utilize the cccDNA to introduce the virus into the hepatoma cell lines. One way to generate the cccDNA is to co-transfect HepG2 cells with two plasmids containing the cccDNA in combination with a Cre-/loxP mediated recombination generating the cccDNA inside the HepG2 cells [89]. Another method involves the introduction of attP/attB sites in the HBV genome inside a plasmid and the expression of a PhiC31 integrase and Sce I endonuclease. The PhiC31 integrase mediates the recombination of the cccDNA at the attP/attB site, whereas the Sce I endonuclease degrades the remaining parental plasmid. Yielding high amounts of cccDNA from a bacterial transformation that could directly be used for the transfection [90]. Although the generated

cccDNA can produce all viral proteins and the pgRNA, the recombinant attL site is introduced between the core promoter and the precore start codon, potentially altering the transcription of precore RNA and the pgRNA.

1.4 Hepatitis B disease

To this point, hepatitis B infection is a significant global health burden, with an estimated 3.8 % of the global population chronically infected with HBV. The prevalence of chronic HBV infections is not equally distributed globally, with the highest prevalance of 7.5 % in Africa, directly followed by the Western Pacific region, with 5.9 % of the population being chronically infected. The European region has an estimated prevalence of 1.5 %, and together with 0.5% in North America, the region with the lowest prevalence [91]. In countries with a high prevalence, most chronic infections result from perinatal transmission or during early childhood exposure. In many low-exposure countries, most infections occur via horizontal transmission [92]. Most of the prevalence stems from infections before the widespread deployment of the vaccine [93]. In 2019, the prevalence of HBV in children younger than five was 6 million (0.9 %), a reduction of 0.4 % compared to the last estimation in 2015 and a significant reduction from the estimated prevalence of 4.7 % in the pre-vaccination era (1980 – 2000). Most of the reduction in prevalence originates from the Western Pacific region and a rigorous vaccination strategy in newborns, bringing the prevalence in children (0.3 %) to lower levels than the eastern Mediterranean region (0.8 %) and similar levels as in the European region (0.3%) [91,94]. The reduction of the HBV prevalence since the introduction of the vaccine is a testament to the success of the vaccine, but in Africa (prevalence of 2.5% of children under five), there is still much to do.

1.4.1 Clinical course of infection

HBV is transmitted when contaminated blood or other body fluids of an infected person get access to the bloodstream via the skin barrier or across mucosal surfaces. Acute hepatitis B infection can range from asymptomatic to symptomatic disease with fever and nausea up to fulminant hepatitis and depends on different factors. In newborns and children, most hepatitis B infections are subclinical, and young patients rarely develop jaundice. In adults, 30-50% of infected individuals develop symptoms, and <1 % of the cases progress to fulminant hepatitis [95]. In an acute infection in adults, it takes approximately four weeks until HBV DNA, HBsAg, and HBeAg can be detected in the serum [96]. HBV DNA and HBsAg persistence correlate with the clinical symptoms and are cleared with the fading of the symptoms. HBeAg is cleared during the peak of the infection, and the production of anti-HBe antibodies is a critical serological marker that indicates the recovery of the infection [97]. Anti-HBc antibodies can be detected shortly before the onset of symptoms. Initially, the anti-HBc antibodies are immunoglobulin M (IgM) class but are replaced by immunoglobulin G (IgG) class antibodies later in the

infection. The transition of the immunoglobulin class allows the diagnostic distinction between an acute or chronic and previously cleared infection. The last antibodies to arise are anti-HBs. The anti-HBs antibodies generally persist and are associated with sterile immunity. Adults undergoing acute hepatitis B resolve the infection in more than 95% of the cases [98]. In Infants, hepatitis B has a much higher chance of progressing into a chronic infection, with the most prominent determinants being the age of the child and the HBeAg status of the mother [99].

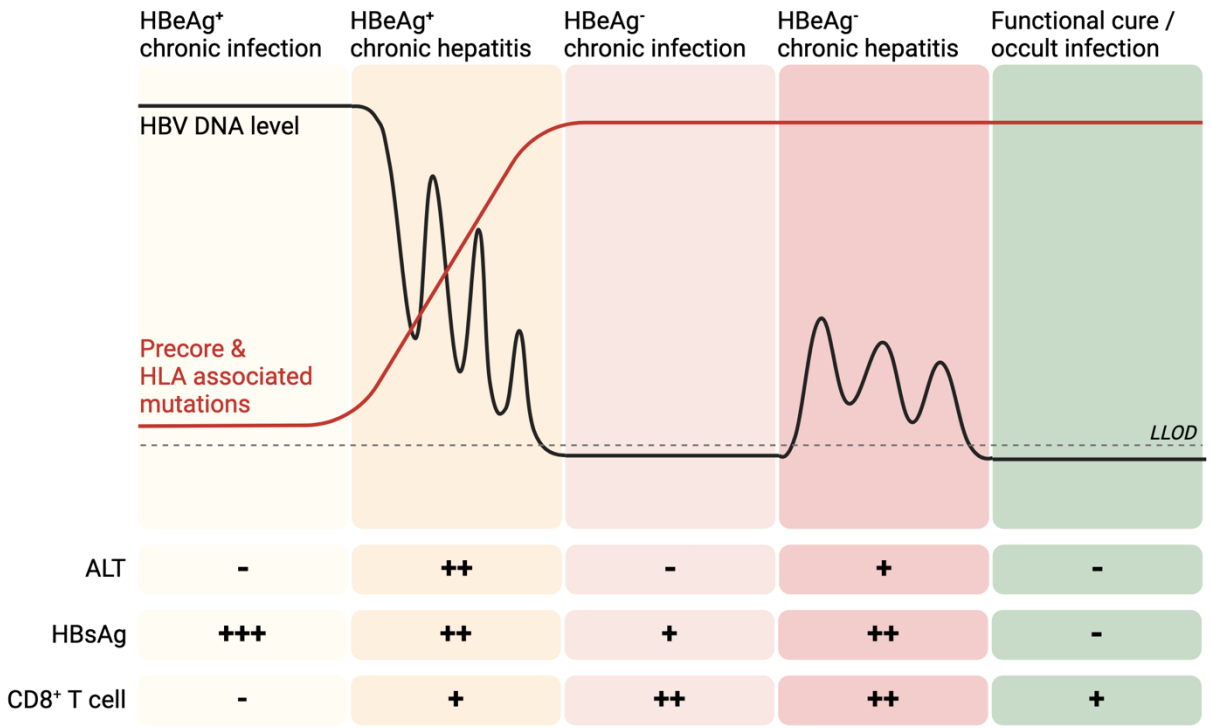

Figure 6 The four phases of chronic hepatitis B and functional cure/occult infection: HBeAg positive chronic infection (light yellow) is characterized by high viral load, high HBsAg levels, and normal ALT levels. No or infrequent occurrences of HLA-associated mutations are found during this phase. The $CD8^+$ T cell immune response against the virus seems non-existing. HBeAg-positive chronic hepatitis (light orange) is characterized by fluctuating viral load, reduced HBsAg levels, and increased ALT levels. There is probably an increase of Precore and HLA-associated mutations found in the viral quasispecies and an increase in $CD8^+$ T cell immune pressure. HBeAg-negative chronic infection (pink) is associated with low or undetected viral load and near-normal ALT levels. Most viruses contain precore and HLA-associated mutations, and the $CD8^+$ T cell immune pressure is high. HBeAg-negative chronic hepatitis (light red) is associated with fluctuating viral load, HBsAg level, and increased ALT levels. Functional cure and occult infection (green) are associated with no detectable HBsAg. The viral load in the serum is undetectable, and ALT levels are normal. Graphical representation was adapted from [100] and created with BioRender.com.

Chronic HBV infection is characterized by the persistence of HBsAg, and HBV DNA for more than six months [101]. The course of the chronic HBV infection is often dynamic and can be divided into different non-sequential phases (Figure 6) [92].

The HBeAg-positive chronic HBV infection is often also called the immune tolerant phase. It is characterized by high viral load, HBeAg in the serum, low ALT levels, and near-normal liver histology [93,102]. Due to the high viral titer in the serum, patients in this phase are highly contagious. This phase

is primarily observed in patients who developed the chronic disease as a newborn or young child and can persist for numerous years [103]. The mechanisms that lead to the loss of immune tolerance and the progression into the next phase are unknown. The HBeAg-positive chronic hepatitis B or immune clearance phase is characterized by an onset of T-cell mediated immune response against the infected hepatocytes. The immune response leads to increased alanine transaminase (ALT) release and decreased HBV DNA levels [96]. As the immune response fluctuates the ALT and DNA levels flare, which is a factor in the development of fibrosis or even cirrhosis [104–106]. The phase ends with a reduction of HBV DNA and an HBeAg seroconversion. The HBeAg seroconversion is the emergence of anti-HBeAg antibodies and is associated with the loss of HBeAg in the serum, and it is believed to be the endpoint of a gradual accumulation of precore and core promoter mutations during the immune clearance phase [107,108]. It is estimated that the yearly rate of spontaneous HBeAg seroconversion is between 2 – 15 % [109,110]. The HBeAg-negative chronic HBV infection or previously inactive carrier phase is characterized by the presence of anti-HBe antibodies in combination with near-normal serum ALT levels and HBV DNA levels below 2000 IU/ml [102]. Patients in the HBeAg-negative chronic hepatitis B phase are seronegative for HBeAg but seropositive for HBsAg. There are detectable HBV DNA levels, but they tend to be lower than in the HBeAg-positive chronic infection. ALT levels are elevated and tend to fluctuate, and liver inflammation at a histological level is detected [102,111]. An increasing chance of fibrosis and cirrhosis and the development of HCC are associated with this phase of chronic infection but can also develop from other phases of chronic infection [112].
Only very few patients with HBeAg-negative chronic HBV infection spontaneously achieve HBsAg seroclearance with or without the development of anti-HBs antibodies [113], termed as functional cure [114]. A functional cure is defined as the absence of HBV DNA and HBsAg in the serum, with persisting cccDNA and possibly chromosomally intgrated HBV DNA in hepatocytes.

The development of HCC is the most significant consequence for patients with chronic hepatitis B and may even develop in patients with effective treatment [115]. Nonetheless, hepatitis B treatment can improve survival and prevent disease progression. The therapy options for patients infected with HBV can be divided into two classes. The first are the immunomodulatory agent's Interferon alpha (IFNa) and pegylated Interferon alpha (PEG-IFNa). They are only used in a small subset of patients. Here, the treatment goal is a long-term control of the virus with a limited duration of therapy. However, the likelihood is low, with approximately 30 % of the patients achieving long-term viral control and only 10 % achieving loss of HBsAg [93,102]. The sub-optimal treatment success is coupled with adverse side effects requiring careful monitoring during therapy [116]. The other classes of treatment agents are directly acting antivirals (DAAs). The nucleoside or nucleotide analogues (NUC) are structural analogues of nucleosides and nucleotides. They inhibit the reverse transcription of the pgRNA to the rcDNA, one

of the later steps in the viral replication cycle [87]. NUCs are very potent in suppressing the viral DNA levels and have few adverse effects, making them the first-line treatment option in most patients [93]. Unfortunately, due to their mode of action, they do not impact the HBsAg levels or directly degrade the cccDNA; therefore, lifelong treatment is required in most patients [117].

1.5 Immune response against the hepatitis B virus

1.5.1 Role of the innate immune response in an HBV infection.

Innate immunity is widely recognized as the direct defense mechanism against invading pathogens. It acts as the first line of defense and remains active until the adaptive immune response takes over and successfully eradicates the infection. The role of the innate immune system in HBV infections has been the subject of debate. Due to the poor induction of inflammatory cytokines, it was unclear if the innate immune system recognizes the virus [118]. Recent studies have shown that parts of the innate immune system consistently contribute to the response. The inadequate recognition is likely due to limited sensing combined with active suppression from the virus [118]. Part of the belief for the "evasion" of innate immunity was that an HBV infection only triggers weak interferon alpha or beta (IFN-α, INF-β) expression [119–121]. In this project, I focused on the role of $CD8^+$ T cell responses, which are part of the adaptive immune response and, therefore, described in more detail below.

1.5.2 Role of the adaptive immune response in an HBV infection.

Adaptive immunity is a crucial aspect of the immune system. Unlike innate immunity, adaptive immunity targets pathogens with high specificity. It encompasses humoral immunity, which produces pathogen-specific antibodies generated by B lymphocytes. In addition to the humoral response, adaptive immunity provides a cell-mediated response via different types of T lymphocytes. Immunological memory, which is responsible for preventing subsequent reinfections from previous infections or vaccination, is also a function of adaptive immunity. In HBV infections, adaptive immunity is the primary host determinant for the infection outcome [122].

1.5.2.1 B lymphocyte (B cell) response to HBV infection

Antibodies secreted from B cells are the central part of the humoral response. B cells recognize pathogens by binding to an antigen via the B cell receptor (BCR) in lymph nodes. With the antigen bound to the BCR, the B cell activation can be T-cell-dependent or independent. When activated, the B cell secretes antibodies with high binding specificity [123]. With the presence of anti-HBs antibodies and HBsAg-specific B cells from vaccination or recovered acute HBV infection, the humoral immune response plays a crucial role in protecting the host from subsequent HBV infections [124]. The high

amount of HBsAg in the blood is believed to absorb and bind the circulating anti-HBsAg antibodies, complicating attachment to virions [125].

1.5.2.2 T lymphocyte response to HBV infection.

The cell-mediated immunity of the adaptive immune system consists of the T lymphocytes (T cells). T cells can be divided into two groups depending on the occurrence of either the CD4 or the CD8 co-receptor. The T lymphocytes expressing the CD4 ($CD4^+$ T cells) co-receptor are also called T helper cells (T_h cells) and play an essential role in the immune response by regulating the activation of cells from innate and adaptive immunity. T lymphocytes expressing the CD8 ($CD8^+$ T cells) co-receptor on the surface are also called cytotoxic T lymphocytes (CTL), which can kill infected cells that present HLA class I molecules with pathogen epitopes [123]. In a self-limited acute HBV infection, it is believed that $CD4^+$ and $CD8^+$ T cells both play an essential role in controlling the infection and that a dysregulation of the adaptive immune system leads to the persistence of the viral infection [122].

A robust $CD4^+$ T cell response could be detected in patients who cleared an acute HBV infection, while the $CD4^+$ T cell response is weak in chronically infected patients [126–128]. Despite the observed association between $CD4^+$ T cells in patients, it was demonstrated in chimpanzees that the depletion of the $CD4^+$ T cells during the acute infection did not affect the subsequent clearance of the infection [129]. However, another study in chimpanzees showed that the depletion of $CD4^+$ T cells before the infection reduced $CD8^+$ T cell response, resulted in a persistent infection [130]. The findings suggest that $CD4^+$ T cells play a crucial indirect role in the clearance of the infection by $CD8^+$ T cells.
A study in PEG-IFN-α treated patients was able to demonstrate that HBeAg-positive patients who undergo an HBeAg seroconversion display a higher frequency of circulating $CXCR5^+$ $CD4^+$ T cells compared to patients that do not undergo an HBeAg seroconversion, suggesting a potential role of the $CD4^+$ T cells in the HBeAg seroconversion [131].

$CD8^+$ T cell response to HBV infection

$CD8^+$ T cells play an essential role in antiviral defense, which also applies to an HBV infection. In an acute infection, a polyclonal $CD8^+$ T cell response can be detected in patients who clear the infection [132]. The antigen receptors on the surface of $CD8^+$ T cells comprise two polypeptide chains, the TCR alpha and TCR beta chains. Gamma and delta chains can also be found in a small subset of T cells but play a lesser role. Each heterodimer consists of a variable, a constant, and a transmembrane domain [123]. The variable domain of the alpha- and beta-chain can further be divided into variable region (V) and joining region (J). Similar to a heavy antibody chain, the beta chain also includes a diversity region (D). The three different complementarity-determining regions (CDR) are found on the TCR alpha chain

in the V region, with the CDR3 region overlapping into the J region. The CDR1 and CDR2 are located in the V region on the TCR beta region, whereas the CDR3 overlaps the V, D, and J regions [133]. The TCR, combined with the CD8 co-receptor, interacts with a short amino acid fragment "epitope" bound to the HLA class I molecule (Figure 7 A). In contrast to antibodies, the T-cell can only recognize the epitope when bound to an HLA molecule.

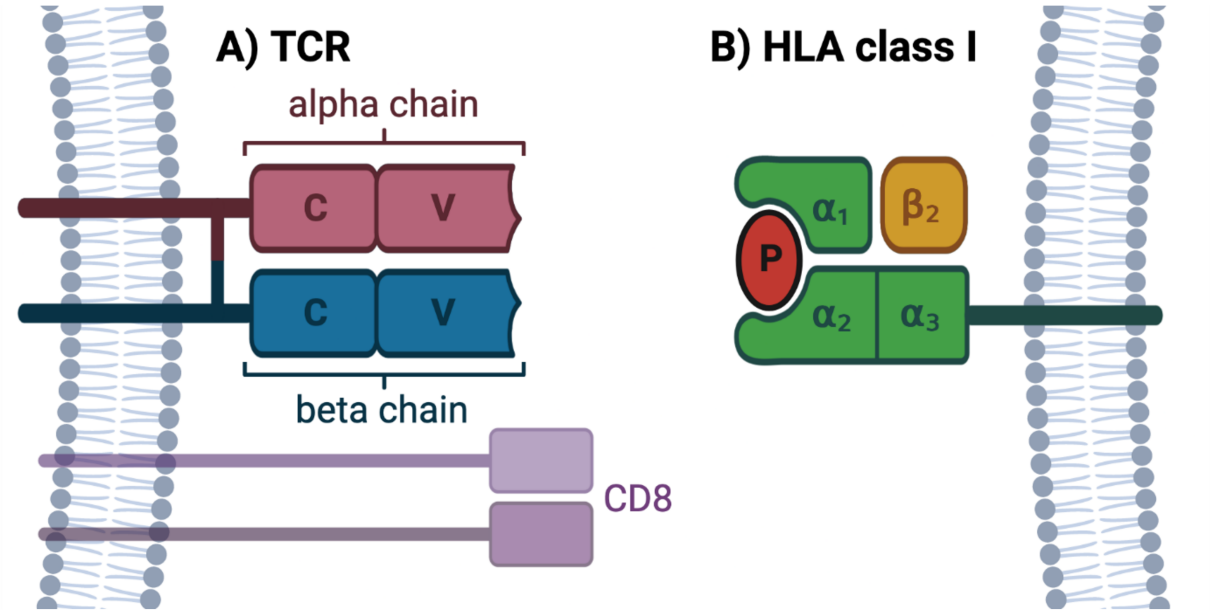

Figure 7 Interaction between the HLA class I molecule with the antigen and the CD8⁺ T cell receptor: A) T cell receptor (TCR) alpha chain (red) or beta chain (blue) containing the constant and variable region. In violet, the CD8 co-receptor. B) HLA class I molecule with the three alpha (α) subunits (green) and the beta2 (β_2) subunit holding the viral peptide (P, red). The Graphic representation was created using templates from BioRender.com.

Human Leukocyte Antigen (HLA) class I molecules are ubiquitously expressed on the surface of all nucleated cells and exhibit high polymorphism. The HLA class I molecule comprises a complex, highly polymorphic alpha chain, and a conserved β_2 microglobulin subunit (Figure 7 B). The alpha chain can be divided into three domains: α_1, α_2, and α_3. The α_1 and α_2 domains form the peptide-binding groove supported by the β_2 microglobulin subunit from below. The peptide is an integral part of the HLA class I molecule, and in its absence, the molecule would be unstable [123]. The HLA loci are considered some of the most variable loci in mammals, presenting different epitopes between individuals.

Due to the structure of the HLA class I molecule, only small peptide fragments can be presented. Antigens must undergo processing before being presented by the MHC class I molecule. Specifically, HBV proteins are first ubiquitinated and transported to the proteasome. The proteasome degrades the protein into small peptides. These fragments are then translocated into the endoplasmic reticulum (ER) lumen via the transporter associated with antigen processing (TAP) heterodimeric polypeptide. Within the ER lumen, newly synthesized HLA alpha chains are stabilized by calnexin until the β_2 microglobulin

subunit is bound. Once the HLA α/β_2 complex has been released from calnexin, it binds to an array of proteins such as Tapasin. Tapasin mediates the binding of the HLA α/β_2 complex to TAP, where the antigen is incorporated in the HLA α/β_2 complex. Incorporating the peptide allows the final folding of the HLA molecule and subsequent transport to the cell membrane, where the complex is presented to the TCR [123].

Although activation of $CD8^+$ T cells can be observed in an acute self-limiting HBV infection, the situation looks entirely different in a chronic HBV infection. In chronic HBV infection, HBV-specific $CD8^+$ T cell frequency is reportedly low in the blood and liver [134,135]. Moreover, the HBV-specific $CD8^+$ T cells are unable to exercise their capacity to proliferate, secrete cytokines, or destroy infected cells [134,136–138]. Nevertheless, nuanced differences can be observed considering the different phases of chronic infection. HBc- and polymerase-specific but not HBsAg-specific $CD8^+$ T cells could be detected in chronic HBV patients with low viremia [139]. In line with these findings, it was also demonstrated that significantly higher frequencies of HBc-specific $CD8^+$ T cells were detected in HBeAg-negative patients compared to HBeAg-positive patients [140].

As $CD8^+$ T cells and indirectly $CD4^+$ T cells play an essential role in the clearance of acute infection and their dysfunction is associated with persistent infection, evasion mechanisms of HBV came into focus. As already described, perinatal transmission accounts for the majority of chronically infected patients. It was found that over 90% of infected newborns of HBeAg-positive mothers developed a chronic infection compared to less than 10% of HBeAg-negative mothers, linking the persistancy of the virus to the HBeAg molecule [141]. Further, it was established that HBeAg but not HBsAg is able to pass into the placenta [142,143] and, in mice, would alter the immune function in the offspring [144,145]. Hence, these observations support the notion that the presence of HBeAg may interfere with the central T cell tolerance during the maturation in the thymus.
Besides the different viral proteins' immunomodulating functions, many viruses are known to develop mutations to avoid immune recognition. This is especially true in viruses with high mutation rates due to the reverse transcriptase like the Human immunodeficiency virus (HIV) and HBV. Mutations related to $CD8^+$ T cell selection pressure are found in HBV epitopes and are specific to different HLA molecules [146–149]. Interestingly, the frequency of HLA class-I associated mutations in chronic HBV correlates with the infected patient's HBeAg status, observing a significant increase in HBeAg-negative infections [150]. The increase of HLA class I associated mutations in combination with an increase in the frequency of HBV-specific $CD8^+$ T cells in the HBeAg negative chronic phase leads to the assumption that the loss of HBeAg may be associated with an increase of selection pressure and the need for the virus to select $CD8^+$ T cell evasion substitutions.

1.6 Aim of the project

Despite the availability of a highly effective vaccine, the hepatitis B virus continues to pose a significant health burden globally, and there is an urgent need for better therapy options. Unfortunately, many aspects of the virus remain poorly understood, partly because no simple animal or robust cell culture models are available, making studying the virus inaccessible to many researchers. Therefore, this project aimed to establish a cell culture assay that utilizes the viral cccDNA as a transcriptional template in hepatocellular carcinoma cell lines and study viral transcription and translation. Although cccDNA transfection assays already exist, they rely on modifications in the genome for the generation of cccDNA, which may have consequences for the transcription of viral RNAs.

Although HBeAg is conserved in all orthohepadnaviridae, it is unnecessary for viral replication. Recent research has revealed various immunotolerogenic and immunomodulatory functions of the viral protein. Further, evidence suggests that HBeAg plays a crucial role in the persistence of viral infection. However, the HBeAg, with its immune evasion properties, is often lost during chronic infection. The loss is coupled with an increase in HBc-specific $CD8^+$ T cells and HLA class I associated substitutions, particularly in the core ORF of the virus in HBeAg negative chronic infection. This raises the question of whether HBeAg, which shares amino acid sequences with the core protein, could become a burden for the virus rather than a benefit. Therefore, the cccDNA model system was utilized to determine if HBeAg is a significant source for epitopes targeted by core-specific $CD8^+$ cells and whether its loss could contribute to a $CD8^+$ T cell immune evasion strategy.

2 Materials

During this project, the following materials were used according to the description in the method section of the chapter.

2.1 Bacterial culture

2.1.1 Bacterial strains

Table 1 Bacterial strains used in this project

Name	Characteristics/Function/Properties	Company
NEB® 5-alpha Competent *E. coli*	Φ80 Δ(lacZ)M15; recA1; endA1; hsdR17, fhuA2	New England BioLabs

2.1.2 Bacterial outgrowth media

Table 2 bacterial outgrowth media used.

Product	Company
SOC Outgrowth Medium	New England BioLabs
LB-Agar	Carl Roth GmBH + Co. KG
LB-Medium (Lennox) 5 g/l NaCl	Carl Roth GmBH + Co. KG

2.2 Cell culture

2.2.1 Cell lines

HEK293T

HEK293T (ATCC: CLR-3216) are adherent growing epithelial-like cells derived from human embryonic kidney 293 cells. The cell line expresses a mutated SV40 large T-antigen. Due to the large SV40 T-antigen, it can replicate vectors carrying the SV40 region of replication [151]. The cell line can produce high titers of retrovirus [152]. In this project, the cell line was used to produce lentiviral particles. The cell line was grown in DMEM containing 10% FCS, 100 U/ml Penicillin, and 100 U/ml Streptomycin.

Phoenix-GALV

Phoenix cells are derived from HEK293T (ATCC: CLR-3216) cells. The cell line is capable of generating helper-free second-generation retrovirus. The cell line is capable of producing gag-pol and envelope proteins that are needed for viral assembly. This allows the generation of second-generation retrovirus without needing helper plasmids containing gag-pol or the envelope. The cell line uses the gibbon ape leukemia virus (GALV) envelop protein, which targets the GLVR-1 surface receptor [153]. GALV envelope is specifically used when human lymphocytes are targeted for gene transfer with a retrovirus, resulting

in a higher transfection efficiency than amphotropic envelope proteins like VSV-G [154]. The cell line was grown in IMDM containing 10% FCS, 100 U/ml Penicillin, and 100 U/ml Streptomycin. Dr. Miriam Heemskerk kindly provided the cell line during the MOI-funded stay in her laboratory in Leiden, Netherlands.

K562 [HLA-A*02]

The K562 cells (ATCC: CCL-243) are a leukemic cell line derived from human bone marrow isolates [155]. The suspension cell line expresses the HLA-A*02 molecule on the cell surface. The cell line was grown in IMDM containing 10% FCS, 100 U/ml Penicillin, and 100 U/ml Streptomycin. Dr. Miriam Heemskerk kindly provided the cell line during the MOI-funded stay in her laboratory in Leiden, Netherlands.

Hep G2

Hep G2 (ATCC: HB-8065) are adherent growing epithelial-like cells. The cell line was derived from a liver hepatocellular carcinoma of a 15-year-old Caucasian male [156]. In this project, derivates of the cell line were used for different purposes.

Hep G2-hNTCP

The Hep G2-hNTCP cell line is a derivate of the Hep G2 (ATCC: HB-8065) cell line. The cell line contains a stably transfected human sodium taurocholate co-transporting polypeptide (hNTCP). NTCP is a critical receptor needed for the entry of the hepatitis B and D viruses [68]. When not specified otherwise, the cell line was grown in DMEM or IMDM containing 10% FCS, 100 U/ml Penicillin, and 100 U/ml Streptomycin. The cell line was kindly provided by Thomas Baumert from Strasbourg, France.

Hep G2-P151 ($core_{wt}$)

The Hep G2-P151 cell line is a derivate of the Hep G2 (ATCC: HB-8065) cell line. The cell line contains a stable transduced HBV genotype core sequence-mCherry-CMVpp65 fusion protein. The core contains the HLA-A*02 epitope prototype sequence FLPSDFFPSV. The HBV core sequence is located downstream of an EF1α-Promotor for protein expression and is followed by an 50 amino acid sequence from the CMV UL83 protein, conatining the immunodominant pp65 epitope NLVPMVATV as internal control. When not specified otherwise, the cell line was grown in DMEM or IMDM containing 10% FCS, 100 U/ml Penicillin, and 100 U/ml Streptomycin. Dr. Andreas Walker generated the Hep G2-P151 cell line.

Hep G2-P152 ($core_{F24Y}$)

The Hep G2-P152 cell line is a derivate of the Hep G2 cell line. Here, the core HLA-A*02 epitope contains the F24Y substitution (sequence FLPSDF**Y**PSV). Dr. Andreas Walker generated the Hep G2-P152 cell line.

Jurkat E6.1

The Jurkat E6.1 cell line (ATCC: TIB-152) is a CD4+ T lymphoblast established initially from the peripheral blood of a child with T cell leukemia [157]. The cell line is used to research T lymphocyte signaling pathways and was an essential tool in helping decipher T cell receptor signaling [158].

Jurkat 76 (J76)

The Jurkat 76 cell line is derived from the Jurkat cell line (ATCC: TIB-152). The cell line is deficient in endogenous T cell receptor α and β chain expression. This allows the expression of exogenious T cell receptors [159].

Jurkat 76 mono NFκB (J76m)

The Jurkat 76 mono NFκB cell line is derived from Jurkat 76 cells (J76). The cells lack the endogenous T cell receptor α and β chain. Further, the cell line stably expresses CD8 and contains an NFκB-GFP response element. The NFκB-GFP response element allows the monitoring of the TCR activation [160]. The cell line was grown in IMDM containing 10% FCS, 100 U/ml Penicillin, and 100 U/ml Streptomycin. Besides the J76m without TCR, two variants contain an HLA-A*02-specific TCR that recognizes a core epitope and a TCR that recognizes an HBV surface epitope. Both TCRs are specified in detail in section 2.13.

2.2.2 Cell culture media, buffers, and additives

Table 3 includes a comprehensive list of the cell culture media, buffers, and additives used during this project.

Table 3 Cell culture media, buffers, and additives used in this project.

Product	Company
Dulbecco's Phosphate Buffered Saline (DPBS)	Gibco Life Technologies
Opt-MEM I [1x]	Gibco Life Technologies
FBS Superior	Biochrom GmbH
Dulbecco's Modified Eagle Medium (DMEM) [1x]	Gibco Life Technologies
MEM NEAA [100x]	Gibco Life Technologies
Penicillin/Streptomycin [10.000 U/ml]	Gibco Life Technologies
Iscove's Modified Dulbecco's Medium (IMDM)	Gibco Life Technologies
Recovery Cell Culture Freezing Medium	Gibco Life Technologies
TrypLE	Gibco Life Technologies

2.3 Enzymes

Table 4 Enzymes used in this project.

Product	Function	Company
NcoI-HF	Restriction Endonucleases	New England BioLabs
NotI-HF	Restriction Endonucleases	New England BioLabs
T4 DNA Ligase	DNA-Ligase	New England BioLabs
T5 Exonuclease	Exonuclease	New England BioLabs
DpnI	Methylation sensitive restriction endonucleases	New England BioLabs
Shrimp Alkaline Phosphatase	Dephosphorylation of 5' and 3' end	New England BioLabs

2.4 Flow cytometry

2.4.1 Antibodies & Dyes

For the staining of the cells used in this project, the following antibodies and dyes were used. Unless stated otherwise in the Methods, cells were stained with an antibody for 15 min at 4°C.

Table 5 Antibodies and dyes used in this project.

Antigen	Fluorochrom	Working dilution	Clone	Company	RRID
CD8	AF700	1:100	3B5	Invitrogen	AB_10372957
Mouse TCR β	APC	1:50	H57-597	BD Pharmingen	AB_398534
Viability dye	eFluor 506	1:1000	-	Invitrogen	-
HBcAg	-	1:50	13A9	Invitrogen	AB_1075048
Mouse IgG (L+H)	AF 488	1:500	Polyclonal	Invitrogen	AB_2534069
HLA-ABC	APC	1:100	REA230	Miltenyi Biotec	AB_2819392

2.5 HBV

2.5.1 HBV Reference sequences

The HBV reference genomes used to verify plasmids containing the whole HBV genomes were taken from the Hepatitis B Virus database (https://hbvdb.lyon.inserm.fr/).

Table 6 HBV Reference sequences

Genotype	Accession number	Genome length	Reference
A	X02763	3221	[161]
D	AB219428	3215	[162]

2.5.2 Dusseldorf cohort

The Duesseldorf HBV cohort consists of peripheral blood samples from 544 patients infected with HBV (Table 7). The patient's material is from Germany, the United Kingdom, and the United States of America. All samples were collected after approval of the local ethics committee, and written informed consent was given by all participants. Dr. Tatjana Schwarz generated the sequence information.

Table 7 Patient characteristics of the Duesseldorf cohort.

SD: standard deviation, ALT: alanine aminotransferase, AST: aspartate aminotransferase.

Patients n	544
Sex	n (%)
woman	236 (43.4)
man	293 (53.8)
unknown	15 (2.8)
Age (mean, range)	41, 15-83
ALT (median U/l, range)	35, 6- 1854
AST (median U/l, range)	31, 6- 2613
HBV viral load (mean log IU/ml ± SD)	4.2 ± 1.6
quantitative HBsAg (mean log IU/ml ± SD)	3.6 ± 0.8

The HBV sequences of the cohort can be obtained in GenBank with the Accession number:

- MW845286-MW845312
- MW887641-MW887652
- MW926548-MW926566
- MZ043025-MZ043097
- MZ097624-MZ097884

2.5.3 HBV genomes used for the assay

Four isolates (Table 8) were picked for the cccDNA assay. All four isolates were from male patients with an average age of 27.5 years (23 – 37). The isolates were chosen for having a viral load > 2 million IU/ml, HBeAg and HBsAg positive. The sequences were further analyzed for the BCP, start codon, or G1896A mutations. Genious Prime software was used to generate the consensus sequences for genotypes A and D by aligning all genotypes A (n = 5) or D (n = 43) HBeAg and HBsAg positive sequences.

Table 8 Patient isolates used for the cccDNA generation

No.	ID	Genotype	Viral load (IU/ml)	HLA-A		HLA-B	
#1	FR-HBV238	D	145426465	201	2402	702	1801
#2	DD14-38611	D	7000000	3201	6801	1518	3801
#1	FR-HBV54	A	220199656	201	3001	1302	3901
#2	DD14-28904	A	2474487	201	3101	1801	4002

2.6 Instruments and devices

Table 9 Instuments and devices used in the project.

Function	Name	Company
Flow cytometry	BD Fortessa	Becton, Dickinson and Company
Spectral flow cytometry	Cytek Aurora	Cytek Biosciences
Cell counter	XP-300	Sysmex
Freezing container	Mr. Frosty	Thermo Fischer Scientific
Immunoassay	ARCHITECT i2000SR	Abbott
Spectrophotometer	NanoDrop 2000	Thermo Fisher Scientific
Power supply for gel electrophoresis chamber	EPS301	Biometra
Gel electrophoresis chamber	Maxi	Biometra
Gel electrophoresis chamber	Mini	Biometra
MACS cell separation	MidiMACS Separator	Miltenyi Biotec
Vacuum manifold	Vac-Man	Promeaga

2.7 Peptides

The peptides were obtained with a purity of >70 %, an OH-group at the C-terminal and an NH_2-group at the N-terminal end. The lyophilized peptides were dissolved in DMSO at a 20mg/ml stock concentration and stored at -80°C for further use. The final concentration for exogenous loading of cells was 1 µg/ml.

Table 10 Peptides used in the project

Sequence	Protein	Position	HLA-class I restriction	Company
FLPSDFFPSV	core	18-27	A*02	EMC microcollections GmbH
FLPSDFYPSV	core	18-27	A*02	EMC microcollections GmbH
SIVSPFIPLL	surface	370-379	A*02	EMC microcollections GmbH

2.8 Kits

Table 11 Kits

Name	Company
NEBuilder HiFi DNA Assembly	New England BioLabs
QIAprep Spin Miniprep Kit	Qiagen
GeneJET Gel Extraction Kit	Thermo Scientific
GeneJET PCR clean-up Kit	Thermo Scientific
PureLink™ Expi Endotoxin-Free Maxi Plasmid Purification Kit	Invitrogen
Architect HBeAg reagent Kit	Abbott
Architect HBsAg reagent Kit	Abbott
Anti-APC MicroBeads	Miltenyi Biotec

2.9 Labware

Table 12 Labware and consumables used in this project.

Description	Company
Cryogenic tubes [2 ml]	Greiner Bio-One
LS Columns	Miltenyi Biotec
96-U-Well plate	VWR International
Safe-Lock Tube • 1.5 ml	Eppendorf

• 2.0 ml	
C-Chip Neubauer Improved Disposable Hemocytometer	NanoEntek
Spin column extender [20 ml]	Biozol
T-25 cell culture flask	Sarstedt
T-75 cell culture flask	Sarstedt
T-175 cell culture flask	Sarstedt
Collagen I-coated plate [24-well]	Corning Incorporated
DNA LoBind 1.5 ml Tube	Eppendorf
DNA LoBind 50 ml Tube	Eppendorf
Disposable Polystyrene serological pipette • 5 ml • 10 ml • 25 ml	Corning Incorporated
Conical tube • 15 ml • 50 ml	Sarstedt

2.10 Molecular cloning

2.10.1 Plasmids

Table 13 Plasmids

Name	Feature	Reference / Origin
pUC18	vector with multiple cloning site	RRID:Addgene_500004
pSHH 2.0	Contains the HBV genotype D strain awy genotype twice	provided by Michael Nassal, Freiburg
pMP71 flex	Retroviral transfer vector	Provided by Mirjam H. M. Hemskerk
pMP71 flex TCR a3-b8	Contains the TCRa3-P2A-b8 sequence targeting the HBc_{18-27} epitope	Based on pMP71 flex
pTwist Lenti SFFV Puro WPRE TCRa3-b8	pCCL lentivirus backbone, SFFV promoter, EMCV IRES, contains the TCRa12-P2A-b7.8 sequence targeting HBc_{18-27} epitope	TwistBioscience
pTwist Lenti SFFV Puro WPRE TCRa12-b7.8	pCCL lentivirus backbone, SFFV promoter, EMCV IRES, contains the TCRa12-P2A-b7.8 sequence targeting $HBs_{370-379}$ epitope	TwistBioscience
pNL1.1-Nluc	-	Promega

pNL1.1-Nluc-GTD #1 prototype	Contains the GTD #1 prototype sequence	Based on pNL1.1-Nluc
pNL1.1-Nluc-GTD #1 BCP	Contains the GTD #1 BCP sequence	Based on pNL1.1-Nluc
pNL1.1-Nluc-GTD #1 W28*	Contains the GTD #1 W28* sequence	Based on pNL1.1-Nluc
pNL1.1-Nluc-GTD #1 CTG	Contains the GTD #1 CTG sequence	Based on pNL1.1-Nluc
pNL1.1-Nluc-GTD #2 prototype	Contains the GTD #2 prototype sequence	Based on pNL1.1-Nluc
pNL1.1-Nluc-GTD #2 BCP	Contains the GTD #2 BCP sequence	Based on pNL1.1-Nluc
pNL1.1-Nluc-GTD #2 W28*	Contains the GTD #2 W28* sequence	Based on pNL1.1-Nluc
pNL1.1-Nluc-GTD #2 CTG	Contains the GTD #2 CTG sequence	Based on pNL1.1-Nluc
pNL1.1-Nluc-GTD Consensus prototype	Contains the GTD Consensus prototype sequence	Based on pNL1.1-Nluc
pNL1.1-Nluc-GTD Consensus BCP	Contains the GTD Consensus BCP sequence	Based on pNL1.1-Nluc
pNL1.1-Nluc-GTD Consensus W28*	Contains the GTD Consensus W28* sequence	Based on pNL1.1-Nluc
pNL1.1-Nluc-GTD Consensus CTG	Contains the GTD Consensus CTG sequence	Based on pNL1.1-Nluc
pNL1.1-Nluc-GTA #1 prototype	Contains the GTA #1 prototype sequence	Based on pNL1.1-Nluc
pNL1.1-Nluc-GTA #1 BCP	Contains the GTA #1 BCP sequence	Based on pNL1.1-Nluc
pNL1.1-Nluc-GTA #1 W28*	Contains the GTA #1 W28* sequence	Based on pNL1.1-Nluc
pNL1.1-Nluc-GTA #1 CTG	Contains the GTA #1 CTG sequence	Based on pNL1.1-Nluc
pNL1.1-Nluc-GTA #2 prototype	Contains the GTA #2 prototype sequence	Based on pNL1.1-Nluc
pNL1.1-Nluc-GTA #2 BCP	Contains the GTA #2 BCP sequence	Based on pNL1.1-Nluc
pNL1.1-Nluc-GTA #2 W28*	Contains the GTA #2 W28* sequence	Based on pNL1.1-Nluc
pNL1.1-Nluc-GTA #2 CTG	Contains the GTA #2 CTG sequence	Based on pNL1.1-Nluc
pNL1.1-Nluc-GTA Consensus prototype	Contains the GTA Consensus prototype sequence	Based on pNL1.1-Nluc
pNL1.1-Nluc- GTA Consensus BCP	Contains the GTA Consensus BCP sequence	Based on pNL1.1-Nluc
pNL1.1-Nluc-GTA Consensus A1762T	Contains the GTA Consensus A1762T sequence	Based on pNL1.1-Nluc

pNL1.1-Nluc-GTA Consensus G1764A	Contains the GTA Consensus G1764A sequence	Based on pNL1.1-Nluc
pNL1.1-Nluc-GTA Consensus W28*	Contains the GTA Consensus W28* sequence	Based on pNL1.1-Nluc
pNL1.1-Nluc-GTA Consensus CTG	Contains the GTA Consensus CTG sequence	Based on pNL1.1-Nluc

2.10.2 Primers

Table 14 Primers used for various methods in this project.

Name	Sequence
HBx out F	ATGCGTGGAACCTTTATGGCTC
Core out R	TGCAGAGAGTCCAAGAGTCCTC
HBV Seq 1 F	ACGTCCTTTGTTTACGTCCC
HBV Seq 1 R	AGGAGACTCTAAGGCATCCC
HBV Seq 2 F	GAACATTGTTCACCTCACCATAC
HBV Seq 2 R	TTTCTCATTAACTGTGAGTGGGC
HBV Seq 3 F	GCCATTGGATAAGGGTATTAAACC
HBV Seq 3 R	TAGTCGGAACAGGGTTTACTG
HBV Seq 4 F	CTGCCTCTCACTTATCGTCAATC
HBV Seq 4 R	GGAAAGCCCTACGAACCACTGAAC
HBV Seq 5 F	TGTACAGCATCTTGAGTCCC
HBV Seq 5 R	AGGACAACCGAGTTATCAGTC
pNL out F	CAAGTGCAGGTGCCAGAACATTTC
pNL out R	CGCTCAGGACAATCCTTTGG
TCR-NotI-Fwd	TTACAGGCGGCCGCCACCATGGATTCTTGGACC
TCR-EcoRI-Rev	GGATCCGAATTCAGCTGCTCCATAGCCG
pMP71 fwd:	TGAATTCGGATCCAAGCTTAGGCCTGCTC
pMP71 Rev	CATGGTGGCGGCCGCCT
TCR_b8_out_F	GCGATGGTGAAGAGAAAAGACAGCAGAGGA
TCR_a3_out_R	CGATACGCAGCACAGCGTCCAGCTGTCCAT
GA_GTA_CON_Fwd	GAGCATTGCTCACCTCACCATAC
GA_GTA_CON_Rev	TGCTGGGAGTCCAAGAGTCCTC
GA_GTD_WT2_Fwd	GAGCATTGTTCACCTCACCATAC
GA_GTD_WT2_Rev	TACAGAGAGTCCAAGAGTCCTC
GA_GTD_CON_Fwd	TACAGAGAGTCCAAGAGTCCTC
GA_GTD_CON_Rev	GAGCATTGTTCACCTCACCATAC

2.10.3 Synthesised nucleotide sequences

Table 15 List of Synthesised nucleotide sequences order from TwistBioscience.

Name	Function	Cloned in	Company
TCR-HBc$_{18-27}$	Contains the TCR alpha 3 P2A beta 8 sequence	pMP 71 flex	TwistBioscience
HBV GTD #1 BCP	Contains the A1762T & G1764A mutation	pNL1.1-Nluc – GTD #1 prototype	TwistBioscience
HBV GTD #1 W28*	Contains the G1896A mutation	pNL1.1-Nluc – GTD #1 prototype	TwistBioscience
HBV GTD #1 CTG	Contains the A1814C mutation	pNL1.1-Nluc – GTD #1 prototype	TwistBioscience
HBV GTD #2 BCP	Contains the A1762T & G1764A mutation	pNL1.1-Nluc – GTD #2 prototype	TwistBioscience
HBV GTD #2 W28*	Contains the G1896A mutation	pNL1.1-Nluc – GTD #2 prototype	TwistBioscience
HBV GTD #2 CTG	Contains the A1814C mutation	pNL1.1-Nluc – GTD #2 prototype	TwistBioscience
HBV GTA #1 BCP	Contains the A1762T & G1764A mutation	pNL1.1-Nluc – GTA #1 prototype	TwistBioscience
HBV GTA #1 W28*	Contains the G1896A mutation	pNL1.1-Nluc – GTA #1 prototype	TwistBioscience
HBV GTA #1 CTG	Contains the A1814C mutation	pNL1.1-Nluc – GTA #1 prototype	TwistBioscience
HBV GTA #1 BCP	Contains the A1762T & G1764A mutation	pNL1.1-Nluc – GTA #2 prototype	TwistBioscience
HBV GTA #1 W28*	Contains the G1896A mutation	pNL1.1-Nluc – GTA #2 prototype	TwistBioscience
HBV GTA #1 CTG	Contains the A1814C mutation	pNL1.1-Nluc – GTA #2 prototype	TwistBioscience
HBV GTD consensus BCP	Contains the A1762T & G1764A mutation	pNL1.1-Nluc – GTD consensus prototype	TwistBioscience
HBV GTD consensus W28*	Contains the G1896A mutation	pNL1.1-Nluc – GTD consensus prototype	TwistBioscience
HBV GTD consensus CTG	Contains the A1814C mutation	pNL1.1-Nluc – GTD consensus prototype	TwistBioscience
HBV GTA consensus BCP	Contains the A1762T & G1764A mutation	pNL1.1-Nluc – GTA consensus prototype	TwistBioscience
HBV GTA consensus W28*	Contains the G1896A mutation	pNL1.1-Nluc – GTA consensus prototype	TwistBioscience
HBV GTA consensus CTG	Contains the A1814C mutation	pNL1.1-Nluc – GTA consensus prototype	TwistBioscience

2.11 Reagents and Chemicals

Table 16 List of reagents and chemicals used in this project.

Product	Company
CutSmart buffer [10x]	New England BioLabs,
NEBuffer 4 [10x]	New England BioLabs
T4 DNA Ligase reaction buffer [10x]	New England BioLabs
TransIT-LT1	Mirus Bio LLC
Nuclease-Free Water, sterile	VWR
Ampicillin Sodium Salt powder	Carl Roth
Trypanblue	Gibco
Ethanol Absolut [≥ 99.5%]	Merck
2-Propanol [≥ 99.9%]	Carl Roth
Dimethylsulfoxid (DMSO) [99.8%]	Carl Roth
BD FACS Clean	Becton, Dickinson and Company
BD FACS Flow	Becton, Dickinson and Company
BD FACS Rinse	Becton, Dickinson and Company
eBioscience IC-Fixation buffer	Invitrogen
eBioscience permeabilisation buffer [10x]	Invitrogen
GeneRuler 1 kB Plus DNA Standard	Thermo Fisher Scientific
Tris-Borate-EDTA (TBE) buffer [10x]	Sigma
TriTrack DNA loading dye	Thermo Fisher Scientific
Anti-APC MicroBeads	Miltenyi Biotec
Accutase Cell Detachment Solution	BioLegend
RetroNectin	TaKaRa
Human Serum Albumin	Sigmaaldrich

2.12 Software

Table 17 List of Software used in this project.

Product	Company
BioRender.com	Science Suite, Inc. Canada
DeepL Translate for Mac	DeepL SE
FlowJo 10.9	Becton, Dickinson and Company, USA
Geneious Prime 2022	Biomatters Inc.
GraphPad Prism 10	GraphPad Software, LLC.
Grammarly.com	Grammarly Inc. USA

LanguageTool for Desktop 1.6.7	Language Tooler GmbH
Libkey Nomad 1.28	Third Iron, LLC
Microsoft Office 365	Microsoft Corporation
Papers v4.37	Digital Science & Research Solutions, Inc.
Sciebo	ownCloud GmbH distributed by Hochschulcloud NRW

2.13 T-Cell Receptor

During the project different T-cell receptors (TCR) were used. The nucleotide sequence was synthesized by TwistBioscience. The complete sequences are attached in the supplements.

HBc_{18-27} TCR

The Hepatitis B virus $core_{18-27}$ specific TCR is HLA-A*02 restricted and targes the FLPSDFFPSV peptide processed from the HBV core protein amino acid position 18 to 27. The TCR alpha chain consists of the T-cell receptor alpha (TRA) 3 locus containing the complementarity-determining region 3 (CDR3) with the amino acid sequence CATWLSGSARQLTF. The TCR beta chain consists of the T-cell receptor beta (TRB) 8 locus containing the CDR3 amino acid sequence CASSNRASSYNEQFF. The entire nucleotide sequence was obtained from Patent US10004801B2, submitted by Antonio Bertoletti and Adam Gehring [163]. For this project, the constant region was exchanged to a murine alpha and beta constant region, allowing higher expression levels on the cell surface [164,165]. Prof. Ulrike Protzer and Dr. Karin Wisskirchen kindly provided the sequence information.

$HBs_{270-379}$ TCR

The Hepatitis B virus $surface_{370-379}$ specific TCR is HLA-A*02 restricted and targes the SIVSPFIPLL peptide processed from the HBV surface protein amino acid position 370 to 379. The TCR alpha chain consists of the T-cell receptor alpha (TRA) 12 locus containing the CDR3 region with the amino acid sequence CAVNLYAGNMLTF. The TCR beta chain consists of the T-cell receptor beta (TRB) 7-8 locus containing the CDR3 amino acid sequence CASSSDFGNQPQHF. The entire nucleotide sequence was obtained from Patent US10004801B2, submitted by Antonio Bertoletti and Adam Gehring [163]. For this project, the constant region was exchanged to a murine alpha and beta constant region, which Prof. Ulrike Protzer and Dr. Karin Wisskirchen kindly provided.

For both TCRs, the final sequence containing the variable alpha and beta chain with the murine constant chain was codon optimized with the HEXplorer/ModCon algorithm [166]. The two chains were combined for expression in the targeted cells by a P2A site. The complete sequence of the clonal genes can be found in the Supplements.

3 Methods

3.1 Mammalian cell culture

3.1.1 Thawing of cryo-conserved mammalian cells

A unique thawing medium was used to thaw the cell lines. The thawing medium consisted of 50% of the subculture medium used for the cell line and 50% fetal bovine serum (FBS). For each cryovial, 30 ml thawing medium was needed. The thawing medium was always prepared shortly before use. The subculturing medium specific for the cell line and the thawing medium were pre-warmed in a water bath at 37°C for 30 minutes as cold media significantly decreased the cell viability [167,168]. A 15 ml conical tube was prepared with 14 ml warm thawing medium. The cells were removed from liquid nitrogen storage and transported on ice. The cryovials were briefly thawn in a water bath at 37°C till no ice was visible. The cells were slowly pipetted from the cryovial into the 15 ml conical tube and centrifuged at 300x RCF for 10 minutes at room temperature (RT). Afterward, the supernatant was discarded, and the cells were resuspended in 15 ml thawing medium. The cells were again centrifuged at 300x RCF for 10 minutes at RT. The supernatant was discarded, and the cells were resuspended in 4 ml (suspension cells) or 8 ml (adherent cells) subculturing medium. The cells were transferred in a T25 cell culture flask and incubated for 24 hours at 37°C 5% CO_2. The next day, the cells were examined under the microscope, and the medium was exchanged. All cell lines used in this project were thawed in the same fashion.

3.1.2 Subculturing of adherent cells

The adherent cells (HEK293T, Phoenix-GALV, and all HepG2 derivates) were cultured at 37°C and 5% CO2 and 80% relative humidity in a T75 cell culture flask. HEK293T and Phoenix-GALV cells were cultivated in IMDM medium supplemented with 10% FBS and 1% Penicillin/Streptomycin (Pen/Strep) solution. HepG2-hNTCP, HepG2-P151, or HepG2-P152 cells were cultivated in IMDM medium supplemented with 10% FBS and 1% Pen/Strep solution when prepared for the T-cell receptor assay or DMEM medium supplemented with 10% FBS and 1% Pen/Strep solution when subcultured for the HBV cccDNA assay. The cells were passaged when >70% confluency was achieved. The cells were washed twice with 15 ml phosphate-buffered saline (PBS). Afterward, 2 ml TrypLE was added to the cells, and the cell culture flask was tilted till all cells were in contact with TrypLE. The cells were incubated for 1 min at RT, and the TrypLE was removed. The flask containing the cells was incubated for 10 min at 37°C and 5% CO_2 in a humidified incubator. After incubation, the cells were collected in 10 ml fresh and pre-warmed culture medium. A fraction (1/3, 1/4, or 1/10) was added to a new T75 cell culture flask containing fresh culture medium and further incubated until at least 70% confluency was reached.

3.1.3 Subculturing of suspension cells

The suspension cell lines (K562, J76 mono NFkB variants) were subcultured in IMDM medium supplemented with 10% FBS and 1% Penicillin/Streptomycin (Pen/Strep) solution. Cells were grown at 37°C, 5% CO_2, and 80% relative humidity in a cell culture incubator. T75 cell culture flasks were used and stored upright in a cell culture incubator for the sub-culture. The passaging of the cells growing in suspension was done by pipetting 3 ml (Mondays) or 5 ml (Fridays) into a new T75 cell culture flask containing 17 – 15 ml fresh medium.

3.1.4 Freezing of mammalian cells

The medium was removed to prepare adherent cells for cryopreservation, and 1 ml was collected for the diagnostics department to test for mycoplasma. The cells were washed twice with PBS, and 2 ml TrypLE was added. The cells were incubated for 10 minutes and resuspended in a culture medium. A small amount was transferred into a safe-lock tube for counting. The cells were transferred to a 50 ml conical tube and centrifuged at 300 RCF for 10 minutes. To prepare suspension cells for cryopreservation, 1 ml medium was collected for the diagnostics department to test for mycoplasma. The cells were transferred in a 50 ml conical tube and centrifuged at 300 RCF for 10 minutes.
Adherent and suspension cells were resuspended in recovery cell culture freezing medium at 5*106 cells/ml. Afterward, the cryotubes were stored in Mr. Frosty's freezing container at -80°C for 2 – 24 hours and then transferred into Nitrogen long-term storage.

3.2 Molecular cloning

All molecular cloning tasks in this project were done using the Gibson assembly or restriction endonuclease methods. Gibson assembly allows the isothermal coupling of two or more DNA fragments with a 15 to 25 base pair (bp) overlap. Generally, the system uses an exonuclease to remove DNA from the 5’ end and anneal the remaining single strand 3’ ends of the fragments. A DNA polymerase closes the gaps introduced by the exonuclease, and a DNA ligase seals the remaining nicks.

3.2.1 Molecular cloning of genotype A and D prototype sequences into pNL1.1-Nluc

The prototype sequences were synthesized and cloned in vectors (pTwist) by Twist Bioscience. Unfortunately, the vectors were of low copy number and yielded inadequate stock concentrations. Therefore, the viral prototype genomes were excised and cloned in pNL1.1-Nluc. The excision was performed with the NcoI-HF restriction endonuclease. The Twist Bioscience vector containing the HBV prototype genome and the pNL1.1-Nluc vectors were digested. The reaction mix was prepared according to Table 18.

Table 18 Reaction mixture for restriction endonuclease.

[1x]	Components
5 µl	CutSmart buffer
1 µl	NcoI-HF
4 µl	Plasmid (pTwist or pNL1.1-Nluc)
to 50 µl	Nuclease-free water

The endonuclease reaction was done for two hours at 37°C. The reaction mixture containing the linearised pNL1.1-Nluc was further incubated for 30 minutes at 37°C with the addition of 1 µl Shrimp Alkaline Phosphatase to dephosphorylate the linear DNA.

The reaction mixture containing the HBV prototype and the vector backbone were separated by 1% agarose gel electrophoresis for one hour at 120 V and 400 mA. The HBV prototype genome gel band was excised under UV light and purified with the GenJet gel extraction Kit from Thermofisher. The agarose gel was dissolved by adding 1:1 volume to weight binding buffer and incubation on a shaking heat block at 56°C, 1000 rpm for up to 5 minutes or when the gel was completely dissolved. 800 µl dissolved agarose gel was transferred to a purification column and centrifuged for 60 seconds at 16000 RCF. The flow-through was discarded, and the column was refilled with dissolved agarose gel and centrifuged. This was repeated until the whole volume was loaded onto a column. The flow-through was discarded, and 700 µl wash buffer was added. The column was again centrifuged at 16000 RCF for 60 seconds, and the flow-through was discarded. The empty column was centrifuged at 16000 RCF for 60 seconds to remove residual wash buffer and transferred onto a 1.5 ml safe lock tube. 50 µl pre-warmed elution buffer was added to the column and incubated for 1 minute. The column was centrifuged for 60 seconds at 12000 RCF and afterward discarded.

The endonuclease reaction mix containing the pNL1.1-Nluc was purified in the same manner as the other reaction mix, with the difference being that no agarose gel was dissolved, and the solution was directly mixed with a 1:1 volume of the binding buffer.

The eluate concentration was determined via spectrophotometer, and a DNA ligation reaction mix was prepared according to Table 19. For best DNA ligation results, the backbone:insert ratio was 1:3.

Table 19 Reaction mixture for DNA ligation.

[1x]	Components
2 µl	T4 DNA ligase buffer [10x]
50 ng	Linear pNL1.1-Nluc vector
150 ng	Linear prototype HBV genome
1 µl	T4 DNA ligase
To 20 µl	Nuclease-free water

The DNA ligase reaction was incubated at room temperature for 15 minutes, and Heat inactivated at 65°C for 10 minutes. The finished DNA ligase reaction was used for bacterial transformation, as explained in section 3.3.1.

3.2.2 Gibson Assembly

3.2.2.1 PCR amplification and linearisation of pNL1.1-Nluc containing HBV prototype variant

The HBeAg mutations were introduced into the prototype variant by Gibson assembly. Therefore, 400 bp long fragments comprising parts of the basal core promoter (BCP) and precore region were synthesized by Twist Bioscience (Figure 8). The lyophilized fragments were dissolved in nuclease-free water for a final concentration of 20 µg/ml.

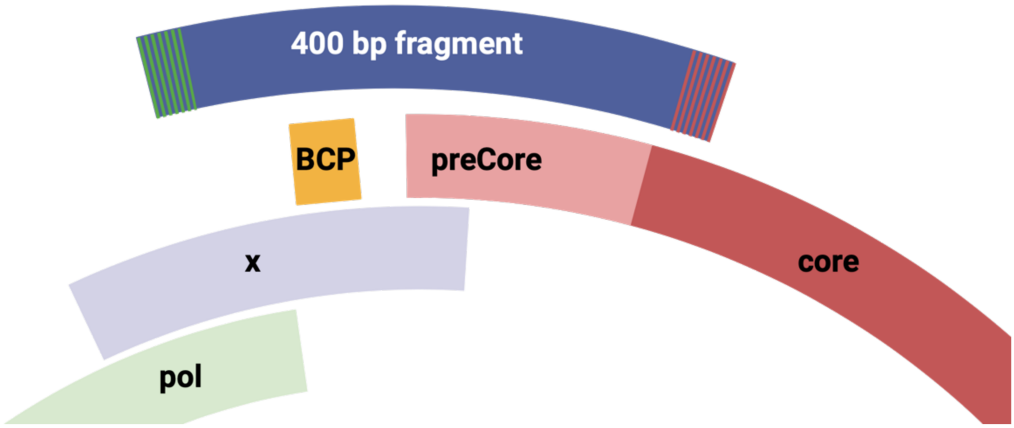

Figure 8 Graphical visualisation: Graphical representataion of the 400 bp fragment containing one of the HBeAg mutations for the Gibson assembly into pNL1.1-Nluc containing the prototype HBV genome.

The pNL1.1-Nluc plasmid containing the prototype variant (backbone) was amplified and linearised by polymerase chain reaction (PCR) to generate the vector containing the HBeAg mutation. The linear length was 5933 bp. Depending on the isolate, specific primers were used (Table 20).

Table 20 Primers used to prepare the DNA for Gibson assembly.

Isolate	Forward primer	Reverse primer
Genotype A #1	GA_GTA_CON_Fwd	GA_GTA_CON_Rev
Genotype A #2	GA_GTA_CON_Fwd	GA_GTA_CON_Rev
Genotype A consensus	GA_GTA_CON_Fwd	GA_GTA_CON_Rev
Genotype D #1	Seq 2 F	Core out R
Genotype D #2	GA_GTD_WT2_Fwd	GA_GTD_WT2_Rev
Genotype D consensus	GA_GTD_CON_Fwd	GA_GTD_CON_Rev

The PCR was performed with the Q5 DNA polymerase to minimize the DNA polymerase error rate and prevent the A-tailing that occurs with the Taq DNA polymerase. The PCR master mix was pipetted according to Table 21.

Table 21 Reaction mixture for the Q5 PCR to generate the linear pNL1.1-Nluc backbone.

Volume [1x]	Components
35.5 µl	Nuclease-free water
10 µl	Q5 buffer
1 µl	dNTPs [10 mM]
1 µl	Forward primer [10 µmol]
1 µl	Reverse primer [10 µmol]
0.5 µl	Q5 DNA polymerase
49 µl	Total voume

The backbone stock was diluted to less than 50 ng/µl to avoid spill-over of the unmodified backbone during bacterial transformation. The master mix was briefly centrifuged on a small benchtop centrifuge, and 1 µl (<50 ng/µl) of the pNL1.1-Nluc plasmid containing the prototype variant was added to the master mix. The reaction mix was again briefly centrifuged and placed in the PCR thermocycler. The PCR thermocycler operated according to program GA-HBe (Table 22).

Table 22 PCR program GA-HBe for the amplification of the 5933 bp long pNL1.1-Nluc

Step	Time [seconds]	Temperature [°C]	Cycle
Melting	30	98	
Melting	10	98	30
Annealing	30	65	
Elongation	190	72	
Elongation	120	72	

3.2.2.2 PCR amplification of the T-cell receptor constructs and pMP71 flex for gibson assembly

The constructs containing the sequence of the alpha and beta chain of the HBc_{18-27} and $HBs_{370-379}$ T-cell receptor (TCR) were initially ordered from the company Twist Bioscience. They were cloned into the lentiviral transfer vector pTwist Lenti SFFV Puro WPRE. The HBc_{18-27} TCR construct needed to be cloned into the retroviral transfer vector pMP71 flex due to safety regulations regarding lentivirus in the laboratory of Prof. Mirjam H. M. Heemskerk, where I went for the MOI stay abroad.

Therefore, two separate PCR were performed, one to amplify the insert containing the TCR (1800 bp) and the other to amplify and linearise pMP71 flex (backbone) with a length of 4500 bp. The master mix for both reactions was identical except for the primers (Table 23).

Table 23 Primers used to prepare the DNA for the Gibson assembly.

Name	Forward primer	Reverse primer
HBc_{18-27} TCR (insert)	TCR-NotI-Fwd	TCR-EcoRI-Rev
pMP71 flex (backbone)	pMP71 Fwd	pMP71 Rev

The PCR was performed with the Q5 DNA polymerase to minimize the DNA polymerase error rate and prevent the A-tailing that occurs with the Taq DNA polymerase. The PCR master mix was pipetted according to Table 24.

Table 24 Reaction mixture of the Q5 PCR to generate the linear DNA for the Gibson assembly.

Volume [1x]	Components
35.5 µl	Nuclease-free water
10 µl	Q5 buffer
1 µl	dNTPs [10 mM]
1 µl	Forward primer [10 µmol]
1 µl	Reverse primer [10 µmol]
0.5 µl	Q5 DNA polymerase
49 µl	Total voume

The insert and backbone stock were diluted to less than 50 ng/µl to minimize spill-over during bacterial transformation. The master mix was briefly centrifuged on a small benchtop centrifuge, and 1 µl (<50 ng/µl) of the vector was added to the designated master mix. The reaction mix was again briefly centrifuged and placed in the PCR thermocycler. The PCR thermocycler operated according to program GA-TCR_I (Table 25) and GA-TCR_B (Table 26).

Table 25 PCR program GA-TCR_I for the amplification of the insert containing the TCR sequence (1800 bp).

Step	Time [seconds]	Temperature [°C]	Cycle
Melting	30	98	
Melting	10	98	30
Annealing	30	69	
Elongation	54	72	
Elongation	120	72	

Table 26 PCR programm GA-TCR_B for the amplification of the linear pMP71 flex vector (4500 bp).

Step	Time [seconds]	Temperature [°C]	Cycle
Melting	30	98	
Melting	10	98	30
Annealing & Elongation	180	72	
Elongation	120	72	

3.2.2.3 PCR control and DpnI

After the PCR, 6 µl of the mix was run on a 1% agarose gel containing four drops of Ethidiumbromid (0.025%) for 1 hour at 100 V, 400 mM to verify the successful amplification of the linear backbone. The GeneRuler 1 kb Plus DNA ladder was used as a size control. To the remaining 44 µl of the reaction mix, 5 µl CutSmart and 1 µl DpnI were added to remove the remaining circular backbone. The mix was incubated for one hour at 37°C.

3.2.2.4 Purification of PCR product

After the reaction, the DNA was purified with the Thermofischer PCR clean-up kit. For this purpose, the 50 µl reaction mix containing the linear DNA backbone was combined with an equal volume binding buffer. The mixture containing the buffer and the DNA was pipetted onto the purification column. The column was centrifuged for 60 seconds at 12000 RCF in a table-top centrifuge. The flow-through was discarded, and 700 µl wash buffer was added. The column was again centrifuged at 12000 RCF for 60 seconds, and the flow-through was discarded. The empty column was centrifuged at 12000 RCF for 60 seconds and transferred onto a 1.5 ml safe lock tube. 50 µl pre-warmed elution buffer was added to the column and incubated for 1 minute. The column was centrifuged for 60 seconds at 12000 RCF and afterward discarded. A spectrophotometer measured the purified DNA concentration.

3.2.2.5 Gibson assembly

The amount of DNA molecules in pmol must be calculated for the Gibson assembly reaction. This depends on the length (number of nucleotides) and the mass in µg of the DNA.

$$pmol\ DNA = \mu g\ DNA\ x\ \frac{pmol}{660pg}\ x\ \frac{10^6 pg}{1}\ \mu l\ x\ \frac{1}{N}$$

N is the number of nucleotides, $\frac{pmol}{660pg}$ is the avarage molecular weight of a nucleotide pair.

The calculation can quickly be done by numerous online tools provided by many companies, e.g., BioMath from Promega "https://www.promega.de/en/resources/tools/biomath/" (Accessed 28. January 2024). The Gibson assembly was performed in a PCR reaction tube according to Table 27. The best results were obtained with a ratio for backbone:insert of 1:2

Table 27 Reaction mixture of the Gibson assembly.

[1x]	Components
0.1 pmol	Insert DNA
0.05 pmol	Backbone DNA
10 µl	HiFi DNA assembly master mix
ad 20 µl	Nuclease-free water

The isothermal Gibson assembly was carried out in a PCR thermocycler in one cycle at 50°C for 30 minutes. The lid had a temperature of 52°C. Afterward, the thermocycler cooled down to 4°C for several minutes.

3.3 Vector stock generation

3.3.1 Transformation of chemically competent bacteria

For the transformation of the vector into bacteria, the NEB® 5-alpha Competent E. coli were used. The bacteria were taken from the -80°C storage (2 ml tube, 50 µl) and were thawed on ice for 10 minutes. Afterwards, 1 µl from the Gibson assembly or restriction endonuclease reaction was pipetted to the bacterial culture. The bacterial cultures were again placed on ice for 30 minutes. After incubation, the bacteria were transferred to a heat block and "heat shocked" at 42°C for 30 seconds. After that, the bacteria were again incubated on ice for 5 minutes. In the next step, 950 µl SOC medium pre-warmed at 37°C was added and placed on a heat-block (37°C) rotating at 250 rpm for 1 hour. After the incubation, 100 µl was platted on a pre-warmed lysogeny broth (LB) agar plate containing ampicillin (100 µg/ ml). The bacterial cultures were incubated for 16 - 18 hours at 37°C. Bacterial colonies, containing the desired plasmid, were transferred individually in 6 ml pre-warmed LB medium and incubated for an additional 16 - 18 hours at 37°C in a rotating wheel.

3.3.2 Analytic plasmid preparation

For the analytic plasmid preparation (mini prep), 2 ml were transferred into a 2 ml safe-lock tube and centrifuged for 5 minutes at 12.000 RCF. The supernatant was discarded, and the bacterial pellet was prepared with the QIAprep Spin Miniprep Kit from Qiagen. The pellet was resuspended in 250 µl P2 buffer. The bacteria were lysed with the addition of 250 µl P2 buffer. The 2 ml tubes were inverted five times and incubated for 5 minutes at room temperature (RT). The lysis was stopped by the addition of 350 µl N3 buffer. The lysed bacteria were centrifuged for 10 minutes at 20000 RCF. The clear supernatant was pipetted in a QIAprep spin column and centrifuged for 60 seconds at 20000 RCF. The plasmid DNA was washed in the next step by adding 750 µl PE buffer containing ethanol. The spin column was centrifuged at 20000 RCF for 60 seconds, and the flow-through was discarded. Subsequently, the spin column was transferred to a 1.5 ml safe-lock tube. To elute the plasmid DNA, 50 µl nuclease-free water was added to the center of the spin column and incubated for 1 min at RT. The spin column was centrifuged for 60 seconds at 20000 RCF and removed from the 1.5 ml safe-lock tube afterward. The eluted DNA concentration was measured by a spectrophotometer.

3.3.3 Sanger Sequencing

The purified plasmids were partially sequenced by LGC genomics using the Sanger Sequencing technique to verify the analytical plasmid preparation. Usually, only the cloning site or the position of the HBeAg mutation was sequenced. Therefore, a 1.5 ml safe-lock tube was prepared and labeled. For the sequencing, 1000 ng of plasmid was needed in a final volume of 12 µl. Additionally, 2 µl of the site-specific primer (10 µM) was added. The obtained data was analyzed with the help of Geneious Prime software.

3.3.4 Stock plasmid preparation (maxi prep)

After the plasmids were verified by sanger-sequencing, 1 ml of the remaining bacterial culture stored at 4°C was used to inoculate 300 - 600 ml of LB medium. The culture was incubated in a rotary shaker for 18 -20 hours at 37°C. The bacterial culture was centrifuged at 2800 RCF for 30 minutes at 4°C, and the supernatant was discarded. The bacterial pellet was resuspended with phosphate-buffered saline (PBS) and transferred into a 50 ml conical tube. The culture was centrifuged at 3200 RCF for 30 minutes at 4°C, and afterward, the supernatant was discarded. The pellets were stored at -20 °C or directly prepared. The PureLink Expi Endotoxin-free Maxi Plasmid Purification Kit from Invitrogen was used to purify the plasmid DNA. At first, the bacterial pellet was resuspended with 6 ml of R3 buffer. The breakdown of the bacterial cells was achieved by adding 6 ml L7 lysis buffer and incubating for 5 minutes. The lysis was stopped by adding 6 ml N3 precipitation buffer. The lysed cells were loaded onto a lysate clarification column and centrifuged at 1000 RCF for 5 minutes. The column was discarded, and

2.5 ml endotoxin removal buffer was added to the flow-through. The 50 ml conical tube was inverted ten times and loaded into a DNA-binding column. The DNA-binding column was centrifuged at 1000 RCF for 1 minute. The flow-through was discarded, and 20 ml W8 wash buffer was added to the DNA-binding column. The column containing the wash buffer was centrifuged for 1 minute at 1000 RCF and transferred to a new 50 ml conical tube. 15 ml E4 elution buffer was added to the DNA-binding column and incubated for 1 minute. Afterward, the conical tube was centrifuged for 1 minute at 1000 RCF. The DNA-binding column was discarded, and 10.5 ml ice-cold isopropanol was added to the eluate. To precipitate the DNA, the 50 ml conical tube was centrifuged at 12000 RCF for 30 minutes at 4°C. The supernatant was discarded, and the visible DNA pellet was resuspended in 70% ethanol. The DNA was again centrifuged at 3200 RCF for 30 minutes. The supernatant was discarded, and the DNA pellet was air-dryed for 15 - 30 minutes. The dry pellet was then resuspended in 200 µl TE buffer, and the concentration was determined using a spectrophotometer. The volume was adjusted to store the stock at 2 µg/µl at -20°C.

3.3.5 Nanopore Sequencing

Plasmid stock was sequenced by Nanopore sequencing to verify the plasmid and avoid mutation that may be introduced. Therefore, 1000 ng plasmid was linearized by a restriction endonuclease. All plasmids contained an Nco restriction site; 0.5 µl (1000 ng) plasmid stock was added to 43.5 µl nuclease-free water. 5 µl CutSmart buffer and 1 µl NEB Nco-I HF were added and incubated at 37°C for one hour, and the enzyme was inactivated at 80°C for 20 minutes. Yara Fröhlich or Anja Voges did the sequencing in-house. The obtained data was analyzed with the help of Geneious Prime software.

3.4 Introducing exogenous TCR in J76 mono NFκB cells by transduction

3.4.1 Generating retroviral or lentiviral particles

The cells were cultured in IMDM as described in section 3.1. The cells were seeded at $4x10^6$ cells per T75 cell culture flask in 15 ml IMDM (10% FBS, 1% Pen/Strep). Afterward, the cells were incubated overnight at 37°C and 5% CO_2. The next day, the confluency was checked under light microscopy. The confluency of the cells was aimed at 50-60 %, and the cells should stretch over the surface of the cell culture flask. Three hours before the transfection, the old medium was removed, and 9 mL of fresh medium was added to the cells. The transfection agent, Mirus TransLT1, and Opti-MEM were placed at room temperature (RT) approximately 10 – 15 minutes before the transfection. The Transfection mix was pipetted according to Table 28 (retrovirus) or Table 29 (lentivirus) in a 2 ml safe-lock tube.

Table 28 Reaction mixture for the transfection of Phoenix-GALV cells.

[1x]	Components
900 µl	Opti-MEM
5 µg	Transfer DNA (pMP71 flex with $HBc1_{8-27}$ specific TCR)

Table 29 Reaction mixture for the transfection of HEK293T cells.

[1x]	Components
900 µl	Opti-MEM
5 µg	Transfer DNA (pTwist Lenti SFFV Puro WPRE with $_{HBs370-379}$ specific TCR)
3,5 µg	Packaging plasmid pCMV8.74 (P3)
1,5 µg	Envelope plasmid pMD2.G (P4)

The transfection mix was carefully mixed by flicking the 2 ml tube and incubating for 5 minutes before adding 15 µl (retrovirus) or 30 µl (lentivirus) TransLT1. The transfection mix was incubated for 15 – 20 minutes at RT and carefully pipetted into the T75 cell culture flask. The cells were incubated at 37°C, 5% CO_2, and >80% humidity overnight. The medium was discarded the following day, and 15 ml fresh IMEM was added to the T75 cell culture flask. The cells were again incubated overnight at 37°C, 5% CO_2, and >80% humidity. Forty-eight hours after the transfection, the viral particles were harvested. Therefore, 28 cryo-vials were prepared. The cell supernatant with the viral particles was filtered through a 0.45 µm polyethersulfone (PES) or cellulose acetate filter. The cryo-viles were filled with 500 µl of the filtered supernatant and stored at -80°C until further use.

3.4.2 Transduction of J76 mono NFκB cells with retroviral or lentiviral particles

For the viral transduction of J76 mono NFκB cells 24-well non-tissue culture coated plates were treated with 400 µl RetroNectin (30 µg/ml) and incubated overnight at 4°C. The Retronectin was removed and the plate was blocked for 30 minutes ar RT with 500 µl of a 2% Human Serum Albumine in PBS solution. The blocking solution was removed and the wells of the plate were washed once with 500 µl PBS. The PBS was discarded and 250 µl lenti- or retrovirus was added per well. The 24-well plate was centrifuged at 4°C and 2000 RCF for 30 minutes. The viral supernatant was discarded and the plate was washed with 500 µl 2% human serum albumine solution. The J76 mono NFκB cells were diluted to 4x105 cells/ml and 500 µl of the cells in IMDM was pipetted into the wells. The cells were incubated over night at 37°C, 5% CO_2, and >80% humidity. The next day the the cells were transfered to a 6 well plate and the medium was exchanged. The cells were incubated at 37°C, 5% CO_2, and >80% humidity for two to three days depending on the growth of the cells. The cells were transferred to a T25 cell culture flask and the transduction effieciency was analysed by flourescence activated cell sorting (FACS).

3.4.3 Analysis of transduction efficiency in J76 mono NFκB cells

Via fluorescence-activated cell sorting (FACS), the success of the viral transduction was tested. The J76 mono NFkB wildtype cells were cultivated and analyzed with the transduced cells as a control. The staining was done by transferring 10,000 - 50,000 cells into a FACS tube. At least 1 ml FACS buffer (PBS with 2% FBS) was added to the cells. The cells were centrifuged for 5 minutes at 500 RCF and 4°C. The supernatant was discarded, and the FACS tube was shortly vortexed to resuspend the cell pellet. 100 µl eFluor 506 Viability dye (1:1000 diluted) was added to the cells and incubated for 15 minutes at 4°C. After the incubation period, 1 ml FACS buffer was added, and the cells were centrifuged at 500 RCF for 5 minutes at 4°C. The supernatant was discarded, and the FACS tube was shortly vortexed to resuspend the cell pellet. 100 µl FACS buffer containing anti-CD8-AF700 (diluted 1:100) and anti-mTCRb-APC (diluted 1:50) antibodies were used to resuspend the cells. The cells were incubated for 15 minutes at 4°C, and 1 ml FACS buffer was added afterwards. The cells were centrifuged at 500 RCF for 5 minutes at 4°C and washed twice. After the final wash step, the cells were resuspended in 100 µl FACS buffer and acquired on a Cytek Aurora or BD LSR Fortessa flow cytometer. Single stained cells were used to compensate for spectral overlay. The BD FACS Diva software automatically calculated the compensation matrix. The data was analyzed by using the FlowJo V10.9 software.

3.4.4 Magnetic activated cell sorting (MACS) of TCR positive J76 mono NFκB cells

The MACS cell separation system allowed the enrichment of the J76 mon NFκB cells containing the recombinant T-cell receptor. To separate the cells that differ only in the presence of the TCR, indirectly labeled beads targeting the APC fluorochrome on the anti-mTCRb antibody were used. At first, the cells were counted, and <107 cells were centrifuged at 300 RCF for 10 minutes. The cells were resuspended in 100 µl running buffer (500 ml PBS, 2.5 ml EDTA, and 13 ml (40g/L) human albumin) containing 2 µl anti-mTCRb antibody. The labeling with the antibody was done for 15 minutes in the dark at 4°C. The labeled cells were washed twice with 1 ml running buffer in the centrifuge for 10 minutes at 300 RCF and 4°C. The anti-APC microbeads were mixed, and 100 µl was used to resuspend the cells after the washing. Afterward, the cells and the beads were incubated for 15 minutes at 4°C. The cells were washed with 5 ml running buffer and centrifuged for 10 minutes at 300 RCF and 4°C. The cell pellet was resuspended in 500 µl running buffer.

After the cells were labeled, an LS column containing a pre-separation filter was placed in the magnet. The column was rinsed with 3 ml running buffer, and the flow-through was collected in a 15 ml conical tube. Then, the cell suspension was applied through the filter onto the column. The unlabeled cells were collected in a 15 ml conical tube. The column was rinsed three times with 3 ml running buffer. After the column reservoir was empty, the pre-separation filter was discarded, and the column was

removed from the magnets and placed onto a 15 ml conical tube. 5 ml running buffer was pipetted onto the column, and the labeled cells were flushed using the plunger.

After separation, the purity of the unlabeled and labeled fractions was analyzed by flow cytometry as described in section 3.4.3. The cells were cultured at 37°C, 5% CO2, and >80% humidity until sufficient cells were grown to be frozen and stored.

3.5 HBV cccDNA cell culture assay

3.5.1 Generation of HBV genotype A and D cccDNA

The Hepatitis B virus genome was cloned into pNL1.1-Nluc and was flanked by the restriction enzyme site C/CATGG, which can be cut with the NcoI enzyme. As the pNL1.1-Nluc plasmid backbone (3110 bp) and the HBV sequence (~3,200 bp) were of similar size, a second restriction endonuclease (NotI) was used to digest the pNL1.1-Nluc plasmid further and therefore make the extraction of the HBV genome simpler (Plasmid map provided in the Supplements). The enzymatic reaction mix was pipetted according to Table 30. Per variant, 80 µg plasmid was needed, and the plasmid stock was diluted to 2 µg/µl.

Table 30 Restriction endonuclease reaction to separate the HBV genome from the pNL1.1-Nluc vector.

Volume [1x]	Components
16 µL	NcoI-HF (20 U/µl, NEB R3193L)
16 µL	NotI-HF(20 U/µl, NEB R3189L)
40 µL	Plasmid (80 µg)
40 µL	10x CutSmart Buffer
288 µL	Nuclease-free water
400 µL	Total volume

The reaction was incubated at 37°C for three hours and heat-inactivated at 80°C for 20 minutes when not directly processed. After the enzymatic reaction, 80 µl loading dye (6x) was added, and the DNA was separated on a 0.9% agarose gel electrophoresis. The agarose was melted in 1x TRIS-Borat-EDTA buffer, and four drops of Ethidiumbromid (0.025%) were added 5 minutes after the boiling. The GeneRuler 1kb Plus DNA ladder was used as a size control. The agarose gel was run at 140 V and 400 mA for 3 hours. The band at 3200 bp containing the HBV genome was extracted from the agarose gel under UV light and transferred into several 2 ml safe-lock tubes to distribute the gel weight so it did not exceed 1 mg/2 ml safe-lock tube. Typically, twelve 2 ml safe-lock tubes were needed.

The linear DNA was extracted with the Thermofisher GenJet gel extraction Kit. The GenJet gel extraction kit was used to work with up to 1 mg of agarose gel per purification column. The agarose gel was dissolved by adding 1:1 volume to weight binding buffer and incubation on a shaking heat block at 56°C, 1000 rpm for up to 5 minutes or when the gel was completely dissolved. 800 µl dissolved agarose gel was transferred to a purification column and centrifuged for 1 min at 16000 RCF. The flow-through was discarded, and the column was refilled with dissolved agarose gel and centrifuged. This was repeated until the whole volume was loaded onto a column. The flow-through was discarded, and 700 µl wash buffer was added. The column was again centrifuged at 16000 RCF for 60 seconds, and the flow-through was discarded. The empty column was centrifuged at 16000 RCF for 60 seconds to remove residual wash buffer and transferred onto a 1.5 ml safe lock tube. 50 µl pre-warmed elution buffer was added to the column and incubated for 1 minute. The column was centrifuged for 60 seconds at 12000 RCF and afterward discarded. The eluate of all the columns were pooled, and a spectrophotometer measured the purified DNA concentration.

To form the viral cccDNA, single strands of the HBV genome were ligated. The ligation reaction was diluted to prevent excessive ligation of two or more DNA fragments so that the DNA concentration did not exceed 2 ng/µl. The DNA ligation mixture was prepared according to Table 31.

Table 31 Ligation of the HBV genome to form the cccDNA.

Volume [1x]	Components
2000 µL	T4 Ligase Buffer 10x
X	Linear HBV (< 30.000 ng)
250 µL	T4 Ligase (Cat. No. M0202L, NEB)
Up to 20 mL	Nuclease-free water
20 mL	Total Volume

The DNA ligation was done for one hour at room temperature, and the subsequent concentration of the cccDNA was immediately carried on afterward. To concentrate the cccDNA, the Thermofisher GenJet PCR clean-up Kit was used in combination with a Vac-Man Vacuum manifold. Four clean-up columns were used per DNA ligation mix (20 ml). As the columns can only carry 800 µl liquid, the columns were connected to column extension tubes, allowing the column to carry 20 ml liquid. The columns were connected to the vacuum manifold. The 20 ml DNA ligation mix was combined with 20 ml binding buffer and shortly inverted. In each column, 10 ml of the mixture was added, and the vacuum was applied. After the columns were dry, the extenders were removed, and the column was loaded with 800 µl wash buffer. The vacuum was applied, and after the wash buffer passed through,

the columns were removed from the vacuum manifold and placed into 2 ml tubes. The columns were centrifuged for 1 minute at 16000 RCF to remove residual wash buffer and placed in a 1.5 ml safe-lock tube. The cccDNA was then eluted in 53 µl elution buffer (10 mM Tris-HCl, ph 8.5). The columns were centrifuged, and the eluted 53 µl was used to elute a second column.

A T5 exonuclease reaction was performed to remove linear HBV genomes. The T5 exonuclease reaction mix was pipetted according to Table 32.

Table 32 T5 Exonuclease reaction to remove linear HBV genomes.

Volumes [1x]	Components
6 µl	Buffer 10x (Buffer 4)
53 µL	DNA from the T4 ligase reaction
1 µl	T5 Exonuclease (Cat. No. M0663S, NEB)
60 µL	Total Volume

The enzymatic reaction was incubated for one hour at 37°C, and 12 µl loading dye (6x) was added to stop the reaction. The cccDNA was applied to a 0.9% agarose gel to separate single HBV genome cccDNA from circular DNA containing two or more HBV genomes. The agarose gel electrophoresis ran for two hours at 120V and 400 mM. Afterward the single genome cccDNA was excised from the agarose gel under the UV light. The cccDNA band was due to the supercoiling located at size location or 2100 bp. The cccDNA was purified via the Thermo Scientific GenJet gel extraction kit similar in precedure as meantioned above. The cccDNA was eluted in 60 µl and the elutant was used for several columns. The cccDNA concentration was determined via spectrophotometer and stored at -20°C till futher use.

3.5.2 Transfecting HepG2-hNTCP cells with HBV cccDNA

Before transfection of HepG2-hNTCP cells with the cccDNA, a specific assay medium had to be prepared. The medium consisted of DMEM with 2% FBS, 4% PEG-8000, and 2% DMSO. This medium composition allowed the reinfecting of HepG2-hNTCP from formed HBV virus particles [88]. In later experiments, this was abandoned as it introduced more disadvantages than advantages, and the J76 mono NFkB cells reacted sensitively to PEG-8000 and DMSO. At the same time as the change away from the assay-specific medium, the cells were also switched from DMEM to IMDM, which had no consequences for the HepG2-hNTCP cells but was required for the J76 mono NFkB cells.

The HepG2-hNTCP cells were cultured in a T75 cell culture flask as described in section 3.1.2. For the cccDNA assay, the cells were washed twice with a sufficient amount of PBS and detached from the flask with TrypLE. The cells were counted in a Neubauer chamber, and 100.000 HepG2-hNTCP cells/ml were

pipetted into a collagen I treated 24-well plate plate (1 ml/well). The cells were incubated overnight at 37°C 5% CO_2 and >80% humidity.

The next step was only done when using an assay-specific medium. When IMDM was used, the next step was the transfection of the cells. The next day, the cell attachment was monitored under the microscope, and the medium was removed. The cells were washed twice with 500 µl PBS, and 500 µl assay-specific medium was added. The cells were incubated overnight at 37°C, 5% CO_2 and >80% humidity.

Two to three hours before the transfection, the old medium was exchanged for 500 µl fresh medium. The transfection agent, Mirus TransLT1, and Opti-MEM were placed at room temperature (RT) approximately 10 – 15 minutes before the transfection. The Transfection mix was pipetted according to Table 33 in a 2 ml safe-lock tube. The transfection mix was prepared according to the wells needed.

Table 33 Reaction mixture for one well for the transfection of HepG2-hNTCP cells with HBV cccDNA.

Per well	Components
Up to 50 µl	Opti-MEM
500 ng	cccDNA

After an incubation of 5 minutes at room temperature, Mirus TransLT1 reagent (2.5 µl TransLT1/ µg DNA) was added to the mixture and gently mixed by pipetting. The reaction was incubated for 30 minutes at room temperature, and 50 µl/well were pipetted dropwise onto the cells. The 24-well plate containing the transfected cells was gently swayed and incubated at 37°C 5% CO_2 and >80% humidity overnight. The next day, 500 µl fresh medium was added to each well. The cells were incubated till the HBV markers, the core staining assay, or the J76 mono NFκB experiments were done.

3.5.3 Detection of HBeAg and HBsAg

After the HepG2-hNTCP cells were transfected with HBV cccDNA, the HBeAg and HBsAg were measured from the supernatant. This was done by removing the supernatant from the well and pipetting it into a 2 ml safe-lock tube. HBeAg and HBsAg were measured on the Abbott Architect i2000 immunoassay analyzer, Abbott HBeAg, and HBsAg reaction kits. The supernatant was pipetted into a 5 ml sample tube and loaded onto the immunoassay via a sample rack. The obtained data was a signal-to-cutoff ratio (S/CO) calculated from the internal standard in the reaction kit. The data was analyzed and visualized with Microsoft Excel and GraphPad Prism 10 software.

3.6 HBV core protein and HLA class I molecule staining

After the transfection of the HepG2-hNTCP cells with the HBV cccDNA or in the HepG2-P151/152 cells, the HBV core protein was stained from cells cultured in collagen-I coated 24-well plates. For the cccDNA experiments, the staining was done four days after transfection. The cells were washed twice with 500 µl PBS and incubated for 5 minutes with 100 µl Accutase to detach them. The reaction was stopped by adding 400 µl FACS buffer (PBS, 2% FBS), and the cell suspension was transferred to a FACS tube. The cells were centrifuged and resuspended in FACS buffer twice for 5 minutes at 500 RCF. A 1:1000 viability dye eFluor 506 dilution was prepared in FACS buffer, and the cells were resuspended in 100 µl of the prepared viability dye solution. The cell suspension was labeled for 15 minutes in the dark at 4°C. Afterward, 500 µl FACS buffer was added, and the cell suspension was centrifuged at 500 RCF for 5 minutes.

For HLA class I molecule staining a 1:100 dilution of the anti-HLA-ABC APC antibody was prepared in FACS buffer. The cells were resuspended in 100 µl antibody solution and incubated for 15 minutes in the dark at 4°C. Afterward, 500 µl FACS buffer was added, and the cell suspension was centrifuged at 500 RCF for 5 minutes. After the viability or HLA class I molecule staining, the cells were resuspended in 100 µl IC Fixation buffer and incubated for 20 minutes at 4 °C in the dark. After the incubation, 400 µl permeabilization (perm) buffer (1x) was added, and the cell suspension was centrifuged at 500 RCF for 5 minutes. This step was performed once more, and afterward, the cells were resuspended in 100 µl perm buffer containing 1:50 diluted anti-HBVcore antibody. The intracellular staining was incubated in the dark for 30 minutes at 4°C. 400 µl perm buffer was added, and the cells were centrifuged at 500 RCF for 5 minutes. The cells were resuspended in 100 µl perm buffer containing 1:500 anti-mouse IgG secondary antibody and incubated for 15 minutes at 4°C in the dark. After the incubation, 400 µl perm buffer was added, and the cells were centrifuged at 500 RCF for 5 minutes. This washing step was repeated twice. After washing, the cells were resuspended in 100 µl FACS buffer and acquired on a BD LSR Fortessa flow cytometer. Single stained cells were used to compensate for spectral overlay. The BD FACS Diva software automatically calculated the compensation matrix. The data was analyzed by using the FlowJo V10.9 software.

3.7 T-cell receptor activation assay

The T-cell receptor (TCR) activation assay was performed with J76 mono NFκB cells containing an HBc18-27 specific or HBs370-379 specific TCR. The J76 mono NFκB cells were co-cultured with HepG2-P151/P152 expressing the HBV core protein, or HepG2-hNTCP cells transfected with HBV cccDNA (section 3.5.2). The HepG2 derivates were cultured with 100.000 cells/well in a collagen-I coated 24-well plate for co-culturing. For the experiments involving the HepG2-hNTCP cells, the J76 mono NFκB cells were added on the evening of the third day after the transfection with the HBV cccDNA. Therefore,

the culture medium from the HepG2 cells was removed and replaced with 1 ml fresh IMDM containing 100.000 J76 mono NFκB cells. Each experimental setup contained untransfected HepG2-hNTCP cells co-cultured with the J76 mono NFκB cells as a negative control. HepG2-hNTCP cells loaded with one µg of the corresponding peptide were used as a positive control. The cells were co-cultured for 16 hours at 37°C, 5% CO_2 and >80% humidity. The staining was handled on ice or at 4°C. The supernatant was transferred into FACS tubes, and the wells were washed twice with PBS. The supernatant from the washing steps was transferred into the FACS tubes. The J76 mono NFκB cells are firmly attached; therefore, all cells were treated with 100 µl Accutase to detech every cell. The cells were incubated for 10 minutes and resuspended in 400 µl FACS buffer. The cells were transferred into the FACS tubes. The tubes were then centrifuged at 300 RCF for 10 minutes, and the cells were resuspended in 100 µl FACS buffer and transferred into a 96-well U-bottom plate. 150 µl FACS buffer was added, and the cells were centrifuged at 300 RCF for 10 minutes. The supernatant was discarded, and the 96-well plate was shortly vortexed to resuspend the cell pellet. 100 µl eFluor 506 Viability dye (1:1000 diluted) was added to the cells and incubated for 15 minutes at 4°C. After incubation, 150 µl FACS buffer was added, and the cells were centrifuged at 500 RCF for 10 minutes at 4°C. The supernatant was discarded, and the 96-well plate was shortly vortexed to resuspend the cell pellet. 100 µl FACS buffer containing anti-CD8-AF700 (diluted 1:100) and anti-mTCRb-APC (diluted 1:50) antibodies were used to resuspend the cells. The cells were incubated for 15 minutes at 4°C, and 150 µl FACS buffer was added afterwards. The cells were centrifuged at 500 RCF for 5 minutes at 4°C and washed twice. After the final wash step, the cells were resuspended in 100 µl FACS buffer and acquired on a BD LSR Fortessa flow cytometer. Single stained cells were used to compensate for spectral overlay. The BD FACS Diva software automatically calculated the compensation matrix. The data was analyzed by using the FlowJo V10.9 software.

3.8 Statistical analysis

The data was analyzed and visualized with the help of GraphPad Prism 10 software. The Shapiro-Wilk test was used to test the data for normal distribution. The Grubbs test identified outliers. For the statistical analysis of the data, an unpaired two-tailed Student's t-test was used to compare two separate groups, and a one-way analysis of variance was used when comparing three or more separate groups. The corresponding statistical test was used for each experiment, as indicated in the figure legends. A p-value of ≤ 0.05 was considered statistically significant.

4 Results

4.1 HBV precore variants in the Duesseldorf cohort

The precore mRNA translates into the precore protein, which comprises the initial 149 amino acids of the core protein sequence and a 29 amino acid N-terminal extension. Part of the N-terminal extension is a signal peptide that targets the precore protein to the endoplasmic reticulum. This allows the subsequent processing and secretion of HBeAg in high amounts from the infected cells.

HBeAg positivity is associated with elevated serum HBV DNA levels and increased infectiousness [169]. During acute infection, HBeAg is the first serological marker to undergo a seroconversion, indicating the next step, an HBsAg seroconversion, and eventually the viral clearance. In a chronic HBV infection, the HBeAg seroconversion may occur only after years or even decades. Nevertheless, the loss of HBeAg during chronic infection is used to help categorize the different stages of a chronic HBV infection. Loss of HBeAg marks the passage from the second phase, HBeAg-positive chronic hepatitis, to the third phase, the HBeAg-negative chronic infection. The second phase is often called an immune-active phase, with fluctuating ALT levels as its hallmark. It is believed that a T cell-mediated immune response to infected cells leads to fluctuating ALT levels and a decrease in HBV DNA levels [169]. The third phase is often called the inactive hepatitis phase, with undetectable or low HBV DNA levels and normal ALT levels.

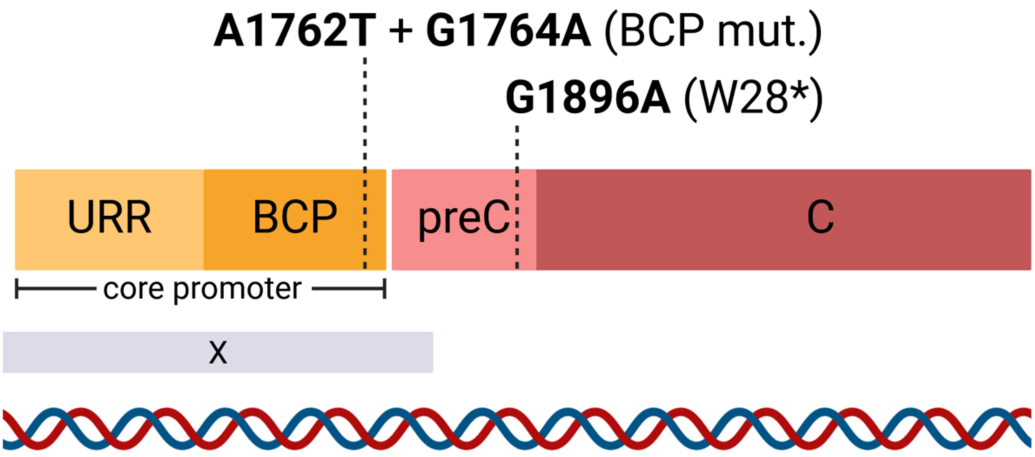

Figure 9 Graphical representation of the viral core promoter and the preC/C open reading frame with mutations altering HBeAg secretion: In yellow, the core promoter contains the upper regulatory region (URR) and the basal core promoter region (BCP). In the BCP region, an HBeAg-altering double mutation can be found at the nucleotide positions G1764A and A1762T. This combination of the two nucleotide mutations is called the BCP double mutation (BCP mut.). Another HBeAg altering mutation can be found at the end of the preC (light red) at nucleotide position 1896. The exchange from guanine to adenine results in a premature translation stop. The X ORF is represented in purple. The double-strand DNA of the cccDNA is represented in blue and red. The graphical representation was created with BioRender.com

Comparing the viral sequences found in the first two phases with the ones in the last two phases, it becomes clear that upon transition from an HBeAg seropostive to an HBeAg seronegative state, mutations associated with altered HBeAg secretion are selected in the viral quasispecies (Figure 9). The mutation at nucleotide position 1896 exchanges guanine for an adenine, resulting in a stop codon at position 28 of the precore reading frame [170,171]. Another prominent HBeAg-altering mutation is a double mutation in the basal core promoter (BCP), which is responsible for the expression of the precore and pregenomic RNA. Viral variants containing G1764A and A1762T mutations still express HBeAg but at reduced levels [172–174].

In this chapter, I analyzed the distribution of HBeAg-altering mutations in the Duesseldorf HBV cohort. This multi-center cohort comprised 544 patients with various diagnostic and sequence information which were generated by Tatjana Schwarz during her PhD studies [175] and can be obtained in GenBank with the Asccession numbers MW845286-MW845312, MW887641-MW887652, MW926548-MW926566, MZ043025-MZ043097, MZ097624-MZ097884.

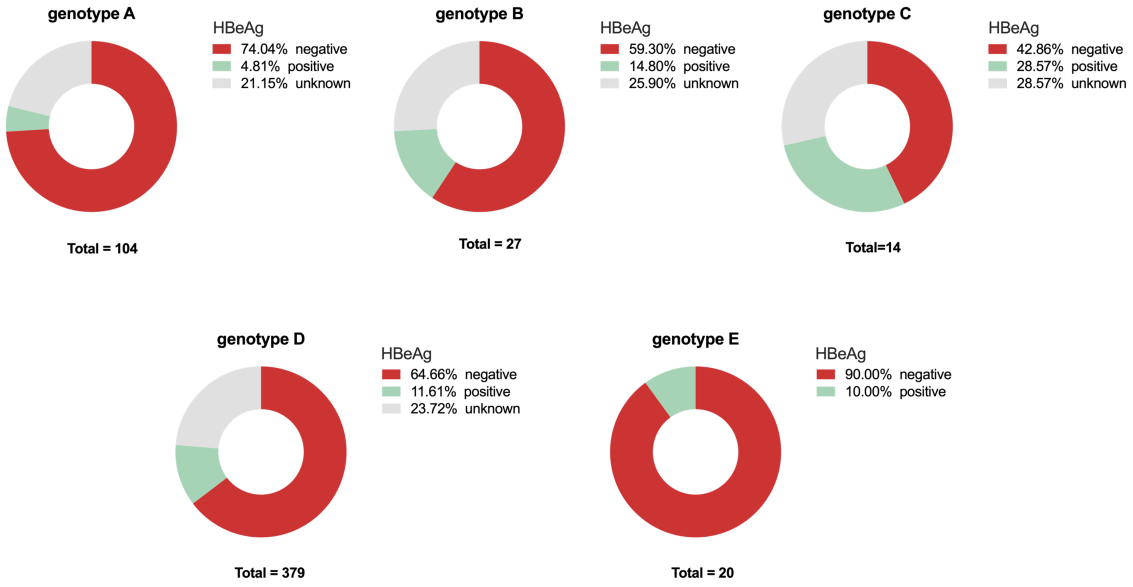

Figure 10 HBeAg status grouped by genotype A-E: The genotypes were partitioned into HBeAg negative (Red), HBeAg positive (green), and HBeAg status unknown (gray). The percentage (%) is given in the legend, and the total number of patients is listed below the diagram.

The frequency of the HBeAg-positive and HBeAg-negative infections for each genotype (Figure 10) was assessed. Due to the geographical distributions of the HBV genotypes, the Dusseldorf cohort, consisting mainly of German patients, includes 104 genotype A and 379 genotype D sequences. The distribution of HBeAg-positive and HBeAg-negative infections was similar across the genotypes. The cohort primarily comprises HBeAg-negative infections, ranging from 42.86% in genotype C to 90% in genotype E. The high proportion of HBeAg-negative patients in the cohort can be attributed in part to the age of

the patients (mean: 41 years). Additionally, the proportion of the rate of unknown HBeAg status was similar for each genotype, ranging from 21.15% to 28.57%. Genotype E was the only exception where HBeAg-status was known for each patient. Patients with an unknown HBeAg status were excluded from further analysis concerning the HBeAg variability or distribution of the different HBeAg-altering mutations.

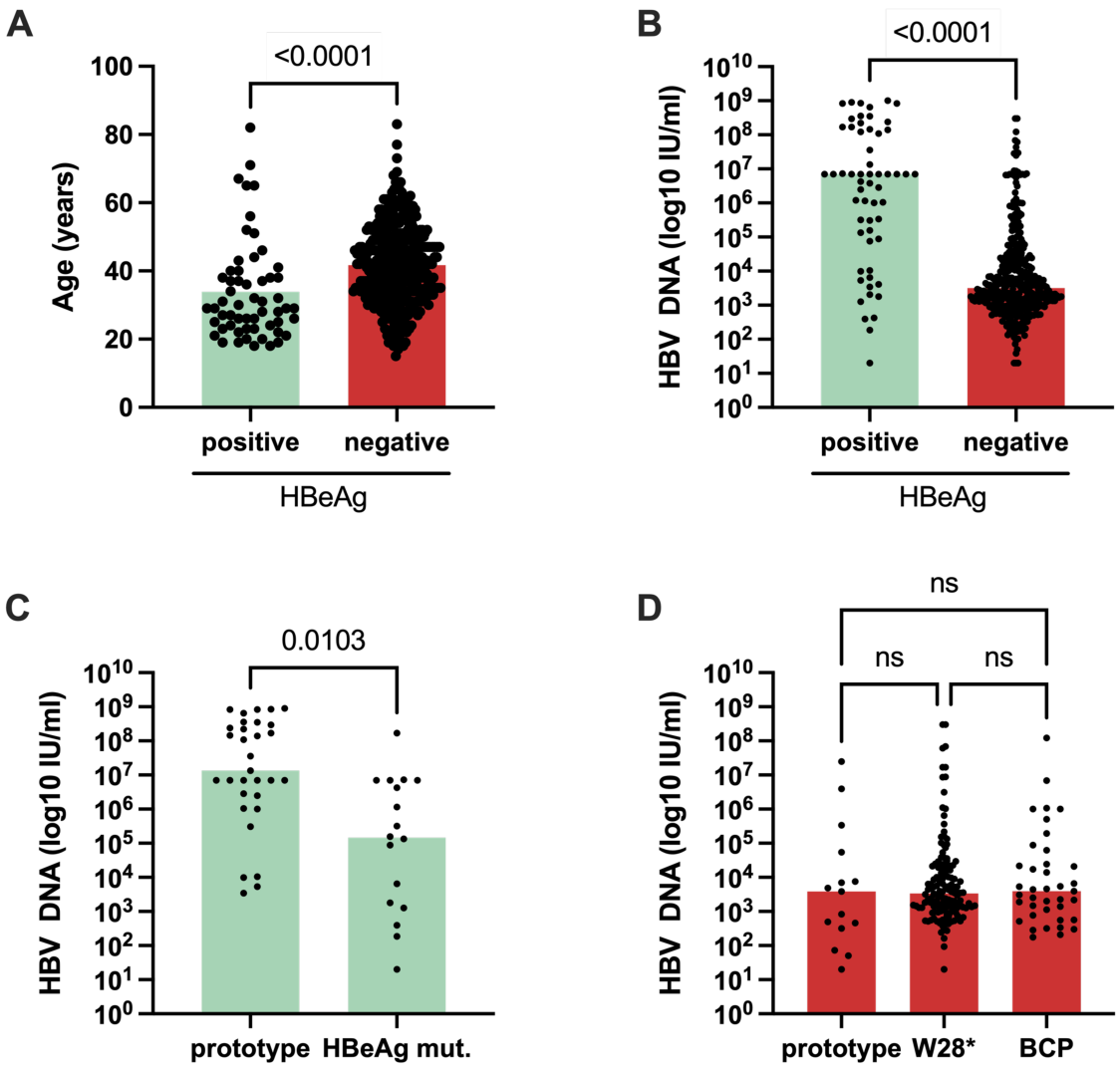

Figure 11 Age and viral load distribution between HBeAg-positive and HBeAg-negative patients: A) The age at sample date was plotted for HBeAg-positive (green) and HBeAg-negative (red) patients. B) HBV DNA levels in International Units (IU)/ml on a logarithmic scale (log10) between HBeAg-positive (green) and HBeAg-negative (red) patients. C) HBV DNA levels in IU/ml on a logarithmic scale for HBeAg-positive (green) patients divided between precore prototype sequences and sequences containing the BCP double mutation, the W28* mutation, or a combination of both. D) HBV DNA levels in IU/ml on a logarithmic scale for HBeAg-negative (red) patients divided between precore prototype sequences, sequences containing the W28* mutation, and sequences containing the BCP double mutation. Sequences containing both mutations were assigned in the W28* group. Statistical significance was calculated using an unpaired two-tailed Student's t-test to compare two groups and a one-way analysis of variance to compare three groups.

After understanding that the largest part of infections in the Dusseldorf cohort were HBeAg-negative, the age distribution between HBeAg-positive and HBeAg-negative infections was examined. HBeAg-positive HBV-infected patients are significantly ($p < 0.0001$) younger than HBeAg-negative HBV-infected patients in the cohort (Figure 11 A). This data is essential as it demonstrates the connection between age and the HBeAg status and partly explains the high proportion of HBeAg-negative patients in the cohort. Inversed to the age but in line with the chronic stage, patients with an HBeAg-positive HBV infection exhibited a significantly higher viral load ($p < 0.0001$) compared to HBeAg-negative HBV-infected patients in the cohort (Figure 11 B). This data aligns with the classification of HBV chronic stages and demonstrates the drastic change in viral load between HBeAg-positive and HBeAg-negative patients.

It is worth noting that mutations affecting the HBeAg could be observed in patients who tested positive for HBeAg. Most of these mutations involve the BCP mutation in either single or double configuration but can also include the W28* mutation. A statistically significant reduction in HBV DNA ($p = 0.0103$) was observed in these patients compared to those without an HBeAg-altering mutation (Figure 11 C). This is important as it suggests that the accumulation of HBeAg-altering mutations is not sudden but indicates a hidden conflict between the virus and the immune system. In this process, over time, the virus could possibly gain an advantage by losing HBeAg. On the other hand, no significant differences between the variants could be discerned in HBeAg-negative infected patients (Figure 11 D). This indicates that the HBeAg-altering mutations did not differ in their impact on the viral load and that other circumstances, like the number of accumulated mutations in the virus or an immune pressure, could be responsible for the loss of replication fitness.

4.1.1 Frequency of HBV precore variants in the Duesseldorf cohort

A comprehensive analysis of the different HBeAg-altering mutations in different genotypes was performed (Figure 12, Table 34). The analysis included all HBV sequences from the Duesseldorf cohort with known HBeAg status. The analysis aimed to establish an understanding of the frequency and diversity of HBeAg-altering mutations. Besides the two well-known HBeAg altering mutations (A1762T + G1764A & G1896A), different precore start codon mutations were detected. The mutations were at positions 1814, 1815, and 1816, resulting in the loss of the typical start codon AUG.

Mutations in the BCP region were only considered in the analysis when they occurred as the previously described double mutation (A1762T + G1764A). Other variants at the two nucleotide positions were not counted. The different precore start codon mutations were grouped in the analysis to simplify the graphs.

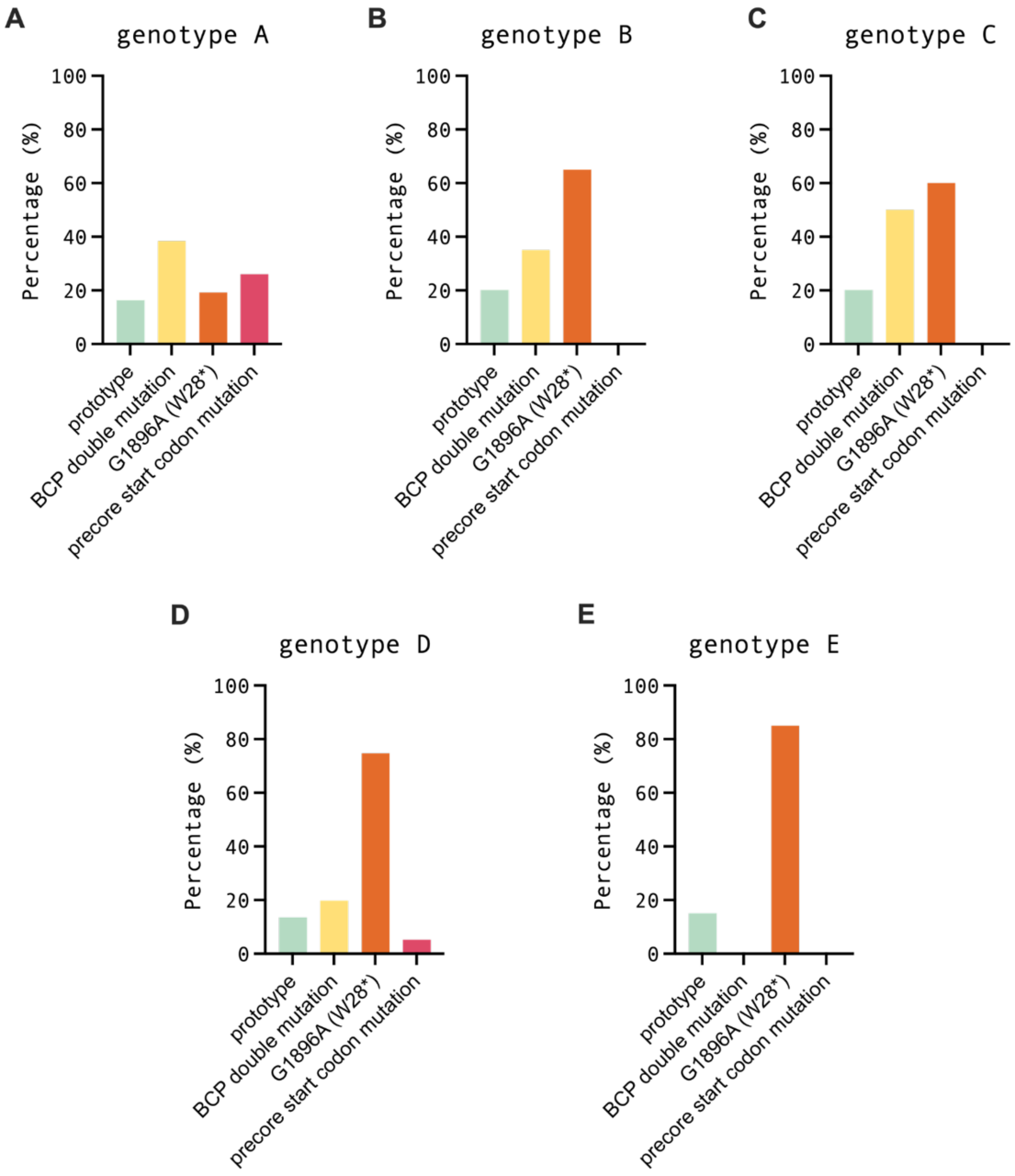

Figure 12 Distribution of HBeAg variants in genotype A-E: The percentage of the four different HBeAg variants for each genotype was plotted in columns. The prototype variant (light green) consists of no mutation at nucleotide position 1762 (BCP), 1764 (BCP), 1814 – 1816 (start codon), and 1896. The BCP double mutation (yellow) only contains the variants with an A1762T and G1764A mutation. The G1896A (W28*) mutation (orange) only includes sequences with the G1896A mutation. The precore start codon mutation variant (pink) has any mutation at position 1814 – 1816.

In patients with an HBV genotype A infection (Figure 12 A), the most common HBeAg variant involved the BCP double mutation (38.4%). The prototype (16.4%) variant and the W28* mutation (19.2%) variant were distributed similarly in genotype A. Apart from the BCP double mutation, the precore start codon mutation was highly prevalent in genotype A (26.0%). In contrast, it was absent in genotype B, C, and E sequences and only played a minor role in genotype D (5.2%) sequences (Figure 12 B-E).

In genotypes B, C, D, and E, the W28* mutation was the most common HBeAg-altering mutation. Whereas in genotypes D and E, the W28* mutation dominated the viral sequences, the BCP double mutation was much more common in genotypes B and C sequences. It is worth noting that although there were only a few genotype E sequences, they all exclusively contained either the HBeAg prototype variant or the W28* mutation variant, with no BCP double mutation or the Start codon mutation detected. Genotypes B and C were similarly prevalent to genotype E in the cohort. However, the BCP double mutation could be detected in both genotypes, excluding the size as a possible explanation. This data demonstrates that the genotypes differ in their distribution of HBeAg-altering mutation.

During the analysis, it became clear that many sequences did not exclusively possess single mutations but a combination of the HBeAg-altering mutations. Therefore, a more specific analysis was carried out. The trough analysis was limited to genotypes A and D. Genotypes B, C, and E were excluded due to the small numbers of sequence data available. Genotype A and D were further divided into HBeAg positive (HBeAg +) and HBeAg-negative (HBeAg -). Sequencing data was available for 43 HBeAg positive and 245 HBeAg negative variants for patients infected with genotype D.

HBeAg-positive genotype D sequences exhibited predominantly prototype variants (65.1 %) at the defined nucleotide positions, as displayed in Table 34. Consistent with expectations, single nucleotide mutations in the Basal core promoter region could be detected in a subset of the sequences (16.3 %). Additionally, the HBeAg altering BCP double mutation was detected in 11.6 % of HBeAg-positive sequences. Interestingly, the W28* mutation, while not unprecedented in other cohorts, was detected in several HBeAg-positive sequences. Although the underlying reasons remain unknown, potential explanations will be explored later during the discussion. No precore start codon mutations were detected in the HBeAg-positive sequences. The genotype A sequences from HBeAg-positive patients presented a comparable pattern to the genotype D sequences, with the caveat that only five sequences were available for analysis. As anticipated, the prototype variant was predominantly observed in most sequences.

The investigation into HBeAg-negative sequences revealed a more complex image. In most HBeAg-negative genotype D and A sequences, at least one of the three HBeAg-altering mutations could be detected. However, a small percentage of genotype D (4.5%) and A (16.4%) sequences lacked a nucleotide mutation at the two BCP positions, the precore start codon nucleotides, or the position responsible for the W28* mutation. Similar to the occurrence of HBeAg-altering mutations in HBeAg-positive sequences, prototype variants in sequences from HBeAg-negative patients can not be explained entirely. Unknown substitutions or an accumulation of different mutations affecting replication may be responsible for the loss of HBeAg in these variants. In the examination of HBeAg-negative sequences, distinctions in the distribution of HBeAg-altering mutations between genotypes A

and D could be observed. Specifically, the W28* mutation appeared as the most prevalent variant in genotype D sequences, detected in 47.3% of sequences, compared to just 12.9% in genotype A sequences. This suggests a preference for the W28* mutation in genotype D. Conversely, the BCP double mutation emerged as the predominant HBeAg-altering mutation in genotype A, appearing in 32.8% of sequences, as opposed to just 11.6% in genotype D sequences. Furthermore, the start codon mutation variants were notably frequent in genotype A (21.8%) but relatively rare in genotype D (2.4%), similar to the BCP double mutation.

Table 34 HBeAg altering mutations in genotype A and D

BCP		precore start codon			W28	genotype D				genotype A			
1762	1764	1814	1815	1816	1896	HBeAg +		HBeAg-		HBeAg +		HBeAg-	
A	G	A	T	G	G	n (43)	%	n (245)	%	n (5)	%	n (73)	%
.	.	.	.	.	.	28	65.1	11	4.5	4	80.0	12	16.4
T	.	.	.	.	A	0	0.0	3	1.2	0	0.0	1	1.4
T	A	.	.	.	A	2	4.7	42	17.1	0	0.0	2	2.7
T	R	.	.	.	A	0	0.0	2	0.8	0	0.0	0	0.0
T	T	C	.	.	A	0	0.0	1	0.4	0	0.0	0	0.0
G	.	.	.	.	A	0	0.0	2	0.8	0	0.0	0	0.0
G	C	.	.	.	A	0	0.0	2	0.8	0	0.0	0	0,0
C	T	.	.	.	A	0	0.0	1	0.4	0	0.0	0	0.0
.	.	.	.	.	A	1	2.3	116	47.3	0	0.0	10	12.9
.	.	C	.	.	A	0	0.0	1	0.4	0	0.0	0	0.0
.	.	M	.	.	A	0	0.0	0	0.0	0	0.0	0	0.0
.	.	T	.	.	A	0	0.0	1	0.4	0	0.0	0	0.0
.	A	.	.	.	A	2	4.7	18	7.3	0	0.0	1	1.4
.	A	.	.	T	A	0	0.0	2	0.8	0	0.0	0	0.0
.	C	.	.	.	A	0	0.0	1	0.4	0	0.0	0	0.0
.	R	.	.	.	A	0	0.0	4	1.6	0	0.0	0	0.0
.	T	.	.	.	A	2	4.7	20	8.2	0	0.0	0	0.0
T	.	.	.	.	.	1	2.3	0	0.0	0	0.0	0	0.0
T	A	.	.	.	.	5	11.6	7	2.9	1	20.0	24	32.8
T	A	.	.	T	.	0	0.0	1	0.4	0	0.0	1	1.4
T	A	C	.	.	.	0	0.0	0	0.0	0	0.0	3	4.1
.	.	.	.	T	.	0	0.0	4	1.6	0	0.0	1	1.4
.	.	.	A	.	.	0	0.0	0	0.0	0	0.0	1	1.4
.	.	.	C	.	.	0	0.0	0	0.0	0	0.0	2	2.6
.	.	C	.	.	.	0	0.0	2	0.8	0	0.0	10	13.7
.	.	T	.	.	.	0	0.0	0	0.0	0	0.0	2	2.7
.	A	.	.	.	.	0	0.0	0	0.0	0	0.0	3	4.1
.	A	.	.	T	.	0	0.0	1	0.4	0	0.0	0	0.0
.	A	C	.	.	.	0	0.0	1	0.4	0	0.0	0	0.0
.	R	.	.	.	.	1	2.3	0	0.0	0	0.0	0	0.0
.	T	.	.	.	.	1	2,3	1	0.4	0	0.0	0	0.0
.	T	.	C	.	.	0	0.0	1	0.4	0	0.0	0	0.0

After examining the frequency of the individual mutations, the frequency of combinations of the mutations at the specified nucleotide positions was examined. Given that the W28* mutation was the most prevalent variant in HBeAg-negative genotype D sequences, observing its combinations with other mutations was not surprising. In genotype D sequences, it was frequently found with the BCP double mutation (17.1%) or BCP single nucleotide mutations (22.3%). However, this combination was less common in genotype A (5.5%). In genotype D, a combination of a precore start codon mutation with the W28* mutation was rare (2%) and nonexistent in genotype A, which is notable considering that the precore start codon variants were more frequent in this genotype. The combination of BCP with a start codon mutation was infrequently detected in genotype D (1.2%) or genotype A (5.5%).

In the Duesseldorf cohort, the HBV genotype D exhibited a high level of homogeneity in developing HBeAg-altering mutations, with a preference for the W28* stop mutation. On the other hand, genotype A sequences showed more heterogeneity with regard to HBeAg-altering mutations. The BCP double mutation was the most common HBeAg-altering mutation, followed by the start codon mutation. Although the variability of HBeAg-altering mutations in genotype D was more homogenous, sequences from this genotype more often possessed combinations of mutations compared to genotype A sequences.

4.1.2 Distribution of the 1858 nucleotide variants in genotype A and D

Next, the analysis focused on the distribution of thymine (T) or cytosine (C) at the nucleotide position 1858 in genotypes A and D. It is believed that the substitution of guanine with adenine at position 1896 (G1896A, W28* mutation) prohibits the formation of the epsilon structure of the pregenomic RNA in sequences containing a cytosine at position 1958 [66,176].

It is considered that the occurrence of thymine or cytosine at position 1858 is associated with the HBV genotype. In the Duesseldorf cohort, all HBeAg-negative genotype D sequences contain thymine at this position. In contrast, the majority (79.22%, n = 61) of genotype A sequences have cytosine at the same position (Figure 13 A). However, thymine was still detected in 20.78% (n = 16) of genotype A sequences at the specified position.

Subsequently, the HBeAg-negative genotype A sequences were further examined for the W28* mutation and the nucleotide choice at position 1858. All genotype A sequences with a W28* mutation (n = 14) also had thymine at nucleotide position 1858 (Figure 13 B). In contrast, in genotype A sequences where other HBeAg-altering mutations were detected, the majority (96.61%, n = 57) had cytosine, and only 3.39% (n = 2) contained thymine at this position.

The analysis revealed that most genotype A sequences contained a cytosine at nucleotide position 1858. Still, thymine was also present at that position in some genotype A sequences. In contrast, genotype D sequences showed a substantial preservation of thymine at nucleotide position 1858. Indeed, this indicates a genotype-distinctive preference for a specific nucleotide at position 1858. Furthermore, when comparing genotype A sequences that contained the W28* mutation to those that did not, a correlation was found between the HBeAg mutation and the nucleotide selection at position 1858. Implying that the nucleotide at position 1858 may influence the selection of HBeAg-altering mutations and could potentially account for the heterogeneous emergence of HBeAg-altering mutations in genotype A.

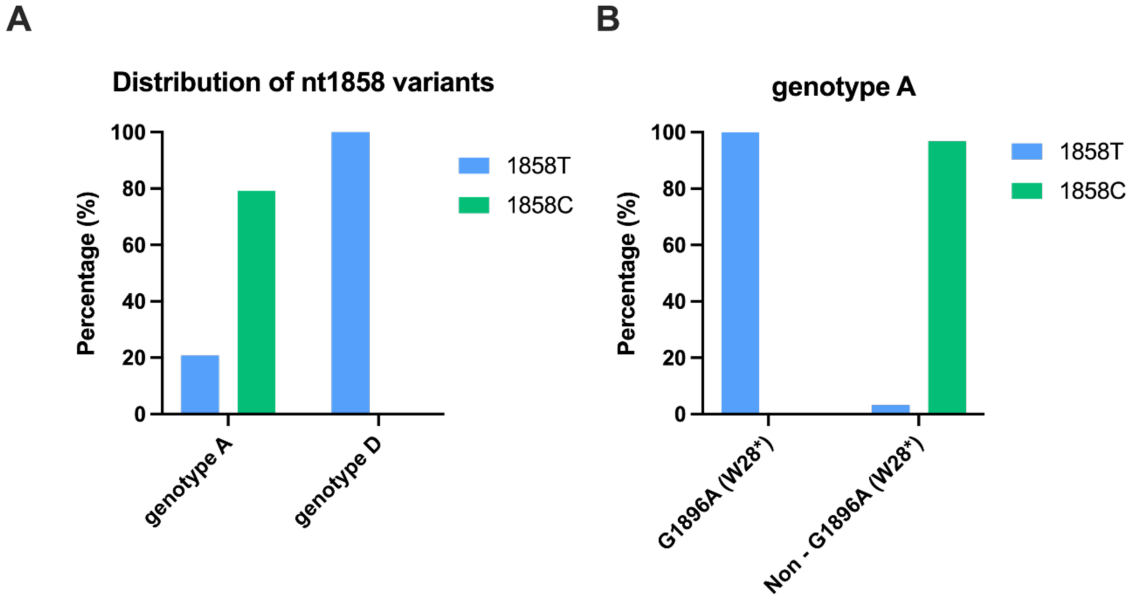

Figure 13 Frequency of the 1858 nucleotide variants in genotype A and D: A) Frequency of the 1858T (blue) and 1858C (green) variant in genotype A and D. B) Percentage of genotype A HBeAg negative sequences that harbor the 1858T (blue) or 1858C (green) variant in sequences that have the G1896A mutation versus sequences that have other HBeAg altering mutations (BCP double mutation, Start codon mutation).

4.2 Establishing an HBV cell culture assay

Hepatitis B virus exclusively infects human hepatocytes [13]. Chimpanzees are the only immune-competent animal model and were crucial for developing HBV vaccines [177]. However, ethical considerations have prohibited using chimpanzees in research in the European Union and the United States of America. The available cell culture systems have different disadvantages and often cannot sustain full viral replication [74,178,179]. One way around this is to integrate the viral genome into the cell line and couple it with a strong promoter. This system enabled the investigation of some elements of viral replication and generated high viral titers for reinfection in hepatoma cell lines. One drawback of the integration is that comparing variants with slight variations is time-consuming, as a stable cell line must be generated for each variant. Instead of infecting the cells with viral particles, a new

approach involved using viral covalently closed circular DNA (cccDNA), which resembles a small plasmid, to transfect the cells. Most cccDNA transfection systems use components like Cre/loxP systems or attA/attB endonuclease, which introduce small artificial sites in the genome [180,181].
One objective of this project was to develop a cccDNA system devoid of artificial elements while allowing for a fast generation of specific variants.

4.2.1 Generating the HBV cccDNA via ligation

Tatjana Schwarz established a protocol for amplifying the whole HBV genome that is suitable for sequencing. The system generates two overlapping amplicons, "core" and "polymerase". Initially, the intention was to utilize the system to amplify specific HBV isolates and create the cccDNA by combining the two fragments using Gibson assembly. While it was possible to generate the HBV cccDNA from isolates through PCR amplification and subsequent Gibson assembly, it was only possible in small quantities. This was insufficient to yield the amount of cccDNA needed for transfection and was therefore abandoned.

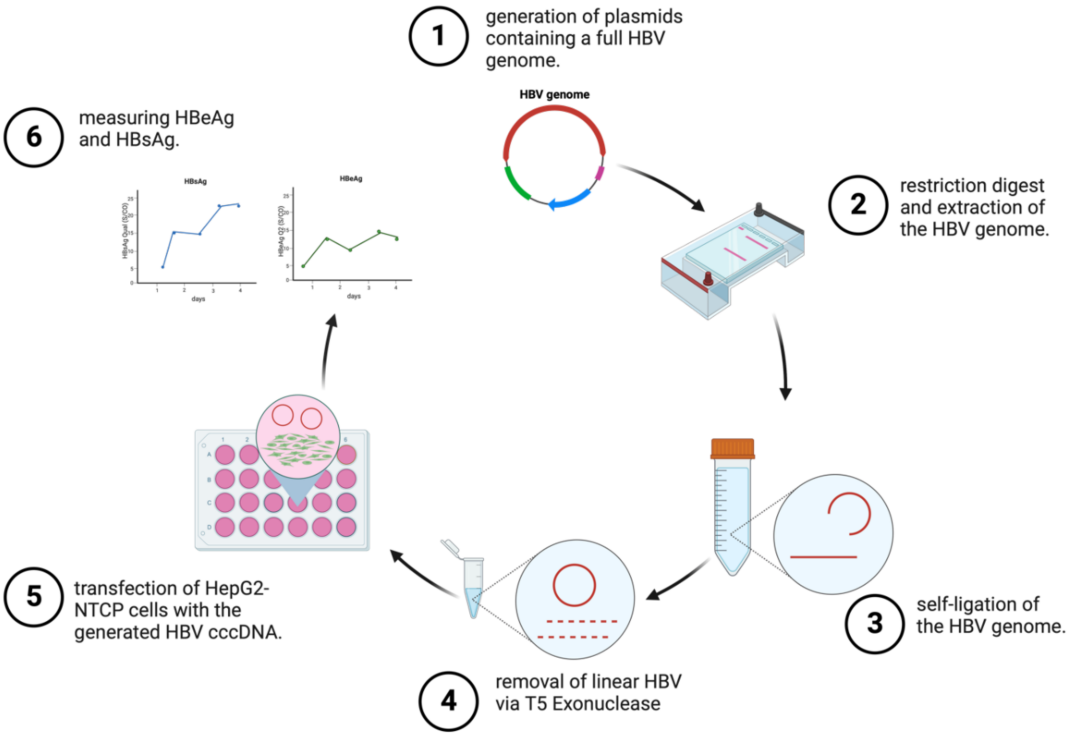

Figure 14 HBV cccDNA ligation assay: Graphical representation of the cccDNA formation and use in the HBV cell culture assay. Step 1) The generation of a plasmid containing a complete HBV genome and providing high concentrations via Maxi prep. Step 2) Restriction digest and extraction of the entire HBV genome. Separation from the backbone via gel electrophoresis. Step 3) Self-ligation of the linear HBV genome in a large volume to prevent the ligation of two or more genomes. Step 4) Removal of partially ligated or linear fragments via T5 Exonuclease and subsequent gel electrophoresis. Step 5) Transfection of cccDNA into HepG2-hNTCP cell line. Step 6) Measuring different parameters in the supernatant (HBeAg and HBsAg) via an immunoassay system. Illustration created with Biorender.com

Therefore, a switch to a method first described by Mutz et al. [182] was done. This involved cloning the entire HBV genome into a plasmid (Figure 14-1). After the plasmid containing the HBV genome was generated and validated, the next step was to cut out the HBV genome and separate it from the backbone (Figure 14-2). Once isolated, the linear HBV genome was self-ligated to form the cccDNA (Figure 14-3). The final step involved the removal of linear or partially ligated genomes using the T5 Exonuclease (Figure 14-4). The resulting cccDNA was then utilized to transfect HepG2-hNTCP cells (Figure 14-5). The cells were monitored during the assay, and the released HBeAg and HBsAg were documented (Figure 14-6).

The DNA generated from the assay steps (Figure 14) was subjected to agarose gel electrophoresis to demonstrate the method (**Figure 15**). The DNA concentration used for the gel electrophoresis in **Figure 15** does not represent the DNA concentration used for the assay and was much lower.

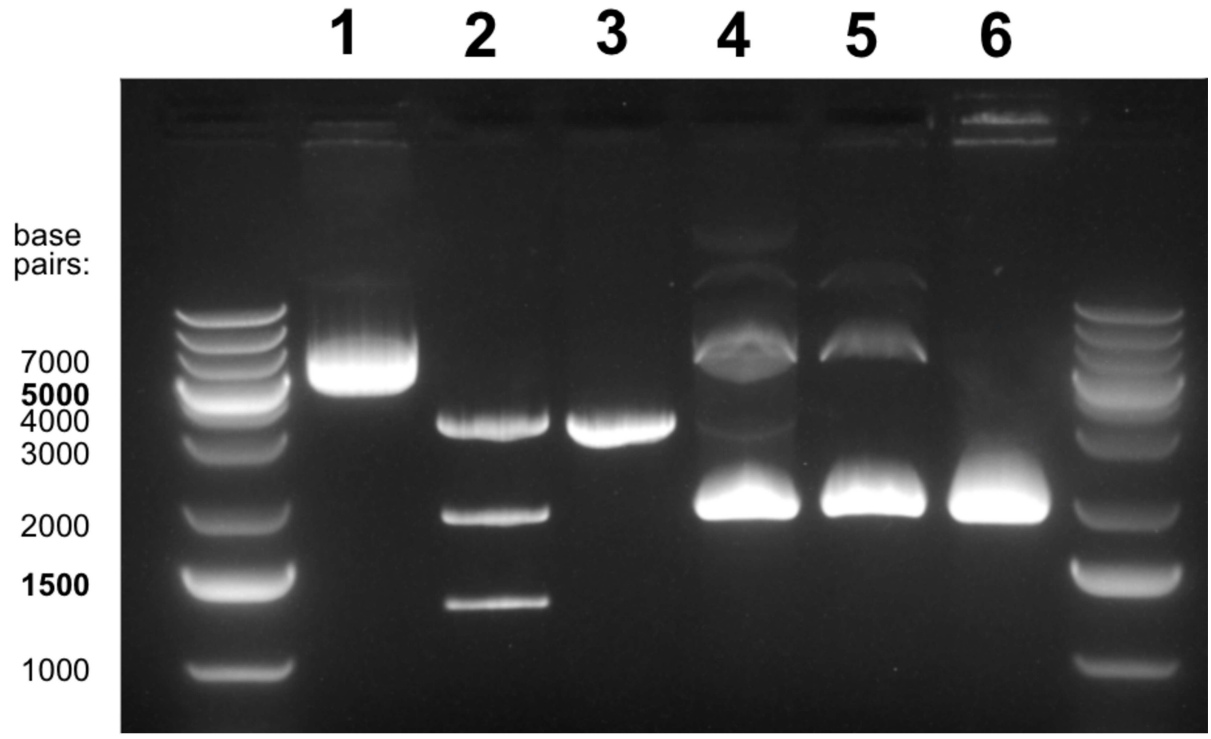

Figure 15 Representive agarose gel electrophoresis showing the DNA from the subsequent steps of generating cccDNA: A 1 % agarose gel was utilized, and the DNA concentration was adjusted to 2000 ng/well where applicable. GeneRuler 1kb plus DNA ladder was used to track DNA fragments. The figure was cropped below 1000 bp for size reasons. No bands were observed below this threshold. Lane 1: Plasmid pNL1.1-Nluc containing HBV genotype D genome (6298 bp). Lane 2: Plasmid after 1-hour restriction digest with NcoI and NotI enzymes. Bands at 3188 bp (HBV genome), 1875 bp, and 1235 bp (pNL1.1-Nluc). Lane 3: Isolated and purified linear HBV genome. Lane 4: Genome after ligation with T4 ligase for 2 hours. Single-genome cccDNA was supercoiled and displays a band at approx. 2100 bp. Lane 5: HBV Genome after 1-hour T5 exonuclease reaction. Lane 6: single-genome cccDNA after isolation and purification.

In the first lane after the DNA ladder, the pNL1.1-Nluc plasmid containing the HBV genome is visible, with a length of 6298 base pairs (bp). Moving on to the second lane, the plasmid was restriction digested with the NcoI and *Not*I enzymes, resulting in three bands. The HBV genome band is observed at 3188 bp for genotype D. The two other bands (1235 bp, 1875 bp) resulted from the *Not*I digestion of the backbone. After the isolating step, the linear HBV genome can be seen in the third lane. Less than 5 % of DNA was lost during the restriction digestion and isolation steps. Following the isolation, the linear HBV DNA was used to form the cccDNA by self-ligating in a T4 ligase reaction. The results from the ligation step can be seen in the fourth lane. As the cccDNA tends to supercoil, the band was found to be around 2100 bp on an agarose gel. Several other bands could be observed along the cccDNA band. The bands resulted from the ligation of several HBV genomes together. The ligation step was the most critical part of the generation of cccDNA and could result in the loss of > 50% of DNA usable for cccDNA. Moving to the agarose gel's fifth lane, linear fragments were eliminated using T5 exonuclease. Other bands were still present, representing circular DNA formed from two or more HBV genomes. Consequently, the band was again isolated and purified to obtain only cccDNA containing one HBV genome (Lane 6).

Each step of the generation of cccDNA was relatively simple molecular biology. However, the difficulties with ligating low concentrations of DNA in large volumes and the consequential loss of DNA in combination with the high concentration needed made the process complicated and time-consuming.

4.2.2 HBV genomes and patient isolates

Different HBV sequences were needed to generate cccDNA to see if HBeAg can contribute to viral $CD8^+$ T cell escape. Instead of reference sequences, patient isolates were used, as this project wanted to explore whether the different HBeAg-altering mutations could have different effects on isolates. Further, using patient isolates from the Duesseldorf cohort allowed a more granular selection, as many diagnostic markers were known. Selecting isolates from patients in the immune tolerance stage (HBeAg-positive) of the chronic infection was essential. The sequences from viruses in the immune tolerance stage should not have developed many mutations yet to evade the immune pressure. Therefore, viral isolates with a high viral load and a positive HBeAg status were chosen (Table 35).

Table 35 Patient isolates: Four patient isolates were selected for use in the cccDNA assay.

Name	ID	Genotype	viral load	HBeAg status	Sex	Age	HLA-A		HLA-B	
GTD #1	FR-HBV238	D	145426465	positive	M	23	2	24	7	18
GTD #2	DD14-38611	D	7000000	positive	M	27	32	68	15	38
GTA #1	FR-HBV54	A	220199656	positive	M	37	2	30	13	39
GTA #2	DD14-28904	A	2474487	positive	M	23	2	31	18	40

Further, the genomes of the selected isolates were screened for mutations at nucleotide positions 1762 and 1764 in the basal core promoter, mutations at position 1814-1816 in the precore start codon, and position 1896. Further, the isolates were screened for immune substitutions in the HLA-A02 core$_{18-27}$ epitope.

Besides these four isolates, a consensus sequence of all HBeAg positive genotypes A or D was generated. Whether the generated consensus sequences could produce HBeAg or HBsAg needed to be clarified. It would present a prototype sequence devoid of patient-specific mutations.

4.2.3 Establishing an HBV cccDNA cell culture assay

These experiments aimed to see whether the assay procedure would function and whether HBeAg and HBsAg could be detected in the supernatant. The use of patient isolates always carried the risk that the sequenced genome was not replication-competent and, consequently, did not produce HBeAg or HBsAg. Therefore, the first attempts of the cccDNA assay were made with one of the patient isolates and with cccDNA generated from plasmid pSHH 2-1. This plasmid was known to produce a replication-competent genotype D virus [9,183,184]. The immunoassay system used to measure HBeAg and HBsAg uses a signal-to-cutoff (S/CO) ratio by measuring the signal strength of a sample and the signal strength of an internal cutoff [185]. Samples with a S/CO ratio > 1.0 were defined as positive.

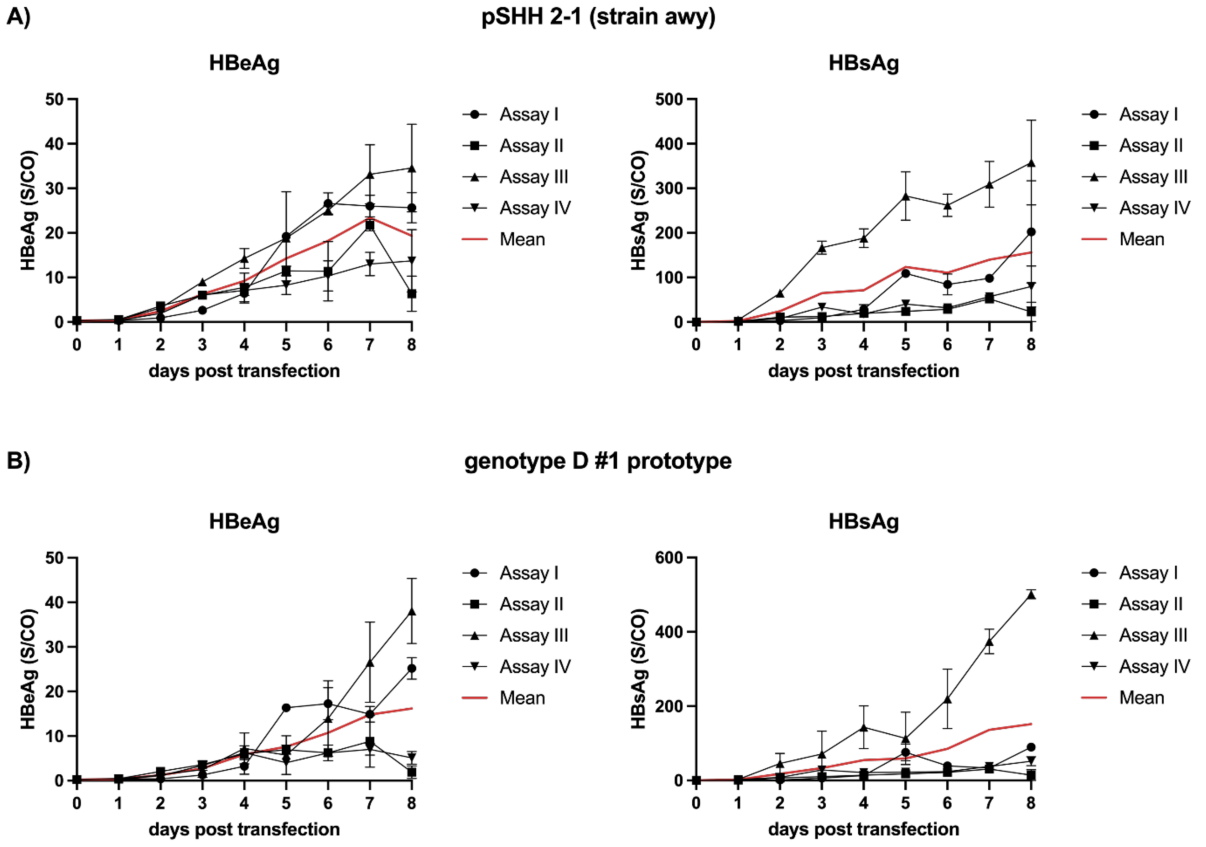

Figure 16 Establishing HBV cccDNA assay: HBeAg and HBsAg levels in the supernatant from pSHH 2-1 (A) and genotype D isolate #1 prototype (B) variants. Signal-to-cutoff (S/CO) ratio was measured with the Architect i2000 immunoassay system. Each experiment used 200.000 HepG2-NTCP cells/well with 250 ng cccDNA/well.

The HBeAg levels in the supernatant increased for both variants throughout the experiments (Figure 16 A-B). The pSHH 2-1 variant did not yield a positive HBeAg S/CO ratio on the first day after transfection. The first detectable mean positive HBeAg S/CO ratio of 2.43 ± 1.04 was observed on the second day after transfection (Figure 16 A). The highest mean HBeAg S/CO ratio recorded within the experimental timeframe was 23.39 ± 9.04 on the seventh day after transfection. The highest overall recorded HBeAg S/CO ratio was 41.5 in Assay III on the eighth day after transfection.

The genotype D isolate #1 prototype variant behaved similarly to the pSHH 2-1 variant in that the mean HBeAg S/CO ratio was first positive on the second day after transfection (Figure 16 B). The highest mean HBeAg S/CO ratio of 16.17 ± 15.65 and the highest recorded HBeAg S/CO ratio of 32.89 were detected on the eighth day after transfection.

Even though both variants secreted HBeAg into the supernatant, it appears that the pSHH 2-1 variant consistently displayed higher HBeAg levels compared to the genotype D prototype variant. The complete dataset and an inter-assay comparison are provided in the supplements.

HBsAg was detected in the supernatant for both variants, and the concentration increased during the experimental timeframe (Figure 16 A-B). For pSHH 2-1, the first positive HBsAg S/CO ratio was reached on the first day after transfection in most replicates. The mean HBsAg S/CO rato was 2.27 ± 1.9. Similarly, for the genotype D prototype, a positive HBsAg S/CO ratio was reached in all assays on the first day after transfection. The results indicate that HBsAg is detected earlier in the supernatant than HBeAg. The highest mean HBsAg S/CO ratio between the assays for the pSHH 2-1 variant was recorded eight days into the experimental setup. HBsAg reached a S/CO ratio of 156.10 ± 143.9. For the genotype D prototype variant, the highest mean HBsAg S/CO ratio was similarly detected on the last day and was 151.85 ± 150.2. The highest recorded HBsAg S/CO ratio was 425.5 for the pSHH 2-1 variant and 509.92 for the genotype D prototype variant. Compared to HBeAg for both variants, much higher HBsAg levels were detected in the supernatant. The complete dataset and an inter-assay comparison are provided in the supplements.

The results of the experiments demonstrated the important fact that the in-vitro-generated cccDNA can be used to transcribe HBeAg and HBsAg and that the antigens are released into the supernatant. While the assays exhibited considerable variability across experiments, the findings suggest that both variants showed similar behavior

HBV genotype A prototype variants

Once the in-vitro-generated cccDNA was confirmed to transcribe RNA in HepG2-hNTCP cells after transfection, leading to the detection of HBeAg and HBsAg in the supernatant, the next step involved testing the remaining genotype A and D prototype variants.

However, due to increasing intraassay variation observed from the fifth day onward and often S/CO ratios below one on the first day, the recording period of HBeAg and HBsAg after transfection was shortened. This adjustment to the experimental setup allowed for more repetitions due to the saved cccDNA.

A steady increase of HBeAg and HBsAg over time was detected for the two genotype A isolates and the consensus variant. (Figure 17 A-C). Although there were variations between the experiments when looking at the mean HBeAg S/CO ratios between the variants, differences could be detected. Isolate #1 prototype had the highest mean HBeAg S/CO ratio (4.08 ± 3.5) compared to the other variants (isolate #2: 2.96 ± 0.54; consensus: 2.80 ± 1.89) on the second day after transfection. One day later, the mean HBeAg S/CO ratio increased to 9.32 ± 9.03 for isolate #1. Similar to the day before, the mean HBeAg S/CO ratio was lower for isolate #2 (6.68 ± 1.70) and consensus (6.34 ± 4.4). On the fourth day, the mean HBeAg S/CO ratio for isolate #1 reached 14.23 ± 11.86, shortly followed by the S/CO ratio of consensus (13.72 ± 8.74) and isolate #2 (12.11 ± 2.94). Regarding the fifth day, HBeAg S/CO ratios did not increase as rapidly as they did in the first few days, where a near doubling could be observed. The mean HBeAg S/CO ratio for isolate #1 reached 21.68 ± 23.24 compared to 18.11 ± 4.3 for isolate #2 and 17.50 ± 12.31 for the consensus variant. Despite isolate #1 having a higher mean HBeAg S/CO ratio than isolate #2, isolate #2 showed the smallest deviation between single assays.

Interestingly but not unexpectedly, the mean HBsAg ratios for the prototype variants did not correlate with the HBeAg ratios. The HBsAg levels were considerably higher than the HBeAg levels across all samples. Further, High HBeAg levels did not automatically mean high HBsAg levels. For example, isolate #1 exhibited the highest HBeAg levels (day 5 HBsAg S/CO ratio: 21.68 ± 23.24) but had lower maximum HBsAg levels (day 5 HBsAg S/CO ratio: 273.80 ± 281.58) compared to the consensus variant (day 5 HBsAg S/CO ratio: 310.76 ± 210.50). Similarly, isolate #2 displayed comparable HBeAg levels, but much lower HBsAg levels (day 5 HBsAg S/CO ratio: 92.87 ± 19.25) compared to isolate #1 (day 5 HBsAg S/CO ratio: 273.80 ± 281.58) and consensus (day 5 HBsAg S/CO ratio: 310.76 ± 210.50).

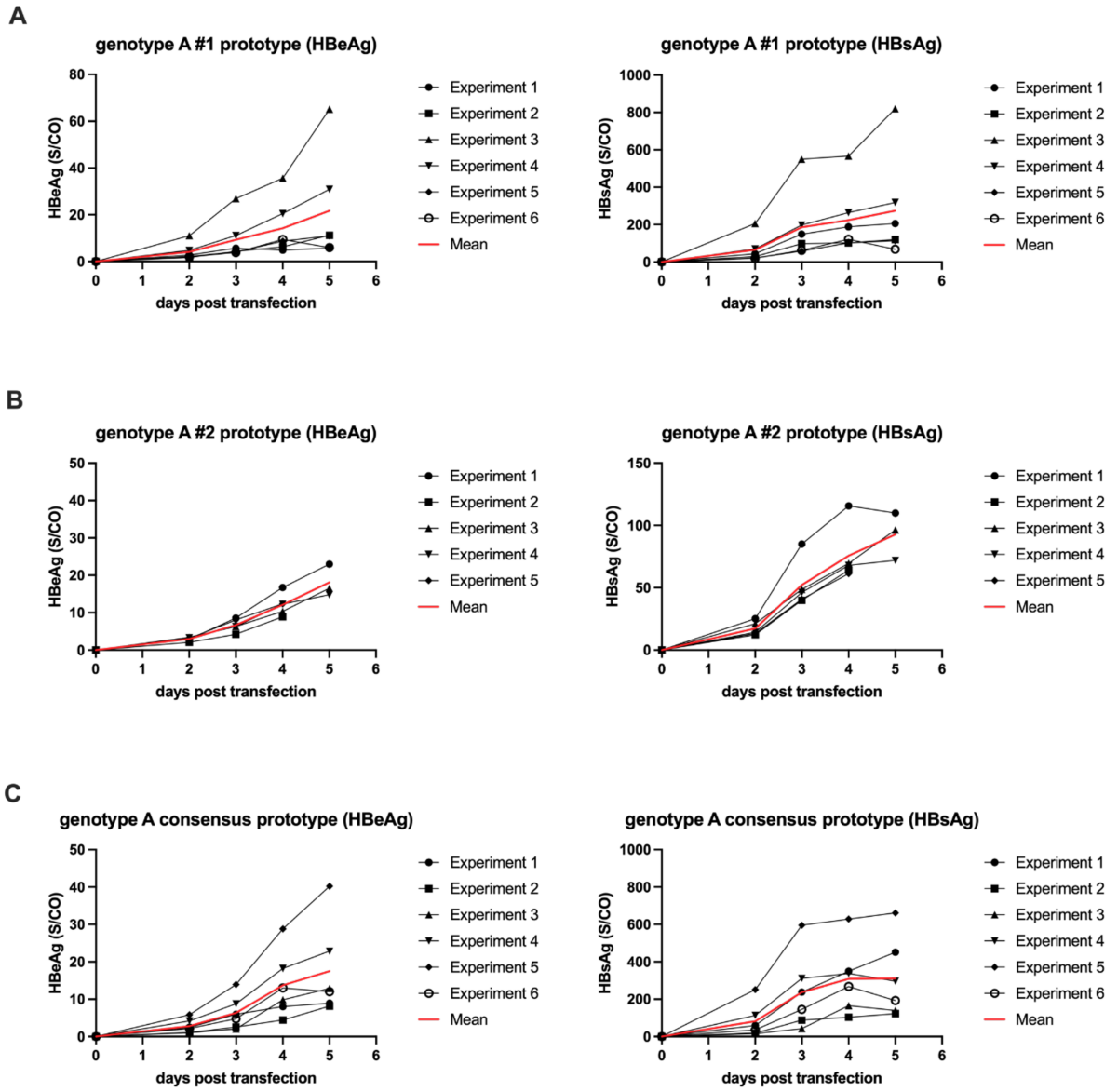

Figure 17 genotype A prototype variants: Graphical visualization of the HBeAg and HBsAg signal-to-cutoff (S/CO) ratio for the different genotype A prototype variants. Each graph contains the S/CO for the different experiments and a mean (red) S/CO generated from the presented experiments. The different variants used different scaling. A) HBeAg and HBsAg ratio from the second to the fifth day for isolate #1. B) HBeAg and HBsAg ratio from the second to the fifth day for isolate #2. C) HBeAg and HBsAg ratio from the second to the fifth day for the consensus sequence.

The experiments demonstrated that HBeAg and HBsAg are controlled differently by the virus. Different promoters regulate both antigens and individual mutations in the S gene may account for the differences in HBsAg levels among the isolates. Furthermore, the results showed considerable variability between the experiments, similar to those conducted in comparison with the pSHH 2-1 plasmid. However, overall, both genotype A isolates and the consensus were capable of transcribing and translating HBeAg and HBsAg.

HBV genotype D prototype variants

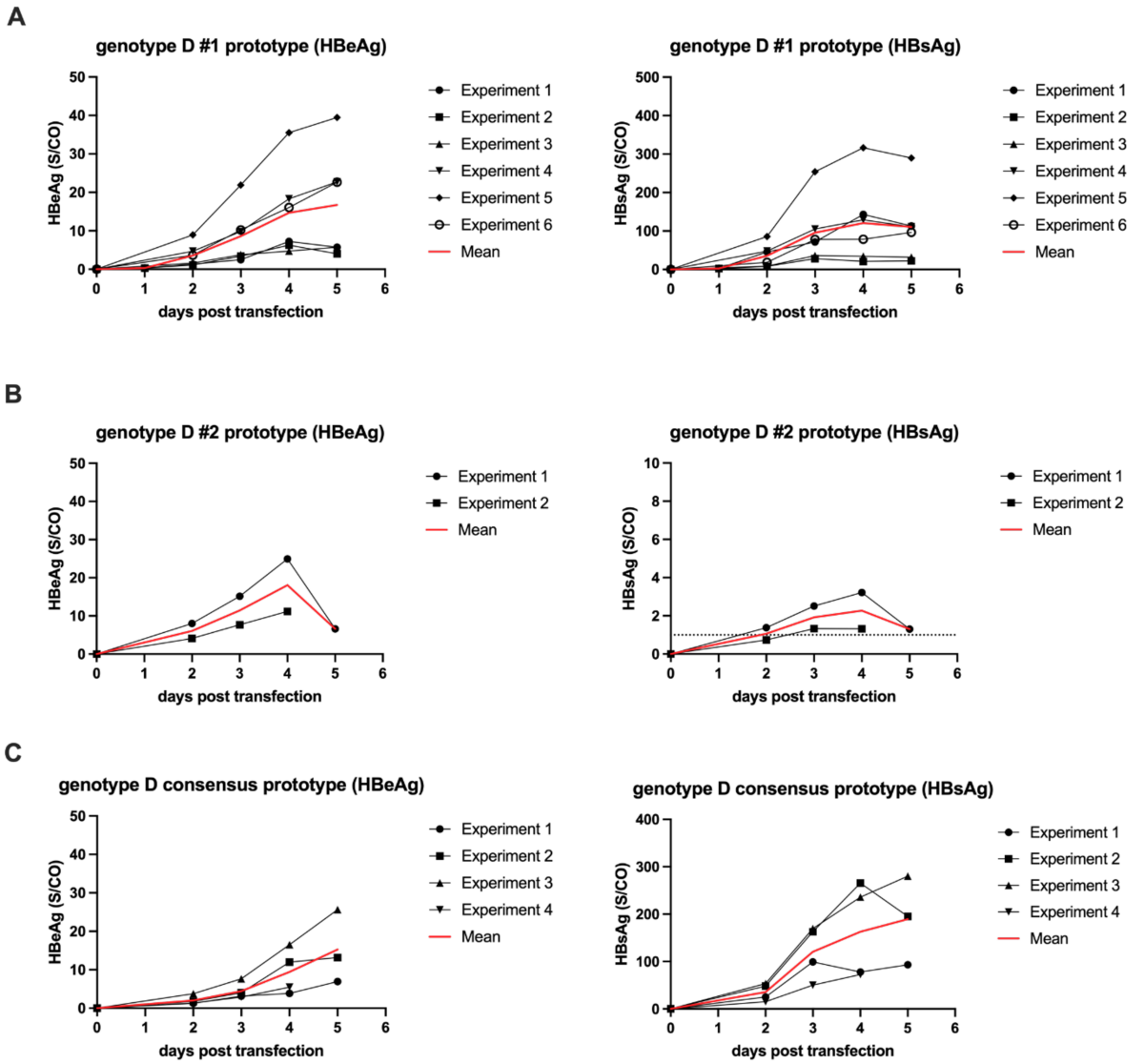

Figure 18 genotype D prototype variants: Graphical visualization of the HBeAg and HBsAg signal-to-cutoff (S/CO) ratio for the different genotype D prototype variants. Each graph contains the S/CO ratio for the different experiments and a mean (red) S/CO ratio generated from the presented experiments. The different variants used different scaling. A) HBeAg and HBsAg ratio from the second to the fifth day for isolate #1. B) HBeAg and HBsAg ratio from the second to the fifth day for isolate #2. The dotted line represented the S/CO ratio of one. C) HBeAg and HBsAg ratio from the second to the fifth day for the consensus sequence.

The two genotype A isolates and the generated consensus variant proved to generate HBeAg and HBsAg. Next were the different genotype D prototype variants from two isolates and the consensus. Unfortunately, only for isolate #1 and the consensus prototype variant, both HBeAg and HBsAg could be detected at reasonable levels (Figure 18 A, C). Genotype D isolate #2 was abandoned after two experiments due to the lack of HBsAg in the supernatant (Figure 18 B). The highest mean S/CO ratio for HBeAg (18.05 ± 9.72) and HBsAg (2.26 ± 1.34) was measured on day four of both experiments.

Isolate #2 was sequenced, and a mutation in the S ORF that was not present in the isolate's original sequence was detected.

In isolate #1 and the consensus prototype variants, there was a doubling of the S/CO ratio per day when observing the HBeAg levels in the first few days. The initial mean positive HBeAg S/CO ratio was 3.55 ± 3.01 for isolate #1 and 2.03 ± 1.16 for consensus on the second day after transfection. By the following day, the HBeAg S/CO ratio had more than doubled, reaching a mean ratio of 8.59 ± 7.32 (isolate #1) and 4.43 ± 2.1 (consensus). Subsequently, on the next day, the HBeAg S/CO ratio nearly doubled again to 14.72 ± 11.61 (isolate #1) and doubled to 9.45 ± 5.8 for the consensus prototype variant. By the fifth day, the HBeAg level for isolate #1 had only slightly increased to 16.72 ± 14.07. The consensus HBeAg levels increased to 15.25 ± 9.52, now closely matching isolate #1 HBeAg levels. These findings suggest that isolate #1 may be able to generate HBeAg faster than the consensus variant. However, by the end of the experiment, both variants produced similar maximum levels of HBeAg.

As for genotype A, the HBsAg levels for both genotype D variants were much higher than their HBeAg levels. Although isolate #1 (35.72 ± 30.11) and consensus (35.54 ± 18.28) initially had similar HBsAg S/CO ratios on the second day after transfection, this started to change for the other days. By the third day, the mean HBsAg levels of the consensus prototype (120.51 ± 107.77) had already reached levels similar to the mean HBsAg levels of isolate #1 on the fourth day (120.38 ± 56.54). Of note is that for isolate #1, the mean HBsAg levels decreased to 110.75 ± 96.20 on the fifth day. In contrast, for the consensus prototype variant, there was a consistent increase in HBsAg (S/CO: 189.51 ± 93.52) until the last day of the experimental setup.

The results demonstrate that similar to genotype A variants, genotype D isolate #1 and the consensus sequence were able to transcribe and translate HBeAg and HBsAg. Interestingly, at least in this experimental setup, it appears that the genotype A variants generally produce higher amounts of HBsAg compared to genotype D variants with similar HBeAg levels. Therefore, these isolates and consensus sequences could be utilized to investigate HBeAg-altering mutations.

4.2.3.1 Quantification of HBV DNA in the rcccDNA assay

The HBeAg and HBsAg levels in the supernatant can be used to determine successful cccDNA expression, whereas measuring HBV DNA levels can indicate viral replication. For the first experiment, both the supernatant and the transfected cells were collected (Figure 19). The HBV DNA levels in the supernatant remained relatively constant (with a mean of 1.8 x 10^7 copies/ml) for the first five days after transfection with the pSHH 2-1 cccDNA. After that, a decline was observed, with a final mean measurement of 2.05 x 10^6 copies/ml. In the case of genotype D #1 prototype cccDNA, there was a constant decline of HBV DNA until day eight, with the mean final HBV DNA level of 1.09 x 10^5 copies /ml. It is important to note that transfection with 250 ng cccDNA (corresponding to 7.24 x 10^{10} copies of HBV DNA) was used, and the cells were only washed once after the transfection. Therefore, there may still be residue cccDNA in the supernatant. Regarding the HBV DNA levels in the cells, there was a decline until day four for both pSHH 2-1 (1.16 x 10^6 copies/ml) and genotype D #1 prototype (7.39 x 10^4 copies/ml) cccDNA. After day four, there was a slight increase in HBV DNA levels for both variants, with 1.67 x 10^5 copies/ml for the genotype D #1 prototype and 2.4 x 10^6 copies/ml for pSHH 2-1. However, since low-level replication was expected, and a cccDNA contamination couldn't be ruled out, HBV DNA measurement was no longer considered for further experiments.

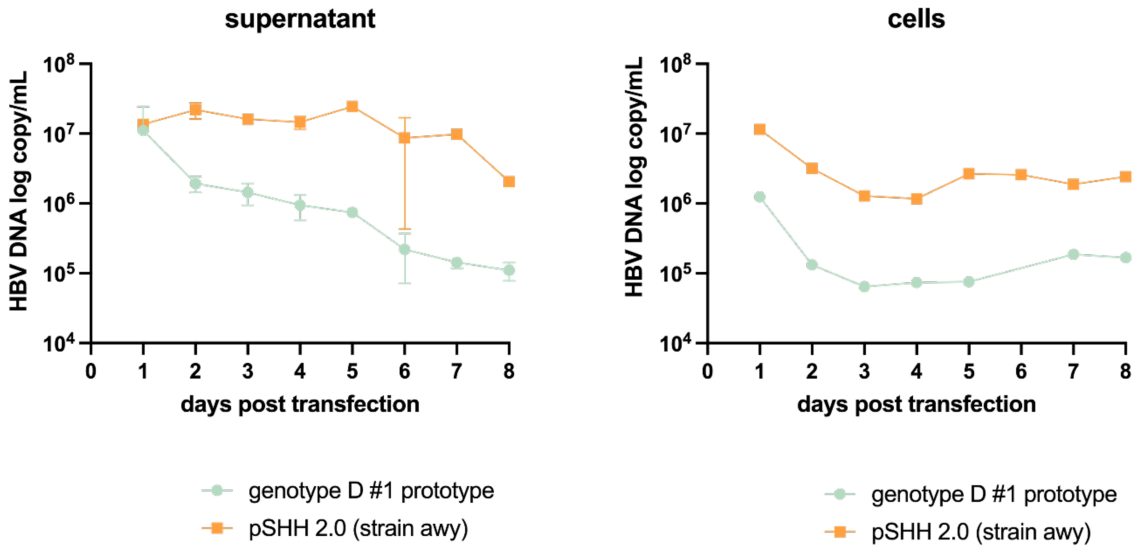

Figure 19 HBV DNA levels: Measurement of HBV DNA levels for genotype D #1 prototype (green) and pSHH 2-1 (orange) cccDNA from assay I. HBV levels were measured from the supernatant or cell lysate by qPCR.

4.2.4 HBeAg and HBsAg S/CO ratio for the HBeAg-altering variants

During the experiments, the medium was exchanged two hours before transfection with cccDNA. The medium exchange was used to measure the HBeAg and HBsAg for day zero. In all experiments performed, the S/CO ratio for HBeAg and HBsAg never exceeded 0.7 and was, therefore, by definition of the manufacturer of the Architect i2000 immunoassay system negative.

HBV genotype A HBeAg-altering variants

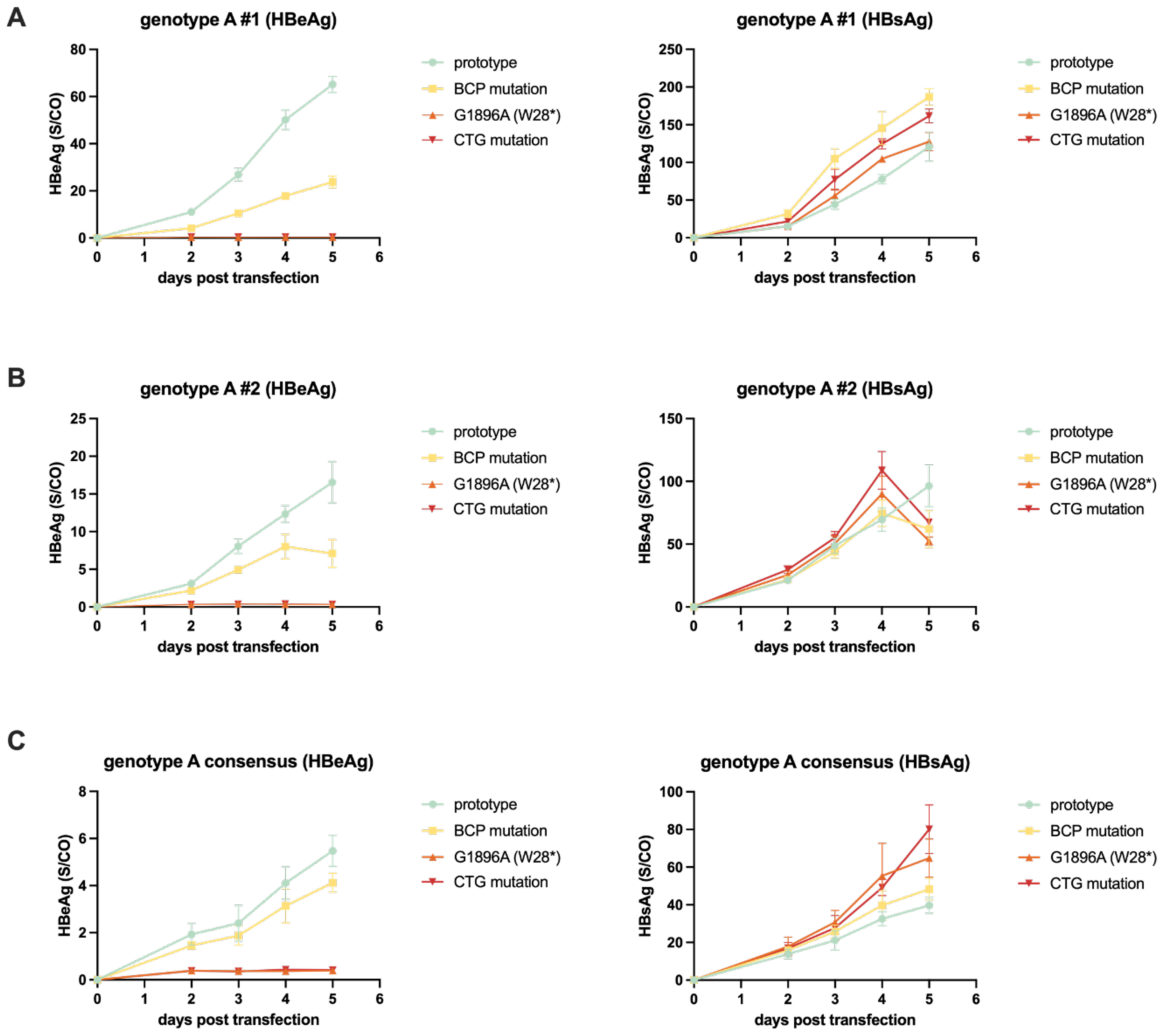

Figure 20 genotype A prototype vs HBeAg variants: Graphical visualization of the HBeAg and HBsAg signal-to-cutoff (S/CO) ratio for genotype A isolate #1, isolate #2, and consensus with the prototype and the different HBeAg variants. Variants were labeled as followed: Prototype (green), BCP double mutation (yellow), G1896A (orange), and CTG mutation (red). A) HBeAg and HBsAg S/CO ratio for isolate #1. B) HBeAg and HBsAg ratio for isolate #2. C) HBeAg and HBsAg ratio for the consensus sequence.

In Figure 20, a representative experiment is described for each genotype A isolate and consensus. For the genotype A isolate #1 prototype variant, the mean HBeAg S/CO ratio was 11.04 ± 1.45 for the second day after transfection, 28.91 ± 2.7 for the third day after transfection, 50.14 ± 4.16 for the fourth day after transfection and 63.19 ± 3.4 for the last day after transfection (Figure 20 A). For the genotype A isolate #1 BCP double mutation (BCP mut.) variant, lower HBeAg S/CO ratios were measured compared to the prototype variant. The mean HBeAg S/CO ratio for the second day was 4.17 ± 0.15. For the third day, the mean S/CO ratio was 10.52+1.01. The mean HBeAg S/CO ratio for the fourth day for the BCP mut. variant was 17.83 ± 0.93 and was followed by a mean HBeAg S/CO ratio of 23.76 ± 2.51 on the fifth day after transfection. For the variants containing the W28* mutation or the CTG

mutation, no positive HBeAg S/CO ratio was recorded. HBsAg S/CO ratios were used as a control, and all genotype A isolate #1 variants displayed similar levels throughout the assays.

The results for genotype A isolate #2 were comparable to genotype A isolate #1, with the prototype variant producing the most HBeAg followed by the BCP mut. variant (Figure 20 B). The G1896A stop mutation, and the start codon mutation did not produce HBeAg. For HBsAg isolate #2, similar but overall lower S/CO ratios were measured compared to the HBsAg S/CO ratio measured for genotype A isolate #1, except for day five, where the S/CO ratio decreased compared to the ratio on day four.

The experiment with the genotype A consensus cccDNA showed an increase in HBeAg and HBsAg over time for the prototype and BCP mutation variants and only an increase in HBsAg over time for the W28* mutation and CTG mutation variants (Figure 20 C). The prototype variant had the highest S/CO ratio on day five (HBeAg: 5.47 ± 0.65; HBsAg: 39.74 ± 4.2). Similarly, for the BCP mutation variant, a mean S/CO of 4.12 ± 0.40 (HBeAg) and 48.28 ± 5.87 (HBsAg) were measured on the fifth day of the experiment. The G1896A and CTG variants never showed S/CO ratios above 0.5 for HBeAg in the supernatant. The HBsAg S/CO ratio reached the maximum recorded on day five with 64.82 ± 10.17 for the G1896A variant and 80.09 ± 12.97 for the CTG variant.
Interestingly, genotype A isolate #1 displayed the most pronounced contrast between the prototype and the BCP mutation. In Isolate #2 and the consensus variant, the HBeAg level of the BCP mutation was closer to the prototype.

HBV Genotype D HBeAg-altering variants

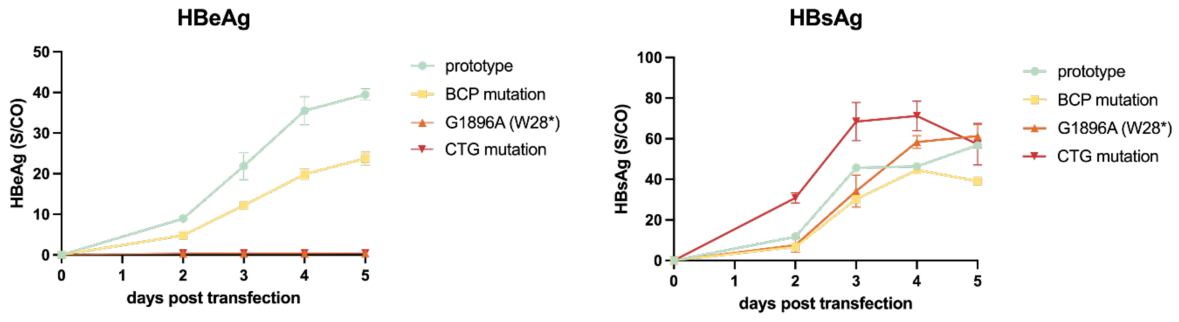

Figure 21 genotype D isolate #1 prototype vs HBeAg variants: Graphical representation of the signal-to-cutoff (S/CO) ratio of HBeAg and HBsAg concerning genotype D isolate #1 with prototype and different HBeAg variants. The variants were labeled as follows: Prototype (green), BCP double mutation (yellow), G1896A stop-mutation (W28*) (orange), and CTG mutation (red).

Figure 21 describes representative experiments for the genotype D isolate #1 HBeAg altering mutations. Genotype D isolate #1 showed similar results to the genotype A variants. The prototype

variant produced the most HBeAg, followed by the BCP mutation. For the prototype variant, the mean S/CO ratio was 8.95 ± 0.89 for the second day, 21.87 ± 3.34 for the third day, 35.50 ± 3.50 for the fourth day, and 39.47 ± 1.39 for the fifth day. For the BCP mutation variant, the mean S/CO ratio was 4.79 ± 0.60 for the second day, 12.16 ± 0.50 for the third day, 19.86 ± 1.21 for the fourth day, and 23.75 ± 1.57 for the fifth day. As for the genotype A variants, no HBeAg was detected for the genotype D W28* mutation or the CTG mutation. Both variants exhibited an HBeAg S/CO ratio of less than 0.60 despite an HBsAg S/CO ratio comparable to the prototype and BCP mutation variants.

The mutations affecting HBeAg showed similar behavior regardless of the genotype. Compared to the HBeAg-altering mutation from the same isolate, the prototype variant produced the highest amount of HBeAg in the supernatant. The W28* and CTG mutations led to very low to undetectable levels of HBeAg. HBsAg levels were consistent across the variants, suggesting comparable transcription and translation. All data points are provided in the supplements.

HBeAg and HBsAg levels from HepG2-hNTCP cells transfected in Jurkat medium

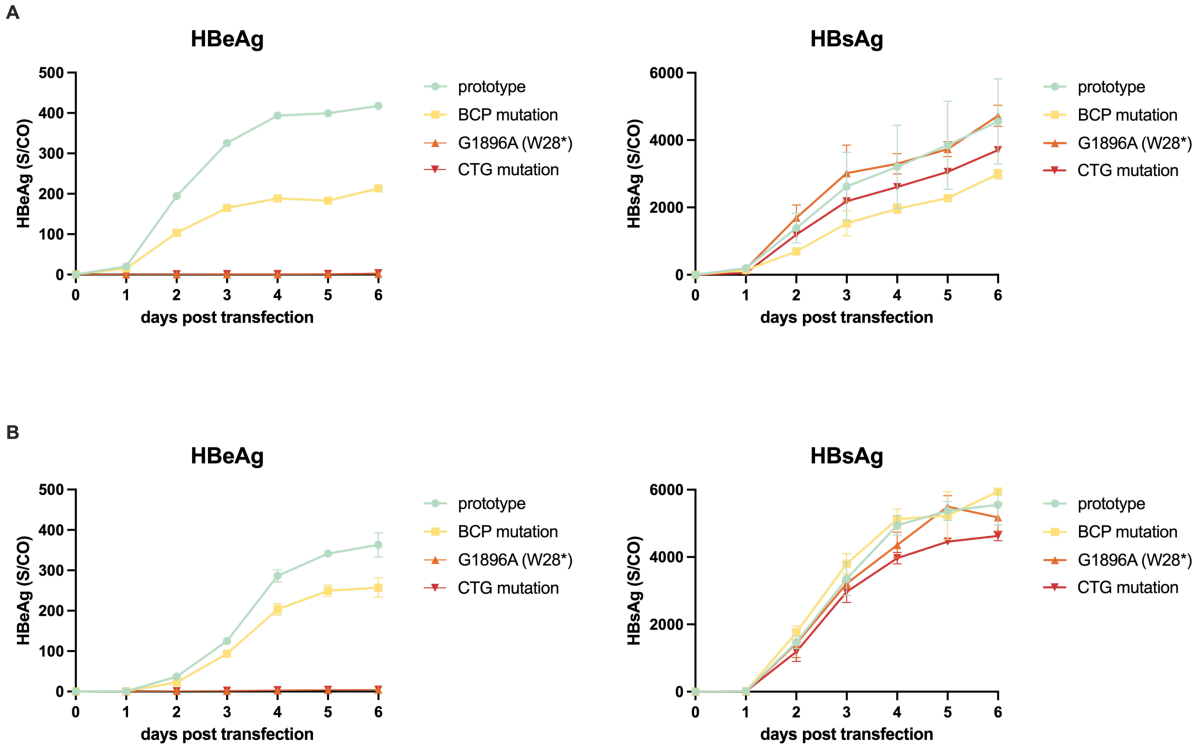

Figure 22 genotype A and D consensus prototype vs HBeAg variants in jurkat medium: Graphical representation of the signal-to-cutoff (S/CO) ratio of HBeAg and HBsAg concerning (A) genotype D and (B) A consensus with prototype and different HBeAg variants. The variants were labeled as follows: Prototype (green), BCP double mutation (yellow), G1896A stop-mutation (W28*) (orange), and CTG mutation (red).

Initially, the experiments were conducted using parameters designed to allow reinfection of HBV. This approach was based on data published by Michailidis et al. [88], which demonstrated that the reinfection efficiency is significantly enhanced by the inclusion of 4% polyethylene glycol 8000 (PEG 8000) and 2% dimethyl sulfoxide (DMSO) in the culture medium. While it was known that DMSO particularly affected the growth of HepG2-hNTCP cells, this was deemed acceptable in light of the potential for viral reinfection. For experiments in which the HepG2-hNTCP cells interacted with Jurkat cells, the medium formulation was modified to remove DMSO and PEG 8000. This was due to the Jurkat cells showing a high sensitivity to these additives, unlike the HepG2-hNTCP cells. As a result, the modified medium led to higher HBeAg and HBsAg S/CO ratios compared to the original replication medium (Figure 22).

In the presence of the Jurkat medium, the consensus variants displayed much higher levels of HBeAg and HBsAg for both the prototype and BCP mutation compared to experiments where the replication medium was used. Still, the prototype variants produced the highest amount of HBeAg, followed by the BCP mutation. Intriguingly, the W28* or CTG mutation variants showed a positive HBeAg S/CO ratio, albeit considerably lower than the prototype and the BCP mutation.

Exemplarily for genotype D consensus (Figure 22 A), this means that for the prototype variant, the mean S/CO ratio was 20.00 ± 2.21 on the first day, 194.50 ± 18.29 on the second day, 325.50 ± 82.51 on the third day, 393.23 ± 60.82 on the fourth day, and 417.92 ± 105.24 on the fifth day. The mean BCP variant HBeAg S/CO ratio was 15.53 ± 3.29 on the first day, 103.55 ± 22.48 on the second day, 164.65 ± 64.45 on the third day, 188.93 ± 19.43 on the fourth day, and 212.96 ± 43.11 on the fifth day. For the G1896A and CTG variants on days four and five, positive HBeAg S/CO ratios were recorded. The highest mean HBeAg S/CO ratio was 1.76 ± 0.13 for G1896A and 3.41 ± 1.76 for the CTG variant on the fifth day after transfection of cccDNA.

Similar to the replication medium, the HBsAg S/CO ratio between the variants did not vary extensively using the Jurkat medium, indicating similar transcription and translation.
Culturing the HepG2-hNTCP cells in the Jurkat medium increased the levels of HBeAg and HBsAg due to the absence of PEG-8000 and DMSO. However, the reduction in HBeAg mirrored the results obtained with the replication medium. This allowed a normalized comparison between the variants irrespective of the medium used. Higher levels of HBeAg and HBsAg in the Jurkat medium were preferable, and consequently, further experiments were exclusively conducted in a medium without PEG-8000 or DMSO.

4.2.5 Normalized HBeAg and HBsAg levels of HBV precore variants

The prior experiments demonstrated that there was some inter-assay variability. Therefore, the signal-to-cutoff ratio in each experiment was normalized (fold change) to the corresponding prototype S/CO ratio. The closer the value gets to 1, the more similar the HBeAg or HBsAg levels were to the readings for the prototype. Figure 23 shows the fold change for HBeAg between the prototype and the HBeAg altering mutation for genotype A and D consensus over time. Normalization led to a much smoother variation. For example, the BCP mutation variant in genotype A now reduced HBeAg production by 25% (0.75 fold change) compared to the prototype from the second to the fifth day of the measurement. In the W28* and the CTG mutation variants, the HBeAg production was drastically reduced by at least 80% (0.20 fold change) compared to the prototype from the second day onward.

For genotype D, similar to genotype A, the fold change between the days did not vary much. Compared to the prototype, the BCP mutation variant had a reduction of 47% in HBeAg in the supernatant. The fold change increased to 0.50 on the third day, 0.47 on the fourth day, and 0.45 on the fifth day. For the W28* mutation, the reduction in HBeAg was already 97% (0.03 fold change) on the second day compared to the prototype. For the CTG mutation, the reduction in HBeAg was 95% on the second day compared to the prototype and only increased slightly to 96% on the fifth day.

Comparing the fold change on one day would be sufficient to compare the different variants from this data. The fourth day was chosen as it was a balance between sufficient HBeAg and HBsAg levels in the supernatant and still stable assay conditions.

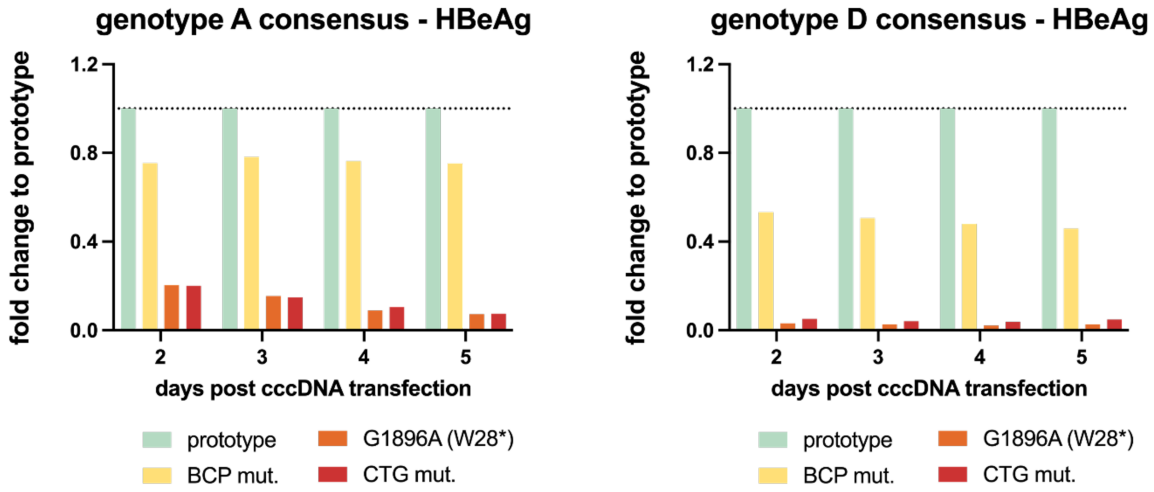

Figure 23 Time period of HBeAg levels normalized to prototype: Graphical representation of genotype A and D consensus HBeAg levels over time. The variants were labeled as follows: Prototype (green), BCP double mutation (yellow), G1896A stop-mutation (orange), and CTG mutation (red). The variant's S/CO ratio was normalized to the prototype S/SO ratio (fold-change). The pointed line represents the prototype (1x).

The goal was to examine if the HBeAg-altering mutations could have an impact between the different isolates or between the genotypes.

Genotype A

For genotype A, the consensus, isolate #1, and isolate #2 variants were compared (Figure 24). The HBeAg levels in the different HBeAg-altering mutations were compared to those in the prototype in each variant. For the consensus of genotype A, two additional variants were generated. They consist of the single mutations from the BCP double mutation (A1862T or G1864A). The objective was to identify if a single mutation or only the combination of both mutations is responsible for reducing HBeAg in the supernatant (Figure 24 A). For the A1862T mutation, an 8% (p = ns) reduction in HBeAg was observed, resulting in a 0.92 ± 0.13 fold change compared to the prototype. Comparably, the G1864A mutation showed an increase of 1% in HBeAg, resulting in a fold change of 1.01 ± 0.16 (p = ns) compared to the prototype. The two single mutations did not influence the HBeAg production compared to the prototype, so they were not further persuaded in the patient isolates.
In contrast to the individual mutations, the BCP double mutation resulted in a 37% ($p < 0.0001$) reduction of HBeAg compared to the prototype. A comparable reduction was observed in patient isolate #1 (42%, $p < 0.0001$). For patient isolate #2, the BCP mutation resulted in a 22% ($p = 0.0385$) reduction of HBeAg, less than for the other two variants.

Introducing the W28* or the CTG mutation reduced the HBeAg production almost entirely. Introducing the W28* mutation resulted in a 97% reduction of HBeAg ($p < 0.0001$) for the consensus, a 98% reduction ($p < 0.0001$) in isolate #1 and isolate #2 compared to the corresponding prototype variants. Similar to the W28* mutation, introducing the CTG mutation resulted in a 93% ($p < 0.0001$) reduction of HBeAg in the consensus, 95% ($p < 0.0001$) reduction in isolate #1, and a 98% ($p < 0.0001$) reduction in isolate #2.

Comparing HBeAg production for genotype A across all experiments, the results demonstrated that the two isolates and the consensus behaved similarly for the different HBeAg-altering mutations. The decline or absence of HBeAg across the isolates and consensus for the HBeAg altering variants was statistically significant compared to the prototype. The BCP single mutations A1862T and G1864A did not exhibit a decline of HBeAg compared to the prototype, and the shift in HBeAg level was not statistically significant.

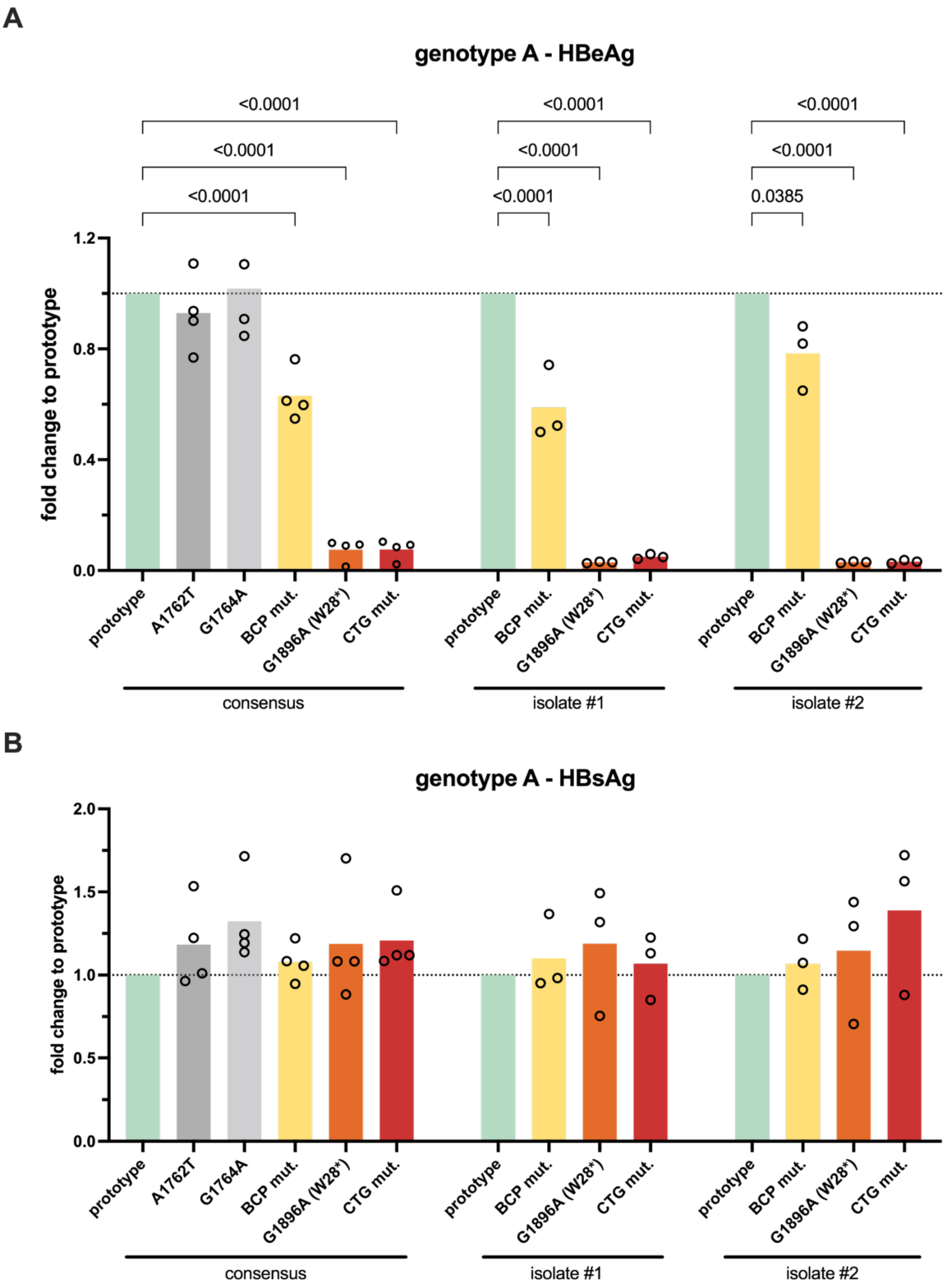

Figure 24 Genotype A HBeAg and HBsAg levels normalized to prototype: Graphical representation of genotype A isolate #1, isolate #2, and consensus HBeAg-altering variants normalized to the prototype variant on the fourth day of individual experiments. The variant's S/CO ratio was normalized for each experiment to the prototype S/SO ratio (fold-change). The pointed line represents the prototype (1x). The variants were labeled as follows: Prototype (green), BCP double mutation (yellow), W28* mutation (orange), and CTG mutation (red). Statistical significance was calculated using a one-way analysis of variance to compare three samples. Statistically not significant values were not stated. Panel A) HBeAg in genotype A consensus, isolate #1 and #2 normalized to prototype on the fourth day after transfection. Panel B) HBsAg in genotype A consensus, isolate #1 and #2 normalized to prototype on the fourth day after transfection.

Besides monitoring the HBeAg levels, it was crucial to measure the HBsAg levels. HBsAg in the supernatant is not connected to HBeAg or the core protein production. Therefore, it served as an independent control to monitor the transcription and translation from the cccDNA during the assay.
Although the HBsAg levels differ from the prototype in some experiments, the mean of experiments shows similar levels, albeit slightly elevated (Figure 24 B). Statistical analysis did not result in a significant mean fold change compared to the prototype variants. This observation is crucial as it indicates that alterations in the HBeAg levels arise from HBeAg-modifying mutations rather than general variations in the transfection or translation of the cccDNA during the assay.
In detail, this means that for the BCP double mutation, the fold change to the prototype was 1.07 ± 0.11 in the consensus. With the A1862T and G1864A mutation, the HBsAg fold change was 1.18 ± 0.26 and 1.32 ± 0.26. The W28* mutation resulted in a fold change of 1.18 ± 0.35, and the start codon mutation resulted in a fold change of 1.20 ± 0.20. In isolate #1, introducing the BCP double mutation resulted in a fold change of 1.10 ± 0.23. The introduction of the G1896A stop-mutation resulted in a fold change of 1.18 ± 0.38, and the CTG mutation resulted in a fold change of 1.06 ± 0.19. For isolate #2, the HBsAg levels of the BCP double mutation were 1.06 ± 0.15 higher than for the prototype. Similarly, the HBsAg levels for the G1896A stop-mutation and CTG mutation were 1.14 ± 0.38 and 1.38 ± 0,44 higher than for the prototype.

Genotype D

Upon analyzing the levels of HBeAg and HBsAg in different isolates and the consensus for genotype D, a pattern similar to genotype A was observed (Figure 25). The introduction of the BCP double mutation, W28* mutation, or the CTG mutation resulted in a statistically significant reduction in HBeAg levels among the two isolates and the consensus (Figure 25 A). Notably, the HBsAg levels showed no significant variation across the variants, suggesting no significant global change in transcription or translation of the cccDNA (Figure 25 B). This observation confirms that the reduction of HBeAg is specifically related to the inserted mutation.
Looking in detail at the results showed that the BCP double mutation in the genotype D consensus resulted in a 44% ($p < 0.0001$) decrease in HBeAg compared to the prototype. Additionally, the W28* or the CTG mutation caused a 97% ($p < 0.0001$) reduction in HBeAg in the supernatant compared to the prototype. Patient isolate #1, with a BCP double mutation introduced, exhibited a 35% mean reduction in HBeAg ($p < 0.0001$) in the supernatant compared to the prototype. Introducing the W28* mutation resulted in a 94% decrease in HBeAg levels in the supernatant. Similarly, introducing the CTG mutation also led to a 97% reduction ($p < 0.0001$) in HBeAg compared to the prototype levels.

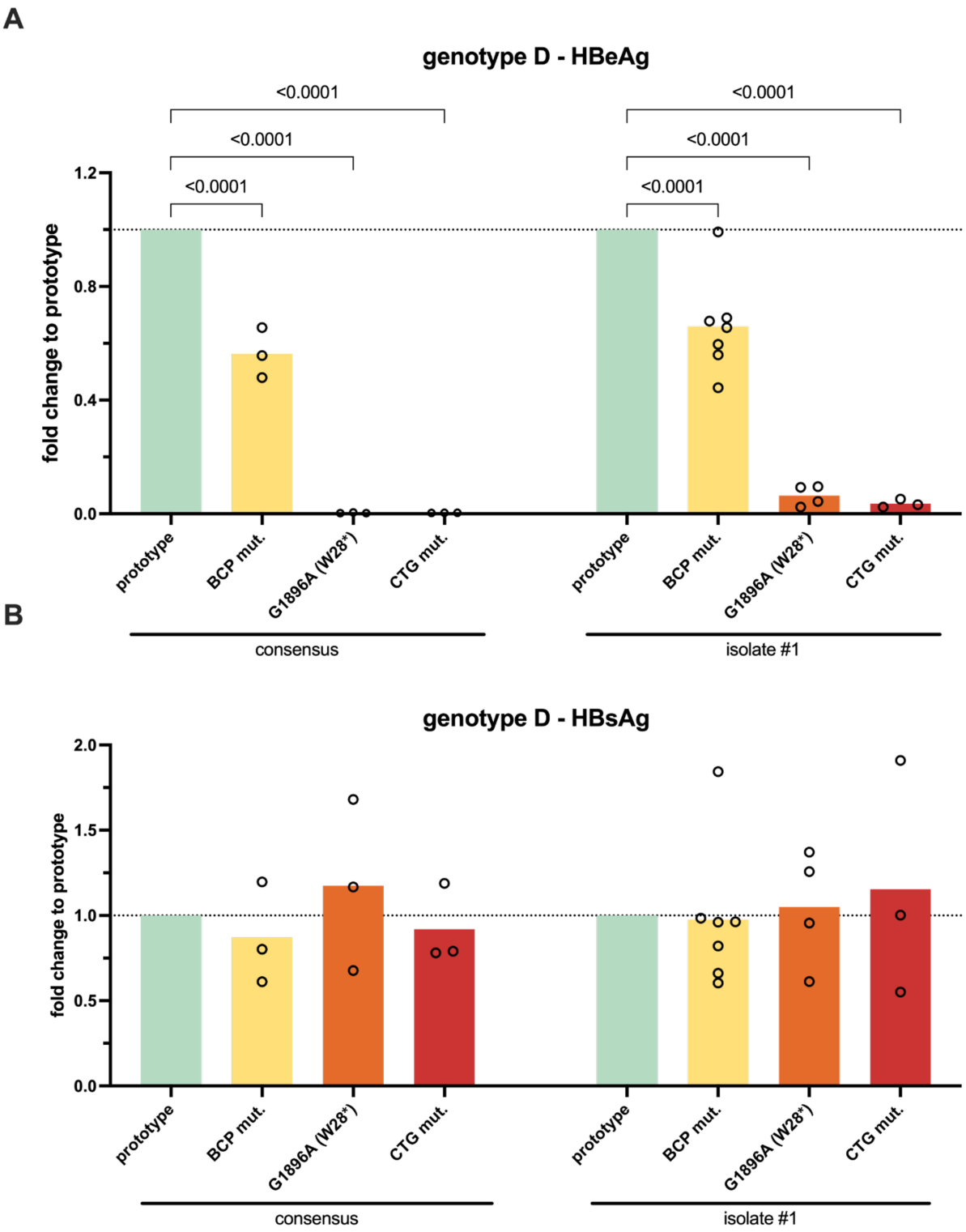

Figure 25 Genotype D HBeAg and HBsAg levels normalized to prototype: Graphical representation of genotype D isolate #1 and consensus HBeAg-altering variants normalized to the prototype variant on the fourth day of individual experiments. The variant's S/CO ratio was normalized for each experiment to the prototype S/SO ratio (fold-change). The pointed line represents the prototype (1x). The variants were labeled as follows: Prototype (green), BCP double mutation (yellow), G1896A stop-mutation (W28*) (orange), and CTG mutation (red). Statistical significance was calculated using a one-way analysis of variance. Statistically insignificant values were not stated. Panel A) HBeAg in genotype D consensus and isolate #1 normalized to prototype on the fourth day after transfection. Panel B) HBsAg in genotype D consensus and isolate #1 normalized to prototype on the fourth day after transfection.

As observed in genotype A (Figure 24), the HBsAg levels remained consistent between the prototype and the HBeAg-altering variants, indicating no significant alterations in the expression of other HBV proteins despite the reduced HBeAg levels resulting from the introduced mutations.
In detail, this meant a 13% (ns) reduction in HBsAg for genotype D consensus when the BCP double mutation was introduced. Introducing the W28* mutation led to a mean increase of 17% compared to the prototype, while the CTG mutation resulted in a mean decrease of 8%. The patient isolate #1 sequences, which contained the BCP double mutation, exhibited an average 8% reduction in HBsAg compared to the prototype, which was in line with the consensus. The variant containing the W28* mutation showed a 4% increase in HBsAg, while the CTG mutation variant displayed an average increase of 15%.

Based on these findings, it can be concluded that the HBV cell culture assay using cccDNA is a viable method for comparing different HBV variants regarding HBeAg and HBsAg expression levels. Concerning HBeAg altering mutations, no significant differences were observed between genotypes A and D. In both genotypes, the BCP double mutation resulted in a reduction but no loss of HBeAg. Additionally, in both genotypes, the W28* and the CTG mutation resulted in the loss of HBeAg.

4.3 HBV core protein staining in transfected HepG2-hNTCP

The preceding chapters have demonstrated that the HBV cccDNA assay was a viable tool that permitted the testing of various HBV variants in their native sequence context. The ease of using HBeAg and HBsAg in the supernatant as markers for the expression of viral products enabled analysis between the HBeAg-altering variants. Despite the precore protein sharing a large part of the amino acid sequence with the HBV core protein, the core protein is translated from the pregenomic mRNA [186]. Although both proteins originate from different mRNAs, both are regulated by the same promoter [187]. This makes the core protein a crucial marker to consider when analyzing HBeAg-altering mutations. Unfortunately, the HBV core protein can not be monitored similarly to HBeAg and HBsAg, so an additional assay was established. It was essential to explore whether mutations impacting HBeAg would significantly affect the expression of the HBV core protein.

4.3.1 Percentage of HBV core positive HepG2-hNTCP cells

A flow cytometry staining was established to measure the HBV core directly in the cells. HepG2-hNTCP cells were transfected with cccDNA and cultured for four days. The core protein was stained by indirect antibody staining with an HBV core-specific antibody and a secondary antibody containing an Alexa Fluor 488 fluorophore. A representative gating strategy for the HBV core staining with a selection of HepG2-hNTCP cells by forward and sideward scatter, narrowing down to single cells, and further

selection of living cells is shown in Figure 26 A. Cells were analyzed on the Alexa Fluor 488 channel and compared to the negative control (NC; Figure 26 B). For genotype A, the different variants showed similar positive rates (Figure 26 C). For genotype D, the HepG2-hNTCP population positive for the core protein was also similar between the different variants. (Figure 26 D).

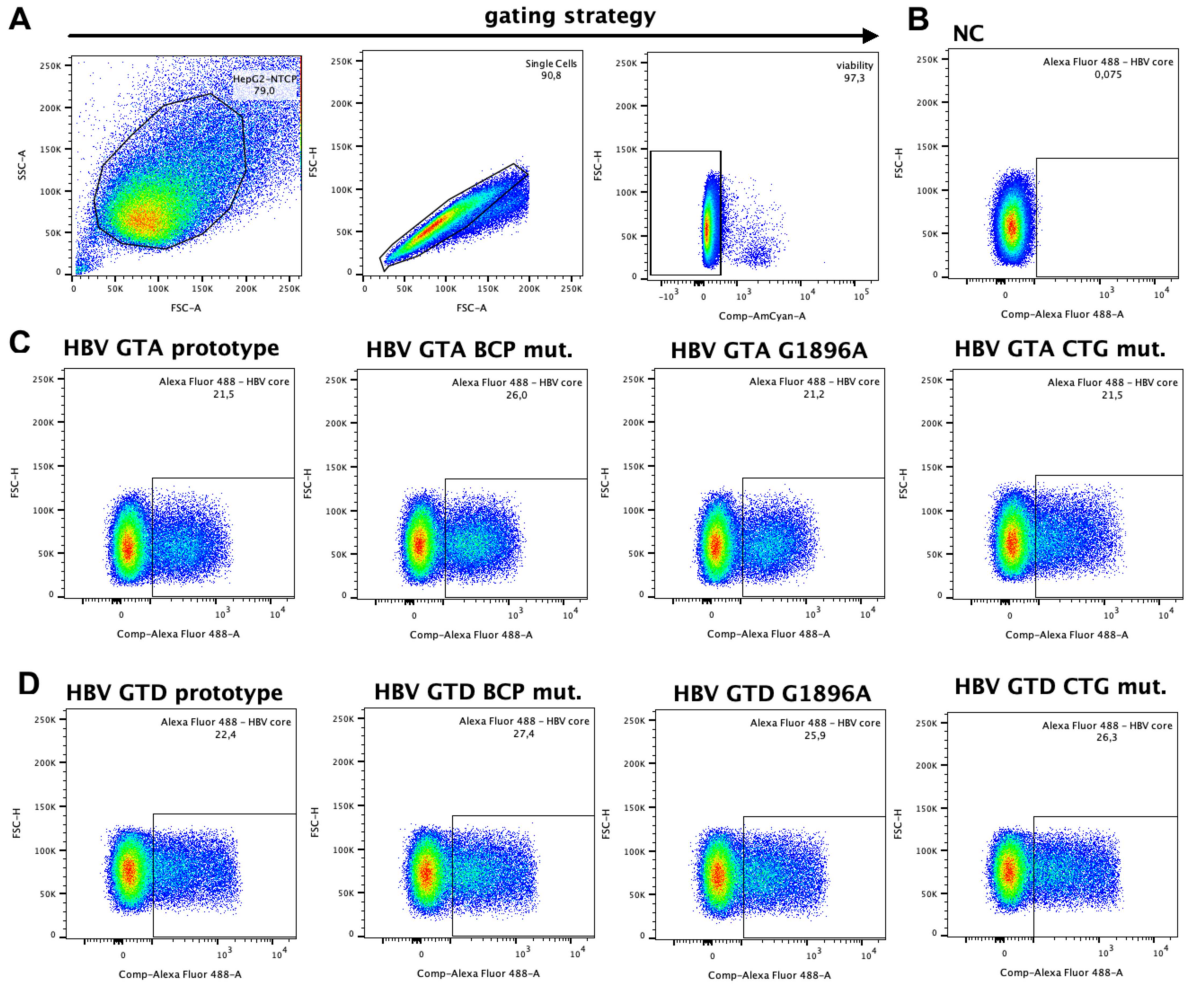

Figure 26 HBV core protein levels in HepG2-hNTCP cells transfected with different HBeAg variants: A) displays the gating strategy for the analyzed HepG2-hNTCP population. B) Intracellular HBV core protein staining in HepG2-hNTCP without transfected cccDNA. C) Intracellular HBV core protein staining in genotype A HBeAg variants. D) Intracellular HBV core protein staining in genotype D HBeAg variants.

After several repetitions, the results showed only small difference in HBV core expression between the different variants (Figure 27). In genotype A, 23.6% ± 4.8 cells were HBV core positive in the prototype variant. In the variant containing the BCP double mutation, 27.5% ± 5.6 (n = 6) of the cell populations were positive for the HBV core protein. For the W28* mutation (n = 4), the mean HBV core positive population was 21.2% ± 5.2. In the CTG mutation variant (n = 4), 26.4% ± 5.6 of the population were positive for the core protein.

In genotype D, 20.9% ± 6.4 of the cells transfected with the prototype variant were HBV core positive. Transfection of HepG2-hNTCP cells with the BCP double mutation cccDNA (n = 4) resulted in a mean of 24.4% ± 4.1 HBV core positive population. Transfecting the cells with the W28* mutation cccDNA (n = 4) resulted in a mean of 17.3% ± 7.0 HBV core positive population. Using the CTG mutation construct (n = 3) resulted in a mean of 20.6% ± 4.3 of the HBV core positive cell population. Overall, the frequency of HBV core positive HepG2-hNTCP cells was comparable for the different variants.

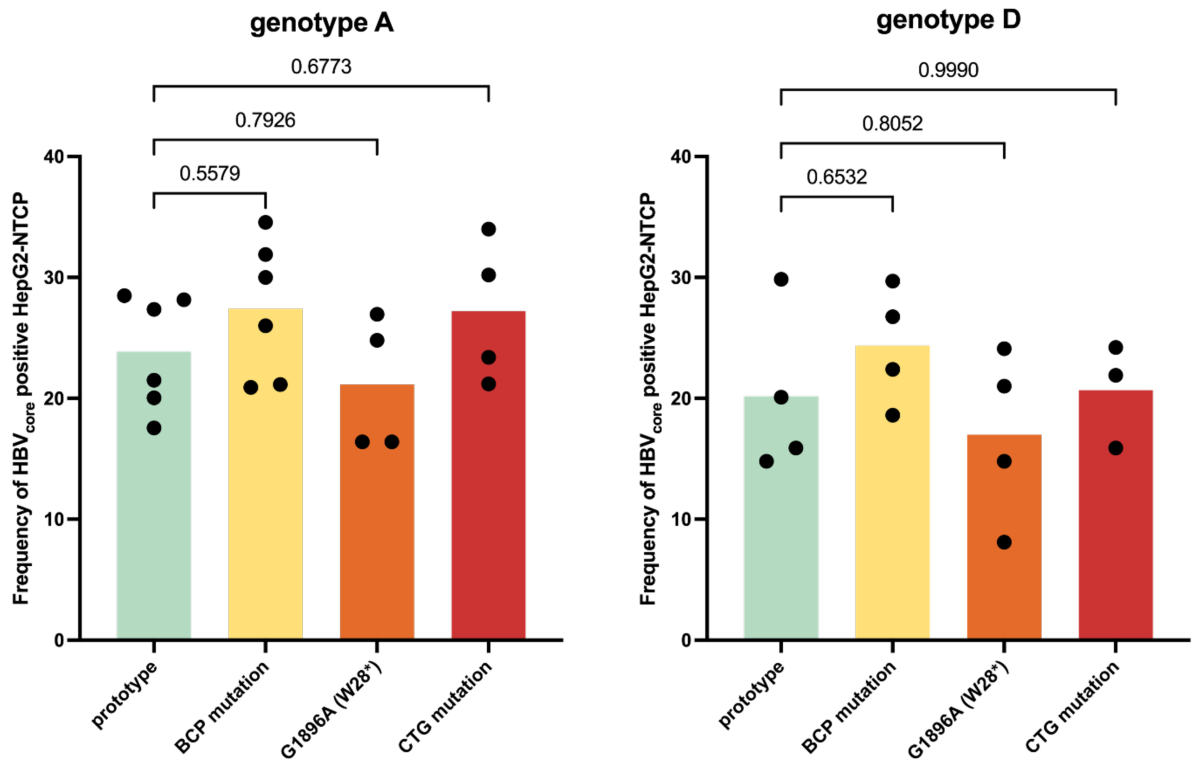

Figure 27 Frequency of HBV core protein positive HepG2-hNTCP population in genotypes A and D: The variants were labeled as follows: Prototype (green), BCP double mutation (yellow), G1896A (orange), and CTG mutation (red). Each dot represents an experiment. Statistical significance was calculated using a one-way analysis of variance.

4.3.2 Mean fluorescence intensity of HepG2-hNTCP cells containing HBV core

Besides analyzing the frequency of HBV core protein positive cell population, the mean fluorescence intensity (MFI) was examined (Figure 28). It allows to detect differences in HBV core levels inside the cells.

For genotype A prototype (n = 6), the MFI was 399 ± 75. For the BCP double mutation (n = 6), the MFI was 401 ± 60. The MFI for the W28* mutation was 280 ± 41 and therefore the lowest compared to the prototype (p = 0.0546). The CTG mutation displayed a MFI of 408 ± 94. Besides the W28* mutation, all other variants displayed similar MFI. The W28* mutation variant showed a lower MFI. The implications were not fully clear, but even if there were a reduction in HBV core levels, they were still not significant.

In genotype D, the recorded MFI closely resembled that of genotype A. The prototype variant (n =4) exhibited an MFI of 480 + 51. The MFI for the BCP double mutation (n = 4, 447 + 49) and the CTG mutation (n =3, 463 + 64) were comparable. Meanwhile, the W28* mutation in genotype D also showed the lowest MFI (n = 4, 352 ± 68), consistent with genotype A. Similar to genotype A, the decrease in fluorescence intensity was not statistically significant and was not expected to impact the display of viral epitopes significantly.

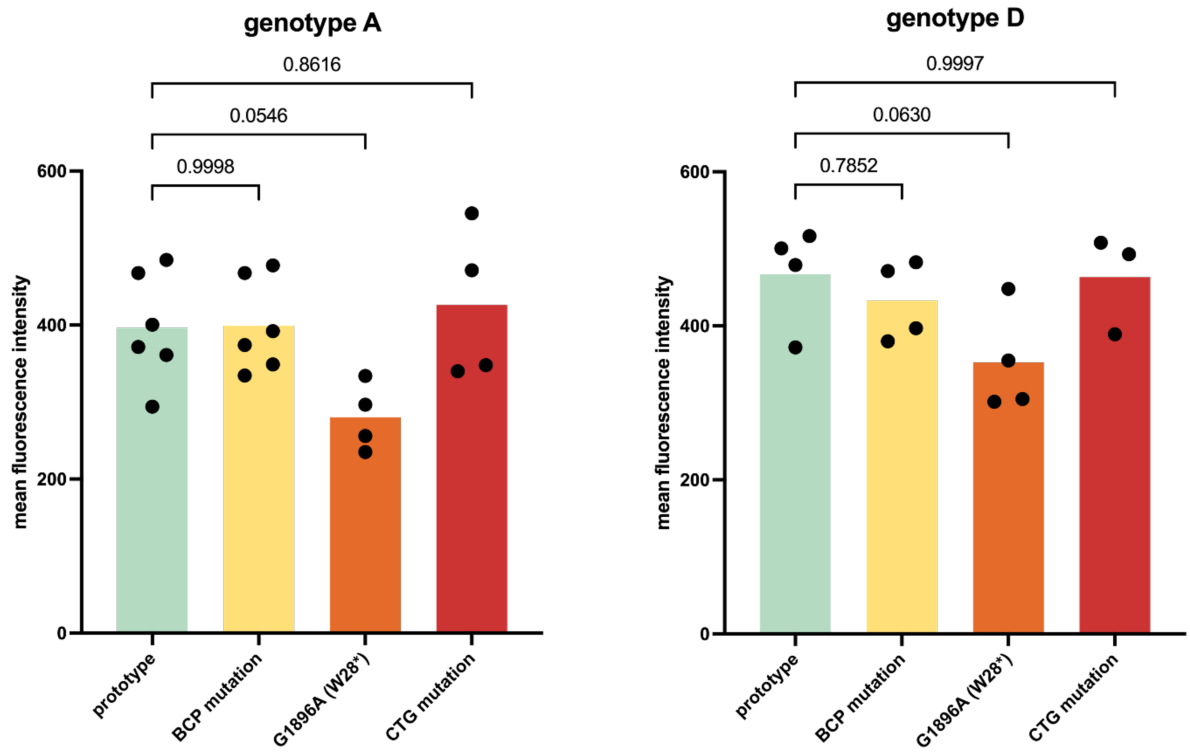

Figure 28 Mean fluorescence intensity (MFI) of HBV core protein positive HepG2-hNTCP population in genotypes A and D: The variants were labeled as follows: Prototype (green), BCP double mutation (yellow), G1896A (orange), and CTG mutation (red). Each dot represents an experiment. Statistical significance was calculated using a one-way analysis of variance. MFI was calculated with FlowJo.

4.3.3 HLA class I molecules on transfected HepG2-hNTCP cells

In the past, publications have suggested that HBeAg downregulates HLA molecules in infected hepatocytes. Due to the established assay, verifying these claims in cell culture was possible. The HepG2-hNTCP cells were stained with an HLA-ABC antibody to observe the surface expression of the HLA molecules on cells containing HBV. A representative gating startegy is shown in Figure 29. The cells were initially gated by forward and sideward scatter, then gated on single cells. Subsequently, only living cells were selected and then divided into HBV core protein negative and positive populations. For the HBV core protein-positive cells (Alexa Fluor 488 positive), the mean fluorescence intensity (MFI) of APC (anti-HLA-ABC) was calculated.

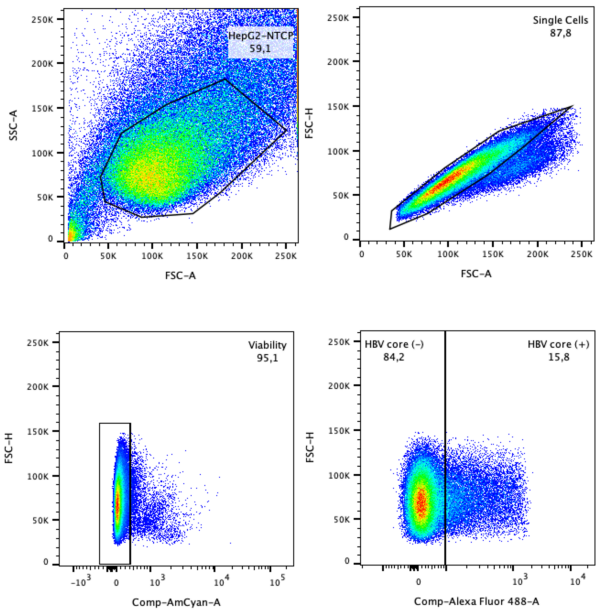

Figure 29 Gating strategy for analyzing HLA class I molecules on HepG2-hNTCP cells: HepG2-hNTCP cells were gated on forward and sideward scatter. In the next step, single cells were selected and gated to include only living cells. The living cells were separated into an HBV core positive and negative population.

Four days after transfection, the HepG2-hNTCP cells with the varying genotype A HBV isolate #2 variants were stained with an anti-HLA-ABC antibody, and the MFI was calculated (Figure 30). Non-transfected HepG2-hNTCP cells were used as a control. The different variants of genotype A isolate #2 did not show meaningful differences in the MFI between each other. Similarly, the difference between non-transfected and transfected cells was negligible. Therefore, contrary to what was suggested, it seems that in this experimental setup, at least HBeAg has no downregulatory effect on HLA molecules.

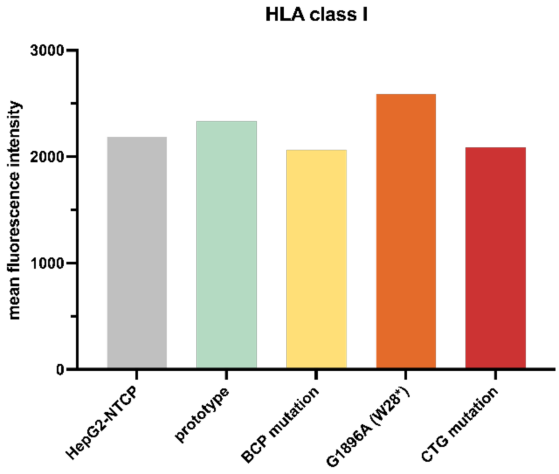

Figure 30 Mean fluorescence intensity (MFI) of anti-HLA class I (A, B, and C) antibody (APC) in HepG2-hNTCP: The MFI for the anti-HLA antibody was calculated in the HBV core positive population in cells transfected with genotype A isolate #2 variants and living cells in the control (HepG2-NTCP). The variants were labeled as follows: HepG2-NTCP (grey), Prototype (green), BCP double mutation (yellow), W28*mutation (orange), and CTG mutation (red).

In detail, for non-transfected HepG2-hNTCP cells, the MFI for the anti-HLA-ABC antibody was 2188. The cells transfected with the HBeAg prototype had an MFI of 2337. For the BCP double mutation, the MFI for the anti-HLA-ABC antibody was 2060. The HepG2-hNTCP cells transfected with the G1896A stop-mutation variant displayed the highest calculated MFI of 2586. When the cells were transfected with the CTG mutation, the MFI for the HLA-ABC antibody was 2091.

4.4 Abundance of HBeAg-derived peptides recognized by $CD8^+$ T cells

Throughout the project, it was consistently demonstrated that the different HBeAg variants deviated in the HBeAg levels found in the supernatant. The prototype variants of the two genotypes exhibited robust production of HBeAg. However, introducing the BCP double mutation in the promoter reduced HBeAg compared to the prototype. The W28* and the CTG mutation led to a near-complete loss of HBeAg in the supernatant. All this while the HBsAg levels in the supernatant remained unaffected, indicating no systematic reduction in transcription or translation. Furthermore, the project demonstrated that the intracellular HBV core protein levels for the HBeAg-altering variants were similar to those of the prototype variant.

With this information in place, the objective was to explore the significance of HBeAg in the viral immune evasion from the adaptive immune system. Although HBV-specific $CD8^+$ T cells play a critical role in the immune control of a hepatitis B virus infection [122], they display an exhausted (HBV polymerase specific $CD8^+$ T cells) or memory-like (HBV core specific $CD8^+$ T cells) state during chronic HBV infections [139]. In the event of an HBeAg seroconversion, there is typically an increase in liver inflammation in combination with reduced viral replication [188] and activation of $CD8^+$ T cells [189]. It appears that during the HBeAg-positive chronic infection, there is a state of "tolerance" from the immune system. Even though the perceived tolerance and rise of activated $CD8^+$ T cells are linked to the HBeAg status, it is unclear how and if the HBeAg itself is involved. This project aimed to investigate the involvement of HBeAg-derived peptides in the recognition of infected cells by $CD8^+$ T cells.

To recap, the HBeAg precursor, even though it is translated from a different transcript than the core protein, shares its amino acid sequence. Therefore, the question was whether peptides of both proteins could be presented at the surface of infected cells by HLA class I molecules and recognized by core-specific $CD8^+$ T cells. Fortunately, the immunodominant HLA-A*02 restricted core-specific $CD8^+$ T cell epitope against the FLPSDFFPSV sequence at the core protein's amino acid position 18 to 27 (HBc_{18-27}) is well described [146], and a corresponding epitope-reactive T-cell receptor sequence is available [163].

A modified reporter cell line was used to investigate whether mutations that reduce HBeAg production also reduce epitope abundance. Prof. Dr. Mirjam H.M Heemskerk from Leiden, Netherlands, developed the reporter cell line. The reporter cell line is a Jurkat cell initially selected for lacking the endogenous T-cell receptor alpha and beta genes. The cells were further modified to express CD8 on the cell surface and gained the ability to produce eGFP upon binding of NFkB to a response element [190]. To analyze the epitope abundance in the different HBeAg variants, the HBc_{18-27}-specific TCR was introduced, and the activation of the reporter cell line was compared (Figure 31).

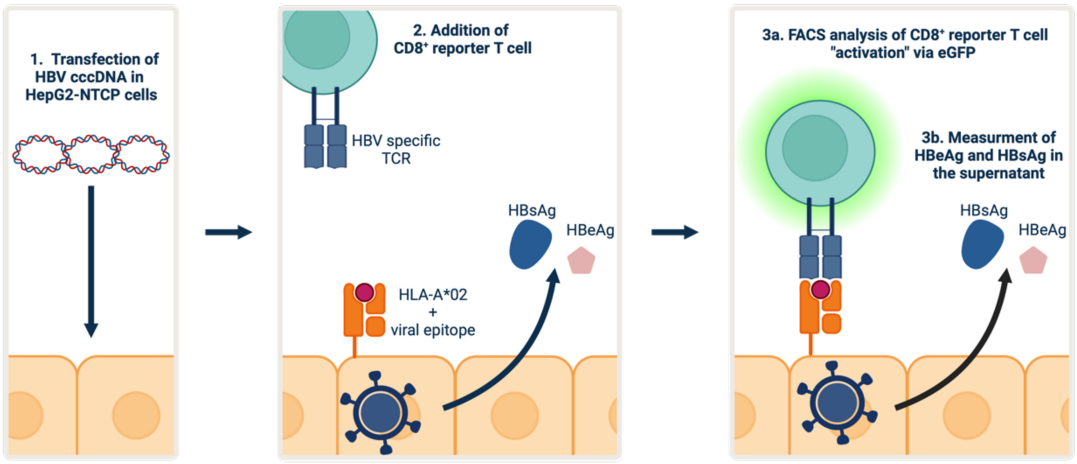

Figure 31: Graphical representation for Jurkat 76 mono NFkB reporter cell line activation upon binding to the HLA-A*02 restricted viral epitope.

4.4.1 Generating the HBV $core_{18-28}$ specific reporter cell line

Initially, the human T-cell receptor's (TCR) alpha and beta constant regions were substituted with a corresponding murine constant region, significantly improving the presentation on the cell surface due to better TCR/CD3 stability [164,165]. Prof. Ulrike Protzer kindly provided the murine constant region sequence. Subsequently, during the MOI-funded stay abroad in Leiden, retroviruses carrying the TCR alpha and beta gene sequence information were generated by transfecting Pheonix-GALV cells. The retroviruses were harvested and utilized to transduce J76 mono NFkB cells (J76mNFkB). The successful transduction was confirmed using an anti-mouse TCR beta (mTCRb) antibody, as the wild-type J76mNFkB cells lacked murine TCR on the cell surface (Figure 32 A).

As can be seen in Figure 32 B, the transduction worked well with 49.3 % of the cells expressing the murine TCR beta constant region on the cell surface. To increase the number of J76mNFkB cells containing the HBV-specific TCR, they were sorted via magnetic beads (MACS) separation (Figure 32 C). This increased the number of J76mNFkB cells possessing the HBc_{18-27} TCR to 96.7 %. After enrichment with MACS, the HBV core-specific TCR functionality presented on the J76m NFkB was tested in combination with K562 cells, which are frequently used as antigen-presenting cells (APC) that can present exogenously loaded peptides [191].

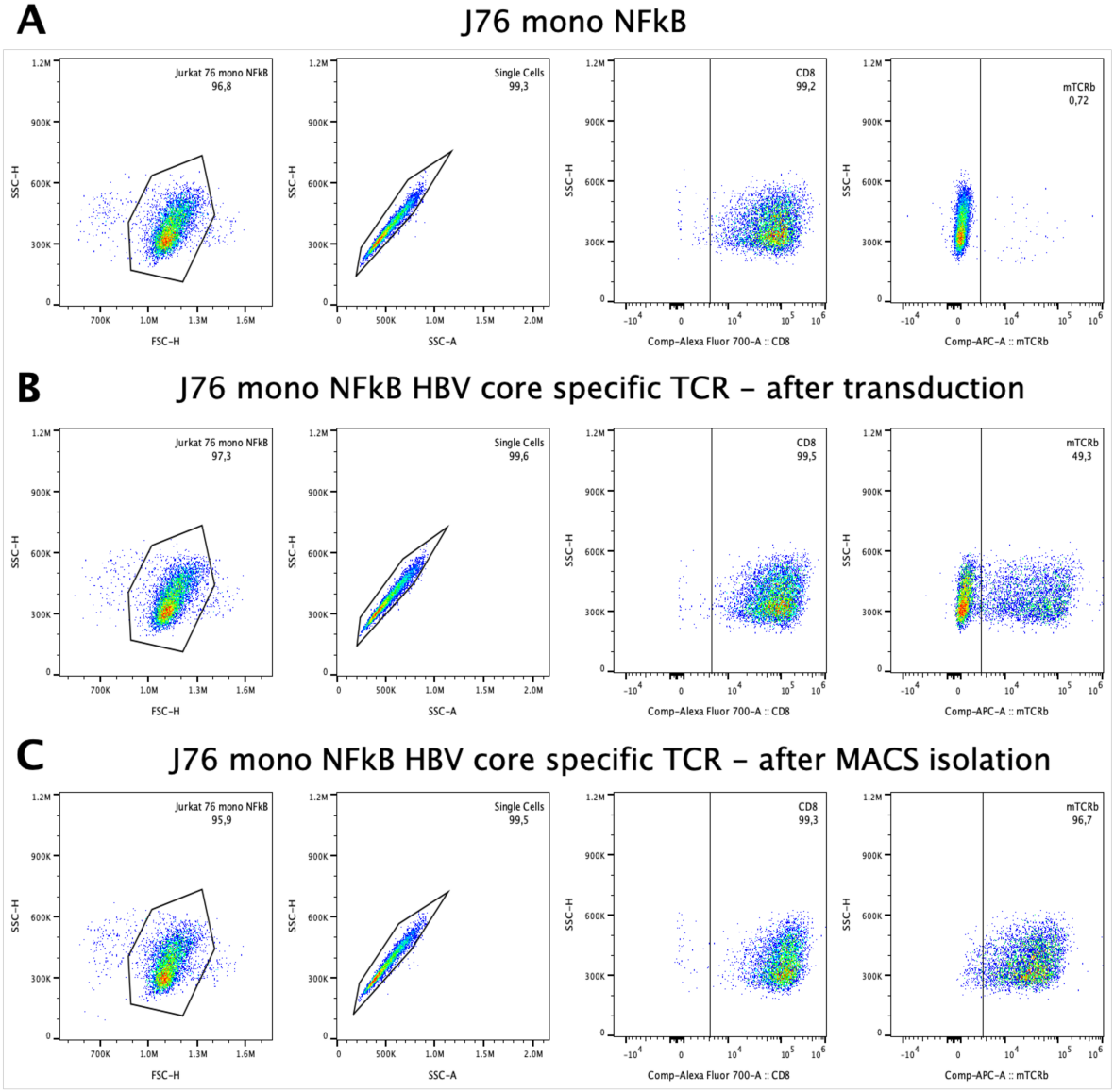

Figure 32 Creation of J76 mono NFkB cells expressing the HBc_{18-27} specific T-Cell receptor (TCR): A) represents the flow cytometry analysis of wild-type J76 mono NFkB cells. B) displays the flow cytometry analysis of J76 mono NFkB cells expressing the HBc_{18-27} specific TCR after transduction. C) A display of the flow cytometry analysis of the J76 mono NFkB cells expressing the HBc_{18-27} specific TCR after magnet-activated cell sorting (MACS) with a murine TCR beta chain positive population increase.

Due to low stimulus of the NFkB pathway through the growth factors in the culture medium unstimulated cells positive for eGFP could be detected (Figure 33 A) After stimulating the cells with TransAct, an artificial T cell activation reagent, 93.8 % were activated after 12 hours (Figure 33 B) demonstrating a functioning TCR signaling pathway and acted as a control for the NFkB response element. To evaluate the recognition of the specific HBc_{18-27} epitope, the peptide was loaded on K562-HLA-A*2 cells and incubated for 12 hours with the J76mNFkB containing the HBc_{18-27}-specific TCR. 39.0 % of the cell population was activated (Figure 33 C). Activation of J76mNFkB by K562-HLA-A2 with the HBc_{18-27} peptide demonstrated the functionality of the TCR.

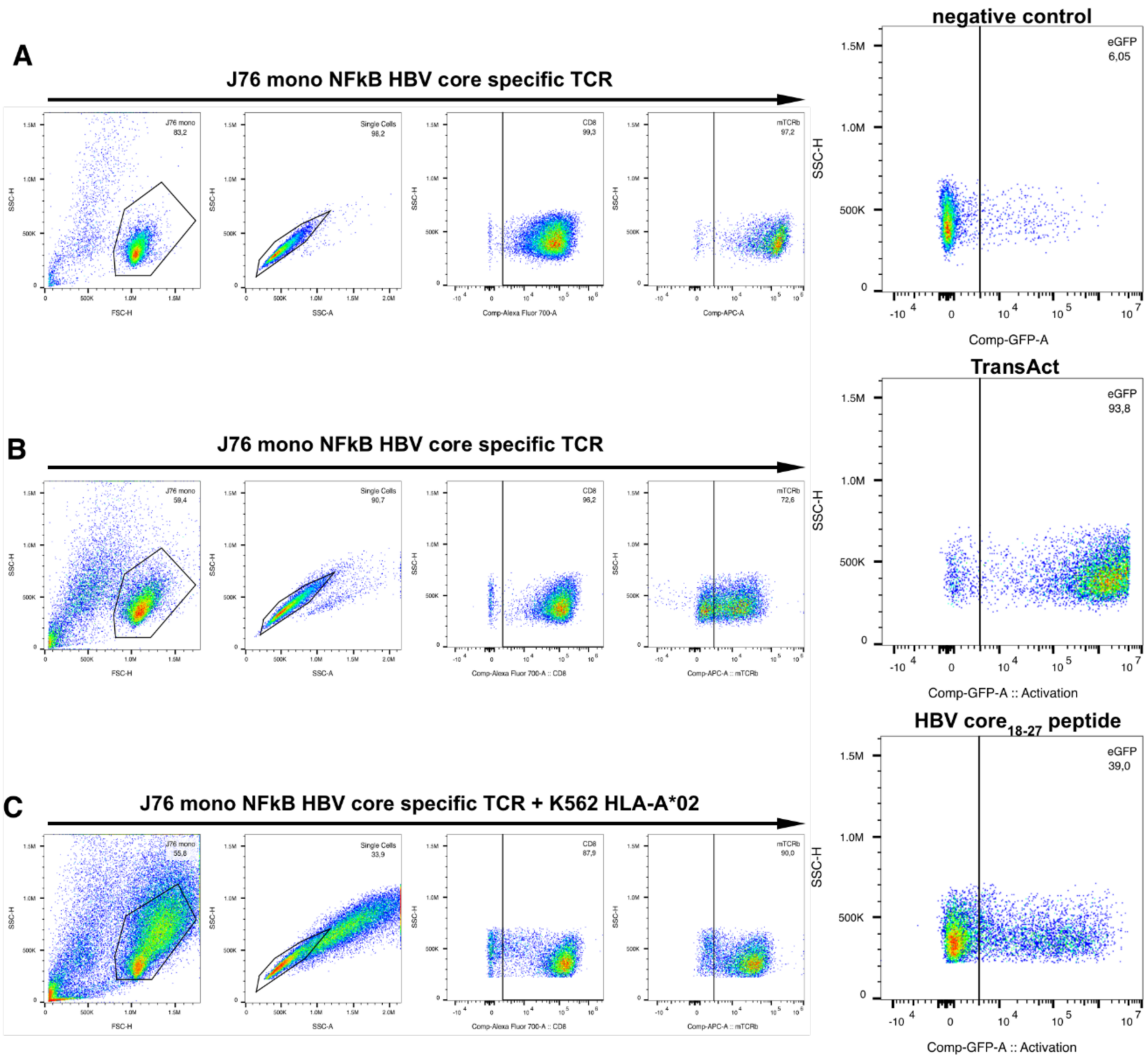

Figure 33 Gating strategy and activation of J76 mono NFkB cells expressing the HBc_{18-27} specific T-Cell receptor (TCR) with TransAct or exogen peptide: A) gating strategy and activation profile of J76 mono NFkB cells with HBc_{18-27} TCR when cultured. B) Gating strategy and activation profile of J76 mono NFkB cells with HBc_{18-27} TCR after activation via TransAct for 12 hours. C) Gating strategy and activation profile of J76 mono NFkB cells with HBc_{18-27} TCR after co-culture for 12 hours with K562-HLA-A*2 cells loaded with FLPSDFFPSV peptide.

4.4.2 Evaluating the function of the HBV $core_{18-27}$ specific TCR

Although the functionality of the T-cell receptor (TCR) was previously tested using exogenously presented peptides on K562 cells, it was critical to investigate the functionality of the TCR with endogenously processed peptides from expressed core proteins. Further, the specific epitope was not only used as it was well described and had a TCR sequence available but there was also a known HLA-A*02 restricted escape substitution present, changing the amino acid phenylalanine (F) to tyrosine (Y) at position 24 (F24Y) [192].

Therefore, HepG2 cells stably expressing the HBV core protein prototype ($core_{wt}$) or a variant containing the F24Y substitution ($core_{F24Y}$) were used to activate the J76mNFkB cells (Figure 34 A). The cells expressing the $core_{wt}$ were able to activate a mean of 14.7 % (n = 4) $core_{18-27}$-specific J76m NFkB cells.

In contrast, the cells expressing the $core_{F24Y}$ activated a mean of 0.4 % (n = 4) of the $core_{18-27}$-specific J76m NFkB cell population. The reduction in activated reporter cells was statistically significant (p = 0.0010).

Subsequently, the reporter cells were tested in the HBV assay containing the genotype D isolate #1 prototype construct and the same construct with the addition of the F24Y substitution (Figure 34 B). In the assay, the transfected prototype variant activated a mean of 7.2 % (n = 3) of the HBc_{18-27}-specific reporter cells. The same variant containing the F24Y mutation resulted in a mean activation of 0.1 % of the reporter cells. The reduction in activated reporter cells was statistically significant (p = 0.0312).

The results indicate that the reporter cells recognized the endogenously presented core peptide from the prototype variants in the tested cells and the HBV assay. However, introducing the known escape substitution F24Y, resulted in both set-ups to the (near) loss of recognition of the peptide on the cell surface.

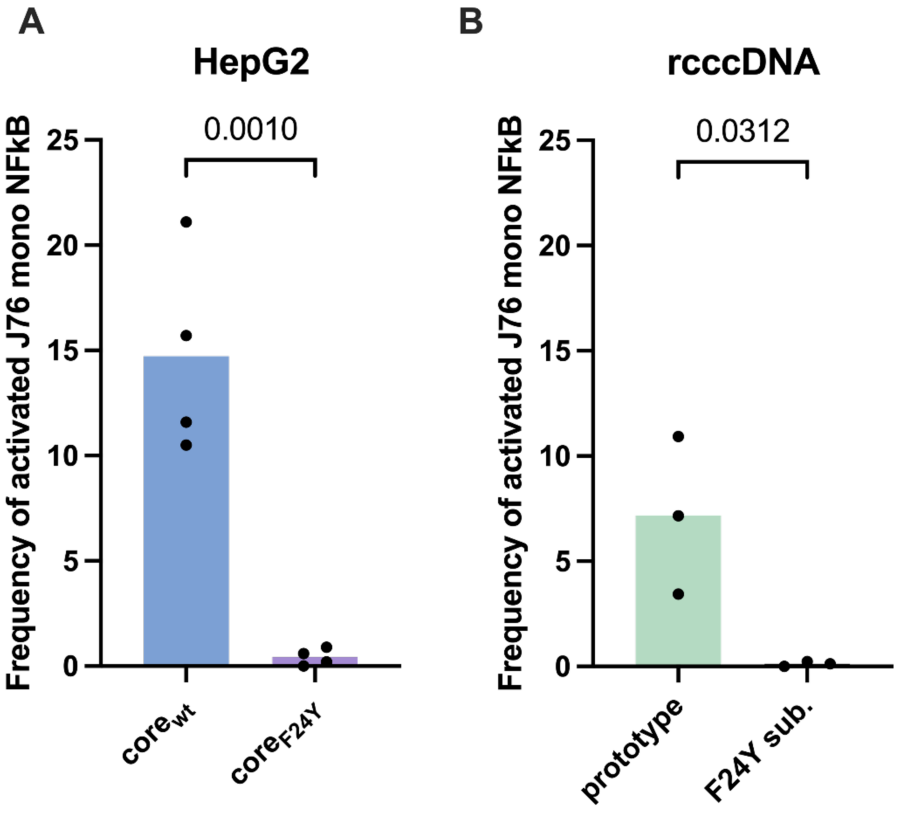

Figure 34 Frequency of activated J76 mono NFkB HBc_{18-27} TCR cells co-cultured with different HepG2 variants: A) Frequency of activated J76 mono NFkB HBc_{18-27} TCR cells co-cultured with HepG2-151 (blue, $core_{wt}$, n= 4) and HepG2-152 (purple, $core_{F24Y}$, n = 4). B) Frequency of activated J76 mono NFkB HBc_{18-27} TCR cells co-cultured with HepG2-hNTCP cells transfected with genotype D isolate #1 prototype (green, n = 3) and prototype with the F24Y mutation (black, F24Y sub.; n = 3). Statistical analysis was conducted by t-test using GraphPad prism.

4.4.3 Abundance of HBeAg as dominating factor for activation of HBV core-specific TCR

Using the data gathered from past experiments, the question of whether the loss of HBeAg decreases the core-specific epitope abundance could now be examined. The experiment involved transfecting HepG2-hNTCP cells with the cccDNA from the different HBeAg variants and incubating the cells for three days. Late in the evening of the third day, the Jurkat 76 mono NFkB cells containing the recombinant T-cell receptor (TCR) were added. The cells were prepared for flow cytometry and analyzed on the morning of the fourth day.

Reporter cells containing an HBV core-specific TCR

For genotype A, the activation of the reporter cells was examined with isolate #2. Transfecting the HepG2-hNTCP cells with the prototype variant and co-culturing the reporter cells led to a mean activation frequency for the reporter cell of 6.3 % (Figure 35 A). Co-culturing the reporter cells with the HepG2-hNTCP transfected with the BCP double mutation variant resulted in an activation of 4.4 %. Therefore, when the HBeAg level was reduced by the BCP double mutation, it affected the frequency of activated reporter cells containing the HBV core-specific TCR. Although there was a reduction, it was statistically not significant ($p = 0.3367$). In HepG2-hNTCP cells with the W28* mutation variant, only 0.8 % of the reporter cells could be activated. Therefore, the loss of HBeAg due to introducing the W28* mutation resulted in a statistically significant reduction ($p = 0.0017$) of activated reporter cells compared to the prototype.

The activation frequency of the reporter cells carrying the HBV core TCR was further assessed in variants of genotype D isolate #1 (Figure 35 A). When the reporter cells were co-cultured with HepG2-hNTCP cells transfected with the prototype variant, the mean frequency of activated cells was 5.7%. In HepG2-hNTCP cells transfected with a variant containing the BCP double mutation, only 3.2 % of the reporter cells were activated. As observed in genotype A, a decrease in HBeAg levels resulting from the BCP mutation also led to a reduction in the frequency of activated reporter cells. However, the reduction in activation compared to the prototype was not statistically significant ($p = 0.0904$).

When examining the W28* mutation, which leads to the near loss of HBeAg in the supernatant, only 0.9 % of reporter cells were activated. This represents a statistically significant ($p = 0.0010$) reduction compared to the prototype variant.

Consequently, within the study design, the loss of HBeAg as a result of the described HBeAg-altering mutations significantly influenced the frequency of activated reporter cells containing an HBV core-specific T-cell receptor.

Reporter cells containing an HBV surface-specific TCR

To rule out that the different core variants influence global epitope processing or presentation, a TCR against the HBsAg-derived epitope was used as a control. Therefore, a J76 mono NFkB cell line containing a T-cell receptor (TCR) specific for the surface$_{370-379}$ (HBs$_{370-379}$) epitope (SIVSPFIPLL) was created. The T-cell receptor sequence used in this project was published by Antonio Bertoletti [163]. As for the core-specific TCR, the human constant region on the HBV surface-specific TCR was exchanged for a murine constant region.

The frequency was measured when co-culturing the J76 mono NFkB cells containing the HBs$_{370-379}$ specific TCR with HepG2-hNTCP transfected with HBeAg variants in genotype A isolate #2 (Figure 35 B). In combination with the prototype variant, 3.6 % of the reporter cells were activated. Similar activation levels were achieved with the BCP double mutation (3.8%) and the W28* mutation (3.2%). In co-culturing the HBs$_{370-379}$ reporter cells with HepG2-hNTCP cells containing genotype D isolate #1 prototype, 3.6 % of the reporter cells were activated. Using the BCP double mutation, 3.8 % of the reporter cells were activated. The W28* mutation resulted in an activation of 3.6% of reporter cells. The change in the frequency of activated reporter cells from the prototype to the HBeAg-altering mutations was not significant in genotype A (BCP mutation: $p = 0.9437$; W28* mutation: $p = 0.6160$) or genotype D (BCP mutation: $p = 0.9437$; W28* mutation: $p = 0.9988$).

This indicates that the changes due to the HBeAg-altering mutations do not affect epitopes from other viral proteins.

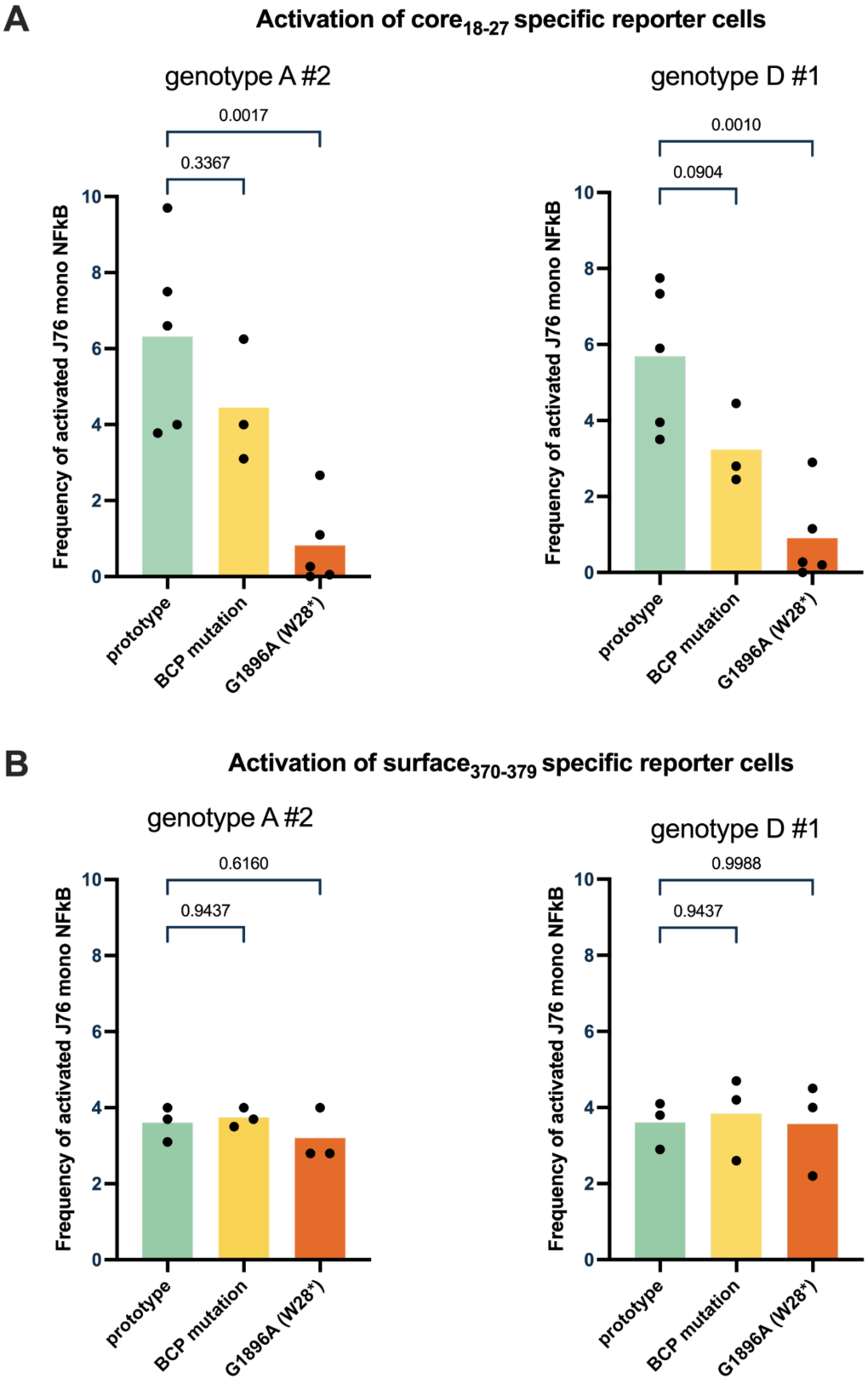

Figure 35 Frequency of activated J76 mono NFkB HBc_{18-27} TCR and $HBs_{370-379}$ TCR cells co-cultured with HepG2-hNTCP cells transfected with HBeAg variants: The HBeAg variants were labeled as follows: Prototype (green), BCP double mutation (yellow), and W28* (orange). A) Mean frequency of activated J76 mono NFkB HBc_{18-27} co-cultured with HepG2-hNTCP cells transfected with HBeAg variants from genotype A isolate #2 and genotype D isolate #1. B) Mean frequency of activated J76 mon NFkB $HBs_{370-379}$ co-cultured with HepG2-hNTCP cells transfected with HBeAg variants from genotype A isolate #2 and genotype D isolate #1. Statistical significance was calculated using a one-way analysis of variance.

5 Discussion

As viruses require a host cell for replication, the different viral realms developed many ways to achieve replication and evade the host immune system. The small hepatitis B virus with its overlapping reading frames is no different. The virus can only infect hepatocytes, the primary parenchymal tissue of the liver, in humans and a few apes [193]. HBV binds to the sodium-taurocholate cotransporting polypeptide (NTCP), and the virus is released into the host cell cytoplasm. The discovery of NTCP [68] was a critical achievement and fuelled the hope for better cell culture replication models. Indeed, the knowledge helped to advance the understanding of entry for the virus [194–196] and improved the infectivity of hepatoma cell lines [197]. However, cell line infection remains challenging despite these advances, with low reinfection rates compared to in vivo infection, indicating that some parameters are still missing.

Further down the line in the replication, the nucleocapsid containing the relaxed circular DNA (rcDNA) is transported to the host cell nucleus, and the rcDNA is released. The rcDNA is repaired to form the covalently closed circular DNA. The cccDNA serves as the template for all viral transcripts and is also the initiation point of the cell culture assay established during this project. The idea for using the cccDNA during this work was to have a method to introduce HBV into hepatoma cell lines that would be more flexible in modifying the genome compared to the production of viral particles and, at the same time, relying on the natural transcription mechanics compared to other DNA originating HBV models that use foreign sequences [89,90]. The viral transcripts consist of the pregenomic RNA (pgRNA), which serves as the template for the viral genome, as well as the viral polymerase and core protein (HBc). The PreS1/preS2/S mRNAs translate into the different HBsAgs found on the viral envelope and are secreted in high amounts into the serum [198]. The HBsAg is an important serological marker as its loss indicates the clearance of an acute HBV infection and a functional cure from therapy. Further, it was used to monitor the progression of the cccDNA HBV model. Another transcript from the cccDNA is the precore mRNA, which translates into the Hepatitis B virus e-antigen (HBeAg). HBeAg is secreted from infected hepatocytes and has, among other things, an immunomodulatory function [60]. Moreover, HBeAg is an important factor leading to the persistence of the virus [141]. Despite its immunoregulatory function, HBeAg can be lost during chronic infection, leading to what is known as the HBeAg seroconversion. This phenomenon is accompanied by a decrease in the viral load [92] and an increase in $CD8^+$ T cell selection pressure against HBc [140].

This project aimed to investigate the correlation between the Hepatitis B virus e-antigen (HBeAg) and the emergence of $CD8^+$ T cells, specifically whether HBeAg is responsible for the abundance of HBV core-specific $CD8^+$ T cell epitopes. In this chapter, the findings of this project will be discussed and their implications for our scientific understanding of the hepatitis B virus.

5.1 HBeAg, its mutation, and the worldwide distribution

HBeAg is derived from the precore protein. The precore protein comprises the HBc amino acid (aa) sequence and a 29 aa-long N-terminal extension. The first 19 aa belongs to a signal peptide cleaved during maturation. HBeAg is not translated from the same RNA as HBc, and in its mature form, it still consists of a ten aa long N-terminal extension but lacks most of the C-terminal domain found in the HBc. In a 2020 editorial, Wolfram Gerlich, Dieter Glebe, Anna Kramvis, and Lars Magnius argue that the protein should not be called precore or HBeAg, falsely suggesting a precursor to HBc and, in the worst case, mistaken for the envelope protein [22]. They argue that although the two proteins share large parts of their sequence, they have different non-overlapping functions. HBc's purpose is the initiation of the encapsidation of the pgRNA and the nucleocapsid formation.

On the other hand, HBeAg can not form the nucleocapsid and is repeatedly shown to have immunoregulatory functions [60]. Besides its function, HBeAg is a serological marker that can vanish from the patient's blood [199]. When HBeAg is lost, and anti-HBeAg is detected, it is referred to as HBeAg seroconversion. In the case of an acute infection, it can be an early indication of viral clearance [66]. However, during chronic infection, HBeAg seroconversion may only occur after several years or even decades. The Duesseldorf cohort includes patients of genotypes A, B, C, D, and E, with a majority being HBeAg-negative. The HBeAg status can be attributed to the cohort's average age of 41 years and the more significant presence of genotypes A and D.

Several studies reported that in Europe, the Mediterranean, and Africa, 90% of chronically infected patients over 20 years had an HBeAg seroconversion [200–202]. However, in Asia, only 5% of those chronically infected at the same age showed HBeAg seroconversion, as reported by Hadzyannis in 2011 [203]. In separate studies, it was demonstrated that the average age for seroconversion was 27 years for genotype B and 35 years for genotype C [107,110]. In a European cohort, the mean age for HBeAg seroconversion was 19.5 years for genotype A and 18 years for genotype D [204]. It is interesting to note that a significant number of Danish HBV patients, including genotypes A, B, C, and D, did not show any differences in the age for HBeAg seroconversion despite belonging to different genotypes. The study suggests that factors other than genotype may play a role in the rate of HBeAg seroconversion [205]. In the Dusseldorf cohort, genotype C has the lowest number of HBeAg seroconverted patients. However, since the number of patients with genotype C is small, other factors not considered in the analysis may also play a role. Regardless of any differences in the rate of HBeAg seroconversion between the genotypes, it should demonstrate that with an average age of 41 years, many of the patients enrolled in the Duesseldorf cohort should be HBeAg negative.

Two mutations are often described to be found in virus sequences of HBeAg-negative patients. The first is a mutation at the nucleotide position in 1896, changing a guanine to an adenine (G1896A) [170]. The change in nucleotide results in a change of codon from TGG representing tryptophan (W) to TAG

(W28*), resulting in the Amber stop codon on the penultimate codon of the precore N-terminal extension [171]. Introducing a stop codon will abort the translation into the precore protein from the precore RNA. The other mutation, the basal core promotor double mutation (BCP mut.), consists of two nucleotide exchanges at positions 1762 and 1764 on the HBV genome. At nucleotide position 1762, an exchange from adenine to thymine (A1762T) occurs, and at nucleotide position 1764, an exchange from guanine to adenine (G1764A) occurs [172,173].

Contrary to the Amber stop codon, the BCP mutation only reduces HBeAg levels and does not suppress HBeAg [206,207]. Other rare HBeAg-altering mutations are described in the literature. In African sequences, a Kozak mutation was found at nucleotide position 1808 – 1813 that, similar to the BCP double mutation, reduces HBeAg levels. The Kozak sequence mutation was detected in HBeAg-positive acute infected patients in similar frequency as in chronically infected patients, suggesting a conserved mutation found in specific groups and not selected by immune pressure and not playing a part in the HBeAg seroconversion [208]. Also mainly described in African patients is a mutation in the signal peptide sequence of precore at nucleotide position 1862, changing guanine into thymine (G1862T). Besides the observation that in cell culture, the mutation leads to an intracellular accumulation of HBeAg and only a reduction in the serum, little is known [209]. The mutation was not considered in the analysis of HBeAg mutations in the Duesseldorf cohort as it was not present, and similar to the Kozak mutation, it is believed that this mutation plays no role in HBeAg seroconversion.

Besides the two mentioned mutations, in the Duesseldorf cohort, several mutations were found in the precore start codon at the nucleotide position 1814-1816. In the literature, information about these mutations is scarce and only described in a few Asian patients [210–212] and a larger group of HBeAg-negative patients infected with genotype A from Rwanda [213]. What gathered interest in the precore start codon mutations was that the different HBeAg mutations are not equally distributed between the genotype. The G1896A (W28*) stop-mutation was the most prevalent in genotypes B, C, D, and E but was rare in genotype A. The BCP double mutation and precore start codon mutations were more frequent in genotype A compared to genotypes B, D, and E. The reason for the low frequency of G1896A mutations in genotype A is another mutation in the precore at nucleotide position 1858. In genotypes A and F, most sequences contain a cytosine at position 1858; in genotypes D, B, and C, thymine is found at the same position [214]. The combination between the nucleotides at the positions 1858C and 1896G does not play a role in HBeAg. However, it belongs to the epsilon stem loop on the pregenomic RNA (pgRNA), which is highly important for localizing the viral polymerase [66]. The introduction of the G1896A stop-mutation in sequences containing 1858C destabilized the epsilon stem loop of the pgRNA [176]. This explains the low frequency of G1896A stop-mutations in genotype A of the Duesseldorf cohort, as most contain the 1858C variant. Still, the HBeAg seroconversion is observed

in genotype A at similar rates to genotype D [203,204]. In the cohort, most HBeAg negative genotype A sequences contain the BCP mutation, which aligns with other studies [215,216] where they found that 40% and 32% of the analyzed sequences contain the BCP double mutation. Both studies do not explain why large proportions of their genotype A HBeAg negative samples do not display the BCP double nor G1896A stop-mutation. In the Duesseldorf cohort, most of the HBeAg negative sequences that do not contain a BCP or G1896A stop-mutation could be attributed to the precore start codon mutations. Therefore, it was proposed in this project that other mutations, especially the precore start codon mutations, could account in some form for the HBeAg seroconversion in genotype A. Besides a higher frequency of BCP double mutations in genotype A, the cohort displayed the highest frequency in genotype C. This is also in line with the literature where it was found in 25 % of genotype C sequences compared to 7 % of genotype B in Malaysian patients [217] or 40 % (genotype C) compared to 27 % (genotype B) in Vietnamesian patients [218].

These studies and the data from this cohort show that the various HBeAg mutations are found in most HBeA-negative patients alone or in combination. Furthermore, many different studies demonstrate that the described HBeAg mutations are only found in small quantities in HBeAg-positive patients but in high quantities in HBeAg-negative patients, linking the HBeAg seroconversion with these mutations [107,205,219–222]. Nevertheless, all this demonstrates that the mutations are closely related to HBeAg seroconversion, but not why it could be an advantage for the virus.

A cccDNA HBV cell culture model was established to understand better and explain the virological advantages of the HBeAg seroconversion.

5.2 Establishing an HBV cccDNA hepatoma cell model

Despite years of research into HBV, no universal high-throughput cell culture model is available to support the entire viral life cycle. Although infection with HBV virions has been successful in primary human hepatocytes (PHH), this approach has limitations, including limited availability, no expansion in culture, and a rapid loss of susceptibility to HBV infection [87,223–225]. Further, the use of virions is not flexible when testing different variants of the same genome, as was attempted in this work. A virion-producing cell line would have to be established for each variant. As establishing a model that allowed flexible changes in the viral genome was an integral part of this work, using PHH combined with virions was ruled out.

Various plasmid-driven HBV models, using CMV as a promoter or an overlengh HBV genome, offer great flexibility for producing different variants [195,197,226,227]. Moreover, using these systems would have been much less time-consuming than the cccDNA method ultimately chosen during this work. However, the HBV plasmid systems have, besides some more negligible disadvantages, the critical disadvantage that they do not generate covalently closed circular DNA (cccDNA) in the nucleus of the

transfected cells [228–231] and therefore omitting not only the viral entry but also the formation of the cccDNA and the transcription from the cccDNA. In contrast to the plasmid systems, Guo et al. showed that artificially generated cccDNA behaves more similarly to the natural life cycle [90]. Furthermore, transfected cccDNA generates significantly higher amounts of HBsAg and slightly lower HBeAg levels than CMV-driven 1.1x HBV genome and non-CMV-driven 1.3x HBV genome systems [181], demonstrating the differences in transcription activity. For this project's aim of researching the interaction between infected cells and the HLA class I-associated immune response, a cccDNA-based method was the best option to generate realistic transcription levels.

As a result, alternative methods for cccDNA generation were explored. The most notable method for cccDNA generation entails the usage of ΦC31 DNA recombinase and I-SceI endonuclease, as reported in studies conducted by Guo et al. [90], Li et al. [232], and Yan et al. [181], or Cre/LoxP, as demonstrated by Kruse et al. [233] and Wu et al. [234]. These systems are valuable for evaluating new cccDNA-targeted therapeutic approaches. However, introducing small sequences into the genome could impact the virus's life cycle, which heavily relies on overlapping genetic information and structure. In a scholarly article by Mutz et al. [182], a method to synthesize native cccDNA was presented, albeit on a smaller scale. Ultimately, this method was selected and modified to meet the requirements of this project.

The prevalence of genotypes A and D was highest in the cohort. Consequently, the analysis was focused on these two genotypes in the cccDNA model. In order to generate HBeAg variants, two HBeAg-positive patient isolates were selected as a base for each genotype. The selection criteria for the isolates included a high viral load and the absence of mutations in the basal core promoter or precore. Furthermore, HBeAg-positive consensus sequences were generated for both genotypes. The rationale behind generating the consensus sequences was the potential to use them as a genotype-specific reference sequence, as individual isolates from patients may have unknown variations that could affect the viral life cycle. At the project's onset, there was only one mention of an HBV genotype B consensus sequence generated from 63 patient isolates from China that was able to replicate [235]. Therefore, it was necessary to clarify whether the consensus sequences generated in the present project could replicate. The project was able to demonstrate that both the genotypes A and D consensus sequences were capable of producing HBeAg and HBsAg and had the potential to function as genotype reference genomes for comparison. Subsequently, a genotype C consensus sequence was also published [236], indicating the growing interest in such reference genomes. In addition to the genotype consensus sequences, the study demonstrated that both genotype A prototypes' isolate variants could generate HBeAg and HBsAg. For genotype D, only isolate #1 could produce HBeAg and HBsAg. The analysis of the preS1/preS2/S open reading frame of isolate #2 revealed a single nucleotide mutation not present in the original isolate, indicating that the mutation must have been introduced at some stage in the

plasmid synthesis. All sequences were subsequently checked for similar mutations, but none were found.

Comparing the prototype cccDNA with other methods is complicated as different factors can affect the outcome, including the genotype, cell lines, transfection reagents, starting concentrations, or media compositions. In the literature, HBsAg levels at day four to five have been reported to range from a S/CO ratio of 4 to 100, while the HBeAg levels at the same time points range from a S/CO ratio of 4 to 20 [90,234–236]. These levels are comparable to those detected during this project for both genotypes using media containing PEG-8000 and DMSO. Unfortunately, HBV DNA levels measured during this work did not indicate signs of newly produced virions. This could be due to cccDNA in the supernatant surpassing small amounts of newly produced virions. Attempts were made to wash the cells with PBS after transfection to remove excessive cccDNA, but the HepG2-hNTCP cells did not tolerate the washing well and detached from the cell culture plate.

This could be attributed to harsher growth conditions or transfection-induced stress. In HepG2-hNTCP cells infected with virions, HBV DNA levels in the supernatant were detected [88,237]. However, for other cccDNA models, no evidence for replication was provided [90,181,233–235,238]. While it has been demonstrated that HBV DNA levels can increase in HepG2-hNTCP cells, there is no reason to believe that the cccDNA method cannot yield new HBV virions. However, the concentrations are likely low and could remain under the amount of input cccDNA still found in the supernatant.

Nonetheless, the inability to measure newly produced HBV DNA is a significant disadvantage of the cccDNA model used during this work. Recently, a group around Yu demonstrated 2023 an HBV model that uses pgRNA instead of cccDNA to transfect HepG2-hNTCP cells [239]. The elegance of this model is that the RNA is incapable of transcribing the different HBV proteins, and the presence of HBeAg, HBc, or HBsAg proves that the pgRNA was reverse transcribed into relaxed circular DNA, which was further converted into cccDNA, the only template for transcription.

Besides the problems with detecting HBV DNA, this work could prove that the cccDNA method, after introducing the HBeAg modifying mutations, could replicate the characteristics found in patients with these mutations. Introducing the G1896A mutation abolishes HBeAg secretion without interfering with HBsAg secretion. Further, it was demonstrated that introducing the start codon mutation A1814C in genotypes A and D had similar effects to the G1896A stop-mutation. Introducing the mutations made the variant incapable of producing HBeAg, all without interfering with the HBsAg production.

This is especially interesting as it indicates that the start codon mutation could indeed be a surrogate for the G1896A stop-mutation, especially in genotype A. Similar to what is written in the literature [172,206,207], single basal core promoter (BCP) mutations in this work did not influence the HBeAg production. Introducing the double mutation in the BCP region reduced but did not stop the HBeAg production. Interestingly, in a cohort of Malaysian patients, it was demonstrated that the BCP double

mutation (S/CO ratio of 108) halves the HBeAg levels compared to patients without (S/CO ratio of 217) the BCP double mutation [217]. A ratio of reduction similar to what was observed in this work with the cccDNA model.

One highly discussed topic is whether the BCP double mutation that reduces the HBeAg increases the transcription of the pgRNA and, therefore, the viral load. Several studies could demonstrate a transcriptional increase of pgRNA with the introduction of the BCP double mutation [172,173,240,241]. However, other studies did not find an increase in pgRNA transcription [242–244]. Although no pgRNA or HBV DNA levels besides the cccDNA could be measured in this work, an increased pgRNA transcription activity should increase HBc levels in the infected cells. In this project, no significant increase in HBc was observed in the BCP double mutation variant, leaning more to the side of no aggravated pgRNA transcription.

Another problem that was briefly touched on but should be addressed is the use of PEG-8000 and DMSO in the cell culture medium. While true, it was impressively demonstrated to be essential for the viral entry [88] and, therefore, must be used in methods that use infection as a starting point or have the research focus on understanding the viral entry. It seems that many groups [90,181,233–235,238], including this project, used this "entry medium" only for the reason that a complete viral life cycle should be possible, but neither being able to demonstrate reinfection of cells nor explaining why it is vital for the specific research. Due to the co-cultivation with Jurkat cells in this project, the additives had to be removed. Although the ratio between the prototype and the HBeAg variants stayed the same, the concentration of HBeAg and HBsAg increased 10-fold. This suggests that PEG-8000 and DMSO highly influence the transfection efficiency and the metabolism of HepG2-NTCP cells even though the appearance unter the microsope is unchanged. During this project, transfection efficiency tests with PEG-8000 and DMSO were conducted and demonstrated that both additives decreased the transfection efficiency significantly (Data not shown). Therefore, using PEG-8000 and DMSO should be evaluated in methods involving transfection. Hopefully, the mode of entry of the virus will be better understood in the future, making the use of the additives unnecessary.

5.3 The role of Hepatitis B e-antigen in the HLA class I associated immune escape

Even though not all the functions of HBeAg are known, there is a clear picture that it is beneficial for viral persistence. It was demonstrated that HBeAg could cross the human placenta [143] and that over 90% of infected newborns from HBeAg-positive mothers develop a chronic infection. However, fewer than 10% of infected newborns from HBeAg-negative mothers develop chronic infections [141], directly linking the progression of the viral infection to the HBeAg. At least during chronic infection, HBeAg serves as a strong HLA class II tolerogene [245,246] that can suppress the formation of anti-HBcAg directed antibodies in transgenic mice [144]. That raises the question of why the virus introduces mutations that alter the secretion of HBeAg during chronic infection.

The reason for the HBeAg seroconversion is unclear, but it is believed to be due to immunological pressure [60,247]. Predicting the onset of an HBeAg seroconversion is difficult. However, several studies showed that a decrease in HBV DNA levels and an enhanced hepatitis activity are signs of an impending HBeAg seroconversion [248–252]. One study in genotype C, a genotype known for high BCP double mutation rates in HBeAg-negative patients, demonstrated an increase in BCP double mutation five years before the HBeAg seroconversion could be detected compared to a control group [253]. That was before a decrease in HBV DNA levels or an increase in G1896A mutations was detected in those patients. The HBV DNA level decline and increased G1896A mutation could only be detected three years before the HBeAg seroconversion. A large longitudinal study in the USA demonstrated that in HBeAg-positive patients, the BCP double mutation rate significantly increased with the patient's age but stayed at similar levels in HBeAg-negative patients [216]. These findings indicate that, in some instances, the BCP double mutation could act as a stop-gap for the virus before introducing other HBeAg-altering mutations.

This project aimed to understand the implications of the HBeAg seroconversion in the context of $CD8^+$ T cell-directed immune response. To this end, a reporter cell line that produces GFP upon activation of an HBV-directed T-cell receptor was developed. With the help of the reporter cell line, the question of Whether HBeAg-derived peptides dominate the HLA-presented epitope landscape in infected hepatocytes should be clarified.

This project focused on a well-described HLA-A*02 restricted immunodominant [254] epitope FLPSDFFPSV targeted by $CD8^+$ T cells [255], which is found in the HBV core region (HBc_{18-27}). HLA-A*02 restricted substitutions in the epitope lead to viral variants that eclipse the $CD8^+$ T cell response [146]. The reporter cell line equipped with a TCR specific for the HBc_{18-27} epitope was first tested on HepG2

cells expressing HBcAg under the control of a CMV promoter containing a prototype variant and an F24Y substitution variant. The F24Y substitution in the epitope replaces the third Phenylalanine with a Tyrosine. The HBcAg-expressing cell line eclipsed a more robust reporter cell activation compared to experiments with the cccDNA. This can be attributed to a higher number of cells presenting the epitope combined with a higher concentration of HBcAg under a CMV promoter control. Compared to the prototype, the F24Y mutation led to a dramatic decrease in the reporter cell line activation. Similar but weaker observations were made in the cccDNA assay. This demonstrated the function of the $HBc_{18\text{-}27}$ epitope-specific TCR.

After establishing the reporter cell line, it was tested on various HBeAg-altering variants. When the BCP double mutation variant was introduced, the activation of the reporter cells was reduced by almost 50% compared to the prototype variants of genotypes A and D. Furthermore, when the G1896A mutation (W28*) or A1814C mutation (CTG) variant were introduced, the activation of reporter cells was reduced by around 80% in both genotypes. These results suggest that HBeAg-derived peptides may play a more prominent role in activating $CD8^+$ T cells than HBcAg-derived peptides in this setting. However, the data does not provide insight into why HBeAg-originating peptides are responsible for the majority of activated reporter cell lines. In previous studies, it was demonstrated that when artificially expressed at similar levels, HBeAg and HBcAg-derived peptides independently presented on HLA class I molecules can equally activate HBV-specific $CD8^+$ T cells in transgenic mice or endogenously presented on HepG2 cells [256–258].

These findings indicate that both proteins can be a potential source for epitopes. However, these studies did not consider potential differences in transcription for precore RNA or pgRNA due to the experimental setup.

Despite this, the results of this project align with Frelin et al.'s [247] assumption, further supporting their hypothesis that cytosolic HBeAg may be a more effective target for $CD8^+$ T cells than HBcAg. They based their assumption on the observation that HBV-specific $CD8^+$ T cells elicited only a very transient liver injury in transgenic mice expressing HBcAg in the hepatocytes compared to HBeAg-expressing transgenic mice, where the liver injury was more prolonged.

5.4 Outlook

Increasing our understanding of virus-host interactions is essential when we want to understand why this infection can develop into a chronic stage, why the virus can thrive in the so-called tolerant stage, what triggers the HBeAg seroconversion, or what the tipping point is where the immune system starts to act on the virus again.

In this project, results supported the hypothesis that although secreted HBeAg is beneficial for the virus during acute infection and establishing a chronic infection, the cytosolic HBeAg or its precursor, which are degraded to be presented as peptides on HLA class I molecules, could be a burden for the virus at some point during chronic hepatitis. The $CD8^+$ T cell-directed selection pressure on the virus significantly increases in HBeAg-negative chronic disease ([150], data in review). Selection of HBeAg negative variants could be an overarching mechanism to escape the onset of HBV-specific $CD8^+$ T cell immune response before making the development of specific mutations in the targeted epitopes necessary. Another possibility is that viruses with core mutation have no growth advantages since most of the epitopes are derived from the HBeAg.

Aligning with the findings from this project that HBeAg is responsible for a large part of the activation of the reporter cells are findings that indicate that human hepatocytes, compared to other cells, are not ideal antigen-presenting cells [259]. They further demonstrated that the quantity of viral antigen presented on HLA class I molecules is the primary factor determining a $CD8^+$ T cell response and that limited peptide concentrations on hepatocytes stimulated $CD8^+$ T cell degranulation instead of the release of cytokines. This could indicate that HBcAg-derived antigens are initially insufficient to activate a robust $CD8^+$ T cells response in HBeAg negative variants and, therefore, have a selection advantage for the virus. Still, this can only be part of the story as HLA-restricted substitutions are detected. A benefit of the loss of HBeAg compared to substitutions in the viral epitopes could be that the substitutions tend to influence viral replication, leading to a reduced viral load [175]. Although it is not entirely ruled out that HBeAg altering mutations may negatively affect viral replication, the data in this work implies that only little to no effect on HBcAg and HBsAg production is observed. Longitudinal sequence data of chronic HBV patients passing from the HBeAg-positive chronic infection into the HBeAg-positive chronic hepatitis and, further, the loss of HBeAg would be highly beneficial in understanding the evolution of HBeAg-altering mutations and substitutions in $CD8^+$ T cell-targeted epitopes.

Overall, this project's findings that HBeAg is responsible for the abundance of HBV core-specific epitopes are a first step in better understanding the mechanisms behind the HBeAg seroconversion and could help develop better HBV therapies, such as CAR-T cell based therapy.

6 Bibliography

[1] Neukamm Judith, Pfrengle Saskia, Molak Martyna, Seitz Alexander, Francken Michael, Eppenberger Partick, Avanzi Charlotte, Reiter Ella, Urban Christian, Welte Beatrix, Stockhammer Philipp W, Teßmann Barbara, Herbig Alexander, Harvati Katerina, Nieselt Kay, Krause Johannes, Schuenemann Verena J. 2000-year-old pathogen genomes reconstructed from metagenomic analysis of Egyptian mummified individuals. BMC Biology 2020;18:108. https://doi.org/10.1186/s12915-020-00839-8.

[2] Kocher Arthur, Papac Luka, Barquera Rodrigo, Key Felix M, Spyrou Maria A, Hübler Ron, Rohrlach Adam B, Aron Franziska, Kühnert Denise, et al. Ten millennia of hepatitis B virus evolution. Science 2021;374:182–8. https://doi.org/10.1126/science.abi5658.

[3] Mühlemann Barbara, Jones Terry C, Damgaard Peter de Barros, Allentoft Morten E, Shevnina Irina, Logvin Andrey, Usmanova Emma, Panyushkina Irina P, Boldgiv Bazartseren, Bazartseren Tsevel, Tashbaeva Kadicha, Merz Victor, Lau Nina, Smrčka Václav, Voyakin Dmitry, Kitov Egor, Epimakhov Andrey, Pokutta Dalia, Vicze Magdolna, Price T Douglas, Moiseyev Vyacheslav, Hansen Anders J, Orlando Ludovic, Rasmussen Simon, Sikora Martin, Vinner Lasse, Osterhaus Albert DME, Smith Derek J, Glebe Dieter, Fouchier Ron AM, Drosten Christian, Sjögren Karl-Göran, Kristiansen Kristian, Willerslev Eske. Ancient hepatitis B viruses from the Bronze Age to the Medieval period. Nature 2018;557:418–23. https://doi.org/10.1038/s41586-018-0097-z.

[4] Blumberg BS, ALTER HJ, VISNICH S. A New Antigen in Leukemia Sera. JAMA 1965;191:541–6. https://doi.org/10.1001/jama.1965.03080070025007.

[5] Blumberg BS, Phil D, Gerstley BJS, Hungerford DA, London WT, Sutnick AI. A Serum Antigen (Australia Antigen) in Down's Syndrome, Leukemia, and Hepatitis. Annals of Internal Medicine 1967;66:924–31. https://doi.org/10.7326/0003-4819-66-5-924.

[6] Prince AM. An antigen detected in the blood during the incubation period of serum hepatitis. Proceedings of the National Academy of Sciences 1968;60:814–21. https://doi.org/10.1073/pnas.60.3.814.

[7] Dane DS, Cameron CH, Briggs Moya. VIRUS-LIKE PARTICLES IN SERUM OF PATIENTS WITH AUSTRALIA-ANTIGEN-ASSOCIATED HEPATITIS. The Lancet 1970;295:695–8. https://doi.org/10.1016/s0140-6736(70)90926-8.

[8] Robinson William S, Clayton David A, Greenman Richard L. DNA of a Human Hepatitis B Virus Candidate. Journal of Virology 1974;14:384–91. https://doi.org/10.1128/jvi.14.2.384-391.1974.

[9] Will Hans, Cattaneo Roberto, Koch Hans-Georg, Darai Gholamreza, Schaller Heinz, Schellekens HŬub, Eerd Peer MCA van, Deinhardt Friedrich. Cloned HBV DNA causes hepatitis in chimpanzees. Nature 1982;299:740–2. https://doi.org/10.1038/299740a0.

[10] Gerlich Wolfram H. Medical Virology of Hepatitis B: how it began and where we are now. Virology Journal 2013;10:239. https://doi.org/10.1186/1743-422x-10-239.

[11] Tiollais Pierre, Pourcel Christine, Dejean Anne. The hepatitis B virus. Nature 1985;317:489–95. https://doi.org/10.1038/317489a0.

[12] Ganem Don, Prince Alfred M. Hepatitis B Virus Infection — Natural History and Clinical Consequences. The New England Journal of Medicine 2004;350:1118–29. https://doi.org/10.1056/nejmra031087.

[13] Hu Jianming, Seeger Christoph. Hepadnavirus Genome Replication and Persistence. Cold Spring Harbor Perspectives in Medicine 2015;5:a021386. https://doi.org/10.1101/cshperspect.a021386.

[14] Lauber Chris, Seitz Stefan, Mattei Simone, Suh Alexander, Beck Jürgen, Herstein Jennifer, Börold Jacob, Salzburger Walter, Kaderali Lars, Briggs John AG, Bartenschlager Ralf. Deciphering the Origin and Evolution of Hepatitis B Viruses by Means of a Family of Non-enveloped Fish Viruses. Cell Host & Microbe 2017;22:387-399.e6. https://doi.org/10.1016/j.chom.2017.07.019.

[15] Magnius Lars, Mason William S, Taylor John, Kann Michael, Glebe Dieter, Dény Paul, Sureau Camille, Norder Heléne, Consortium ICTV Report. ICTV Virus Taxonomy Profile: Hepadnaviridae. The Journal of General Virology 2020;101:571–2. https://doi.org/10.1099/jgv.0.001415.

[16] Galibert Francis, Mandart Elisabeth, Fitoussi Françoise, Tiollais Pierre, Charnay Patrick. Nucleotide sequence of the hepatitis B virus genome (subtype ayw) cloned in E. coli. Nature 1979;281:646–50. https://doi.org/10.1038/281646a0.

[17] Locarnini Stephen, Zoulim Fabien. Molecular Genetics of HBV Infection. Antiviral Therapy 2010;15:3–14. https://doi.org/10.3851/imp1619.

[18] Molnar-Kimber KL, Summers J, Taylor JM, Mason WS. Protein covalently bound to minus-strand DNA intermediates of duck hepatitis B virus. Journal of Virology 1983;45:165–72. https://doi.org/10.1128/jvi.45.1.165-172.1983.

[19] Kay Alan, Zoulim Fabien. Hepatitis B virus genetic variability and evolution. Virus Research 2007;127:164–76. https://doi.org/10.1016/j.virusres.2007.02.021.

[20] Nassal Michael, Schaller Heinz. Hepatitis B virus replication. Trends in Microbiology 1993;1:221–8. https://doi.org/10.1016/0966-842x(93)90136-f.

[21] Rieger Andrea, Nassal Michael. Distinct requirements for primary sequence in the 5′- and 3′-part of a bulge in the hepatitis B virus RNA encapsidation signal revealed by a combined in vivo selection/ in vitro amplification system. Nucleic Acids Research 1995;23:3909–15. https://doi.org/10.1093/nar/23.19.3909.

[22] Gerlich Wolfram H, Glebe Dieter, Kramvis Anna, Magnius Lars O. Peculiarities in the designations of hepatitis B virus genes, their products, and their antigenic specificities: a potential source of misunderstandings. Virus Genes 2020;56:109–19. https://doi.org/10.1007/s11262-020-01733-9.

[23] Beck Juergen, Nassal Michael. Hepatitis B virus replication. World Journal of Gastroenterology 2007;13:48. https://doi.org/10.3748/wjg.v13.i1.48.

[24] Urban Stephan, Schulze Andreas, Dandri Maura, Petersen Joerg. The replication cycle of hepatitis B virus. Journal of Hepatology 2010;52:282–4. https://doi.org/10.1016/j.jhep.2009.10.031.

[25] Ryu Dong-Kyun, Ahn Byung-Yoon, Ryu Wang-Shick. Proximity between the cap and 5′ ε stem–loop structure is critical for the suppression of pgRNA translation by the hepatitis B viral polymerase. Virology 2010;406:56–64. https://doi.org/10.1016/j.virol.2010.07.005.

[26] Nassal Michael, Junker-Niepmann Michael, Schaller Heinz. Translational inactivation of RNA function: Discrimination against a subset of genomic transcripts during HBV nucleocapsid assembly. Cell 1990;63:1357–63. https://doi.org/10.1016/0092-8674(90)90431-d.

[27] Ou JH, Bao H, Shih C, Tahara SM. Preferred translation of human hepatitis B virus polymerase from core protein- but not from precore protein-specific transcript. Journal of Virology 1990;64:4578–81. https://doi.org/10.1128/jvi.64.9.4578-4581.1990.

[28] Hulo Chantal, Castro Edouard de, Masson Patrick, Bougueleret Lydie, Bairoch Amos, Xenarios Ioannis, Mercier Philippe Le. ViralZone: a knowledge resource to understand virus diversity. Nucleic Acids Research 2011;39:D576–82. https://doi.org/10.1093/nar/gkq901.

[29] Schlicksup Christopher John, Laughlin Patrick, Dunkelbarger Steven, Wang Joseph Che-Yen, Zlotnick Adam. Local Stabilization of Subunit–Subunit Contacts Causes Global Destabilization of Hepatitis B Virus Capsids. ACS Chemical Biology 2020;15:1708–17. https://doi.org/10.1021/acschembio.0c00320.

[30] Seifer M, Standring DN. A protease-sensitive hinge linking the two domains of the hepatitis B virus core protein is exposed on the viral capsid surface. Journal of Virology 1994;68:5548–55. https://doi.org/10.1128/jvi.68.9.5548-5555.1994.

[31] Böttcher B, Wynne SA, Crowther RA. Determination of the fold of the core protein of hepatitis B virus by electron cryomicroscopy. Nature 1997;386:88–91. https://doi.org/10.1038/386088a0.

[32] Zlotnick Adam, Venkatakrishnan Balasubramanian, Tan Zhenning, Lewellyn Eric, Turner William, Francis Samson. Core protein: A pleiotropic keystone in the HBV lifecycle. Antiviral Research 2015;121:82–93. https://doi.org/10.1016/j.antiviral.2015.06.020.

[33] Wynne SA, Crowther RA, Leslie AGW. The Crystal Structure of the Human Hepatitis B Virus Capsid. Molecular Cell 1999;3:771–80. https://doi.org/10.1016/s1097-2765(01)80009-5.

[34] Gallina A, Bonelli F, Zentilin L, Rindi G, Muttini M, Milanesi G. A recombinant hepatitis B core antigen polypeptide with the protamine-like domain deleted self-assembles into capsid particles but fails to bind nucleic acids. Journal of Virology 1989;63:4645–52. https://doi.org/10.1128/jvi.63.11.4645-4652.1989.

[35] Bruss V, Ganem D. The role of envelope proteins in hepatitis B virus assembly. Proceedings of the National Academy of Sciences 1991;88:1059–63. https://doi.org/10.1073/pnas.88.3.1059.

[36] Gilbert Robert JC, Beales Lucy, Blond Donatienne, Simon Martha N, Lin Beth Y, Chisari Francis V, Stuart David I, Rowlands David J. Hepatitis B small surface antigen particles are octahedral. Proceedings of the National Academy of Sciences 2005;102:14783–8. https://doi.org/10.1073/pnas.0505062102.

[37] McAleer William J, Buynak Eugene B, Maigetter Robert Z, Wampler D Eugene, Miller William J, Hilleman Maurice R. Human hepatitis B vaccine from recombinant yeast. Nature 1984;307:178–80. https://doi.org/10.1038/307178a0.

[38] Hildt E, Urban S, Hofschneider PH. Characterization of essential domains for the functionality of the MHBst transcriptional activator and identification of a minimal MHBst activator. Oncogene 1995;11:2055–66.

[39] Oess S, Hildt E. Novel cell permeable motif derived from the PreS2-domain of hepatitis-B virus surface antigens. Gene Therapy 2000;7:750–8. https://doi.org/10.1038/sj.gt.3301154.

[40] Seyec J Le, Chouteau P, Cannie I, Guguen-Guillouzo C, Gripon P. Infection Process of the Hepatitis B Virus Depends on the Presence of a Defined Sequence in the Pre-S1 Domain. Journal of Virology 1999;73:2052–7. https://doi.org/10.1128/jvi.73.3.2052-2057.1999.

[41] Glebe Dieter, Urban Stephan. Viral and cellular determinants involved in hepadnaviral entry. World Journal of Gastroenterology 2007;13:22. https://doi.org/10.3748/wjg.v13.i1.22.

[42] Bartenschlager R, Schaller H. Hepadnaviral assembly is initiated by polymerase binding to the encapsidation signal in the viral RNA genome. The EMBO Journal 1992;11:3413–20. https://doi.org/10.1002/j.1460-2075.1992.tb05420.x.

[43] Zoulim F, Seeger C. Reverse transcription in hepatitis B viruses is primed by a tyrosine residue of the polymerase. Journal of Virology 1994;68:6–13. https://doi.org/10.1128/jvi.68.1.6-13.1994.

[44] Radziwill G, Tucker W, Schaller H. Mutational analysis of the hepatitis B virus P gene product: domain structure and RNase H activity. Journal of Virology 1990;64:613–20. https://doi.org/10.1128/jvi.64.2.613-620.1990.

[45] Menéndez-Arias Luis, Álvarez Mar, Pacheco Beatriz. Nucleoside/nucleotide analog inhibitors of hepatitis B virus polymerase: mechanism of action and resistance. Current Opinion in Virology 2014;8:1–9. https://doi.org/10.1016/j.coviro.2014.04.005.

[46] Wei Xin, Peterson Darrell L. Expression, Purification, and Characterization of an Active RNase H Domain of the Hepatitis B Viral Polymerase*. Journal of Biological Chemistry 1996;271:32617–22. https://doi.org/10.1074/jbc.271.51.32617.

[47] Terradillos Olivier, Billet Olivier, Renard Claire-Angélique, Levy Rafael, Molina Thierry, Briand Pascale, Buendia Marie Annick. The hepatitis B virus X gene potentiates c-myc-induced liver oncogenesis in transgenic mice. Oncogene 1997;14:395–404. https://doi.org/10.1038/sj.onc.1200850.

[48] Chirillo Paolo, Pagano Sabrina, Natoli Gioacchino, Puri Pier Lorenzo, Burgio Vito Lelio, Balsano Clara, Levrero Massimo. The hepatitis B virus X gene induces p53-mediated programmed cell death. Proceedings of the National Academy of Sciences 1997;94:8162–7. https://doi.org/10.1073/pnas.94.15.8162.

[49] Bouchard Michael J, Schneider Robert J. The Enigmatic X Gene of Hepatitis B Virus. Journal of Virology 2004;78:12725–34. https://doi.org/10.1128/jvi.78.23.12725-12734.2004.

[50] Belloni Laura, Pollicino Teresa, Nicola Francesca De, Guerrieri Francesca, Raffa Giuseppina, Fanciulli Maurizio, Raimondo Giovanni, Levrero Massimo. Nuclear HBx binds the HBV minichromosome and modifies the epigenetic regulation of cccDNA function. Proceedings of the National Academy of Sciences 2009;106:19975–9. https://doi.org/10.1073/pnas.0908365106.

[51] Magnius Lars O, Espmark Ake. A NEW ANTIGEN COMPLEX CO-OCCURRING WITH AUSTRALIA ANTIGEN. Acta Pathologica Microbiologica Scandinavica Section B Microbiology and Immunology 1972;80B:335–7. https://doi.org/10.1111/j.1699-0463.1972.tb00167.x.

[52] Standring DN, Ou JH, Masiarz FR, Rutter WJ. A signal peptide encoded within the precore region of hepatitis B virus directs the secretion of a heterogeneous population of e antigens in Xenopus oocytes. Proceedings of the National Academy of Sciences 1988;85:8405–9. https://doi.org/10.1073/pnas.85.22.8405.

[53] Bruss Volker, Gerlich Wolfram H. Formation of transmembraneous hepatitis b e-antigen by cotranslational in vitro processing of the viral precore protein. Virology 1988;163:268–75. https://doi.org/10.1016/0042-6822(88)90266-8.

[54] Revill Peter, Yuen Lilly, Walsh Renae, Perrault Marie, Locarnini Stephen, Kramvis Anna. Bioinformatic analysis of the hepadnavirus e-antigen and its precursor identifies remarkable sequence conservation in all orthohepadnaviruses. Journal of Medical Virology 2010;82:104–15. https://doi.org/10.1002/jmv.21645.

[55] Schlicht HJ, Salfeld J, Schaller H. The duck hepatitis B virus pre-C region encodes a signal sequence which is essential for synthesis and secretion of processed core proteins but not for virus formation. Journal of Virology 1987;61:3701–9. https://doi.org/10.1128/jvi.61.12.3701-3709.1987.

[56] Chen HS, Kew MC, Hornbuckle WE, Tennant BC, Cote PJ, Gerin JL, Purcell RH, Miller RH. The precore gene of the woodchuck hepatitis virus genome is not essential for viral replication in the natural host. Journal of Virology 1992;66:5682–4. https://doi.org/10.1128/jvi.66.9.5682-5684.1992.

[57] Tsai Kuen-Nan, Ou Jing-Hsiung James. Hepatitis B virus e antigen and viral persistence. Current Opinion in Virology 2021;51:158–63. https://doi.org/10.1016/j.coviro.2021.10.003.

[58] Liu Hui, Cheng Junjun, Viswanathan Usha, Chang Jinhong, Lu Fengmin, Guo Ju-Tao. Amino acid residues at core protein dimer-dimer interface modulate multiple steps of hepatitis B virus replication and HBeAg biogenesis. PLoS Pathogens 2021;17:e1010057. https://doi.org/10.1371/journal.ppat.1010057.

[59] Messageot Fabienne, Salhi Samia, Eon Patricia, Rossignol Jean-Michel. Proteolytic Processing of the Hepatitis B Virus e Antigen Precursor CLEAVAGE AT TWO FURIN CONSENSUS SEQUENCES*. Journal of Biological Chemistry 2003;278:891–5. https://doi.org/10.1074/jbc.m207634200.

[60] Milich David R. Is the function of the HBeAg really unknown? Human Vaccines & Immunotherapeutics 2019;15:2187–91. https://doi.org/10.1080/21645515.2019.1607132.

[61] Hong Xupeng, Luckenbaugh Laurie, Mendenhall Megan, Walsh Renae, Cabuang Liza, Soppe Sally, Revill Peter A, Burdette Dara, Feierbach Becket, Delaney William, Hu Jianming. Characterization of Hepatitis B Precore/Core-Related Antigens. Journal of Virology 2021;95. https://doi.org/10.1128/jvi.01695-20.

[62] Kramvis Anna. Genotypes and Genetic Variability of Hepatitis B Virus. Intervirology 2014;57:141–50. https://doi.org/10.1159/000360947.

[63] Lin CL, Kao JH. Hepatitis B Virus Genotypes and Variants. Cold Spring Harbor Perspectives in Medicine 2015;5:a021436–a021436. https://doi.org/10.1101/cshperspect.a021436.

[64] Velkov Stoyan, Ott Jördis J, Protzer Ulrike, Michler Thomas. The Global Hepatitis B Virus Genotype Distribution Approximated from Available Genotyping Data. Genes 2018;9:495. https://doi.org/10.3390/genes9100495.

[65] Sunbul Mustafa. Hepatitis B virus genotypes: Global distribution and clinical importance. World Journal of Gastroenterology 2014;20:5427–34. https://doi.org/10.3748/wjg.v20.i18.5427.

[66] Kramvis Anna. The clinical implications of hepatitis B virus genotypes and HBeAg in pediatrics. Reviews in Medical Virology 2016;26:285–303. https://doi.org/10.1002/rmv.1885.

[67] Schulze Andreas, Gripon Philippe, Urban Stephan. Hepatitis B virus infection initiates with a large surface protein–dependent binding to heparan sulfate proteoglycans. Hepatology 2007;46:1759–68. https://doi.org/10.1002/hep.21896.

[68] Yan Huan, Zhong Guocai, Xu Guangwei, He Wenhui, Jing Zhiyi, Gao Zhenchao, Huang Yi, Qi Yonghe, Peng Bo, Wang Haimin, Fu Liran, Song Mei, Chen Pan, Gao Wenqing, Ren Bijie, Sun Yinyan, Cai Tao, Feng Xiaofeng, Sui Jianhua, Li Wenhui. Sodium taurocholate cotransporting polypeptide is a functional receptor for human hepatitis B and D virus. ELife 2012;1:e00049. https://doi.org/10.7554/elife.00049.

[69] Döring Barbara, Lütteke Thomas, Geyer Joachim, Petzinger Ernst. Chapter Four The SLC10 Carrier Family Transport Functions and Molecular Structure. Current Topics in Membranes 2012;70:105–68. https://doi.org/10.1016/b978-0-12-394316-3.00004-1.

[70] Huang Hsiu-Chen, Chen Chun-Chi, Chang Wen-Cheng, Tao Mi-Hua, Huang Cheng. Entry of Hepatitis B Virus into Immortalized Human Primary Hepatocytes by Clathrin-Dependent Endocytosis. Journal of Virology 2012;86:9443–53. https://doi.org/10.1128/jvi.00873-12.

[71] Herrscher Charline, Roingeard Philippe, Blanchard Emmanuelle. Hepatitis B Virus Entry into Cells. Cells 2020;9:1486. https://doi.org/10.3390/cells9061486.

[72] Tian Ji, Li Cong, Li Wenhui. Entry of hepatitis B virus: going beyond NTCP to the nucleus. Current Opinion in Virology 2021;50:97–102. https://doi.org/10.1016/j.coviro.2021.08.001.

[73] Kann Michael, Schmitz Andre, Rabe Birgit. Intracellular transport of hepatitis B virus. World Journal of Gastroenterology 2007;13:39. https://doi.org/10.3748/wjg.v13.i1.39.

[74] Seeger Christoph, Mason William S. Molecular biology of hepatitis B virus infection. Virology 2015;479:672–86. https://doi.org/10.1016/j.virol.2015.02.031.

[75] Newbold JE, Xin H, Tencza M, Sherman G, Dean J, Bowden S, Locarnini S. The covalently closed duplex form of the hepadnavirus genome exists in situ as a heterogeneous population of viral minichromosomes. Journal of Virology 1995;69:3350–7. https://doi.org/10.1128/jvi.69.6.3350-3357.1995.

[76] Moolla Naazneen, Kew Michael, Arbuthnot Patrick. Regulatory elements of hepatitis B virus transcription. Journal of Viral Hepatitis 2002;9:323–31. https://doi.org/10.1046/j.1365-2893.2002.00381.x.

[77] Summers J, Smith PM, Horwich AL. Hepadnavirus envelope proteins regulate covalently closed circular DNA amplification. Journal of Virology 1990;64:2819–24. https://doi.org/10.1128/jvi.64.6.2819-2824.1990.

[78] Watanabe Tokiko, Sorensen Ericka M, Naito Akira, Schott Meghan, Kim Seungtaek, Ahlquist Paul. Involvement of host cellular multivesicular body functions in hepatitis B virus budding. Proceedings of the National Academy of Sciences 2007;104:10205–10. https://doi.org/10.1073/pnas.0704000104.

[79] Jiang Bingfu, Himmelsbach Kiyoshi, Ren Huimei, Boller Klaus, Hildt Eberhard. Subviral Hepatitis B Virus Filaments, like Infectious Viral Particles, Are Released via Multivesicular Bodies. Journal of Virology 2016;90:3330–41. https://doi.org/10.1128/jvi.03109-15.

[80] Hu Jianming, Protzer Ulrike, Siddiqui Aleem. Revisiting Hepatitis B Virus: Challenges of Curative Therapies. Journal of Virology 2019;93. https://doi.org/10.1128/jvi.01032-19.

[81] Barker LF, Maynard JE, Purcell RH, Hoofnagle JH, Berquist KR, London WT, Gerety RJ, Krushak DH. Hepatitis B Virus Infection in Chimpanzees: Titration of Subtypes. Journal of Infectious Diseases 1975;132:451–8. https://doi.org/10.1093/infdis/132.4.451.

[82] D'Ugo Emilio, Argentini Claudio, Giuseppetti Roberto, Canitano Andrea, Catone Stefania, Rapicetta Maria. The woodchuck hepatitis B virus infection model for the evaluation of HBV therapies and vaccine therapies. Expert Opinion on Drug Discovery 2010;5:1153–62. https://doi.org/10.1517/17460441.2010.530252.

[83] Dandri Maura, Burda Martin R, Török Eva, Pollok Joerg M, Iwanska Alicja, Sommer Gunhild, Rogiers Xavier, Rogler Charles E, Gupta Sanjeev, Will Hans, Greten Heiner, Petersen Joerg. Repopulation of mouse liver with human hepatocytes and in vivo infection with hepatitis B virus. Hepatology 2001;33:981–8. https://doi.org/10.1053/jhep.2001.23314.

[84] Gripon P, Diot C, Thézé N, Fourel I, Loreal O, Brechot C, Guguen-Guillouzo C. Hepatitis B virus infection of adult human hepatocytes cultured in the presence of dimethyl sulfoxide. Journal of Virology 1988;62:4136–43. https://doi.org/10.1128/jvi.62.11.4136-4143.1988.

[85] Galle Peter R, Hagelstein Jens, Kommerell Burkhard, Volkmann Martin, Schranz Peter, Zentgraf Hanswalter. In vitro experimental infection of primary human hepatocytes with hepatitis B virus. Gastroenterology 1994;106:664–73. https://doi.org/10.1016/0016-5085(94)90700-5.

[86] Hantz O, Parent R, Durantel D, Gripon P, Guguen-Guillouzo C, Zoulim F. Persistence of the hepatitis B virus covalently closed circular DNA in HepaRG human hepatocyte-like cells. Journal of General Virology 2009;90:127–35. https://doi.org/10.1099/vir.0.004861-0.

[87] Li Feng, Wang Zhuo, Hu Fengyu, Su Lishan. Hepatitis B Virus Infection, Molecular Virology to Antiviral Drugs. Advances in Experimental Medicine and Biology 2019;1179:109–35. https://doi.org/10.1007/978-981-13-9151-4_5.

[88] Michailidis Eleftherios, Pabon Jonathan, Xiang Kuanhui, Park Paul, Ramanan Vyas, Hoffmann Hans-Heinrich, Schneider William M, Bhatia Sangeeta N, Jong Ype P de, Shlomai Amir, Rice Charles M. A robust cell culture system supporting the complete life cycle of hepatitis B virus. Scientific Reports 2017;7:16616. https://doi.org/10.1038/s41598-017-16882-5.

[89] Qi Zhihua, Li Gaiyun, Hu Hao, Yang Chunhui, Zhang Xiaoming, Leng Qibin, Xie Youhua, Yu Demin, Zhang Xinxin, Gao Yueqiu, Lan Ke, Deng Qiang. Recombinant Covalently Closed Circular Hepatitis B Virus DNA Induces Prolonged Viral Persistence in Immunocompetent Mice. Journal of Virology 2014;88:8045–56. https://doi.org/10.1128/jvi.01024-14.

[90] Guo Xiaoyan, Chen Ping, Hou Xiaohu, Xu Wenjuan, Wang Dan, Wang Tian-yan, Zhang Liping, Zheng Gang, Gao Zhi-liang, He Cheng-Yi, Zhou Boping, Chen Zhi-Ying. The recombined cccDNA produced using minicircle technology mimicked HBV genome in structure and function closely. Scientific Reports 2016;6:25552. https://doi.org/10.1038/srep25552.

[91] WHO. Global progress report on HIV, viral hepatitis and sexually transmitted infections. 2021.

[92] Seto Wai-Kay, Lo Ying-Ru, Pawlotsky Jean-Michel, Yuen Man-Fung. Chronic hepatitis B virus infection. The Lancet 2018;392:2313–24. https://doi.org/10.1016/s0140-6736(18)31865-8.

[93] Yuen Man-Fung, Chen Ding-Shinn, Dusheiko Geoffrey M, Janssen Harry LA, Lau Daryl TY, Locarnini Stephen A, Peters Marion G, Lai Ching-Lung. Hepatitis B virus infection. Nature Reviews Disease Primers 2018;4:18035. https://doi.org/10.1038/nrdp.2018.35.

[94] WHO. Global hepatitis report. 2017.

[95] McMahon BJ, Alward WLM, Hall DB, Heyward WL, Bender TR, Francis DP, Maynard JE. Acute Hepatitis B Virus Infection: Relation of Age to the Clinical Expression of Disease and Subsequent Development of the Carrier State. Journal of Infectious Diseases 1985;151:599–603. https://doi.org/10.1093/infdis/151.4.599.

[96] Liaw Yun-Fan, Chu Chia-Ming. Hepatitis B virus infection. The Lancet 2009;373:582–92. https://doi.org/10.1016/s0140-6736(09)60207-5.

[97] Liang T Jake. Hepatitis B: The virus and disease. Hepatology 2009;49:S13–21. https://doi.org/10.1002/hep.22881.

[98] Tassopoulos Nicolaos C, Papaevangelou George J, Sjogren Maria H, Roumeliotou-karayannis Anastasia, Gerin John L, Purcell Robert H. Natural history of acute hepatitis B surface antigen-positive hepatitis in Greek adults. Gastroenterology 1987;92:1844–50. https://doi.org/10.1016/0016-5085(87)90614-7.

[99] Chang Mei-Hwei. Natural history of hepatitis B virus infection in children. Journal of Gastroenterology and Hepatology 2000;15:E16–9. https://doi.org/10.1046/j.1440-1746.2000.02096.x.

[100] Fanning Gregory C, Zoulim Fabien, Hou Jinlin, Bertoletti Antonio. Therapeutic strategies for hepatitis B virus infection: towards a cure. Nature Reviews Drug Discovery 2019;18:827–44. https://doi.org/10.1038/s41573-019-0037-0.

[101] Fong Tse-Ling, Bisceglie Adrian M Di, Biswas Robin, Waggoner Jeanne G, Wilson Leonard, Claggett Janet, Hoofnagle Jay H. High levels of viral replication during acute hepatitis B infection predict progression to chronicity. Journal of Medical Virology 1994;43:155–8. https://doi.org/10.1002/jmv.1890430210.

[102] Lampertico Pietro, Agarwal Kosh, Berg Thomas, Buti Maria, Janssen Harry LA, Papatheodoridis George, Zoulim Fabien, Tacke Frank. EASL 2017 Clinical Practice Guidelines on the management of hepatitis B virus infection. Journal of Hepatology 2017;67:370–98. https://doi.org/10.1016/j.jhep.2017.03.021.

[103] Lok Anna SF, Lai Ching-Lung, Wu Pui-Chee, Leung Elsie KY, Lam Tat-Shun. Spontaneous hepatitis B e antigen to antibody seroconversion and reversion in Chinese patients with chronic

hepatitis B virus infection. Gastroenterology 1987;92:1839–43. https://doi.org/10.1016/0016-5085(87)90613-5.

[104] Fattovich Giovanna, Rugge Massimo, Brollo Lucio, Pontisso Patrizia, Noventa Franco, Guido Maria, Alberti Alfredo, Realdi Professor Giuseppe. Clinical, virologic and histologic outcome following seroconversion from HBeAg to anti-HBe in chronic hepatitis type B. Hepatology 1986;6:167–71. https://doi.org/10.1002/hep.1840060203.

[105] Yuen Man-Fung, Hui Chee-Kin, Cheng Chi-Chung, Wu Chi-Hang, Lai Yim-Ping, Lai Ching-Lung. Long-term follow-up of interferon alfa treatment in chinese patients with chronic hepatitis B infection: The effect on hepatitis B e antigen seroconversion and the development of cirrhosis-related complications. Hepatology 2001;34:139–45. https://doi.org/10.1053/jhep.2001.25273.

[106] Realdi G, Alberti A, Rugge M, Bortolotti F, Rigoli AM, Tremolada F, Ruol A. Seroconversion from hepatitis B e antigen to anti-HBe in chronic hepatitis B virus infection. Gastroenterology 1980;79:195–9. https://doi.org/10.1016/0016-5085(80)90130-4.

[107] Chu Chi–Jen, Hussain Munira, Lok Anna SF. Hepatitis B virus genotype B is associated with earlier HBeAg seroconversion compared with hepatitis B virus genotype C. Gastroenterology 2002;122:1756–62. https://doi.org/10.1053/gast.2002.33588.

[108] Yuen Man-Fung, Sablon Erwin, Yuan He-Jun, Hui Chee-Kin, Wong Danny Ka-Ho, Doutreloigne Joke, Wong Benjamin Chun-Yu, Chan Annie On-On, Lai Ching-Lung. Relationship between the Development of Precore and Core Promoter Mutations and Hepatitis B e Antigen Seroconversion in Patients with Chronic Hepatitis B Virus. The Journal of Infectious Diseases 2002;186:1335–8. https://doi.org/10.1086/344327.

[109] Chu Chia-Ming, Hung Shao-Jen, Lin Justin, Tai Dar-In, Liaw Yun-Fan. Natural history of hepatitis b e antigen to antibody seroconversion in patients with normal serum aminotransferase levels. The American Journal of Medicine 2004;116:829–34. https://doi.org/10.1016/j.amjmed.2003.12.040.

[110] Yuen Man-Fung, Sablon Erwin, Yuan He-Jun, Wong Danny Ka-Ho, Hui Chee-Kin, Wong Benjamin Chun-Yu, Chan Annie On-On, Lai Ching Lung. Significance of hepatitis B genotype in acute exacerbation, HBeAg seroconversion, cirrhosis-related complications, and hepatocellular carcinoma. Hepatology 2003;37:562–7. https://doi.org/10.1053/jhep.2003.50098.

[111] Hadziyannis Stephanos J, Vassilopoulos Dimitrios. Hepatitis B e antigen–negative chronic hepatitis B. Hepatology 2001;34:617–24. https://doi.org/10.1053/jhep.2001.27834.

[112] Trépo Christian, Chan Henry LY, Lok Anna. Hepatitis B virus infection. The Lancet 2014;384:2053–63. https://doi.org/10.1016/s0140-6736(14)60220-8.

[113] Zeisel Mirjam B, Lucifora Julie, Mason William S, Sureau Camille, Beck Jürgen, Levrero Massimo, Kann Michael, Knolle Percy A, Benkirane Monsef, Durantel David, Michel Marie-Louise, Autran Brigitte, Cosset François-Loïc, Strick-Marchand Hélène, Trépo Christian, Kao Jia-Horng, Carrat Fabrice, Lacombe Karine, Schinazi Raymond F, Barré-Sinoussi Françoise, Delfraissy Jean-François, Zoulim Fabien. Towards an HBV cure: state-of-the-art and unresolved questions—report of the ANRS workshop on HBV cure. Gut 2015;64:1314. https://doi.org/10.1136/gutjnl-2014-308943.

[114] Yuen Man–Fung, Wong Danny Ka–Ho, Fung James, Ip Philip, But David, Hung Ivan, Lau Kevin, Yuen John Chi–Hang, Lai Ching–Lung. HBsAg Seroclearance in Chronic Hepatitis B in Asian Patients: Replicative Level and Risk of Hepatocellular Carcinoma. Gastroenterology 2008;135:1192–9. https://doi.org/10.1053/j.gastro.2008.07.008.

[115] Varbobitis Ioannis, Papatheodoridis George V. The assessment of hepatocellular carcinoma risk in patients with chronic hepatitis B under antiviral therapy. Clinical and Molecular Hepatology 2016;22:319–26. https://doi.org/10.3350/cmh.2016.0045.

[116] Lampertico Pietro, Viganò Mauro, Costanzo Giovan Giuseppe Di, Sagnelli Evangelista, Fasano Massimo, Marco Vito Di, Boninsegna Sara, Farci Patrizia, Fargion Silvia, Giuberti Tiziana, Iannacone Claudio, Regep Loredana, Massetto Benedetta, Facchetti Floriana, Colombo Massimo, Group PegBeLiver Study. Randomised study comparing 48 and 96 weeks peginterferon α-2a therapy in genotype D HBeAg-negative chronic hepatitis B. Gut 2013;62:290. https://doi.org/10.1136/gutjnl-2011-301430.

[117] Nassal Michael. HBV cccDNA: viral persistence reservoir and key obstacle for a cure of chronic hepatitis B. Gut 2015;64:1972. https://doi.org/10.1136/gutjnl-2015-309809.

[118] Maini Mala K, Gehring Adam J. The role of innate immunity in the immunopathology and treatment of HBV infection. Journal of Hepatology 2016;64:S60–70. https://doi.org/10.1016/j.jhep.2016.01.028.

[119] Dunn Claire, Peppa Dimitra, Khanna Pooja, Nebbia Gaia, Jones Meleri, Brendish Nathan, Lascar R Monica, Brown David, Gilson Richard J, Tedder Richard J, Dusheiko Geoffrey M, Jacobs Michael, Klenerman Paul, Maini Mala K. Temporal Analysis of Early Immune Responses in Patients With Acute Hepatitis B Virus Infection. Gastroenterology 2009;137:1289–300. https://doi.org/10.1053/j.gastro.2009.06.054.

[120] Stacey Andrea R, Norris Philip J, Qin Li, Haygreen Elizabeth A, Taylor Elizabeth, Heitman John, Lebedeva Mila, DeCamp Allan, Li Dongfeng, Grove Douglas, Self Steven G, Borrow Persephone. Induction of a Striking Systemic Cytokine Cascade prior to Peak Viremia in Acute Human Immunodeficiency Virus Type 1 Infection, in Contrast to More Modest and Delayed Responses in Acute Hepatitis B and C Virus Infections. Journal of Virology 2009;83:3719–33. https://doi.org/10.1128/jvi.01844-08.

[121] Luangsay Souphalone, Gruffaz Marion, Isorce Nathalie, Testoni Barbara, Michelet Maud, Faure-Dupuy Suzanne, Maadadi Sarah, Ait-Goughoulte Malika, Parent Romain, Rivoire Michel, Javanbakht Hassan, Lucifora Julie, Durantel David, Zoulim Fabien. Early inhibition of hepatocyte innate responses by hepatitis B virus. Journal of Hepatology 2015;63:1314–22. https://doi.org/10.1016/j.jhep.2015.07.014.

[122] Bertoletti Antonio, Ferrari Carlo. Adaptive immunity in HBV infection. Journal of Hepatology 2016;64:S71–83. https://doi.org/10.1016/j.jhep.2016.01.026.

[123] Murphy Kenneth, Weaver Casey. Janeway Immunology. 2018.

[124] Trepo Christian. A brief history of hepatitis milestones. Liver International 2014;34:29–37. https://doi.org/10.1111/liv.12409.

[125] Iannacone Matteo, Guidotti Luca G. Immunobiology and pathogenesis of hepatitis B virus infection. Nature Reviews Immunology 2022;22:19–32. https://doi.org/10.1038/s41577-021-00549-4.

[126] Ferrari C, Penna A, Bertoletti A, Valli A, Antoni AD, Giuberti T, Cavalli A, Petit MA, Fiaccadori F. Cellular immune response to hepatitis B virus-encoded antigens in acute and chronic hepatitis B virus infection. Journal of Immunology (Baltimore, Md : 1950) 1990;145:3442–9.

[127] Ferrari C, Bertoletti A, Penna A, Cavalli A, Valli A, Missale G, Pilli M, Fowler P, Giuberti T, Chisari FV. Identification of immunodominant T cell epitopes of the hepatitis B virus nucleocapsid antigen. Journal of Clinical Investigation 1991;88:214–22. https://doi.org/10.1172/jci115280.

[128] Chisari Francis V, Ferrari Carlo. Hepatitis B Virus Immunopathogenesis. Annual Review of Immunology 1995;13:29–60. https://doi.org/10.1146/annurev.iy.13.040195.000333.

[129] Thimme Robert, Wieland Stefan, Steiger Carola, Ghrayeb John, Reimann Keith A, Purcell Robert H, Chisari Francis V. CD8 + T Cells Mediate Viral Clearance and Disease Pathogenesis during Acute Hepatitis B Virus Infection. Journal of Virology 2003;77:68–76. https://doi.org/10.1128/jvi.77.1.68-76.2003.

[130] Asabe Shinichi, Wieland Stefan F, Chattopadhyay Pratip K, Roederer Mario, Engle Ronald E, Purcell Robert H, Chisari Francis V. The Size of the Viral Inoculum Contributes to the Outcome of Hepatitis B Virus Infection. Journal of Virology 2009;83:9652–62. https://doi.org/10.1128/jvi.00867-09.

[131] Zhang Li, Zhang Miao, Li Hu, Chen Zhiwei, Luo Aoran, Liu Bin, Chen Min, Peng Mingli, Ren Hong, Hu Peng. Tfh cell-mediated humoral immune response and HBsAg level can predict HBeAg seroconversion in chronic hepatitis B patients receiving peginterferon-α therapy. Molecular Immunology 2016;73:37–45. https://doi.org/10.1016/j.molimm.2016.03.011.

[132] Chisari Francis V. Viruses, Immunity, and Cancer: Lessons from Hepatitis B. The American Journal of Pathology 2000;156:1117–32. https://doi.org/10.1016/s0002-9440(10)64980-2.

[133] Danska JS, Livingstone AM, Paragas V, Ishihara T, Fathman CG. The presumptive CDR3 regions of both T cell receptor alpha and beta chains determine T cell specificity for myoglobin peptides. The Journal of Experimental Medicine 1990;172:27–33. https://doi.org/10.1084/jem.172.1.27.

[134] Reignat Stephanie, Webster George JM, Brown David, Ogg Graham S, King Abigail, Seneviratne Suranjith L, Dusheiko Geoff, Williams Roger, Maini Mala K, Bertoletti Antonio. Escaping High Viral Load Exhaustion. The Journal of Experimental Medicine 2002;195:1089–101. https://doi.org/10.1084/jem.20011723.

[135] Webster George JM, Reignat Stephanie, Brown David, Ogg Graham S, Jones Louise, Seneviratne Suranjith L, Williams Roger, Dusheiko Geoffrey, Bertoletti Antonio. Longitudinal Analysis of CD8 + T Cells Specific for Structural and Nonstructural Hepatitis B Virus Proteins in Patients with Chronic Hepatitis B: Implications for Immunotherapy. Journal of Virology 2004;78:5707–19. https://doi.org/10.1128/jvi.78.11.5707-5719.2004.

[136] Boni Carolina, Fisicaro Paola, Valdatta Caterina, Amadei Barbara, Vincenzo Paola Di, Giuberti Tiziana, Laccabue Diletta, Zerbini Alessandro, Cavalli Albertina, Missale Gabriele, Bertoletti Antonio, Ferrari Carlo. Characterization of Hepatitis B Virus (HBV)-Specific T-Cell Dysfunction in

Chronic HBV Infection ▿ . Journal of Virology 2007;81:4215–25. https://doi.org/10.1128/jvi.02844-06.

[137] Bengsch Bertram, Martin Bianca, Thimme Robert. Restoration of HBV-specific CD8+ T cell function by PD-1 blockade in inactive carrier patients is linked to T cell differentiation. Journal of Hepatology 2014;61:1212–9. https://doi.org/10.1016/j.jhep.2014.07.005.

[138] Hoogeveen Ruben C, Robidoux Maxwell P, Schwarz Tatjana, Heydmann Laura, Cheney James A, Kvistad Daniel, Aneja Jasneet, Melgaço Juliana G, Fernandes Carlos A, Chung Raymond T, Boonstra Andre, Kim Arthur Y, Baumert Thomas F, Timm Jörg, Lewis-Ximenez Lia L, Tonnerre Pierre, Lauer Georg M. Phenotype and function of HBV-specific T cells is determined by the targeted epitope in addition to the stage of infection. Gut 2018;68:893–904. https://doi.org/10.1136/gutjnl-2018-316644.

[139] Schuch Anita, Alizei Elahe Salimi, Heim Kathrin, Wieland Dominik, Kiraithe Michael Muthamia, Kemming Janine, Llewellyn-Lacey Sian, Sogukpinar Özlem, Ni Yi, Urban Stephan, Zimmermann Peter, Nassal Michael, Emmerich Florian, Price David A, Bengsch Bertram, Luxenburger Hendrik, Neumann-Haefelin Christoph, Hofmann Maike, Thimme Robert. Phenotypic and functional differences of HBV core-specific versus HBV polymerase-specific CD8+ T cells in chronically HBV-infected patients with low viral load. Gut 2019;68:905–15. https://doi.org/10.1136/gutjnl-2018-316641.

[140] Walker Andreas, Schwarz Tatjana, Brinkmann-Paulukat Janine, Wisskirchen Karin, Menne Christopher, Alizei Elahe Salimi, Kefalakes Helenie, Theissen Martin, Hoffmann Daniel, Wiesch Julian Schulze zur, Maini Mala K, Cornberg Markus, Kraft Anke RM, Keitel Verena, Bock Hans H, Horn Peter A, Thimme Robert, Wedemeyer Heiner, Heinemann Falko M, Luedde Tom, Neumann-Haefelin Christoph, Protzer Ulrike, Timm Jörg. Immune escape pathways from the HBV core18-27 CD8 T cell response are driven by individual HLA class I alleles. Frontiers in Immunology 2022;13:1045498. https://doi.org/10.3389/fimmu.2022.1045498.

[141] Hadziyannis Stephanos, Papatheodoridis George. Hepatitis B e Antigen-Negative Chronic Hepatitis B: Natural History and Treatment. Semin Liver Dis 2006;26:130–41. https://doi.org/10.1055/s-2006-939751.

[142] Hsu Hong-Yuan, Chang Mei-Hwei, Hsieh Kue-Hsiung, Lee Chin-Yun, Lin Ho-Hsiung, Hwang Lih-Hwa, Chen Pei-Jer, Chen Ding-Shinn. Cellular Immune Response to HBcAg in Mother-to-Infant Transmission of Hepatitis B Virus. Hepatology 1992;15:770–6. https://doi.org/10.1002/hep.1840150505.

[143] Wang Zhanhui, Zhang Jin, Yang Hong, Li Xiuhui, Wen Shujuan, Guo Yabing, Sun Jian, Hou Jinlin. Quantitative analysis of HBV DNA level and HBeAg titer in hepatitis B surface antigen positive mothers and their babies: HBeAg passage through the placenta and the rate of decay in babies. Journal of Medical Virology 2003;71:360–6. https://doi.org/10.1002/jmv.10493.

[144] Chen Margaret T, Billaud Jean-Noel, Sällberg Matti, Guidotti Luca G, Chisari Francis V, Jones Joyce, Hughes Janice, Milich David R. A function of the hepatitis B virus precore protein is to regulate the immune response to the core antigen. Proceedings of the National Academy of Sciences 2004;101:14913–8. https://doi.org/10.1073/pnas.0406282101.

[145] Tian Yongjun, Kuo Cheng-fu, Akbari Omid, Ou Jing-hsiung James. Maternal-Derived Hepatitis B Virus e Antigen Alters Macrophage Function in Offspring to Drive Viral Persistence after

Vertical Transmission. Immunity 2016;44:1204–14. https://doi.org/10.1016/j.immuni.2016.04.008.

[146] Bertoletti A, Costanzo A, Chisari FV, Levrero M, Artini M, Sette A, Penna A, Giuberti T, Fiaccadori F, Ferrari C. Cytotoxic T lymphocyte response to a wild type hepatitis B virus epitope in patients chronically infected by variant viruses carrying substitutions within the epitope. The Journal of Experimental Medicine 1994;180:933–43. https://doi.org/10.1084/jem.180.3.933.

[147] Kefalakes Helenie, Budeus Bettina, Walker Andreas, Jochum Christoph, Hilgard Gudrun, Heinold Andreas, Heinemann Falko M, Gerken Guido, Hoffmann Daniel, Timm Joerg. Adaptation of the hepatitis B virus core protein to CD8+ T-cell selection pressure. Hepatology 2015;62:47–56. https://doi.org/10.1002/hep.27771.

[148] Timm Joerg, Walker Christopher M. Mutational escape of CD8+ T cell epitopes: implications for prevention and therapy of persistent hepatitis virus infections. Medical Microbiology and Immunology 2015;204:29–38. https://doi.org/10.1007/s00430-014-0372-z.

[149] Maini Mala K, Boni Carolina, Lee Chun Kyon, Larrubia Juan R, Reignat Stephanie, Ogg Graham S, King Abigail S, Herberg Jethro, Gilson Richard, Alisa Akeem, Williams Roger, Vergani Diego, Naoumov Nikolai V, Ferrari Carlo, Bertoletti Antonio. The Role of Virus-Specific Cd8+ Cells in Liver Damage and Viral Control during Persistent Hepatitis B Virus Infection. The Journal of Experimental Medicine 2000;191:1269–80. https://doi.org/10.1084/jem.191.8.1269.

[150] Schwarz Tatjana, Ptok Johannes, Damagnez Maximilian, Menne Christopher, Alizei Elahe Salimi, Habermann Daniel, Hoffmann Daniel, Wiesch Julian zur Schulze, Lauer Georg, Cornberg Markus, Kraft Anke, Gliga Smaranda, Bock Hans Heinrich, Horn Peter, Thimme Robert, Wedemeyer Heiner, Heinemann Falko, Lüdde Tom, Neumann-Haefelin Christoph, Walker Andreas, Timm Jörg. HLA class I-associated mutations are predominantly located in the HBV core protein and restricted to HBeAg-negative HBV infection. Zeitschrift Für Gastroenterologie 2024;62:e60–e60. https://doi.org/10.1055/s-0043-1777662.

[151] DuBridge Robert B, Tang Peter, Hsia Han Chao, Leong Phaik-Mooi, Miller Jeffrey H, Calos Michele P. Analysis of Mutation in Human Cells by Using an Epstein-Barr Virus Shuttle System. Molecular and Cellular Biology 1987;7:379–87. https://doi.org/10.1128/mcb.7.1.379-387.1987.

[152] Pear WS, Nolan GP, Scott ML, Baltimore D. Production of high-titer helper-free retroviruses by transient transfection. Proceedings of the National Academy of Sciences 1993;90:8392–6. https://doi.org/10.1073/pnas.90.18.8392.

[153] Kavanaugh MP, Miller DG, Zhang W, Law W, Kozak SL, Kabat D, Miller AD. Cell-surface receptors for gibbon ape leukemia virus and amphotropic murine retrovirus are inducible sodium-dependent phosphate symporters. Proceedings of the National Academy of Sciences 1994;91:7071–5. https://doi.org/10.1073/pnas.91.15.7071.

[154] Lam John S, Reeves Mark E, Cowherd Robert, Rosenberg Steven A, Hwu Patrick. Improved Gene Transfer into Human Lymphocytes Using Retroviruses with the Gibbon Ape Leukemia Virus Envelope. Human Gene Therapy 1996;7:1415–22. https://doi.org/10.1089/hum.1996.7.12-1415.

[155] Chen TR. Modal karyotype of human leukemia cell line, K562 (ATCC CCL 243). Cancer Genetics and Cytogenetics 1985;17:55–60. https://doi.org/10.1016/0165-4608(85)90101-3.

[156] Knowles Barbara B, Howe Chin C, Aden David P. Human Hepatocellular Carcinoma Cell Lines Secrete the Major Plasma Proteins and Hepatitis B Surface Antigen. Science 1980;209:497–9. https://doi.org/10.1126/science.6248960.

[157] Schneider Ulrich, Schwenk Hans-Ulrich, Bornkamm Georg. Characterization of EBV-genome negative "null" and "T" cell lines derived from children with acute lymphoblastic leukemia and leukemic transformed non-Hodgkin lymphoma. International Journal of Cancer 1977;19:621–6. https://doi.org/10.1002/ijc.2910190505.

[158] Abraham Robert T, Weiss Arthur. Jurkat T cells and development of the T-cell receptor signalling paradigm. Nature Reviews Immunology 2004;4:301–8. https://doi.org/10.1038/nri1330.

[159] Mommaas B, Halteren AG van, Pool J, Veken L van der, Wieles B, Heemskerk MH, Goulmy. E. Adult and cord blood T cells can acquire HA-1 specificity through HA-1 T-cell receptor gene transfer | Haematologica. Haematologica 2005;90:1415–21.

[160] Yu Hui, Lin Liangbin, Zhang Zhiqiang, Zhang Huiyuan, Hu Hongbo. Targeting NF-κB pathway for the therapy of diseases: mechanism and clinical study. Signal Transduction and Targeted Therapy 2020;5:209. https://doi.org/10.1038/s41392-020-00312-6.

[161] Valenzuela Pablo, Quiroga Margarita, Zaldivar Josefina, Gray Patrick, Rutter William J. THE NUCLEOTIDE SEQUENCE OF THE HEPATITIS B VIRAL GENOME AND THE IDENTIFICATION OF THE MAJOR VIRAL GENES. Animal Virus Genetics 1980:57–70. https://doi.org/10.1016/b978-0-12-255850-4.50010-x.

[162] Nagasaki Futoshi, Niitsuma Hirofumi, Cervantes Julieta G, Chiba Masanori, Hong Shan, Ojima Toshiaki, Ueno Yoshiyuki, Bondoc Edgardo, Kobayashi Koju, Ishii Motoyasu, Shimosegawa Tooru. Analysis of the entire nucleotide sequence of hepatitis B virus genotype B in the Philippines reveals a new subgenotype of genotype B. Journal of General Virology 2006;87:1175–80. https://doi.org/10.1099/vir.0.81525-0.

[163] Bertoletti Antonio, Gehring Adam. HBV epitope reactive exogenous T cell receptor (TCR) and uses thereof, 2018.

[164] Cohen Cyrille J, Zhao Yangbing, Zheng Zhili, Rosenberg Steven A, Morgan Richard A. Enhanced Antitumor Activity of Murine-Human Hybrid T-Cell Receptor (TCR) in Human Lymphocytes Is Associated with Improved Pairing and TCR/CD3 Stability. Cancer Research 2006;66:8878–86. https://doi.org/10.1158/0008-5472.can-06-1450.

[165] Sommermeyer Daniel, Uckert Wolfgang. Minimal Amino Acid Exchange in Human TCR Constant Regions Fosters Improved Function of TCR Gene-Modified T Cells. The Journal of Immunology 2010;184:6223–31. https://doi.org/10.4049/jimmunol.0902055.

[166] Ptok Johannes, Müller Lisa, Ostermann Philipp Niklas, Ritchie Anastasia, Dilthey Alexander T, Theiss Stephan, Schaal Heiner. Modifying splice site usage with ModCon: Maintaining the genetic code while changing the underlying mRNP code. Computational and Structural Biotechnology Journal 2021;19:3069–76. https://doi.org/10.1016/j.csbj.2021.05.033.

[167] Baust John M, Campbell Lia H, Harbell John W. Best practices for cryopreserving, thawing, recovering, and assessing cells. In Vitro Cellular & Developmental Biology - Animal 2017;53:855–71. https://doi.org/10.1007/s11626-017-0201-y.

[168] Ramachandran Hari, Laux Jessica, Moldovan Ioana, Caspell Richard, Lehmann Paul V, Subbramanian Ramu A. Optimal Thawing of Cryopreserved Peripheral Blood Mononuclear Cells for Use in High-Throughput Human Immune Monitoring Studies. Cells 2012;1:313–24. https://doi.org/10.3390/cells1030313.

[169] Choi Won-Mook, Choi Jonggi, Lim Young-Suk. Comprehensive Guide to Hepatitis Advances, 2023, p. 183–203. https://doi.org/10.1016/b978-0-323-98368-6.00007-0.

[170] Carman WF, Hadziyannis S, Mcgarvey MJ, Jacyna MR, Karayiannis P, Makris A, Thomas HC. MUTATION PREVENTING FORMATION OF HEPATITIS B e ANTIGEN IN PATIENTS WITH CHRONIC HEPATITIS B INFECTION. The Lancet 1989;334:588–91. https://doi.org/10.1016/s0140-6736(89)90713-7.

[171] Chan Henry LY, Hussain Munira, Lok Anna SF. Different hepatitis b virus genotypes are associated with different mutations in the core promoter and precore regions during hepatitis B e antigen seroconversion. Hepatology 1999;29:976–84. https://doi.org/10.1002/hep.510290352.

[172] Moriyama Kosei, Okamoto Hiroaki, Tsuda Fumio, Mayumi Makoto. Reduced Precore Transcription and Enhanced Core-Pregenome Transcription of Hepatitis B Virus DNA after Replacement of the Precore-Core Promoter with Sequences Associated with e Antigen-Seronegative Persistent Infections. Virology 1996;226:269–80. https://doi.org/10.1006/viro.1996.0655.

[173] Buckwold VE, Xu Z, Chen M, Yen TS, Ou JH. Effects of a naturally occurring mutation in the hepatitis B virus basal core promoter on precore gene expression and viral replication. Journal of Virology 1996;70:5845–51. https://doi.org/10.1128/jvi.70.9.5845-5851.1996.

[174] Li Jie, Buckwold Victor E, Hon Man-wai, Ou Jing-hsiung. Mechanism of Suppression of Hepatitis B Virus Precore RNA Transcription by a Frequent Double Mutation. Journal of Virology 1999;73:1239–44. https://doi.org/10.1128/jvi.73.2.1239-1244.1999.

[175] Schwarz Tatjana. Analyse der Sequenzvariabilität des Hepatitis B Virus unter dem Einfluss der CD8 T-Zellantwort auf Populationsebene. Heinrich-Heine-Universität Düsseldorf, 2022.

[176] Tong SP, Li JS, Vitvitski L, Kay A, Treépo C. Evidence for a base-paired region of hepatitis B virus pregenome encapsidation signal which influences the patterns of precore mutations abolishing HBe protein expression. Journal of Virology 1993;67:5651–5. https://doi.org/10.1128/jvi.67.9.5651-5655.1993.

[177] Wieland Stefan F. The Chimpanzee Model for Hepatitis B Virus Infection. Cold Spring Harbor Perspectives in Medicine 2015;5:a021469. https://doi.org/10.1101/cshperspect.a021469.

[178] Hu Jianming, Lin You-Yu, Chen Pei-Jer, Watashi Koichi, Wakita Takaji. Cell and Animal Models for Studying Hepatitis B Virus Infection and Drug Development. Gastroenterology 2018;156:338–54. https://doi.org/10.1053/j.gastro.2018.06.093.

[179] Gripon Philippe, Rumin Sylvie, Urban Stephan, Seyec Jacques Le, Glaise Denise, Cannie Isabelle, Guyomard Claire, Lucas Josette, Trepo Christian, Guguen-Guillouzo Christiane. Infection of a human hepatoma cell line by hepatitis B virus. Proceedings of the National Academy of Sciences 2002;99:15655–60. https://doi.org/10.1073/pnas.232137699.

[180] Kay Mark A, He Cheng-Yi, Chen Zhi-Ying. A robust system for production of minicircle DNA vectors. Nature Biotechnology 2010;28:1287–9. https://doi.org/10.1038/nbt.1708.

[181] Yan Zhipeng, Zeng Jing, Yu Youjun, Xiang Kunlun, Hu Hui, Zhou Xue, Gu Lili, Wang Li, Zhao Jie, Young John AT, Gao Lu. HBVcircle: A novel tool to investigate hepatitis B virus covalently closed circular DNA. Journal of Hepatology 2017;66:1149–57. https://doi.org/10.1016/j.jhep.2017.02.004.

[182] Mutz Pascal, Metz Philippe, Lempp Florian A, Bender Silke, Qu Bingqian, Schöneweis Katrin, Seitz Stefan, Tu Thomas, Restuccia Agnese, Frankish Jamie, Dächert Christopher, Schusser Benjamin, Koschny Ronald, Polychronidis Georgios, Schemmer Peter, Hoffmann Katrin, Baumert Thomas F, Binder Marco, Urban Stephan, Bartenschlager Ralf. HBV Bypasses the Innate Immune Response and Does not Protect HCV From Antiviral Activity of Interferon. Gastroenterology 2018;154:1791-1804.e22. https://doi.org/10.1053/j.gastro.2018.01.044.

[183] Chang CM, Jeng KS, Hu CP, Lo SJ, Su TS, Ting LP, Chou CK, Han SH, Pfaff E, Salfeld J. Production of hepatitis B virus in vitro by transient expression of cloned HBV DNA in a hepatoma cell line. The EMBO Journal 1987;6:675–80. https://doi.org/10.1002/j.1460-2075.1987.tb04807.x.

[184] Chou Chen-Kung, Wang Li-Hsien, Lin Hsing-Mei, Chi Chin-Wen. Glucocorticoid stimulates hepatitis B viral gene expression in cultured human hepatoma cells. Hepatology 1992;16:13–8. https://doi.org/10.1002/hep.1840160104.

[185] Moretti Marco, Pieretti Barbara, Masucci Annamaria, Sisti Davide, Rocchi Marco, Delprete Ernesto. Role of Signal-to-Cutoff Ratios in Hepatitis C Virus Antibody Detection. Clinical and Vaccine Immunology 2012;19:1329–31. https://doi.org/10.1128/cvi.00175-12.

[186] Seeger Christoph, Mason William S. Hepatitis B Virus Biology. Microbiology and Molecular Biology Reviews 2000;64:51–68. https://doi.org/10.1128/mmbr.64.1.51-68.2000.

[187] YUH CHIOU-HWA, Chang YUH-LONG, Ting LING-PAI. Transcriptional regulation of precore and pregenomic RNAs of hepatitis B virus. JOURNAL OF VIROLOGY 1992:4073–84.

[188] Lok Anna Suk-Fong. Hepatitis B Treatment: What We Know Now and What Remains to Be Researched. Hepatology Communications 2019;3:8–19. https://doi.org/10.1002/hep4.1281.

[189] Tsai SL, Chen PJ, Lai MY, Yang PM, Sung JL, Huang JH, Hwang LH, Chang TH, Chen DS. Acute exacerbations of chronic type B hepatitis are accompanied by increased T cell responses to hepatitis B core and e antigens. Implications for hepatitis B e antigen seroconversion. Journal of Clinical Investigation 1992;89:87–96. https://doi.org/10.1172/jci115590.

[190] Rosskopf Sandra, Leitner Judith, Paster Wolfgang, Morton Laura T, Hagedoorn Renate S, Steinberger Peter, Heemskerk Mirjam HM. A Jurkat 76 based triple parameter reporter system to evaluate TCR functions and adoptive T cell strategies. Oncotarget 2018;9:17608–19. https://doi.org/10.18632/oncotarget.24807.

[191] Britten Cedrik M, Meyer Ralf G, Kreer Tanja, Drexler Ingo, Wölfel Thomas, Herr Wolfgang. The use of HLA-A*0201-transfected K562 as standard antigen-presenting cells for CD8+ T lymphocytes in IFN-γ ELISPOT assays. Journal of Immunological Methods 2002;259:95–110. https://doi.org/10.1016/s0022-1759(01)00499-9.

[192] Brinkmann J, Schwarz T, Kefalakes H, Wiesch J Schulze zur, Kraft A, Cornberg M, Hoffmann D, Walker A, Timm J. Differential escape pathways from the dominant CD8 T cell epitope in HBV core18 – 27 depend on the HLA class I genotype. Zeitschrift Für Gastroenterologie 2018;56:E2–89. https://doi.org/10.1055/s-0037-1612872.

[193] Leenders WPJ, Hertogs K, Moshage H, Yap SH. Host and tissue tropism of hepatitis B virus. Liver 1992;12:51–5. https://doi.org/10.1111/j.1600-0676.1992.tb00556.x.

[194] Watashi Koichi, Urban Stephan, Li Wenhui, Wakita Takaji. NTCP and Beyond: Opening the Door to Unveil Hepatitis B Virus Entry. International Journal of Molecular Sciences 2014;15:2892–905. https://doi.org/10.3390/ijms15022892.

[195] Yan Huan, Liu Yang, Sui Jianhua, Li Wenhui. NTCP opens the door for hepatitis B virus infection. Antiviral Research 2015;121:24–30. https://doi.org/10.1016/j.antiviral.2015.06.002.

[196] Wettengel Jochen M, Burwitz Benjamin J. Innovative HBV Animal Models Based on the Entry Receptor NTCP. Viruses 2020;12:828. https://doi.org/10.3390/v12080828.

[197] Urban Stephan, Bartenschlager Ralf, Kubitz Ralf, Zoulim Fabien. Strategies to Inhibit Entry of HBV and HDV Into Hepatocytes. Gastroenterology 2014;147:48–64. https://doi.org/10.1053/j.gastro.2014.04.030.

[198] Siederdissen Christoph Höner Zu, Cornberg Markus. The role of HBsAg levels in the current management of chronic HBV infection. Annals of Gastroenterology 2013;27:105–12.

[199] Song Guangjun, Rao Huiying, Feng Bo, Wei Lai. Prediction of spontaneous HBeAg seroconversion in HBeAg-positive chronic hepatitis B patients during the immune clearance phase. Journal of Medical Virology 2014;86:1838–44. https://doi.org/10.1002/jmv.24032.

[200] Kramvis Anna, Kew Michael C. Epidemiology of hepatitis B virus in Africa, its genotypes and clinical associations of genotypes. Hepatology Research 2007;37:S9–19. https://doi.org/10.1111/j.1872-034x.2007.00098.x.

[201] Iorio Raffaele, Giannattasio Antonietta, Cirillo Francesco, D'Alessandro Luca, Vegnente Angela. Long-Term Outcome in Children with Chronic Hepatitis B: A 24-Year Observation Period. Clinical Infectious Diseases 2007;45:943–9. https://doi.org/10.1086/521864.

[202] Malarnitsi-Puchner A, Papacharitonos S, Sotos D, Tzala L, Psichogiou M, Hatzakis A, Evangelopoulou A, Michalas S. Prevalence study of different hepatitis markers among pregnant Albanian refugees in Greece. European Journal of Epidemiology 1996;12:297–301. https://doi.org/10.1007/bf00145420.

[203] Hadziyannis Stephanos J. Natural history of chronic hepatitis B in Euro-Mediterranean and African Countries. Journal of Hepatology 2011;55:183–91. https://doi.org/10.1016/j.jhep.2010.12.030.

[204] Livingston Stephen E, Simonetti Josephine P, Bulkow Lisa R, Homan Chriss E, Snowball Mary M, Cagle Henry H, Negus Susan E, McMahon Brian J. Clearance of Hepatitis B e Antigen in Patients With Chronic Hepatitis B and Genotypes A, B, C, D, and F. Gastroenterology 2007;133:1452–7. https://doi.org/10.1053/j.gastro.2007.08.010.

[205] Krarup Henrik, Andersen Stig, Madsen Poul Henning, Christensen Peer Brehm, Laursen Alex Lund, Bentzen-Petersen Anne, Møller Jørn M, Weis Nina, group DANHEP. HBeAg and not genotypes predicts viral load in patients with hepatitis B in Denmark: A nationwide cohort study. Scandinavian Journal of Gastroenterology 2011;46:1484–91. https://doi.org/10.3109/00365521.2011.619273.

[206] Laras Andreas, Koskinas John, Hadziyannis Stephanos J. In Vivo Suppression of Precore mRNA Synthesis Is Associated with Mutations in the Hepatitis B Virus Core Promoter. Virology 2002;295:86–96. https://doi.org/10.1006/viro.2001.1352.

[207] Takahashi K, Aoyama K, Ohno N, Iwata K, Akahane Y, Baba K, Yoshizawa H, Mishiro S. The precore/core promoter mutant (T1762A1764) of hepatitis B virus: clinical significance and an easy method for detection. Journal of General Virology 1995;76:3159–64. https://doi.org/10.1099/0022-1317-76-12-3159.

[208] Ahn Sang Hoon, Kramvis Anna, Kawai Shigenobu, Spangenberg Hans Christian, Li Jisu, Kimbi Gerald, Kew Michael, Wands Jack, Tong Shuping. Sequence variation upstream of precore translation initiation codon reduces hepatitis B virus e antigen production. Gastroenterology 2003;125:1370–8. https://doi.org/10.1016/j.gastro.2003.07.016.

[209] Chen Chien Yu, Crowther Carol, Kew Michael C, Kramvis Anna. A valine to phenylalanine mutation in the precore region of hepatitis B virus causes intracellular retention and impaired secretion of HBe-antigen. Hepatology Research 2008;38:580–92. https://doi.org/10.1111/j.1872-034x.2007.00315.x.

[210] Okamoto H, Yotsumoto S, Akahane Y, Yamanaka T, Miyazaki Y, Sugai Y, Tsuda F, Tanaka T, Miyakawa Y, Mayumi M. Hepatitis B viruses with precore region defects prevail in persistently infected hosts along with seroconversion to the antibody against e antigen. Journal of Virology 1990;64:1298–303. https://doi.org/10.1128/jvi.64.3.1298-1303.1990.

[211] Fiordalisi Gianfranco, Cariani Elisabetta, Mantero Giovanni, Zanetti Alessandro, Tanzi Elisabetta, Chiaramonte Maria, Primi Daniele. High genomic variability in the pre-C region of hepatitis B virus in anti-HBe, HBV DNA-positive chronic hepatitis. Journal of Medical Virology 1990;31:297–300. https://doi.org/10.1002/jmv.1890310410.

[212] Santantonio Teresa, Jung Maria-Christina, Miska Stefan, Pastore Giuseppe, Rape Gerd R, Will Hans. Prevalence and type of pre-C HBV mutants in anti-HBe positive carriers with chronic liver disease in a highly endemic area. Virology 1991;183:840–4. https://doi.org/10.1016/0042-6822(91)91022-9.

[213] Norder Heléne, Twagirumugabe Theogene, Said Joanna, Tian Yarong, Tang Ka-Wei, Magnius Lars, Lindh Magnus. High Frequency of Either Altered Pre-Core Start Codon or Weakened Kozak Sequence in the Core Promoter Region in Hepatitis B Virus A1 Strains from Rwanda. Genes 2019;10:182. https://doi.org/10.3390/genes10030182.

[214] Kramvis Anna, Arakawa Kazuko, Yu Mimi C, Nogueira Ramon, Stram Daniel O, Kew Michael C. Relationship of serological subtype, basic core promoter and precore mutations to genotypes/subgenotypes of hepatitis B virus. Journal of Medical Virology 2008;80:27–46. https://doi.org/10.1002/jmv.21049.

[215] Chu Chi-Jen, Keeffe Emmet B, Han Steven-Huy, Perrillo Robert P, Min Albert D, Soldevila-Pico Consuelo, Carey William, Brown Robert S, Luketic Velimir A, Terrault Norah, Lok Anna SF,

Group US HBV Epidemiology Study. Prevalence of HBV precore/core promoter variants in the United States. Hepatology 2003;38:619–28. https://doi.org/10.1053/jhep.2003.50352.

[216] Lau Daryl TY, Ganova-Raeva Lilia, Wang Junyao, Mogul Douglas, Chung Raymond T, Lisker-Melman Mauricio, Chang Kyong-Mi, Shaikh Obaid S, Kleiner David, et al. Precore and Basal Core Promoter Hepatitis B Virus (HBV) Variants Are Present From a Young Age and Differ Across HBV Genotypes. Hepatology 2021;73:1637–51. https://doi.org/10.1002/hep.31506.

[217] Lim Chee Kent, Tan Joanne Tsui Ming, Khoo Jason Boo Siang, Ravichandran Aarthi, Low Hsin Mei, Chan Yin Chyi, Ton So Har. Correlations of HBV Genotypes, Mutations Affecting HBeAg Expression and HBeAg/ anti-HBe Status in HBV Carriers. International Journal of Medical Sciences 2006;3:14–20. https://doi.org/10.7150/ijms.3.14.

[218] Huy Tran Thien Tuan, Ushijima Hiroshi, Quang Vo Xuan, Ngoc Trinh Thi, Hayashi Shigeki, Sata Tetsutaro, Abe Kenji. Characteristics of core promoter and precore stop codon mutants of hepatitis B virus in Vietnam. Journal of Medical Virology 2004;74:228–36. https://doi.org/10.1002/jmv.20175.

[219] Fang Zhong-Liao, Sabin Caroline A, Dong Bai-Qing, Wei Shao-Chao, Chen Qin-Yan, Fang Kong-Xiong, Yang Jin-Ye, Wang Xue-Yan, Harrison Tim J. The association of HBV core promoter double mutations (A1762T and G1764A) with viral load differs between HBeAg positive and anti-HBe positive individuals: A longitudinal analysis. Journal of Hepatology 2009;50:273–80. https://doi.org/10.1016/j.jhep.2008.09.014.

[220] Lindh Magnus, Hannoun Charles, Dhillon Amar P, Norkrans Gunnar, Horal Peter. Core Promoter Mutations and Genotypes in Relation to Viral Replication and Liver Damage in East Asian Hepatitis B Virus Carriers. The Journal of Infectious Diseases 1999;179:775–82. https://doi.org/10.1086/314688.

[221] Chu Chia-Ming, Yeh Chau-Ting, Lee Ching-Song, Sheen I Shyan, Liaw Yun-Fan. Precore Stop Mutant in HBeAg-Positive Patients with Chronic Hepatitis B: Clinical Characteristics and Correlation with the Course of HBeAg-to-Anti-HBe Seroconversion. Journal of Clinical Microbiology 2002;40:16–21. https://doi.org/10.1128/jcm.40.1.16-21.2002.

[222] Alexopoulou Alexandra, Karayiannis Peter. HBeAg negative variants and their role in the natural history of chronic hepatitis B virus infection. World Journal of Gastroenterology 2014;20:7644–52. https://doi.org/10.3748/wjg.v20.i24.7644.

[223] Hayes C Nelson, Chayama Kazuaki. HBV culture and infectious systems. Hepatology International 2016;10:559–66. https://doi.org/10.1007/s12072-016-9712-y.

[224] Verrier Eloi R, Colpitts Che C, Schuster Catherine, Zeisel Mirjam B, Baumert Thomas F. Cell Culture Models for the Investigation of Hepatitis B and D Virus Infection. Viruses 2016;8:261. https://doi.org/10.3390/v8090261.

[225] Guo Hongbo, Urban Stephan, Wang Wenshi. In vitro cell culture models to study hepatitis B and D virus infection. Frontiers in Microbiology 2023;14:1169770. https://doi.org/10.3389/fmicb.2023.1169770.

[226] Sureau Camille, Romet-Lemonne Jean-Loup, Mullins James I, Essex Max. Production of hepatitis B virus by a differentiated human hepatoma cell line after transfection with cloned circular HBV DNA. Cell 1986;47:37–47. https://doi.org/10.1016/0092-8674(86)90364-8.

[227] Ladner SK, Otto MJ, Barker CS, Zaifert K, Wang GH, Guo JT, Seeger C, King RW. Inducible expression of human hepatitis B virus (HBV) in stably transfected hepatoblastoma cells: a novel system for screening potential inhibitors of HBV replication. Antimicrobial Agents and Chemotherapy 1997;41:1715–20. https://doi.org/10.1128/aac.41.8.1715.

[228] Guo Haitao, Jiang Dong, Zhou Tianlun, Cuconati Andrea, Block Timothy M, Guo Ju-Tao. Characterization of the Intracellular Deproteinized Relaxed Circular DNA of Hepatitis B Virus: an Intermediate of Covalently Closed Circular DNA Formation. Journal of Virology 2007;81:12472–84. https://doi.org/10.1128/jvi.01123-07.

[229] Sun Dianxing, Nassal Michael. Stable HepG2- and Huh7-based human hepatoma cell lines for efficient regulated expression of infectious hepatitis B virus. Journal of Hepatology 2006;45:636–45. https://doi.org/10.1016/j.jhep.2006.05.019.

[230] Raney Anneke K, Eggers Carrie M, Kline Eric F, Guidotti Luca G, Pontoglio Marco, Yaniv Moshe, McLachlan Alan. Nuclear Covalently Closed Circular Viral Genomic DNA in the Liver of Hepatocyte Nuclear Factor 1α-Null Hepatitis B Virus Transgenic Mice. Journal of Virology 2001;75:2900–11. https://doi.org/10.1128/jvi.75.6.2900-2911.2001.

[231] Gao Weifan, Hu Jianming. Formation of Hepatitis B Virus Covalently Closed Circular DNA: Removal of Genome-Linked Protein. Journal of Virology 2007;81:6164–74. https://doi.org/10.1128/jvi.02721-06.

[232] Li Wenhui, Urban Stephan. Entry of hepatitis B and hepatitis D virus into hepatocytes: Basic insights and clinical implications. Journal of Hepatology 2016;64:S32–40. https://doi.org/10.1016/j.jhep.2016.02.011.

[233] Kruse Robert L, Legras Xavier, Barzi Mercedes. Cre/LoxP-HBV plasmids generating recombinant covalently closed circular DNA genome upon transfection. Virus Research 2021;292:198224. https://doi.org/10.1016/j.virusres.2020.198224.

[234] Wu Min, Li Jin, Yue Lei, Bai Lu, Li Yaming, Chen Jieliang, Zhang Xiaonan, Yuan Zhenghong. Establishment of Cre-mediated HBV recombinant cccDNA (rcccDNA) cell line for cccDNA biology and antiviral screening assays. Antiviral Research 2018;152:45–52. https://doi.org/10.1016/j.antiviral.2018.02.007.

[235] Zhang Zhenhua, Xia Jianbo, Sun Binghu, Dai Yu, Li Xu, Schlaak Joerg F, Lu Mengji. In vitro and in vivo replication of a chemically synthesized consensus genome of hepatitis B virus genotype B. Journal of Virological Methods 2015;213:57–64. https://doi.org/10.1016/j.jviromet.2014.11.007.

[236] Liao Fenfang, Xie Junmou, Du Rongsong, Gao Wenbo, Lan Lanyin, Wang Min, Rong Xia, Fu Yongshui, Wang Hao. Replication and Expression of the Consensus Genome of Hepatitis B Virus Genotype C from the Chinese Population. Viruses 2023;15:2302. https://doi.org/10.3390/v15122302.

[237] Qiao Luhua, Sui Jianhua, Luo Guangxiang. Robust Human and Murine Hepatocyte Culture Models of Hepatitis B Virus Infection and Replication. Journal of Virology 2018;92. https://doi.org/10.1128/jvi.01255-18.

[238] Li Feng, Cheng Liang, Murphy Christopher M, Reszka-Blanco Natalia J, Wu Yaxu, Chi Liqun, Hu Jianming, Su Lishan. Minicircle HBV cccDNA with a Gaussia luciferase reporter for investigating

HBV cccDNA biology and developing cccDNA-targeting drugs. Scientific Reports 2016;6:36483. https://doi.org/10.1038/srep36483.

[239] Yu Yingpu, Schneider William M, Kass Maximilian A, Michailidis Eleftherios, Acevedo Ashley, Mosimann Ana L Pamplona, Bordignon Juliano, Koenig Alexander, Livingston Christine M, Gijzel Hardeep van, Ni Yi, Ambrose Pradeep M, Freije Catherine A, Zhang Mengyin, Zou Chenhui, Kabbani Mohammad, Quirk Corrine, Jahan Cyprien, Wu Xianfang, Urban Stephan, You Shihyun, Shlomai Amir, Jong Ype P de, Rice Charles M. An RNA-based system to study hepatitis B virus replication and evaluate antivirals. Science Advances 2023;9:eadg6265. https://doi.org/10.1126/sciadv.adg6265.

[240] Yang Danli, Zou Jun, Guan Guiwen, Feng Xiaoyu, Zhang Ting, Li Guixin, Liu Hui, Zheng Huiling, Xi Jingyuan, Yu Guangxin, Dai Lizhong, Lu Fengmin, Chen Xiangmei. The A1762T/G1764A mutations enhance HBV replication by alternating viral transcriptome. Journal of Medical Virology 2023;95:e29129. https://doi.org/10.1002/jmv.29129.

[241] Jammeh Saffie, Tavner Fiona, Watson Roger, Thomas Howard C, Karayiannis Peter. Effect of basal core promoter and pre-core mutations on hepatitis B virus replication. Journal of General Virology 2008;89:901–9. https://doi.org/10.1099/vir.0.83468-0.

[242] Scaglioni Pier Paolo, Melegari Margherita, Wands Jack R. Biologic Properties of Hepatitis B Viral Genomes with Mutations in the Precore Promoter and Precore Open Reading Frame. Virology 1997;233:374–81. https://doi.org/10.1006/viro.1997.8594.

[243] Gv°nther S, Piwon N, Will H. Wild-type levels of pregenomic RNA and replication but reduced pre-C RNA and e-antigen synthesis of hepatitis B virus with C(1653) --> T, A(1762) --> T and G(1764) --> A mutations in the core promoter. Journal of General Virology 1998;79:375–80. https://doi.org/10.1099/0022-1317-79-2-375.

[244] Yoo Byung Chul, Park Joong-Won, Kim Hyung Joon, Lee Dong Ho, Cha Young Ju, Park Sill Moo. Precore and core promoter mutations of hepatitis B virus and hepatitis B e antigen-negative chronic hepatitis B in Korea. Journal of Hepatology 2003;38:98–103. https://doi.org/10.1016/s0168-8278(02)00349-5.

[245] Milich David R, Chen Margaret, Schödel Florian, Peterson Darrell L, Jones Joyce E, Hughes Janice L. Role of B cells in antigen presentation of the hepatitis B core. Proceedings of the National Academy of Sciences 1997;94:14648–53. https://doi.org/10.1073/pnas.94.26.14648.

[246] Diepolder* ‡ Helmut M, Ries‡ Gerhard, Jung* ‡ Maria-Christina, Schlicht§ Hans-Jürgen, Gerlach* ‡ Jörn-Tilman, Grüner‡ Norbert, Caselmann‖ Wolfgang H, Pape* ‡ Gerd R. Differential antigen-processing pathways of the hepatitis B virus e and core proteins. Gastroenterology 1999;116:650–7. https://doi.org/10.1016/s0016-5085(99)70187-3.

[247] Frelin Lars, Wahlström Therese, Tucker Amy E, Jones Joyce, Hughes Janice, Lee Byung O, Billaud Jean-Noel, Peters Cory, Whitacre David, Peterson Darrell, Milich David R. A Mechanism To Explain the Selection of the Hepatitis e Antigen-Negative Mutant during Chronic Hepatitis B Virus Infection. Journal of Virology 2009;83:1379–92. https://doi.org/10.1128/jvi.01902-08.

[248] Liu Chun-Jen, Chen Pei-Jer, Lai Ming-Yang, Lin Feng-Yi, Wang Tzusan, Kao Jia-Horng, Chen Ding-Shinn. Viral factors correlate with hepatitis B e antigen seroconverson in patients with chronic hepatitis B. Liver International 2006;26:949–55. https://doi.org/10.1111/j.1478-3231.2006.01319.x.

[249] Eijk AA Van Der, Niesters HGM, Hansen BE, Heijtink RA, Janssen HLA, Schalm SW, Man RA De. Quantitative HBV DNA levels as an early predictor of nonresponse in chronic HBe-antigen positive hepatitis B patients treated with interferon-alpha. Journal of Viral Hepatitis 2006;13:96–103. https://doi.org/10.1111/j.1365-2893.2005.00661.x.

[250] Fried Michael W, Piratvisuth Teerha, Lau George KK, Marcellin Patrick, Chow Wan-Cheng, Cooksley Graham, Luo Kang-Xian, Paik Seung Woon, Liaw Yun-Fan, Button Peter, Popescu Matei. HBeAg and hepatitis B virus DNA as outcome predictors during therapy with peginterferon alfa-2a for HBeAg-positive chronic hepatitis B. Hepatology 2008;47:428–34. https://doi.org/10.1002/hep.22065.

[251] Mommeja-Marin Herve, Mondou Elsa, Blum M Robert, Rousseau Franck. Serum HBV DNA as a marker of efficacy during therapy for chronic HBV infection: Analysis and review of the literature. Hepatology 2003;37:1309–19. https://doi.org/10.1053/jhep.2003.50208.

[252] Lau George KK, Piratvisuth Teerha, Luo Kang Xian, Marcellin Patrick, Thongsawat Satawat, Cooksley Graham, Gane Edward, Fried Michael W, Chow Wan Cheng, Paik Seung Woon, Chang Wen Yu, Berg Thomas, Flisiak Robert, McCloud Philip, Pluck Nigel, Group Peginterferon Alfa-2a HBeAg-Positive Chronic Hepatitis B Study. Peginterferon Alfa-2a, Lamivudine, and the Combination for HBeAg-Positive Chronic Hepatitis B. The New England Journal of Medicine 2005;352:2682–95. https://doi.org/10.1056/nejmoa043470.

[253] Yamaura Takahiro, Tanaka Eiji, Matsumoto Akihiro, Rokuhara Akinori, Orii Koji, Yoshizawa Kaname, Miyakawa Yuzo, Kiyosawa Kendo. A case-control study for early prediction of hepatitis B e antigen seroconversion by hepatitis B virus DNA levels and mutations in the precore region and core promoter. Journal of Medical Virology 2003;70:545–52. https://doi.org/10.1002/jmv.10429.

[254] Bertoni R, Sidney J, Fowler P, Chesnut RW, Chisari FV, Sette A. Human histocompatibility leukocyte antigen-binding supermotifs predict broadly cross-reactive cytotoxic T lymphocyte responses in patients with acute hepatitis. Journal of Clinical Investigation 1997;100:503–13. https://doi.org/10.1172/jci119559.

[255] Penna A, Chisari FV, Bertoletti A, Missale G, Fowler P, Giuberti T, Fiaccadori F, Ferrari C. Cytotoxic T lymphocytes recognize an HLA-A2-restricted epitope within the hepatitis B virus nucleocapsid antigen. The Journal of Experimental Medicine 1991;174:1565–70. https://doi.org/10.1084/jem.174.6.1565.

[256] Kuhröber A, Wild J, Pudollek HP, Chisari FV, Reimann J. DNA vaccination with plasmids encoding the intracellular (HBcAg) or secreted (HBeAg) form of the core protein of hepatitis B virus primes T cell responses to two overlapping Kb- and Kd-restricted epitopes. International Immunology 1997;9:1203–12. https://doi.org/10.1093/intimm/9.8.1203.

[257] Townsend K, Sällberg M, O'Dea J, Banks T, Driver D, Sauter S, Chang SM, Jolly DJ, Mento SJ, Milich DR, Lee WT. Characterization of CD8+ cytotoxic T-lymphocyte responses after genetic immunization with retrovirus vectors expressing different forms of the hepatitis B virus core and e antigens. Journal of Virology 1997;71:3365–74. https://doi.org/10.1128/jvi.71.5.3365-3374.1997.

[258] Street M, Herd K, Londono P, Doan T, Dougan G, Kast WM, Tindle RW. Differences in the effectiveness of delivery of B- and CTL-epitopes incorporated into the Hepatitis B core antigen

(HBcAg) c/e1-region. Archives of Virology 1999;144:1323–43. https://doi.org/10.1007/s007050050590.

[259] Gehring Adam J, Sun Dianxing, Kennedy Patrick TF, Hoen Esther Nolte-'t, Lim Seng Gee, Wasser Shanthi, Selden Clare, Maini Mala K, Davis Dan M, Nassal Michael, Bertoletti Antonio. The Level of Viral Antigen Presented by Hepatocytes Influences CD8 T-Cell Function. Journal of Virology 2007;81:2940–9. https://doi.org/10.1128/jvi.02415-06.

Eidesstattliche Erklärung

Erklärung

Ich versichere an Eides Statt, dass die Dissertation von mir selbständig und ohne unzulässige fremde Hilfe unter Beachtung der „Grundsätze zur Sicherung guter wissenschaftlicher Praxis an der Heinrich-Heine- Universität Düsseldorf“ erstellt worden ist. Die Arbeit habe ich bisher keinem anderen Prüfungsamt in gleicher oder vergleichbarer Form vorgelegt.

_____ _____

(Ort, Datum) Maximilian Paul Damagnez

List of Figures

List of Tables

Supplements

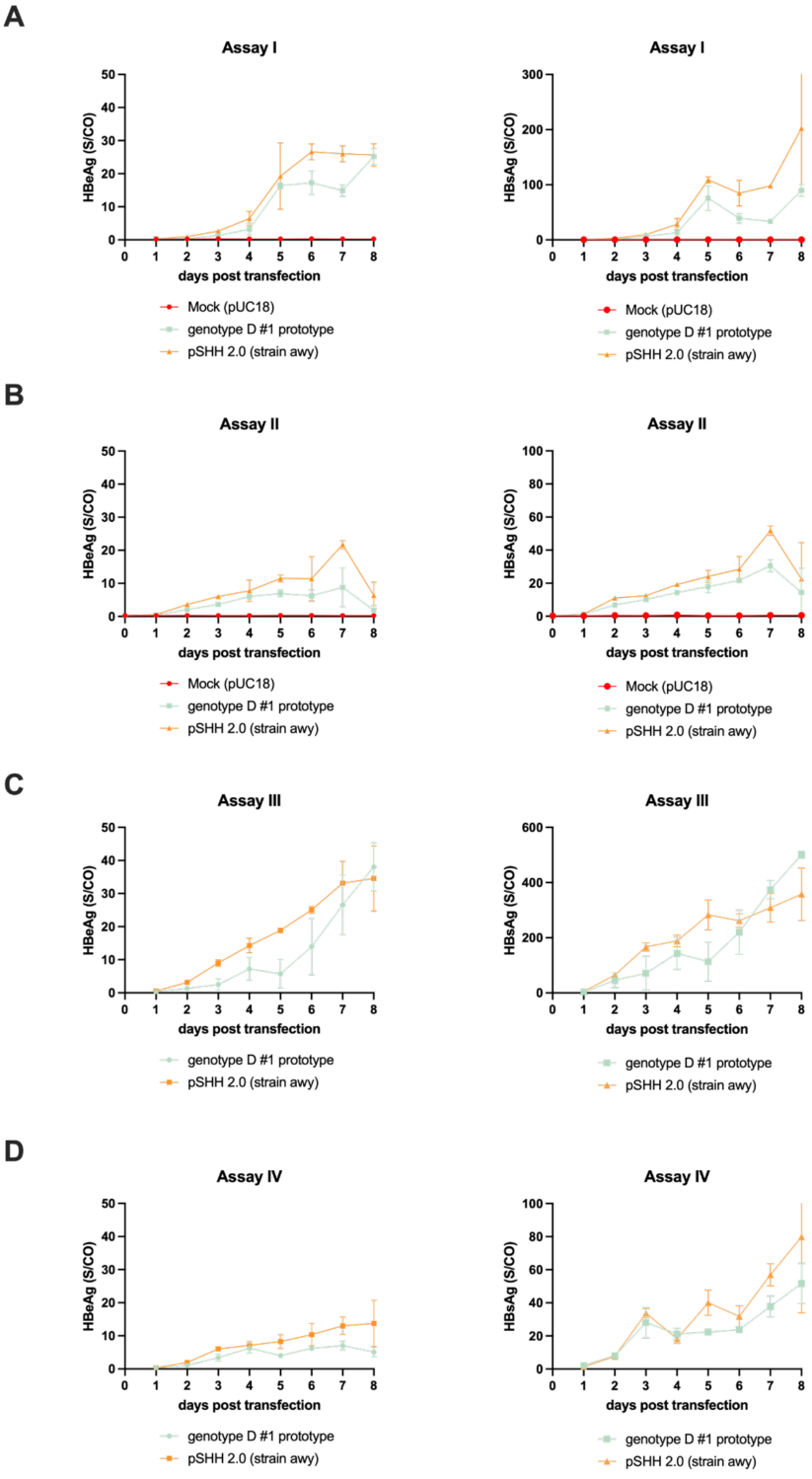

Figure S1 HBV cccDNA assay: HBeAg and HBsAg levels in the supernatant from genotype D #1 prototype (green), pSHH 2-1 (orange) variants and pUC18 (red). Signal-to-cutoff (S/CO) ratio was measured with the Architect i2000 immunoassay system. Each experiment used 200.000 HepG2-NTCP cells/well with 250 ng cccDNA/well. A) HBeAg and HBsAg S/CO ratios during the first experiment. B) HBeAg and HBsAg S/CO ratios during the second experiment. C) HBeAg and HBsAg S/CO ratios during the third experiment. D) HBeAg and HBsAg S/CO ratios during the third experiment.

Supplemental Table 1 pSHH 2-1 HBeAg (S/CO ratio)

days post transfection	Assay I (S/CO ratio)		Assay II (S/CO ratio)		Assay III (S/CO ratio)			Assay IV (S/CO ratio)		
0	-	-	0,306	-	0,385	-	-	0,312	-	-
1	0,324	0,327	0,592	0,55	0,466	0,572	0,519	0,375	0,341	0,343
2	0,747	1,111	3,668	3,557	3,132	3,066	3,253	2,24	1,798	1,773
3	2,842	2,48	6,229	5,774	10,15	8,373	8,508	6,452	6,484	5,307
4	4,869	7,974	10,044	5,48	12,864	16,819	13,12	5,92	7,175	8,223
5	26,306	12,16	12,22	10,707	19,246	18,43	18,837	6,806	10,668	7,375
6	28,305	24,915	16,151	6,682	24,647	26,22	24,334	10,94	13,462	6,721
7	27,777	24,304	22,605	20,83	40,724	30,301	28,353	14,802	14,3	9,989
8	28,041	23,211	3,521	9,147	-	41,526	27,57	16,719	18,729	5,73

Supplemental Table 2 pSHH 2-1 HBsAg (S/CO ratio)

days post transfection	Assay I (S/CO ratio)		Assay II (S/CO ratio)		Assay III (S/CO ratio)			Assay IV (S/CO ratio)		
0	-	-	0,23	-	0,25	-	-	0,5	-	-
1	0,59	0,46	1,96	0,74	4,61	5,44	4,83	1,58	1,21	1,37
2	1,77	4,08	10,41	11,65	69,86	60,86	63,56	8,7	6,18	8,04
3	10,32	9,14	12,04	12,86	179,79	169,82	150,83	31,67	36,89	32,64
4	21,06	35,75	20,12	18,33	193,5	206,18	165,17	15,49	18,66	20,83
5	112,72	104,88	21,41	26,67	309,75	220,37	318,26	32,69	47,78	39,66
6	67,95	101,05	33,9	23,01	289,9	241,13	254,34	30,27	38,86	26,15
7	96,28	99,64	53,81	49,82	366,55	292,18	267,66	63,36	57,64	49,95
8	121,21	283,31	6,98	38,08	-	425,07	290,65	108,45	104,24	26,92

Supplemental Table 3 genotype D isolate #1 prototype HBeAg (S/CO ratio)

days post transfection	Assay I (S/CO ratio)		Assay II (S/CO ratio)		Assay III (S/CO ratio)			Assay IV (S/CO ratio)		
0	-	-	0,248	-	0,355	-	-	0,212	-	-
1	0,354	0,412	0,432	0,447	0,402	0,318	0,289	0,31	0,336	0,336
2	0,312	0,455	2,076	2,055	1,992	0,705	1,275	1,175	1,148	1,021
3	1,717	0,823	3,799	3,418	1,815	1,149	4,483	2,377	3,2	4,561
4	1,923	4,504	6,335	5,665	10,59	3,665	7,476	4,502	7,426	6,836
5	15,723	16,976	6,208	7,644	10,726	3,582	2,907	3,463	4,5	4,137
6	14,749	19,829	7,457	4,968	23,686	8,4	9,726	5,629	6,825	6,191
7	16,122	13,653	4,725	12,921	32,473	31,05	16,221	5,52	7,708	7,885
8	23,433	26,904	2,941	0,888	-	32,896	43,211	3,482	5,595	6,182

Supplemental Table 4 genotype D isolate #1 prototype HBsAg (S/CO ratio)

days post transfection	Assay I (S/CO ratio)		Assay II (S/CO ratio)		Assay III (S/CO ratio)			Assay IV (S/CO ratio)		
0	-	-	0,24	-	0,63	-	-	0,41	-	-
1	1,11	1,06	1,65	1,17	5,23	2,43	1,01	2,07	2,33	2,01
2	0,65	1,46	6,63	7,2	69,9	16,52	50,91	8,6	8,53	7,14
3	9,53	2,92	10,36	9,82	43,84	28,38	142,15	20,04	25,99	38,12
4	6,7	19,55	15,19	13,57	177,11	76,53	175,75	17,51	24,45	21,57
5	59,93	91,49	15,2	20,47	194,69	76,09	68,59	23,18	21,18	22,53
6	32,92	45,52	22,22	21,26	290,22	132,42	236,61	23,49	24,65	23,17
7	35	31,61	27,98	33,15	345,35	366,52	410,59	31,68	37,43	44,22
8	82,54	97,31	24,66	4,22	-	492,91	509,92	39,92	51,02	64,21

Supplemental Table 5 genotype A isolate #1 HBeAg (S/CO ratio)

days post **transfection**	prototype			BCP mutation			G1896A (W28*)			start codon mutation		
0	0,385			0,332			0,348			0,31		
2	9,362	12,013	11,746	4,153	4,042	4,344	0,365	0,342	0,326	0,361	0,352	0,371
3	29,79	24,412	26,536	10,141	9,757	11,668	0,327	0,32	0,327	0,338	0,376	0,382
4	47,2	53,09	-	18,898	17,145	17,451	0,431	0,358	0,372	0,36	0,444	0,373
5	69,175	63,1	63,31	20,951	24,646	25,763	0,337	0,326	0,35	0,38	0,406	0,382

Supplemental Table 6 genotype A isolate #1 HBsAg (S/CO ratio)

days post **transfection**	prototype			BCP mutation			G1896A (W28*)			start codon mutation		
0	0,349			0,375			0,342			0,355		
2	16,62	13,01	16,17	36,48	25,96	33,18	12,01	16,2	17,44	17,25	23,66	24,54
3	51,68	38,63	42,49	120,07	97,4	97,13	45,83	59,44	62,01	61,85	80,35	89,26
4	83,68	71,25	78,58	170,39	135,64	129,64	108,27	102,06	103,91	121,73	119,56	132,17
5	138,29	124,31	99,76	199,31	178,7	182,11	114,92	138,49	129,24	154,12	172,05	158,81

Supplemental Table 7 genotype A isolate #2 HBeAg (S/CO ratio)

days post **transfection**	prototype				BCP mutation				G1896A (W28*)				start codon mutation			
0	0,346				0,375				0,319				0,323			
2	3,129	3,481	3,191	2,601	1,926	2,338	2,427	2,057	0,327	0,349	0,331	0,318	0,388	0,326	0,327	0,341
3	7,512	9,293	8,25	7,134	4,571	5,308	4,884	4,919	0,384	0,42	0,407	0,373	0,327	0,389	0,377	0,363
4	11,917	12,303	13,88	11,259	8,44	8,375	9,544	5,711	0,328	0,343	0,339	0,339	0,381	0,45	0,35	0,372
5	16,994	18,743	17,835	12,588	9,809	6,361	5,716	6,48	0,311	0,365	0,3	0,323	0,39	0,314	0,338	0,311

Supplemental Table 8 genotype A isolate #2 HBsAg (S/CO ratio)

days post transfection	prototype				BCP mutation				G1896A (W28*)				start codon mutation			
0	0				0				0				0			
2	24,63	20,5	18,5	21,11	20,92	23,81	24,37	18,36	21,69	25,02	26,67	29,04	26,27	33,7	29,37	29,48
3	55,5	47,65	50,67	41,17	46,91	45,13	47,71	36,5	56,6	49,84	52,89	41,82	57,93	60,75	50,25	51,45
4	63,81	81,49	72,24	60,88	64,94	89,53	73,85	70,43	94,95	104,09	90,68	70,61	104,5	129,49	107,89	93,56
5	99,89	107,51	106,37	71,83	83,56	59,12	54,62	50,94	53,53	54,36	47,9	54,65	66,09	68,13	68,13	-

Supplemental Table 9 genotype A consensus HBeAg (S/CO ratio)

days post transfection	prototype				BCP mutation				G1896A (W28*)				start codon mutation			
0	0				0				0				0			
2	1,496	2,14	2,48	1,606	1,319	1,481	1,673	1,343	0,42	0,397	0,421	0,334	0,34	0,448	0,373	0,385
3	1,929	2,842	3,238	1,609	1,531	2,231	2,235	1,522	0,354	0,341	0,407	0,385	0,338	0,347	0,376	0,368
4	3,997	4,793	4,461	3,198	2,589	3,574	3,919	2,461	0,35	0,344	0,364	0,42	0,42	0,468	0,386	0,437
5	4,615	5,632	6,209	5,44	3,581	4,425	4,44	4,035	0,366	0,369	0,421	0,423	0,401	0,381	0,395	0,465

Supplemental Table 10 genotype A consensus HBsAg (S/CO ratio)

days post transfection	prototype				BCP mutation				G1896A (W28*)				start codon mutation			
0	0				0				0				0			
2	11,28	13,73	17,25	13,19	15,32	15,07	18,43	14,89	15,42	21,13	22,95	12,07	13,83	18,54	20,34	15,18
3	20,04	21,49	27,8	15,24	23,11	28,98	28,53	22,5	25,88	36,73	35,57	24,52	22,17	31,43	35,09	22,01
4	32,62	36,39	33,68	27,49	33,11	43,85	48,81	33,17	37,6	48,75	56,74	78,41	44,83	52,69	46,19	52,82
5	34,28	38,79	41,94	43,96	41,1	48,81	55,46	47,77	53,15	60,67	68,73	76,73	73,31	95,33	85,65	66,08

Supplemental Table 11 genotype D isolate #1 HBeAg (S/CO ratio)

days post transfection	prototype			BCP mutation			G1896A (W28*)			CTG start codon mutation		
0	0,374			0,483			0			0,348		
2	7,969	9,163	9,728	5,493	4,46	4,446	0,362	0,374	0,346	0,355	0,346	0,424
3	23,844	23,768	18,017	12,189	11,651	12,661	0,339	0,323	0,362	0,357	0,588	0,363
4	35,512	39	31,988	18,745	21,16	19,692	0,362	0,373	0,37	0,37	0,523	0,4
5	40,818	39,569	38,041	21,949	24,51	24,814	0,408	0,41	0,406	0,441	0,449	0,416

Supplemental Table 12 genotype D isolate #1 HBsAg (S/CO ratio)

days post transfection	prototype			BCP mutation			G1896A (W28*)			CTG start codon mutation		
0	0,67			0,58			0,43			0,51		
2	13,42	10,77	10,81	9,1	7,03	4,29	11,45	5,93	5,23	28,02	31,75	32,87
3	45,15	46,96	44,65	19,42	31,03	40,1	28,86	30,53	43,34	78,35	67,46	59,55
4	49,26	42	47,97	49,4	43,37	41,04	56,29	62,03	56,78	71,11	78,53	63,9
5	46,47	43,48	80,52	37,01	36,29	44,18	67,82	59,13	56,87	68,83	53,64	49,28

Supplemental Table 13 genotype D consensus HBeAg (S/CO ratio)

days post transfection	prototype		BCP mutation		G1896A (W28*)		CTG	
0	0,4		0,42		0,443		0,398	
1	29	11	21	9	0,573	0,427	0,412	0,479
2	112	277	39,1	168	0,634	0,565	0,992	1
3	220	431	67,3	262	0,648	0,98	1,079	1,569
4	265	522	56	321	0,783	0,847	0,967	1,983
5	232	567	49	317	1,04	1,03	1,15	2,69
6	247	588	54,9	371	1,624	1,9	1,645	5,167

Supplemental Table 14 genotype D consensus HBsAg (S/CO ratio)

days post transfection	prototype		BCP mutation		G1896A (W28*)		CTG	
0	0,47		0,48		0,48		0,46	
1	133,91	258,87	108,76	164,72	219,81	136,94	37,19	69,28
2	1699	1076	621,71	764	1422	1961	1903	479
3	3345	1904	1787	1264	2425	3609	1087	3278
4	4081	2336	2058	1868	3086	3512	953	4263
5	4770	2924	2329	2228	3576	3890	1060	5050
6	5448	3658	3082	2889	4498	4947	1581	5821

Sequence Information

T-cell Receptor

HBc18-27

TCR alpha 3 variable region

ATGGAAACACTACTTGGAGTCTCACTGGTCATATTATGGTTACAACTTGCGCGAGTCAACAGCCAACAAGGAGAAGAAGATCCTCAAGCTCTATCGATCCAAG
AAGGAGAAAACGCTACGATGAACTGCTCGTACAAGACATCGATCAACAACCTGCAATGGTACCGACAAAACAGCGGAAGAGGACTCGTCCACCTGATCCTGA
TCCGGAGCAATGAACGAGAGAAGCACAGCGGAAGACTTCGAGTGACGCTGGACACGTCGAAGAAGAGCAGCAGCCTGCTGATCACCGCATCAAGAGCAGC
AGACACCGCCTCCTACTTCTGCGCAACATGGCTGAGCGGATCAGCTCGACAGCTGACCTTCGGAAGCGGAACGCAGCTGACCGTGCTGCCGGAC

TCR beta 8 variable region

ATGGATTCTTGGACCCTTTGTTGTGTTTCGCTTTGTATACTTGTCGCTAAACACACCGACGCTGGAGTGATCCAGAGCCCAAGACATGAAGTGACCGAGATGG
GACAAGAAGTGACGCTGCGCTGCAAACCGATCTCCGGACACGACTACCTCTTCTGGTACCGACAAACGATGATGAGAGGACTGGAGCTGCTGATCTACTTCA
ACAACAACGTGCCAATCGACGACTCCGGAATGCCAGAAGATCGCTTCAGCGCCAAGATGCCAAACGCCAGCTTCAGCACGCTGAAGATCCAGCCATCAGAAC
CAAGAGACAGCGCCGTCTACTTCTGCGCTTCATCGAACCGAGCTTCGAGCTACAACGAGCAGTTCTTCGGACCTGGAACAAGATTGACCGTGCTG

HBs370-379

Nucleotide Sequence

TCR alpha 12 variable region

ATGGCAACCAACTTCAGCCTGCTGAAACAAGCTGGAGACGTGGAAGAAAATCCTGGACCGATGAAGAGCCTACGAGTGCTGCTCGTCATCCTATGGCTACAA
CTGAGCTGGGTCTGGAGCCAGCAGAAAGAAGTGGAGCAGAACAGCGGACCGCTATCAGTTCCAGAAGGAGCGATCGCATCGCTGAACTGCACCTACTCGG
ATCGAGGAAGCCAAAGCTTCTTCTGGTACCGCCAATACTCCGGAAAAAGCCCGGAGCTGATCATGTTCATCTACTCCAACGGAGACAAAGAAGATGGAAGAT
TCACAGCGCAGCTGAACAAAGCTTCACAATACGTCTCGCTGCTGATCCGAGACAGCCAACCAAGCGACAGCGCAACCTACCTGTGCGCCGTCAACCTCTACGC
TGGAAACATGCTGACCTTCGGAGGAGGAACACGGCTGATGGTGAAGCCACAC

TCR beta 7.8 variable region

ATGGGAACAAGACTGCTGTGCTGGGTCGTGCTCGGATTCCTCGGAACGGACCACACTGGAGCTGGAGTCAGCCAATCGCCACGCTACAAAGTCGCCAAACG
AGGACAAGACGTGGCGCTGCGCTGCGATCCGATCTCCGGACACGTCAGCCTCTTCTGGTACCAACAAGCGCTCGGACAAGGACCGGAGTTCCTGACCTACTT
CCAAAACGAAGCGCAGCTGGACAAGAGCGGACTACCATCGGACCGCTTCTTCGCCGAGAGACCAGAAGGAAGCGTCAGCACGCTGAAGATCCAAAGAACA
CAACAAGAAGACAGCGCCGTCTACCTGTGCGCTTCGAGCTCCGACTTCGGAAACCAACCGCAACACTTCGGAGATGGAACAAGACTATCGATCCTG

Murin alpha constant region

ATCCAAAACCCAGAACCAGCAGTCTACCAGCTGAAGGACCCAAGAAGCCAAGACAGCACGCTGTGCCTCTTCACCGACTTCGACTCGCAAATCAACGTGCCG
AAGACAATGGAGAGCGGAACCTTCATCACCGACAAATGCGTCCTGGACATGAAAGCCATGGATTCGAAATCCAACGGAGCGATCGCCTGGAGCAACCAGAC
AAGCTTCACGTGCCAAGACATCTTCAAGGAGACCAACGCCACCTACCCATCGAGCGACGTGCCGTGCGACGCTACGCTGACGGAGAAGAGCTTCGAGACCG
ACATGAACCTGAACTTCCAAAACCTCAGCGTGATGGGACTTCGGATCCTGCTGCTGAAAGTCGCTGGATTCAACCTGCTGATGACGCTGCGGCTATGGAGCAG
CTGA

Murine beta constant region

GAAGACCTGCGGAACGTGACGCCACCGAAAGTTTCGCTCTTCGAGCCATCGAAAGCCGAGATCGCCAACAAACAGAAAGCTACACTCGTCTGCCTGGCAAG
AGGATTCTTCCCGGACCACGTGGAGCTGTCATGGTGGGTCAACGGAAAAGAAGTCCACAGCGGCGTCTGCACCGACCCTCAAGCCTACAAGGAATCCAACT
ACAGCTACTGCCTCAGCAGCAGACTTCGAGTCAGCGCAACGTTCTGGCACAATCCAAGAAACCACTTCAGATGCCAAGTCCAGTTCCACGGACTATCGGAAG
AAGACAAGTGGCCCGAAGGAAGTCCAAAGCCCGTCACCCAGAACATTAGCGCAGAAGCCTGGGGACGAGCGGACTGCGGAATCACATCCGCCTCCTACCAC

CAAGGAGTGCTGAGCGCAACGATCCTCTACGAGATCCTGCTCGGAAAAGCTACGCTCTACGCCGTGCTCGTCTCCGGACTCGTGCTGATGGCGATGGTGAAG
AAGAAGAACAGC

Plasmids

pMP71 flex

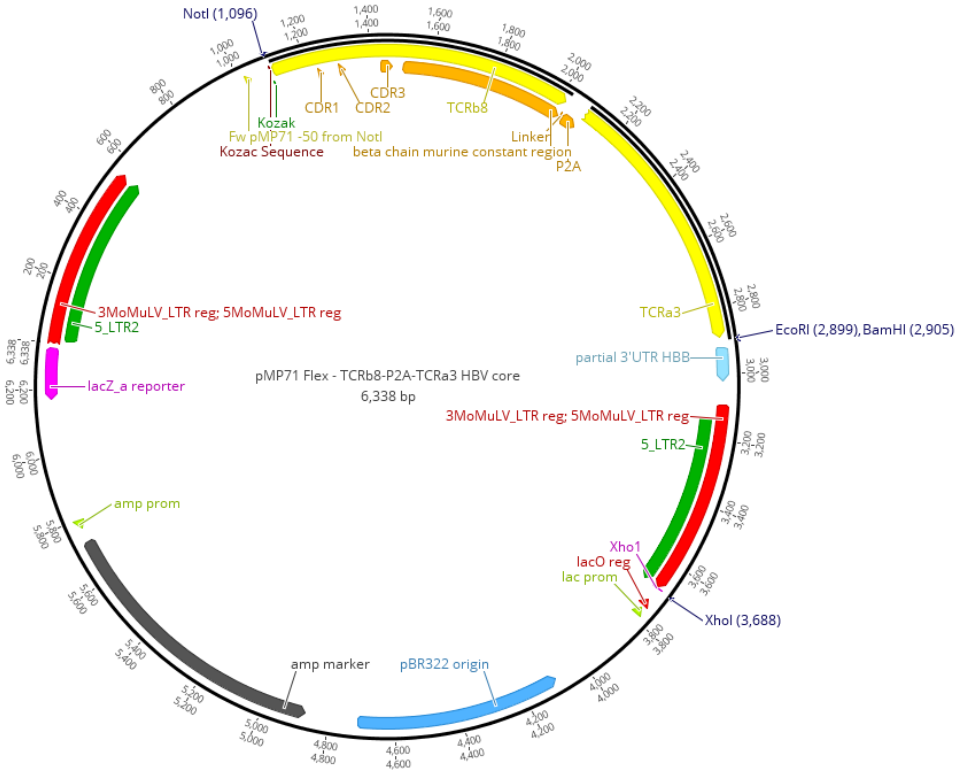

CTAGCTTAAGTAACGCCATTTTGCAAGGCATGGAAAATACATAACTGAGAATAGAGAAGTTCAGATCAAGGTTAGAACAGAGAGACAGCAGAATATGGGCCA
AACAGGATATCTGTGGTAAGCAGTTCCTGCCCCGGCTCAGGGCCAAGAACAGTTGGAACAGCAGAATATGGGCCAAACAGGATATCTGTGGTAAGCAGTTCC
TGCCCCGGCTCAGGGCCAAGAACAGATGGTCCCCAGATGCGGTCCCGCCCTCAGCAGTTTCTAGAGAACCATCAGATGTTTCCAGGGTGCCCCAAGGACCTG
AAATGACCCTGTGCCTTATTTGAACTAACCAATCAGTTCGCTTCTCGCTTCTGTTCGCGCGCTTCTGCTCCCCGAGCTCAATAAAAGAGCCCACAACCCCTCACT
CGGCGCGCCAGTCCTCCGATAGACTGCGTCGCCCGGGTACCCGTATTCCCAATAAAGCCTCTTGCTGTTTGCATCCGAATCGTGGACTCGCTGATCCTTGGGAG
GGTCTCCTCAGATTGATTGACTGCCCACCTCGGGGGTCTTTCATTTGGAGGTTCCACCGAGATTTGGAGACCCCTGCCCAGGGACCACCGACCCCCCCGCCG
GGAGGTAAGCTGGCCAGCGGTCGTTTCGTGTCTGTCTCTGTCTTTGTGCGTGTTTGTGCCGGCATCTAATGTTTGCGCCTGCGTCTGTACTAGTTGGCTAACTA
GATCTGTATCTGGCGGTCCCGCGGAAGAACTGACGAGTTCGTATTCCCGGCCGCAGCCCCTGGGAGACGTCCCAGCGGCCTCGGGGGCCCGTTTTGTGGCC
CATTCTGTATCAGTTAACCTACCCGAGTCGGACTTTTTGGAGCTCCGCCACTGTCCGAGGGGTACGTGGCTTTGTTGGGGGACGAGAGACAGAGACACTTCC
CGCCCCCGTCTGAATTTTTGCTTTCGGTTTTACGCCGAAACCGCGCCGCGCGTCTTGTCTGCTGCAGCATCGTTCTGTGTTGTCTCTGTCTGACTGTGTTTCTGT
ATTTGTCTGAAAATTAGCTCGACAAAGTTAAGTAATAGTCCCTCTCTCCAAGCTCACTTACAGGCGGCCGCCACCATGTCCATCGGCCTGCTGTGCTGTGCCGC
CCTGTCTCTGCTGTGGGCAGGACCAGTGAACGCAGGAGTGACCCAGACACCCAAGTTTCAGGTGCTGAAGACCGGCCAGAGCATGACACTGCAGTGCGCCC
AGGACATGAATCACGAGTACATGTCCTGGTATCGGCAAGACCCTGGCATGGGCCTGAGACTGATCCACTACTCCGTGGGAGCAGGAATCACCGACCAGGGAG
AGGTGCCCAACGGCTATAATGTGAGCAGGTCCACCACAGAGGATTTCCCACTGCGCCTGCTGTCTGCCGCACCTTCTCAGACCAGCGTGTACTTTTGTGCCAG
CTCCTCTGTGACCGGCACAGGCAACTACGGCTATACATTCGGCAGCGGAACCAGGCTGACAGTGGTGGAGGACCTACGTAACGTGACACCACCCAAAGTCTC
ACTGTTTGAGCCTAGCAAGGCAGAAATTGCCAACAAGCAGAAGGCCACCCTGGTGTGCCTGGCAAGAGGGTTCTTTCCAGATCACGTGGAGCTGTCCTGGT
GGGTCAACGGCAAAGAAGTGCATTCTGGGGTCTGCACCGACCCCCAGGCTTACAAGGAGAGTAATTACTCATATTGTCTGTCAAGCCGGCTGAGAGTGTCCG
CCACATTCTGGCACAACCCTAGGAATCATTTCCGCTGCCAGGTCCAGTTTCACGGCCTGAGTGAGGAAGATAAATGGCCAGAGGGGTCACCTAAGCCAGTGA
CACAGAACATCAGCGCAGAAGCCTGGGGACGAGCAGACTGTGGCATTACTAGCGCCTCCTATCATCAGGGCGTGCTGAGCGCCACTATCCTGTACGAGATTCT

GCTGGGAAAGGCCACCCTGTATGCTGTGCTGGTCTCCGGCCTGGTGCTGATGGCCATGGTCAAGAAAAAGAACTCTGGGAGTGGAGCCACAAATTTCTCTCT
GCTGAAACAGGCTGGAGATGTGGAGGAAAACCCCGGCCCTATGAAGAGCCTGCGCGTGCTGCTGGTCATCCTGTGGCTGCAATTGTCCTGGGTGTGGAGCC
AGATCCTGAACGTGGAGCAGTCTCCACAGAGCCTGCACGTGCAGGAGGGCGACTCTACCAACTTCACATGCAGCTTTCCCAGCTCCAATTTCTATGCCCTGCA
CTGGTACCGGTGGGAGACAGCCAAGAGCCCTGAGGCCCTGTTTGTGATGACACTGAACGGCGATGAGAAGAAGAAGGGCAGAATCTCCGCCACCCTGAATA
CAAAGGAGGGCTACTCTTATCTGTACATCAAGGGCAGCCAGCCAGAGGACAGCGCCACCTACCTGTGCGCAAGGAACACAGGCAATCAGTTCTACTTTGGCA
CCGGCACATCCCTGACCGTGATCCCCGATATCCAGAATCCCGAGCCTGCCGTATACCAGCTGAAGGACCCCCGATCTCAGGATAGTACTCTGTGCCTGTTCACC
GACTTTGATAGTCAGATCAATGTGCCTAAAACCATGGAATCCGGAACTTTTATTACCGACAAGTGCGTGCTGGATATGAAAGCCATGGACAGTAAGTCAAACG
GCGCCATCGCTTGGAGCAATCAGACATCCTTCACTTGCCAGGATATCTTCAAGGAGACCAACGCAACATACCCATCCTCTGACGTGCCCTGTGATGCCACCCTG
ACAGAGAAGTCTTTCGAAACAGACATGAACCTGAATTTTCAGAATCTGAGCGTGATGGGCCTGAGAATCCTGCTGCTGAAGGTCGCTGGGTTTAATCTGCTGA
TGACACTGCGGCTGTGGTCCTCATGAATTCGGATCCAAGCTTAGGCCTGCTCGCTTTCTTGCTGTCCCATTTCTATTAAAGGTTCCTTTGTTCCCTAAGTCCAACT
ACTAAACTGGGGGATATTATGAAGGGCCTTGAGCATCTGGATTCTGCCTAGCGCTAAGCTTAACACGAGCCATAGATAGAATAAAAGATTTTATTTAGTCTCCA
GAAAAAGGGGGGAATGAAAGACCCCACCTGTAGGTTTGGCAAGCTAGCTTAAGTAACGCCATTTTGCAAGGCATGGAAAATACATAACTGAGAATAGAGAA
GTTCAGATCAAGGTTAGGAACAGAGAGACAGCAGAATATGGGCCAAACAGGATATCTGTGGTAAGCAGTTCCTGCCCCGGCTCAGGGCCAAGAACAGTTGG
AACAGCAGAATATGGGCCAAACAGGATATCTGTGGTAAGCAGTTCCTGCCCCGGCTCAGGGCCAAGAACAGATGGTCCCCAGATGCGGTCCCGCCCTCAGCA
GTTTCTAGAGAACCATCAGATGTTTCCAGGGTGCCCCAAGGACCTGAAATGACCCTGTGCCTTATTTGAACTAACCAATCAGTTCGCTTCTCGCTTCTGTTCGC
GCGCTTCTGCTCCCCGAGCTCAATAAAAGAGCCCACAACCCCTCACTCGGCGCGCCAGTCCTCCGATAGACTGCGTCGCCCGGGTACCCGTGTTCTCAATAAA
CCCTCTTGCAGTTGCATCCGACTCGTGGTCTCGCTGTTCCTTGGGAGGGTCTCCTCTGAGTGATTGACTGCCCACCTCGGGGGTCTTTCATTCTCGAGCAGCTT
GGCGTAATCATGGTCATAGCTGTTTCCTGTGTGAAATTGTTATCCGCTCACAATTCCACACAACATACGAGCCGGAAGCATAAAGTGTAAAGCCTGGGGTGCCT
AATGAGTGAGCTAACTCACATTAATTGCGTTGCGCTCACTGCCCGCTTTCCAGTCGGGAAACCTGTCGTGCCAGCTGCATTAATGAATCGGCCAACGCGCGGG
GAGAGGCGGTTTGCGTATTGGGCGCTCTTCCGCTTCCTCGCTCACTGACTCGCTGCGCTCGGTCGTTCGGCTGCGGCGAGCGGTATCAGCTCACTCAAAGGC
GGTAATACGGTTATCCACAGAATCAGGGGATAACGCAGGAAAGAACATGTGAGCAAAAGGCCAGCAAAAGGCCAGGAACCGTAAAAAGGCCGCGTTGCTG
GCGTTTTTCCATAGGCTCCGCCCCCCTGACGAGCATCACAAAAATCGACGCTCAAGTCAGAGGTGGCGAAACCCGACAGGACTATAAAGATACCAGGCGTTT
CCCCCTGGAAGCTCCCTCGTGCGCTCTCCTGTTCCGACCCTGCCGCTTACCGGATACCTGTCCGCCTTTCTCCCTTCGGGAAGCGTGGCGCTTTCTCATAGCTC
ACGCTGTAGGTATCTCAGTTCGGTGTAGGTCGTTCGCTCCAAGCTGGGCTGTGTGCACGAACCCCCCGTTCAGCCCGACCGCTGCGCCTTATCCGGTAACTATC
GTCTTGAGTCCAACCCGGTAAGACACGACTTATCGCCACTGGCAGCAGCCACTGGTAACAGGATTAGCAGAGCGAGGTATGTAGGCGGTGCTACAGAGTTCT
TGAAGTGGTGGCCTAACTACGGCTACACTAGAAGAACAGTATTTGGTATCTGCGCTCTGCTGAAGCCAGTTACCTTCGGAAAAAGAGTTGGTAGCTCTTGATC
CGGCAAACAAACCACCGCTGGTAGCGGTGGTTTTTTTGTTTGCAAGCAGCAGATTACGCGCAGAAAAAAAGGATCTCAAGAAGATCCTTTGATCTTTTCTACG
GGGTCTGACGCTCAGTGGAACGAAAACTCACGTTAAGGGATTTTGGTCATGAGATTATCAAAAAGGATCTTCACCTAGATCCTTTTAAATTAAAAATGAAGTTT
TAAATCAATCTAAAGTATATATGAGTAAACTTGGTCTGACAGTTACCAATGCTTAATCAGTGAGGCACCTATCTCAGCGATCTGTCTATTTCGTTCATCCATAGTTG
CCTGACTCCCCGTCGTGTAGATAACTACGATACGGGAGGGCTTACCATCTGGCCCCAGTGCTGCAATGATACCGCGAGACCCACGCTCACCGGCTCCAGATTTA
TCAGCAATAAACCAGCCAGCCGGAAGGGCCGAGCGCAGAAGTGGTCCTGCAACTTTATCCGCCTCCATCCAGTCTATTAATTGTTGCCGGGAAGCTAGAGTAA
GTAGTTCGCCAGTTAATAGTTTGCGCAACGTTGTTGCCATTGCTACAGGCATCGTGGTGTCACGCTCGTCGTTTGGTATGGCTTCATTCAGCTCCGGTTCCCAAC
GATCAAGGCGAGTTACATGATCCCCCATGTTGTGCAAAAAAGCGGTTAGCTCCTTCGGTCCTCCGATCGTTGTCAGAAGTAAGTTGGCCGCAGTGTTATCACTC
ATGGTTATGGCAGCACTGCATAATTCTCTTACTGTCATGCCATCCGTAAGATGCTTTTCTGTGACTGGTGAGTACTCAACCAAGTCATTCTGAGAATAGTGTATGC
GGCGACCGAGTTGCTCTTGCCCGGCGTCAATACGGGATAATACCGCGCCACATAGCAGAACTTTAAAAGTGCTCATCATTGGAAAACGTTCTTCGGGGCGAAA
ACTCTCAAGGATCTTACCGCTGTTGAGATCCAGTTCGATGTAACCCACTCGTGCACCCAACTGATCTTCAGCATCTTTTACTTTCACCAGCGTTTCTGGGTGAGC
AAAAACAGGAAGGCAAAATGCCGCAAAAAAGGGAATAAGGGCGACACGGAAATGTTGAATACTCATACTCTTCCTTTTTCAATATTATTGAAGCATTTATCAG
GGTTATTGTCTCATGAGCGGATACATATTTGAATGTATTTAGAAAAATAAACAAATAGGGGTTCCGCGCACATTTCCCCGAAAAGTGCCACCTGACGTCTAAGA
AACCATTATTATCATGACATTAACCTATAAAAATAGGCGTATCACGAGGCCCTTTCGTCTCGCGCGTTTCGGTGATGACGGTGAAAACCTCTGACACATGCAGCT
CCCGGAGACGGTCACAGCTTGTCTGTAAGCGGATGCCGGGAGCAGACAAGCCCGTCAGGGCGCGTCAGCGGGTGTTGGCGGGTGTCGGGGCTGGCTTAAC
TATGCGGCATCAGAGCAGATTGTACTGAGAGTGCACCATATGCGGTGTGAAATACCGCACAGATGCGTAAGGAGAAAATACCGCATCAGGCGCCATTCGCCAT
TCAGGCTGCGCAACTGTTGGGAAGGGCGATCGGTGCGGGCCTCTTCGCTATTACGCCAGCTGGCGAAAGGGGGATGTGCTGCAAGGCGATTAAGTTGGGTA
ACGCCAGGGTTTTCCCAGTCACGACGTTGTAAAACGACGGCCAGTGAATTAGTACT

pNL1.1-Nluc

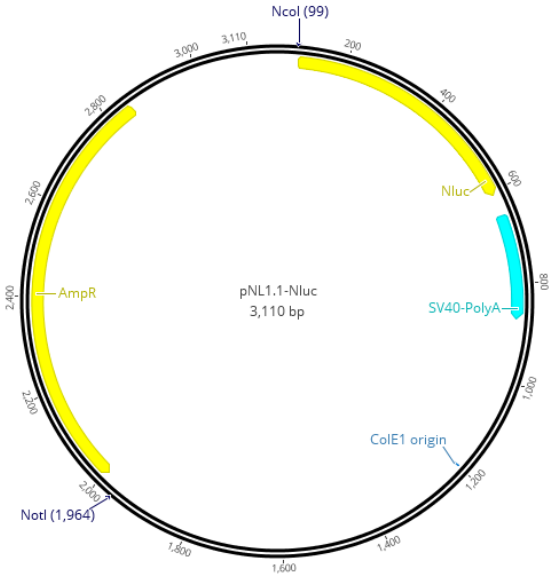

GGCCTAACTGGCCGGTACCTGAGCTCGCTAGCCTCGAGGATATCAAGATCTGGCCTCGGCGGCCAAGCTTGGCAATCCGGTACTGTTGGTAAAGCCACCATG
GTCTTCACACTCGAAGATTTCGTTGGGGACTGGCGACAGACAGCCGGCTACAACCTGGACCAAGTCCTTGAACAGGGAGGTGTGTCCAGTTTGTTTCAGAAT
CTCGGGGTGTCCGTAACTCCGATCCAAAGGATTGTCCTGAGCGGTGAAAATGGGCTGAAGATCGACATCCATGTCATCATCCCGTATGAAGGTCTGAGCGGCG
ACCAAATGGGCCAGATCGAAAAAATTTTTAAGGTGGTGTACCCTGTGGATGATCATCACTTTAAGGTGATCCTGCACTATGGCACACTGGTAATCGACGGGGTT
ACGCCGAACATGATCGACTATTTCGGACGGCCGTATGAAGGCATCGCCGTGTTCGACGGCAAAAAGATCACTGTAACAGGGACCCTGTGGAACGGCAACAAA
ATTATCGACGAGCGCCTGATCAACCCCGACGGCTCCCTGCTGTTCCGAGTAACCATCAACGGAGTGACCGGCTGGCGGCTGTGCGAACGCATTCTGGCGTAA
GGCCGCGACTCTAGAGTCGGGGCGGCCGGCCGCTTCGAGCAGACATGATAAGATACATTGATGAGTTTGGACAAACCACAACTAGAATGCAGTGAAAAAAA
TGCTTTATTTGTGAAATTTGTGATGCTATTGCTTTATTTGTAACCATTATAAGCTGCAATAAACAAGTTAACAACAACAATTGCATTCATTTTATGTTTCAGGTTCA
GGGGGAGGTGTGGGAGGTTTTTTAAAGCAAGTAAAACCTCTACAAATGTGGTAAAATCGATAAGGATCCGTCGACCGATGCCCTTGAGAGCCTTCAACCCAG
TCAGCTCCTTCCGGTGGGCGCGGGGCATGACTATCGTCGCCGCACTTATGACTGTCTTCTTTATCATGCAACTCGTAGGACAGGTGCCGGCAGCGCTCTTCCGC
TTCCTCGCTCACTGACTCGCTGCGCTCGGTCGTTCGGCTGCGGCGAGCGGTATCAGCTCACTCAAAGGCGGTAATACGGTTATCCACAGAATCAGGGGATAAC
GCAGGAAAGAACATGTGAGCAAAAGGCCAGCAAAAGGCCAGGAACCGTAAAAAGGCCGCGTTGCTGGCGTTTTTCCATAGGCTCCGCCCCCCTGACGAGC
ATCACAAAAATCGACGCTCAAGTCAGAGGTGGCGAAACCCGACAGGACTATAAAGATACCAGGCGTTTCCCCCTGGAAGCTCCCTCGTGCGCTCTCCTGTTCC
GACCCTGCCGCTTACCGGATACCTGTCCGCCTTTCTCCCTTCGGGAAGCGTGGCGCTTTCTCATAGCTCACGCTGTAGGTATCTCAGTTCGGTGTAGGTCGTTC
GCTCCAAGCTGGGCTGTGTGCACGAACCCCCCGTTCAGCCCGACCGCTGCGCCTTATCCGGTAACTATCGTCTTGAGTCCAACCCGGTAAGACACGACTTATC
GCCACTGGCAGCAGCCACTGGTAACAGGATTAGCAGAGCGAGGTATGTAGGCGGTGCTACAGAGTTCTTGAAGTGGTGGCCTAACTACGGCTACACTAGAA
GAACAGTATTTGGTATCTGCGCTCTGCTGAAGCCAGTTACCTTCGGAAAAAGAGTTGGTAGCTCTTGATCCGGCAAACAAACCACCGCTGGTAGCGGTGGTTT
TTTTGTTTGCAAGCAGCAGATTACGCGCAGAAAAAAAGGATCTCAAGAAGATCCTTTGATCTTTTCTACGGGGTCTGACGCTCAGTGGAACGAAAACTCACG
TTAAGGGATTTTGGTCATGAGATTATCAAAAAGGATCTTCACCTAGATCCTTTTAAATTAAAAATGAAGTTTTAAATCAATCTAAAGTATATATGAGTAAACTTGG
TCTGACAGCGGCCGCAAATGCTAAACCACTGCAGTGGTTACCAGTGCTTGATCAGTGAGGCACCGATCTCAGCGATCTGCCTATTTCGTTCGTCCATAGTGGCC
TGACTCCCCGTCGTGTAGATCACTACGATTCGTGAGGGCTTACCATCAGGCCCCAGCGCAGCAATGATGCCGCGAGAGCCGCGTTCACCGGCCCCCGATTTGT
CAGCAATGAACCAGCCAGCAGGGAGGGCCGAGCGAAGAAGTGGTCCTGCTACTTTGTCCGCCTCCATCCAGTCTATGAGCTGCTGTCGTGATGCTAGAGTAA
GAAGTTCGCCAGTGAGTAGTTTCCGAAGAGTTGTGGCCATTGCTACTGGCATCGTGGTATCACGCTCGTCGTTCGGTATGGCTTCGTTCAACTCTGGTTCCCAG

CGGTCAAGCCGGGTCACATGATCACCCATATTATGAAGAAATGCAGTCAGCTCCTTAGGGCCTCCGATCGTTGTCAGAAGTAAGTTGGCCGCGGTGTTGTCGC
TCATGGTAATGGCAGCACTACACAATTCTCTTACCGTCATGCCATCCGTAAGATGCTTTTCCGTGACCGGCGAGTACTCAACCAAGTCGTTTTGTGAGTAGTGTA
TACGGCGACCAAGCTGCTCTTGCCCGGCGTCTATACGGGACAACACCGCGCCACATAGCAGTACTTTGAAAGTGCTCATCATCGGGAATCGTTCTTCGGGGCG
GAAAGACTCAAGGATCTTGCCGCTATTGAGATCCAGTTCGATATAGCCCACTCTTGCACCCAGTTGATCTTCAGCATCTTTTACTTTCACCAGCGTTTCGGGGTG
TGCAAAAACAGGCAAGCAAAATGCCGCAAAGAAGGGAATGAGTGCGACACGAAAATGTTGGATGCTCATACTCGTCCTTTTTCAATATTATTGAAGCATTTAT
CAGGGTTACTAGTACGTCTCTCAAGGATAAGTAAGTAATATTAAGGTACGGGAGGTATTGGACAGGCCGCAATAAAATATCTTTATTTTCATTACATCTGTGTGTT
GGTTTTTTGTGTGAATCGATAGTACTAACATACGCTCTCCATCAAAACAAAACGAAACAAAACAAACTAGCAAAATAGGCTGTCCCCAGTGCAAGTGCAGGTG
CCAGAACATTTCTCT

Prototype HBV Sequence

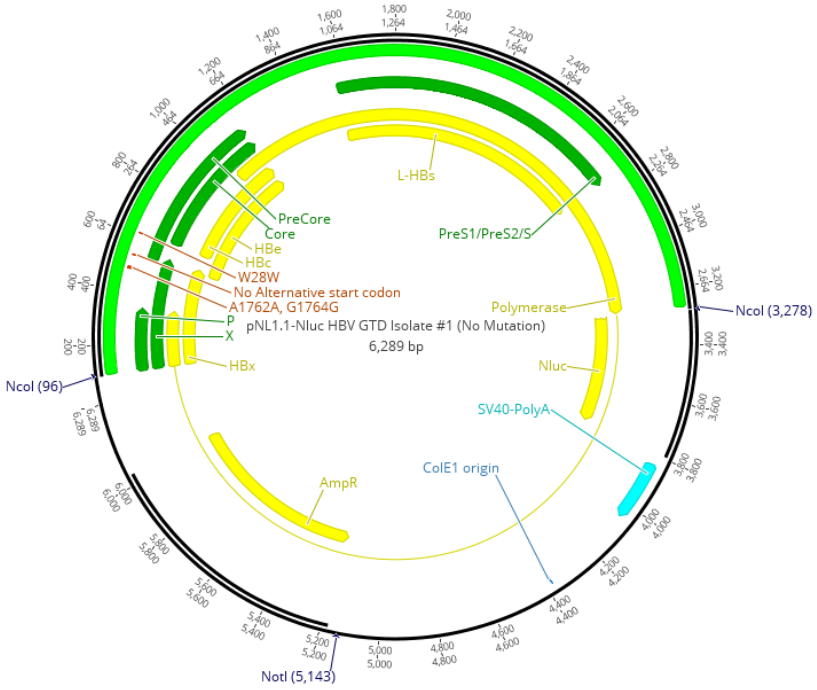

Genotype A isolate #1

CCATGGCTGCTAGGCTGTACTGCCAACTGGATCCTTCGCGGGACGTCCTTTGTTTACGTCCCGTCGGCGCTGAATCCCGCGGACGACCCCTCTCGGGGCCGCT
TGGGACTCTCTCGTCCCCTTCTCCGTCTGCCGTTCCAGCCGACCACGGGGCGCACCTCTCTTTACGCGGTCTCCCCGTCTGTGCCTTCTCATCTGCCGGTCCGT
GTGCACTTCGCTTCACCTCTGCACGTTGCATGGAGACCACCGTGAACGCCCATCAGATCCTGCCCAAGGTCTTACATAAGAGGACTCTTGGACTCCCAGCAAT
GTCAACGACCGACCTTGAGGCTTACTTCAAAGACTGTGTGTTTAAGGACTGGGAGGAGCTGGGGGAGGAGATTAGGTTAAAGGTCTTTGTATTAGGAGGCT
GTAGGCATAAATTGGTCTGCGCACCAGCACCATGCAACTTTTTCACCTCTGCCTAATCATCTCTTGTACATGTCCCACTGTTCAAGCCTCCAAGCTGTGCCTTGG
GTGGCTTTGGGGCATGGACATTGACCCTTATAAAGAATTTGGAGCTACTGTGGAGTTACTCTCGTTTTTGCCTTCTGACTTCTTTCCTTCCGTCAGAGATCTCCT
AGACACCGCCTCAGCTCTGTATCGAGAAGCCTTAGAGTCTCCTGAGCATTGCTCACCTCACCATACTGCACTCAGGCAAGCCATTCTCTGCTGGGGGGAATTG
ATGACTCTAGCTACCTGGGTGGGCAATAATTTGGAAGATCCAGCATCCAGGGATCTAGTAGTCAATTATGTTAATACTAACATGGGTTTAAAGATCAGGCAACTA
TTGTGGTTTCATATATCTTGCCTTACTTTTGGAAGAGAGACTGTACTTGAATATTTGGTCTCTTTCGGAGTGTGGATTCGCACTCCTCCAGCCTATAGACCACCAA
ATGCCCCTATCTTATCAACACTTCCGGAAACTACTGTTGTTAGACGACGGGACCGAGGCAGGTCCCCTAGAAGAAGAACTCCCTCGCCTCGCAGACGCAGATC
TCAATCGCCGCGTCGCAGAAGATCTCAATCTCGGGAATCTCAATGTTAGTATTCCTTGGACTCATAAGGTGGGAAACTTTACGGGGCTTTATTCCTCTACAGTAC
CTATCTTTAATCCTGAATGGCAAACTCCTTCCTTTCCTAGGATTCATTTACAAGAGGACATTATTAATAGGTGTCAACAATTTGTGGGCCCTCTCACTGTAAATGA
AAAGAGAAGATTGAAATTAATTATGCCTGCTAGATTCTATCCTACCCACACTAAATATTTGCCCTTAGACAAAGGAATTAAACCTTATTATCCAGATCAGGTAGTT
AATCATTACTTCCAAACCAGACATTATTTACATACTCTTTGGAAGGCTGGTATTCTATATAAGAGAGAAACCACACGTAGCGCCTCATTTTGCGGGTCACCATATT
CTTGGGAACAAGAGCTACAGCATGGGAGGTTGGTCATCAAAACCTCGCAAAGGCTTGGGGACGAATCTTTCTGTTCCCAACCCTCTGGGATTCTTTCCCGATC
ATCAGTTGGACCCTGCATTCGGAGCCAACTCAAACAATCCAGATTGGGACTTCAACCCCATCAAGGACCACTGGCCAGCAGCCAACCAGGTAGGAGTGGGA

GCATTCGGGCCAGGGCTCACCCCTCCACACGGCGGTATTTTGGGGTGGAGCCCTCAGGCTCAGGGCATATTGACCACAGTGTCAACAATTCCTCCTCCTGCCT
CCACCAATCGGCAGTCAGGAAGGCAGCCTACTCCCATCTCTCCACCTCTAAGAGACAGTCATCCTCAGGCCATGCAGTGGAATTCCACTGCCTTCCACCAAGCT
CTGCAGGATCCCAGAGTCAGGGGTCTGTATTTTCCTGCTGGTGGCTCCAGTTCAGGAACAGTAAACCCTGCTCCGAATATTGCCTCTCACATCTCGTCAATCTCC
GCGAGGACTGGGGACCCTGTGACGATCATGGAGAACATCACATCAGGATTCCTAGGACCCCTGCTCGTGTTACAGGCGGGGTTTTTCTTGTTGACAAGAATC
CTCACAATACCGCAGAGTCTAGACTCGTGGTGGACTTCTCTCAATTTTCTAGGGGGATCACCCGTGTGTCTTGGCCAAAATTCGCAGTCCCCAACCTCCATTCA
CTCACCAACCTCCTGTCCTCCAATTTGTCCTGGTTATCGCTGGATGTGTCTGCGGCGTTTTATCATATTCCTCTTCATCCTGCTGCTATGCCTCATCTTCTTATTGGT
TCTTCTGGATTATCAAGGTATGTTGCCCGTTTGTCCTCTAATTCCAGGATCAACAACAACCAGTACGGGACCATGCAAAACCTGCACGACTCCTGCTCAAGGCA
ACTCTATGTTTCCCTCCTGTTGCTGTACAAAACCTACGGATGGAAATTGCACCTGTATTCCCATCCCATCGTCCTGGGCTTTCGCAAAATACCTATGGGAGTGGG
CCTCAGTCCGTTTCTCTTGGCTCAGTTTACTAGTGCCATTTGTTCAGTGGTTCGTAGGGCTTTCCCCCACTGTTTGGCTTTCAGCTATATGGATGATGTGGTATTG
GGGGCCAAGTCTGTACAGCATCGTGAGTCCCTTTATACCGCTGTTACCAATTTTCTTTTGTCTCTGGGTATACATTTAAACCCTAACAAAACAAAAAGATGGGGT
TATTCCCTAAACTTCATGGGTTACATAATTGGAAGTTGGGGAACGTTGCCACAGGATCATATTGTACAAAAGATCAAACACTGTTTTAGAAAACTTCCTGTTAAC
AGGCCTATTGATTGGAAAGTATGTCAAAGAATTGTGGGTCTTTTGGGCTTTGCTGCTCCATTTACACAATGTGGATATCCTGCCTTAATGCCTTTGTATGCATGTA
TACAAGCTAAACAGGCTTTCACTTTCTCGCCAACTTACAAGGCCTTTCTAAGTAAACAGTACATGAACCTTTACCCCGTTGCTCGGCAACGGCCTGGTCTGTGC
CAAGTGTTTGCTGACGCAACCCCCACTGGCTGGGGCTTGGCCATAGGCCATCAGCGCATGCGTGGAACCTTTGTGGCTCCTCTGCCGATCCATACTGCGGAAC
TCCTAGCCGCTTGTTTTGCTCGCAGCCGGTCTGGAGCAAAGCTCATCGGAACTGACAATTCTGTCGTCCTCTCGCGGAAATATACATCGTTTCCATGG

Genotype A isolate #2

CCATGGCTGCTAGGCTGTACTGCCAACTGGATCCTTCGCGGGACGTCCTTTGTTTACGTCCCGTCGGCGCTGAATCCCGCGGACGACCCCTCTCGGGGCCGCT
TGGGACTCTCTCGTCCCCTTCTCCGTCTGCCGTTCCAGCCGACCACGGGGCGCACCTCTCTTTACGCGGTCTCCCCGTCTGTGCCTTCTCATCTGCCGGTCCGT
GTGCACTTCGCTTCACCTCTGCACGTTGCATGGAGACCACCGTGAACGCCCATCAGATCCTGCCCAAGGTCTTACATAAGAGGACTCTTGGACTCCCAGCAAT
GTCAACGACCGACCTTGAGGCCTACTTCAAAGACTGTGTGTTTAAGGACTGGGAGGAGCTGGGGGAGGAGATTAGGTTAAAGGTCTTTGTATTAGGAGGCT
GTAGGCATAAATTGGTCTGCGCACCAGCACCATGCAACTTTTTCACCTCTGCCTAATCATCTCTTGTACATGTCCCACTGTTCAAGCCTCCAAGCTGTGCCTTGG
GTGGCTTTGGGGCATGGACATTGACCCTTATAAAGAATTTGGAGCTACTGTGGAGTTACTCTCGTTTTTGCCTTCTGACTTCTTTCCTTCCGTCAGAGATCTCCT
AGACACCGCCTCAGCTCTGTATCGAGAAGCCTTAGAGTCTCCTGAGCATTGCTCACCTCACCATACTGCACTCAGGCAAGCCATTCTCTGCTGGGGGGAATTG
ATGACTCTAGCTACCTGGGTGGGTAATAATTTGGAAGATCCAGCATCCAGGGATCTAGTAGTCAATTATGTTAATACTAATATGGGTTTAAAGATCAGGCAACTAT
TGTGGTTTCATATATCTTGCCTTACTTTTGGAAGAGAGACTGTACTTGAATATTTGGTCTCTTTCGGAGTGTGGATTCGCACTCCTCCAGCCTATAGACCACCAAA
TGCCCCTATCTTATCAACACTTCCGGAAACTACTGTTGTTAGACGACGGGACCGAGGCAGGTCCCCTAGAAGAAGAACTCCCTCGCCTCGCAGACGCAGATCT
CAATCGCCGCGTCGCAGAAGATCTCAATCTCGGGAATCTCAATGTTAGTATTCCTTGGACTCATAAGGTGGGAAACTTTACTGGGCTTTATTCCTCTACAGTACC
TATCTTTAACCCTGAATGGCAAACTCCTTCCTTTCCTAAGATTCATTTACAAGAGGACATTATTAATAGGTGTCAACAATTTGTGGGCCCTCTAACTGTAAATGAA
AAGAGAAGATTGAAATTAATTATGCCTGCTAGATTCTATCCTACCCACACTAAATATTTGCCCTTGGACAAAGGAATTAAACCTTATTATCCAGATCAGGTAGTTA
ATCATTACTTCCAAACCAGACATTATTTACATACTCTTTGGAAGGCTGGTATTCTATATAAGAGGGAAACCACACGTAGCGCATCATTTTGCGGGTCACCATATTC
TTGGGAACAAGAGCTACAGCATGGGAGGTTGGTCATCAAAACCTCGCAAAGGCATGGGGACGAATCTTTCTGTTCCCAACCCTCTGGGATTCTTTCCCGATCA
TCAGTTGGACCCTGCATTCGGAGCCAACTCAAACAATCCAGATTGGGACTTCAACCCCATCAAGGACCACTGGCCAGCAGCCAACCAGGTAGGAGTGGGAG
CATTCGGGCCAGGGCTCACCCCTCCACACGGCGGTATTTTGGGGTGGAGCCCTCAGGCTCAGGGCATATTGACCACAGTGTCAACAATTCCTCCTCCTGCCTC
CACCAATCGGCAGTCAGGAAGGCAGCCTACTCCCATCTCTCCACCTCTAAGAGACAGTCATCCTCAGGCCATGCAGTGGAATTCCACTGCCTTCCACCAAGCTC
TGCAGGATCCCAGAGTCAGGGGTCTGTATTTTCCTGCTGGTGGCTCCAGTTCAGGAACAGTAAACCCTGCTCCGAATATTGCCTCTCACATCTCGTCAATCTCC
GCGAGGACTGGGGACCCTGTGACGAACATGGAGAACATCACATCAGGATTCCTAGGACCCCTGCTCGTGTTACAGGCGGGGTTTTTCTTGTTGACAAGAATC
CTCACAATACCGCAGAGTCTAGACTCGTGGTGGACTTCTCTCAATTTTCTAGGGGGATCACCCGTGTGTCTTGGCCAAAATTCGCAGTCCCCAACCTCCAATCA
CTCACCAACCTCCTGTCCTCCAATTTGTCCTGGTTATCGCTGGATGTGTCTGCGGCGTTTTATCATATTCCTCTTCATCCTGCTGCTATGCCTCATCTTCTTATTGGT
TCTTCTGGATTATCAAGGTATGTTGCCCGTTTGTCCTCTAATTCCAGGATCAACAACAACCAGTACGGGACCATGCAAAACCTGCACGACTCCTGCTCAAGGCA
ACTCTATGTTTCCCTCATGTTGCTGTACAAAACCTACGGATGGAAATTGCACCTGTATTCCCATCCCATCGTCCTGGGCTTTCGCAAAATACCTATGGGAGTGGG
CCTCAGTCCGTTTCTCTTGGCTCAGTTTACTAGTGCCATTTGTTCAGTGGTTCGTAGGGCTTTCCCCCACTGTTTGGCTTTCAGCTATATGGATGATGTGGTATTG
GGGGCCAAGTCTGTACAGCATCGTGAGTCCCTTTATACCGCTGTTACCAATTTTCTTTTGTCTCTGGGTATACATTTAAACCCTAACAAAACAAAAAGATGGGGT
TATTCCCTAAACTTCATGGGTTACATAATTGGAAGTTGGGGAACATTGCCACAGGATCATATTGTACAAAAGATCAAACACTGTTTTAGAAAACTTCCTGTTAAC
AGGCCTATTGATTGGAAAGTATGTCAAAGAATTGTGGGTCTTTTGGGCTTTGCTGCTCCATTTACACAATGTGGATATCCTGCCTTAATGCCTTTGTATGCATGTA
TACAAGCTAAACAGGCTTTCACTTTCTCGCCAACTTACAAGGCCTTTCTAAGTAAACAGTACATGAACCTTTACCCCGTTGCTCGGCAACGGCCTGGTCTGTGC
CAAGTGTTTGCTGACGCAACCCCCACTGGCTGGGGCTTGGCCATAGGCCATCAGCGCATGCGTGGAACCTTTGTGGCTCCTCTGCCGATCCATACTGCGGAAC
TCCTAGCCGCTTGTTTTGCTCGCAGCCGGTCTGGAGCAAAGCTCATCGGAACTGACAATTCTGTCGTCCTCTCGCGGAAATATACATCGTTTCCATGG

Genotype A consensus

CCATGGCTGCTAGGCTGTACTGCCAACTGGATCCTTCGCGGGACGTCCTTTGTTTACGTCCCGTCGGCGCTGAATCCCGCGGACGACCCCTCTCGGGGCCGCT
TGGGACTCTCTCGTCCCCTTCTCCGTCTGCCGTTCCAGCCGACCACGGGGCGCACCTCTCTTTACGCGGTCTCCCCGTCTGTGCCTTCTCATCTGCCGGTCCGT
GTGCACTTCGCTTCACCTCTGCACGTTGCATGGAGACCACCGTGAACGCCCATCAGATCCTGCCCAAGGTCTTACATAAGAGGACTCTTGGACTCCCAGCAAT
GTCAACGACCGACCTTGAGGCCTACTTCAAAGACTGTGTGTTTAAGGACTGGGAGGAGCTGGGGGAGGAGATTAGGTTAAAGATCTTTGTATTAGGAGGCT
GTAGGCATAAATTGGTCTGCGCACCAGCACCATGCAACTTTTTCACCTCTGCCTAATCATCTCTTGTACATGTCCCACTGTTCAAGCCTCCAAGCTGTGCCTTGG
GTGGCTTTGGGGCATGGACATTGACCCTTATAAAGAATTTGGAGCTACTGTGGAGTTACTCTCGTTTTTGCCTTCTGACTTCTTTCCTTCCGTCAGAGATCTCCT
AGACACCGCCTCAGCTCTGTATCGAGAAGCCTTAGAGTCTCCTGAGCATTGCTCACCTCACCATACTGCACTCAGGCAAGCCATTCTCTGCTGGGGGGAATTG
ATGACTCTAGCTACCTGGGTGGGTAATAATTTGCAAGATCCAGCATCCAGGGATCTAGTAGTCAATTATGTTAATACTAACATGGGTTTAAAGATCAGGCAACTA
TTGTGGTTTCATATATCTTGCCTTACTTTTGGAAGAGAGACTGTACTTGAATATTTGGTCTCTTTCGGAGTGTGGATTCGCACTCCTCCAGCCTATAGACCACCAA
ATGCCCCTATCTTATCAACACTTCCGGAAACTACTGTTGTTAGACGACGGGACCGAGGCAGGTCCCCTAGAAGAAGAACTCCCTCGCCTCGCAGACGCAGATC
TCAATCGCCGCGTCGCAGAAGATCTCAATCTCGGGAATCTCAATGTTAGTATTCCTTGGACTCATAAGGTGGGAAACTTTACTGGGCTTTATTCCTCTACAGTAC
CTATCTTTAATCCTGAATGGCAAACTCCTTCCTTTCCTAAGATTCATTTACAAGAGGACATTATTAATAGGTGTCAACAATTTGTGGGCCCTCTCACTGTAAATGA
AAAGAGAAGATTGAAATTAATTATGCCTGCTAGATTCTATCCTACCCACACTAAATATTTGCCCTTAGACAAAGGAATTAAACCTTATTATCCAGATCAGGTAGTT
AATCATTACTTCCAAACCAGACATTATTTACATACTCTTTGGAAGGCTGGTATTCTATATAAGAGGGAAACCACACGTAGCGCATCATTTTGCGGGTCACCATATT
CTTGGGAACAAGAGCTACAGCATGGGAGGTTGGTCATCAAAACCTCGCAAAGGCATGGGGACGAATCTTTCTGTTCCCAACCCTCTGGGATTCTTTCCCGATC
ATCAGTTGGACCCTGCATTCGGAGCCAACTCAAACAATCCAGATTGGGACTTCAACCCCATCAAGGACCACTGGCCAGCAGCCAACCAGGTAGGAGTGGGA
GCATTCGGGCCAGGGCTCACCCCTCCACACGGCGGTATTTTGGGGTGGAGCCCTCAGGCTCAGGGCATATTGACCACAGTGTCAACAATTCCTCCTCCTGCCT
CCACCAATCGGCAGTCAGGAAGGCAGCCTACTCCCATCTCTCCACCTCTAAGAGACAGTCATCCTCAGGCCATGCAGTGGAATTCCACTGCCTTCCACCAAGCT
CTGCAGGATCCCAGAGTCAGGGGTCTGTATTTTCCTGCTGGTGGCTCCAGTTCAGGAACAGTAAACCCTGCTCCGAATATTGCCTCTCACATCTCGTCAATCTCC
GCGAGGACTGGGGACCCTGTGACGAACATGGAGAACATCACATCAGGATTCCTAGGACCCCTGCTCGTGTTACAGGCGGGGTTTTTCTTGTTGACAAGAATC
CTCACAATACCGCAGAGTCTAGACTCGTGGTGGACTTCTCTCAATTTTCTAGGGGGATCACCCGTGTGTCTTGGCCAAAATTCGCAGTCCCCAACCTCCAATCA
CTCACCAACCTCCTGTCCTCCAATTTGTCCTGGTTATCGCTGGATGTGTCTGCGGCGTTTTATCATATTCCTCTTCATCCTGCTGCTATGCCTCATCTTCTTATTGGT
TCTTCTGGATTATCAAGGTATGTTGCCCGTTTGTCCTCTAATTCCAGGATCAACAACAACCAGTACGGGACCATGCAAAACCTGCACGACTCCTGCTCAAGGCA
ACTCTATGTTTCCCTCATGTTGCTGTACAAAACCTACGGATGGAAATTGCACCTGTATTCCCATCCCATCGTCCTGGGCTTTCGCAAAATACCTATGGGAGTGGG
CCTCAGTCCGTTTCTCTTGGCTCAGTTTACTAGTGCCATTTGTTCAGTGGTTCGTAGGGCTTTCCCCCACTGTTTGGCTTTCAGCTATATGGATGATGTGGTATTG
GGGGCCAAGTCTGTACAGCATCGTGAGTCCCTTTATACCGCTGTTACCAATTTTCTTTTGTCTCTGGGTATACATTTAAACCCTAACAAAACAAAAAGATGGGGT
TATTCCCTAAACTTCATGGGTTACATAATTGGAAGTTGGGGAACATTGCCACAGGATCATATTGTACAAAAGATCAAACACTGTTTTAGAAAACTTCCTGTTAAC
AGGCCTATTGATTGGAAAGTATGTCAAAGAATTGTGGGTCTTTTGGGCTTTGCTGCTCCATTTACACAATGTGGATATCCTGCCTTAATGCCTTTGTATGCATGTA
TACAAGCTAAACAGGCTTTCACTTTCTCGCCAACTTACAAGGCCTTTCTAAGTAAACAGTACATGAACCTTTACCCCGTTGCTCGGCAACGGCCTGGTCTGTGC
CAAGTGTTTGCTGACGCAACCCCCACTGGCTGGGGCTTGGCCATAGGCCATCAGCGCATGCGTGGAACCTTTGTGGCTCCTCTGCCGATCCATACTGCGGAAC
TCCTAGCCGCTTGTTTTGCTCGCAGCCGGTCTGGAGCAAAGCTCATCGGAACTGACAATTCTGTCGTCCTCTCGCGGAAATATACATCGTTTCCATGG

Genotype D isolate #1

CCATGGCTGCTAGGCTGTGCTGCCAACTGGATCCTGCGCGGGACGTCCTTTGTTTACGTCCCCTCGGCGCTGAATCCCGCGGACGACCCTTCTCGGGGTCGCT
TGGGACTCTCTCGTCCCCTTCTCCGTCTGCCGTTTCGACCGACCACGGGGCGCACCTCTCTTTACGCGGACTCCCCGTCTGTGCCTTCTCATCTGCCGGACCGT
GTGCACTTCGCTTCACCTCTGCACGTCGCATGGAGACCACCGTGAACGCCCACCAAATATTGCCCAAGGTCTTACATAAGAGGACTCTTGGACTCTCTGCAATG
TCAACGACCGACCTTGAGGCATACTTCAAAGACTGTTTGTTTAAAGACTGGGAGGAGTTGGGGGAGGAGATTAGATTAAAGGTCTTTGTACTAGGAGGCTGT
AGGCATAAATTGGTCTGCGCACCAGCACCATGCAACTTTTTCACCTCTGCCTAATCATCTCTTGTTCATGTCCTACTGTTCAAGCCTCCAAGCTGTGCCTTGGGT
GGCTTTGGGGCATGGACATTGACCCTTATAAAGAATTTGGAGCTACCGTGGAGTTACTCTCGTTTTTGCCTTCTGACTTCTTTCCTTCAGTACGAGATCTTCTAG
ATACCGCCTCAGCTCTGTATCGGGATGCCTTAGAGTCTCCTGAACATTGTTCACCTCACCATACTGCACTCAGGCAAGCAATTCTTTGCTGGGGGGAACTAATG
ACTCTAGCTACCTGGGTGGGCGTTAATTTGGAAGATCCAGCATCTAGAGACCTAGTAGTCAGTTATGTCAACACTAATATGGGCCTAAAGTTCAGACAACTCTT
GTGGTTTCACATTTCTTGTCTCACTTTTGGAAGAGAAACAGTTATAGAATATTTGGTGTCTTTCGGAGTGTGGATTCGCACTCCTCCAGCTTATAGACCACCAAA
TGCCCCTATCTTATCAACACTTCCGGAGACTACTGTTGTTAGACGACGAGGCAGGTCCCCTAGAAGAAGAACTCCCTCGCCTCGCAGACGAAGGTCTCAATCG
CCGCGTCGCCGAAGATCTCAATCTCGGGAATCTCAATGTTAGTATTCCTTGGACTCATAAGGTGGGAAACTTTACGGGGCTTTATTCTTCTACTGTACCTGTCTT
TAATCCTCATTGGAAAACACCCTCTTTTCCTAATATACATTTACACCAAGACATTATCAAAAAATGTGAACAGTTTGTAGGCCCACTCACAGTTAATGAGAAAAG
AAGATTGCAATTGATTATGCCTGCTAGGTTTTATCCAAATGTTACCAAATATTTGCCATTGGATAAGGGTATTAAACCTTATTATCCAGAACATCTAGTTAATCATTA

CTTCCAAACTAGACACTATTTACACACTCTATGGAAGGCGGGTATATTATATAAGAGAGAAACAACACATAGCGCCTCATTTTGTGGGTCACCATATTCTTGGGA
ACAAGAGCTACAGCATGGGGCAGAATCTTTCCACCAGCAATCCTCTGGGATTCTTTCCCGACCACCAGTTGGATCCAGCCTTCAGAGCAAACACCGCAAATCC
AGATTGGGACTTCAATCCCAACAAGGACACCTGGCCAGACGCCAACAAGGTAGGAGCTGGAGCATTCGGGCTGGGTTTCACCCCACCGCACGGAGGCCTTT
TGGGGTGGAGCCCTCAAGCTCAGGGCATAATACAAACTTTGCCAGCAAATCCGCCTCCTGCCTCCACCAATCGCCAGTCAGGAAGGCAGCCTACCCCGCTGTC
TCCACCTTTGCGAAACACTCATCCTCAGGCCATGCAGTGGAACTCCACAACCTTCCATCAAACTCTGCAAGATCCCAGAGTGAGAGGCCTGTATTTCCCTGCTG
GTGGCTCCAGTTCAGGAACAGTAAACCCTGTTCCGACTACTGCCTCTCACTTATCGTCAATCTTCTCGAGGATTGGGGACCCTGCGCTGAACATGGAGAACATC
ACATCAGGATTCCTAGGACCCCTTCTCGTGTTACAGGCGGGGTTTTTCTTGTTGACAAGAATCCTCACAATACCGCAGAGTCTAGACTCGTGGTGGACTTCTCT
CAATTTTCTAGGGGGAACTACCGTGTGTCTTGGCCAAAATTCGCAGTCCCCAACCTCCAATCACTCACCAACCTCCTGTCCTCCAACTTGTCCTGGTTATCGTTG
GATGTGTCTGCGGCGTTTTATCATCTTCCTCTTCATCCTGCTGCTATGCCTCATCTTCTTGTTGGTTCTTCTGGACTATCAAGGTATGTTGCCCGTTTGTCCTCTAAT
TCCAGGATCCTCAACCACCAGCACGGGACCATGCAGAACCTGCACGACTCCTGCTCAAGGAACCTCTATGTATCCCTCCTGTTGCTGTACCAAACCTTCGGACG
GAAATTGCACCTGTATTCCCATCCCATCATCCTGGGCTTTCGGAAAATTCCTATGGGAGTGGGCCTCAGCCCGTTTCTCCTGGCTCAGTTTACTAGTGCCATTTG
TTCAGTGGTTCGTAGGGCTTTCCCCCACTGTTTGGCTTTCAGTTATATGGATGATGTGGTATTGGGGGCCAAGTCTGTACAGCATCTTGAGTCCCTTTTTACCGC
TGTTACCAATTTTCTTTTGTCTTTGGGTATACATTTAAACCCTAACAAAACAAAGAGATGGGGTTATTCTCTAAATTTTATGGGTTATGTCATTGGATGTTATGGAT
CATTGCCACAAGAACACATCATACAAAAAATCAAAGACTGTTTTAGAAAACTTCCTGTTAACAGGCCTATTGATTGGAAAGTGTGTCAACGAATTGTGGGCCTT
TTGGGTTTTGCTGCACCTTTTACACAATGTGGTTATCCTGCTTTAATGCCCTTGTATGCATGTATTCAATCTAAGCAGGCTTTCACTTTCTCGCCAACTTACAAGG
CCTTTCTGTGTAAACAATACCTGAACCTTTACCCCGTTGCCCGGCAACGGCCAGGTCTGTGCCAAGTGTTTGCTGACGCAACCCCCACTGGCTGGGGCTTGGT
CATGGGCCATCAGCGCATGCGTGGAACCTTTATGGCTCCTCTGCCGATCCATACTGCGGAACTCCTAGCCGCTTGTTTTGCTTGCAGCAGGTCTGGAGCAAAC
GTTATCGGGACTGATAACTCGGTTGTCCTCTCCCGCAAATATACATCATTTCCATGG

Genotype D isolate #2

CCATGGCTGCTAGGCTGTGCTGCCAACTGGATCCTGCGCGGGACGTCCTTTGTTTACGTCCCGTCGGCGCTGAATCCCGCGGACGACCCTTCTCGGGGTCGCT
TGGGACTCTCTCGTCCCCTTCTCCGTCTGCCGTTTCGACCGACCACGGGGCGCACCTCTCTTTACGCGGACTCCCCGTCTGTGCCTTCTCATCTGCCGGACCGT
GTGCACTTCGCTTCACCTCTGCACGTCGCATGGAGACCACCGTGAACGCCCACCGATTCTTGCCCAAGGTCTTACATAAGAGGACTCTTGGACTCTCTGTAATG
TCAACGACCGACCTTGAGGCATACTTCAAAGACTGTTTGTTCAAAGACTGGGAGGAGTTGGGGGAGGAGATTAGATTAAAGGTCTTTGTACTAGGAGGCTGT
AGGCATAAATTGGTCTGCGCACCAGCACCATGCAACTTTTTCACCTCTGCCTAATCATCTTTTGTTCATGTCCTACTGTTCAAGCCTCCAAGCTGTGCCTTGGGT
GGCTTTGGGGCATGGACATTGATCCTTATAAAGAATTTGGAGCTACTGTGGAGTTACTCTCGTTTTTGCCTTCTGACTTCTTTCCTTCAGTACGTGATCTTCTAG
ATACCGCCTCAGCTCTGTATCGGGAAGCCTTAGAGTCTCCTGAGCATTGTTCACCTCACCATACTGCACTCAGGCAAGCAATTCTGTGCTGGGGGGACCTAATG
ACTCTAGCTACCTGGGTGGGTGGTAATTTGGAAGATCCAATATCCAGGGACCTAGTAGTCAGTTATGTCAACACTAATATGGGCCTAAAGTTCCGGCAACTATT
GTGGTTTCACATTTCTTGTCTCACTTTTGGAAGAGAAACAGTTATAGAGTATTTGGTGTCTTTCGGAGTGTGGATTCGCACTCCTCCAGCTTATAGACCACCAAA
TGCCCCTATCTTATCAACACTTCCGGAGACTACTGTTGTTAGACGACGAGGCAGGTCCCCTAGAAGAAGAACTCCCTCGCCTCGCAGACGAAGGTCTCAATCG
CCGCGTCGCAGAAGATCTCAATCTCGGGAATCTCAATGTTAGTATTCCTTGGACTCATAAGGTGGGAAACTTTACGGGGCTTTATTCTTCTACTGTACCTGTCTT
TAACCCTCATTGGAAAACACCCTCTTTTCCTAATATACATTTACACCAAGACATTATCAAAAAATGTGAACAATTTGTAGGCCCACTCACAGTCAATGAGAAAAG
AAGACTGCAATTGATTATGCCTGCTAGGTTTTATCCAAATGTTACCAAATATTTGCCATTGGATAAGGGTATTAAACCTTATTACCCAGAACATCTAGTTAATCATT
ACTTCCAAACCAGACATTATTTACACACTCTATGGAAGGCGGGTATATTATATAAGAGAGAAACAACACATAGCGCCTCATTTTGTGGGTCACCATATTCTTGGG
AACAAAAGCTACAGCATGGGGCAGAATCTTTCCACCAGCAATCCTCTGGGATTCTTTCCCGACCACCAGTTGGATCCAGCCTTCAGAGCAAACACCGCAAATC
CAGATTGGGACTTCAATCCCAACAAGGACACCTGGCCAGACGCCAACAAGGTAGGAGCTGGAGCATTCGGGCTGGGATTCACCCCACCGCACGGAGGCCTT
TTGGGGTGGAGCCCCCAGGCTCAGGGCATACTACAAACCTTGCCAGCAAATCCGCCTCCTGCCTCTACCAATCGCCAGTCAGGAAGGCAGCCGACCCCGCTG
TCTCCACCTTTGAGAAACACTCATCCTCAGGCCATGCAGTGGAACTCCACAACCTTCCACCAAACTCTGCAAGATCCCAGAGTGAGAGGCCTGTATTTCCCTGC
TGGTGGCTCCAGTTCAGGAACAGTAAACCCTGTTCCGACTACTGTCTCTCCCATATCGTCAATCTTCTCGAAGATTGGGGACCCTGCGCTGAACATGGAGAACA
TCACATCAGGATTCCTAGGACCCCTGCTCGTGTTACAGGCGGGGTTTTTCTTGTTGACAAGAATCCTCACAATACCGCAGAGTCTAGACTCGTGGTGGACTTCT
CTCAATTTTCTAGGGGGAACTACCGTGTGTCTTGGCCAAAATTCGCAGTCCCCAACCTCCAATCACTCACCAACCTCCTGTCCTCCAACTTGTCCTGGTTATCGC
TGGATGTGTCTGCGGCGTTTTATCATCTTCCTCTTCATCCTGCTGCTATGCCTCATCTTCTTGTTGGTTCTTCTGGACTATCAAGGTATGTTGCCCGTTTGTCCTCTA
ATTCCAGGATCTTCAACTACCAGCACGGGCCCATGCAGAACCTGCACGACTCCTGCTCAAGGAACCTCTATGTATCCCTCCTGTTGCTGTACCAAACCTTCGGA
CGGAAATTGCACCTGTATTCCCATCCCATCATCCTGGGCTTTCGGAAAATTCCTATGGGAGTGGGCCTCAGCCCGTTTCTCCTGGCTCAGTTTACTAGTGCCATT
TGTTCAGTGGTTCGTAGGGCTTTCCCCCATTGTTTGGCTTTCAGTTATATGGATGATGTGGTATTGGGGGCCAAGTCTGTACAGCATCTTGAGTCCCTTTTTACC
GCTGTTACCAATTTTCTTTTGTCTTTGGGTATACATTTAAACCCTAACAAAACAAAAAGATGGGGTTACTCTTTACATTTCATGGGCTATGTCATTGGATGTTATG
GGTCATTGCCACAAGATCACATCATACAAAAAATCAAAGAATGTTTTCGAAAACTTCCTGTTAACAGACCTATTGATTGGAAAGTCTGTCAACGTATTGTGGGT
CTTTTGGGTTTTGCTGCCCCTTTTACACAATGTGGTTATCCTGCTTTAATGCCCTTGTATGCATGTATTCAGTCGAAGCAGGCTTTTACTTTCTCGCCAACTTACA

AGGCCTTTCTGTGTAAACAATACCTGAACCTTTACCCCGTTGCCCGGCAACGGCCAGGTCTGTGCCAAGTGTTTGCTGATGCAACCCCCACTGGCTGGGGCTT
GGTCATGGGCCATCAGCGCATGCGTGGAACCTTTCTGGCTCCTCTGCCGATCCATACTGCGGAACTCCTAGCCGCTTGTTTTGCTCGCAGCAGGTCTGGAGCA
AACATTCTCGGGACAGATAACTCTGTTGTTCTCTCCCGCAAATATACATCGTTTCCATGG

Genotype D consensus

CCATGGCTGCTAGGCTGTGCTGCCAACTGGATCCTGCGCGGGACGTCCTTTGTTTACGTCCCGTCGGCGCTGAATCCCGCGGACGACCCTTCTCGGGGCCGCT
TGGGACTCTCTCGTCCCCTTCTCCGTCTGCCGTTTCGACCGACCACGGGGCGCACCTCTCTTTACGCGGACTCCCCGTCTGTGCCTTCTCATCTGCCGGACCGT
GTGCACTTCGCTTCACCTCTGCACGTCGCATGGAGACCACCGTGAACGCCCACCAATTCTTGCCCAAGGTCTTACATAAGAGGACTCTTGGACTCTCTGTAATG
TCAACGACCGACCTTGAGGCATACTTCAAAGACTGTTTGTTTAAAGACTGGGAGGAGTTGGGGGAGGAGATTAGATTAAAGGTCTTTGTACTAGGAGGCTGT
AGGCATAAATTGGTCTGCGCACCAGCACCATGCAACTTTTTCACCTCTGCCTAATCATCTCTTGTTCATGTCCTACTGTTCAAGCCTCCAAGCTGTGCCTTGGGT
GGCTTTAGGGCATGGACATTGACCCTTATAAAGAATTTGGAGCTTCTGTGGAGTTACTCTCGTTTTTGCCTTCTGACTTCTTTCCTTCAGTACGAGATCTTCTAG
ATACCGCCTCAGCTCTGTATCGGGAAGCCTTAGAGTCTCCTGAGCATTGTTCACCTCACCATACTGCACTCAGGCAAGCAATTCTTTGCTGGGGGGAACTAATG
ACTCTAGCTACCTGGGTGGGTGGTAATTTGGAAGATCCAACATCCAGGGACCTAGTAGTCAGTTATGTCAACACTAATATGGGCCTAAAGTTCAGGCAACTATT
GTGGTTTCACATTTCTTGTCTCACTTTTGGAAGAGAAACAGTCATAGAGTATTTGGTGTCTTTCGGAGTGTGGATTCGCACTCCTCCAGCTTATAGACCACCAA
ATGCCCCTATCTTATCAACACTTCCGGAGACTACTGTTGTTAGACGACGAGGCAGGTCCCCTAGAAGAAGAACTCCCTCGCCTCGCAGACGAAGGTCTCAATC
GCCGCGTCGCAGAAGATCTCAATCTCGGGAATCTCAATGTTAGTATTCCTTGGACTCATAAGGTGGGAAACTTTACGGGGCTTTATTCTTCTACTGTACCTGTCT
TTAACCCTCATTGGAAAACACCCTCTTTTCCTAATATACATTTACACCAAGACATTATCAAAAAATGTGAACAATTTGTAGGCCCACTCACAGTCAATGAGAAAA
GAAGACTGCAATTGATTATGCCTGCTAGGTTTTATCCAAATGTTACCAAATATTTGCCATTGGATAAGGGTATTAAACCTTATTATCCAGAACATCTAGTTAATCAT
TACTTCCAAACCAGACATTATTTACACACTCTATGGAAGGCGGGTATATTATATAAGAGAGAAACAACACATAGCGCCTCATTTTGTGGGTCACCATATTCTTGG
GAACAAGAGCTACAGCATGGGGCAGAATCTTTCCACCAGCAATCCTCTGGGATTCTTTCCCGACCACCAGTTGGATCCAGCCTTCAGAGCAAACACCGCAAAT
CCAGATTGGGACTTCAATCCCAACAAGGACACCTGGCCAGACGCCAACAAGGTAGGAGCTGGAGCATTCGGGCTGGGATTCACCCCACCGCACGGAGGCCT
TTTGGGGTGGAGCCCTCAGGCTCAGGGCATACTACAAACCTTGCCAGCAAATCCGCCTCCTGCCTCTACCAATCGCCAGTCAGGAAGGCAGCCTACCCCGCTG
TCTCCACCTTTGAGAAACACTCATCCTCAGGCCATGCAGTGGAACTCCACAACCTTCCACCAAACTCTGCAAGATCCCAGAGTGAGAGGCCTGTATTTCCCTGC
TGGTGGCTCCAGTTCAGGAACAGTAAACCCTGTTCCGACTACTGTCTCTCACATATCGTCAATCTTCTCGAGGATTGGGGACCCTGCGCTGAACATGGAGAAC
ATCACATCAGGATTCCTAGGACCCCTGCTCGTGTTACAGGCGGGGTTTTTCTTGTTGACAAGAATCCTCACAATACCGCAGAGTCTAGACTCGTGGTGGACTTC
TCTCAATTTTCTAGGGGGAACTACCGTGTGTCTTGGCCAAAATTCGCAGTCCCCAACCTCCAATCACTCACCAACCTCCTGTCCTCCAACTTGTCCTGGTTATCG
CTGGATGTGTCTGCGGCGTTTTATCATCTTCCTCTTCATCCTGCTGCTATGCCTCATCTTCTTGTTGGTTCTTCTGGACTATCAAGGTATGTTGCCCGTTTGTCCTC
TAATTCCAGGATCTTCAACCACCAGCACGGGACCATGCAGAACCTGCACGACTCCTGCTCAAGGAACCTCTATGTATCCCTCCTGTTGCTGTACCAAACCTTCG
GACGGAAATTGCACCTGTATTCCCATCCCATCATCCTGGGCTTTCGGAAAATTCCTATGGGAGTGGGCCTCAGCCCGTTTCTCCTGGCTCAGTTTACTAGTGCCA
TTTGTTCAGTGGTTCGTAGGGCTTTCCCCCACTGTTTGGCTTTCAGTTATATGGATGATGTGGTATTGGGGGCCAAGTCTGTACAGCATCTTGAGTCCCTTTTTA
CCGCTGTTACCAATTTTCTTTTGTCTTTGGGTATACATTTAAACCCTAACAAAACAAAAAGATGGGGTTACTCTTTACATTTCATGGGCTATGTCATTGGATGTTAT
GGGTCATTGCCACAAGATCACATCATACAGAAAATCAAAGAATGTTTTAGAAAACTTCCTGTTAACAGGCCTATTGATTGGAAAGTCTGTCAACGTATTGTGGG
TCTTTTGGGTTTTGCTGCCCCTTTTACACAATGTGGTTATCCTGCTTTAATGCCCTTGTATGCATGTATTCAATCTAAGCAGGCTTTCACTTTCTCGCCAACTTACA
AGGCCTTTCTGTGTAAACAATACCTGAACCTTTACCCCGTTGCCCGGCAACGGCCAGGTCTGTGCCAAGTGTTTGCTGACGCAACCCCCACTGGCTGGGGCTT
GGTCATGGGCCATCAGCGCATGCGTGGAACCTTTCTGGCTCCTCTGCCGATCCATACTGCGGAACTCCTAGCCGCTTGTTTTGCTCGCAGCAGGTCTGGAGCA
AACATTCTCGGGACGGATAACTCTGTTGTTCTCTCCCGCAAATATACATCGTTTCCATGG

HBV HBeAg gene fragments for Gibson Assembly

BCP double mutation

Genotype A isolate #1

GGACTCTTGGACTCCCAGCAATGTCAACGACCGACCTTGAGGCTTACTTCAAAGACTGTGTGTTTAAGGACTGGGAGGAGCTGGGGGAGGAGATTAGGTTA
ATGATCTTTGTATTAGGAGGCTGTAGGCATAAATTGGTCTGCGCACCAGCACCATGCAACTTTTTCACCTCTGCCTAATCATCTCTTGTACATGTCCCACTGTTCA
AGCCTCCAAGCTGTGCCTTGGGTGGCTTTGGGGCATGGACATTGACCCTTATAAAGAATTTGGAGCTACTGTGGAGTTACTCTCGTTTTTGCCTTCTGACTTCT
TTCCTTCCGTCAGAGATCTCCTAGACACCGCCTCAGCTCTGTATCGAGAAGCCTTAGAGTCTCCTGAGCATTGCTCACCTCACCA

Genotype A isolate #2

GGACTCTTGGACTCCCAGCAATGTCAACGACCGACCTTGAGGCTTACTTCAAAGACTGTGTGTTTAAGGACTGGGAGGAGCTGGGGGAGGAGATTAGGTTA
ATGATCTTTGTATTAGGAGGCTGTAGGCATAAATTGGTCTGCGCACCAGCACCATGCAACTTTTTCACCTCTGCCTAATCATCTCTTGTACATGTCCCACTGTTCA
AGCCTCCAAGCTGTGCCTTGGGTGGCTTTGGGGCATGGACATTGACCCTTATAAAGAATTTGGAGCTACTGTGGAGTTACTCTCGTTTTTGCCTTCTGACTTCT
TTCCTTCCGTCAGAGATCTCCTAGACACCGCCTCAGCTCTGTATCGAGAAGCCTTAGAGTCTCCTGAGCATTGCTCACCTCACCA

Genotype A consensus

GGACTCTTGGACTCCCAGCAATGTCAACGACCGACCTTGAGGCCTACTTCAAAGACTGTGTGTTTAAGGACTGGGAGGAGCTGGGGGAGGAGATTAGGTTA
ATGATCTTTGTATTAGGAGGCTGTAGGCATAAATTGGTCTGCGCACCAGCACCATGCAACTTTTTCACCTCTGCCTAATCATCTCTTGTACATGTCCCACTGTTCA
AGCCTCCAAGCTGTGCCTTGGGTGGCTTTGGGGCATGGACATTGACCCTTATAAAGAATTTGGAGCTACTGTGGAGTTACTCTCGTTTTTGCCTTCTGACTTCT
TTCCTTCCGTCAGAGATCTCCTAGACACCGCCTCAGCTCTGTATCGAGAAGCCTTAGAGTCTCCTGAGCATTGCTCACCTCACCA

Genotype D isolate #1

GGACTCTTGGACTCTCTGCAATGTCAACGACCGACCTTGAGGCATACTTCAAAGACTGTTTGTTTAAAGACTGGGAGGAGTTGGGGGAGGAGATTAGATTAA
TGATCTTTGTACTAGGAGGCTGTAGGCATAAATTGGTCTGCGCACCAGCACCATGCAACTTTTTCACCTCTGCCTAATCATCTCTTGTTCATGTCCTACTGTTCAA
GCCTCCAAGCTGTGCCTTGGGTGGCTTTGGGGCATGGACATTGACCCTTATAAAGAATTTGGAGCTACCGTGGAGTTACTCTCGTTTTTGCCTTCTGACTTCTT
TCCTTCAGTACGAGATCTTCTAGATACCGCCTCAGCTCTGTATCGGGATGCCTTAGAGTCTCCTGAACATTGTTCACCTCACCA

Genotype D isolate #2

GGACTCTTGGACTCTCTGTAATGTCAACGACCGACCTTGAGGCATACTTCAAAGACTGTTTGTTCAAAGACTGGGAGGAGTTGGGGGAGGAGATTAGATTAA
TGATCTTTGTACTAGGAGGCTGTAGGCATAAATTGGTCTGCGCACCAGCACCATGCAACTTTTTCACCTCTGCCTAATCATCTTTTGTTCATGTCCTACTGTTCAA
GCCTCCAAGCTGTGCCTTGGGTGGCTTTGGGGCATGGACATTGATCCTTATAAAGAATTTGGAGCTACTGTGGAGTTACTCTCGTTTTTGCCTTCTGACTTCTTT
CCTTCAGTACGTGATCTTCTAGATACCGCCTCAGCTCTGTATCGGGAAGCCTTAGAGTCTCCTGAGCATTGTTCACCTCACCA

Genotype D consensus

GGACTCTTGGACTCTCTGTAATGTCAACGACCGACCTTGAGGCATACTTCAAAGACTGTTTGTTTAAAGACTGGGAGGAGTTGGGGGAGGAGATTAGATTAA
TGATCTTTGTACTAGGAGGCTGTAGGCATAAATTGGTCTGCGCACCAGCACCATGCAACTTTTTCACCTCTGCCTAATCATCTCTTGTTCATGTCCTACTGTTCAA
GCCTCCAAGCTGTGCCTTGGGTGGCTTTGGGGCATGGACATTGACCCTTATAAAGAATTTGGAGCTTCTGTGGAGTTACTCTCGTTTTTGCCTTCTGACTTCTT
TCCTTCAGTACGAGATCTTCTAGATACCGCCTCAGCTCTGTATCGGGAAGCCTTAGAGTCTCCTGAGCATTGTTCACCTCACCA

G1896A (W28*)

Genotype A isolate #1

GGACTCTTGGACTCCCAGCAATGTCAACGACCGACCTTGAGGCTTACTTCAAAGACTGTGTGTTTAAGGACTGGGAGGAGCTGGGGGAGGAGATTAGGTTA
AAGGTCTTTGTATTAGGAGGCTGTAGGCATAAATTGGTCTGCGCACCAGCACCATGCAACTTTTTCACCTCTGCCTAATCATCTCTTGTACATGTCCCACTGTTCA
AGCCTCCAAGCTGTGCCTTGGGTGGCTTTAGGGCATGGACATTGACCCTTATAAAGAATTTGGAGCTACTGTGGAGTTACTCTCGTTTTTGCCTTCTGACTTCT
TTCCTTCCGTCAGAGATCTCCTAGACACCGCCTCAGCTCTGTATCGAGAAGCCTTAGAGTCTCCTGAGCATTGCTCACCTCACCA

Genotype A isolate #2

GGACTCTTGGACTCCCAGCAATGTCAACGACCGACCTTGAGGCTTACTTCAAAGACTGTGTGTTTAAGGACTGGGAGGAGCTGGGGGAGGAGATTAGGTTA
AAGGTCTTTGTATTAGGAGGCTGTAGGCATAAATTGGTCTGCGCACCAGCACCATGCAACTTTTTCACCTCTGCCTAATCATCTCTTGTACATGTCCCACTGTTCA
AGCCTCCAAGCTGTGCCTTGGGTGGCTTTAGGGCATGGACATTGACCCTTATAAAGAATTTGGAGCTACTGTGGAGTTACTCTCGTTTTTGCCTTCTGACTTCT
TTCCTTCCGTCAGAGATCTCCTAGACACCGCCTCAGCTCTGTATCGAGAAGCCTTAGAGTCTCCTGAGCATTGCTCACCTCACCA

Genotype A consensus

GGACTCTTGGACTCCCAGCAATGTCAACGACCGACCTTGAGGCCTACTTCAAAGACTGTGTGTTTAAGGACTGGGAGGAGCTGGGGGGAGGAGATTAGGTTA
AAGGTCTTTGTATTAGGAGGCTGTAGGCATAAATTGGTCTGCGCACCAGCACCATGCAACTTTTTCACCTCTGCCTAATCATCTCTTGTACATGTCCCACTGTTCA
AGCCTCCAAGCTGTGCCTTGGGTGGCTTTAGGGCATGGACATTGACCCTTATAAAGAATTTGGAGCTACTGTGGAGTTACTCTCGTTTTTGCCTTCTGACTTCT
TTCCTTCCGTCAGAGATCTCCTAGACACCGCCTCAGCTCTGTATCGAGAAGCCTTAGAGTCTCCTGAGCATTGCTCACCTCACCA

Genotype D isolate #1

GGACTCTTGGACTCTCTGCAATGTCAACGACCGACCTTGAGGCATACTTCAAAGACTGTTTGTTTAAAGACTGGGAGGAGTTGGGGGGAGGAGATTAGATTAA
AGGTCTTTGTACTAGGAGGCTGTAGGCATAAATTGGTCTGCGCACCAGCACCATGCAACTTTTTCACCTCTGCCTAATCATCTCTTGTTCATGTCCTACTGTTCAA
GCCTCCAAGCTGTGCCTTGGGTGGCTTTAGGGCATGGACATTGACCCTTATAAAGAATTTGGAGCTACCGTGGAGTTACTCTCGTTTTTGCCTTCTGACTTCTT
TCCTTCAGTACGAGATCTTCTAGATACCGCCTCAGCTCTGTATCGGGATGCCTTAGAGTCTCCTGAACATTGTTCACCTCACCA

Genotype D isolate #2

GGACTCTTGGACTCTCTGTAATGTCAACGACCGACCTTGAGGCATACTTCAAAGACTGTTTGTTCAAAGACTGGGAGGAGTTGGGGGGAGGAGATTAGATTAA
AGGTCTTTGTACTAGGAGGCTGTAGGCATAAATTGGTCTGCGCACCAGCACCATGCAACTTTTTCACCTCTGCCTAATCATCTTTTGTTCATGTCCTACTGTTCAA
GCCTCCAAGCTGTGCCTTGGGTGGCTTTAGGGCATGGACATTGATCCTTATAAAGAATTTGGAGCTACTGTGGAGTTACTCTCGTTTTTGCCTTCTGACTTCTTT
CCTTCAGTACGTGATCTTCTAGATACCGCCTCAGCTCTGTATCGGGAAGCCTTAGAGTCTCCTGAGCATTGTTCACCTCACCA

CTG start codon mutation

Genotype A isolate #1

GGACTCTTGGACTCCCAGCAATGTCAACGACCGACCTTGAGGCTTACTTCAAAGACTGTGTGTTTAAGGACTGGGAGGAGCTGGGGGGAGGAGATTAGGTTA
AAGGTCTTTGTATTAGGAGGCTGTAGGCATAAATTGGTCTGCGCACCAGCACCCTGCAACTTTTTCACCTCTGCCTAATCATCTCTTGTACATGTCCCACTGTTCA
AGCCTCCAAGCTGTGCCTTGGGTGGCTTTGGGGCATGGACATTGACCCTTATAAAGAATTTGGAGCTACTGTGGAGTTACTCTCGTTTTTGCCTTCTGACTTCT
TTCCTTCCGTCAGAGATCTCCTAGACACCGCCTCAGCTCTGTATCGAGAAGCCTTAGAGTCTCCTGAGCATTGCTCACCTCACCA

Genotype A isolate #2

GGACTCTTGGACTCCCAGCAATGTCAACGACCGACCTTGAGGCTTACTTCAAAGACTGTGTGTTTAAGGACTGGGAGGAGCTGGGGGGAGGAGATTAGGTTA
AAGGTCTTTGTATTAGGAGGCTGTAGGCATAAATTGGTCTGCGCACCAGCACCCTGCAACTTTTTCACCTCTGCCTAATCATCTCTTGTACATGTCCCACTGTTCA
AGCCTCCAAGCTGTGCCTTGGGTGGCTTTGGGGCATGGACATTGACCCTTATAAAGAATTTGGAGCTACTGTGGAGTTACTCTCGTTTTTGCCTTCTGACTTCT
TTCCTTCCGTCAGAGATCTCCTAGACACCGCCTCAGCTCTGTATCGAGAAGCCTTAGAGTCTCCTGAGCATTGCTCACCTCACCA

Genotype A consensus

GGACTCTTGGACTCCCAGCAATGTCAACGACCGACCTTGAGGCCTACTTCAAAGACTGTGTGTTTAAGGACTGGGAGGAGCTGGGGGGAGGAGATTAGGTTA
AAGGTCTTTGTATTAGGAGGCTGTAGGCATAAATTGGTCTGCGCACCAGCACCCTGCAACTTTTTCACCTCTGCCTAATCATCTCTTGTACATGTCCCACTGTTCA
AGCCTCCAAGCTGTGCCTTGGGTGGCTTTGGGGCATGGACATTGACCCTTATAAAGAATTTGGAGCTACTGTGGAGTTACTCTCGTTTTTGCCTTCTGACTTCT
TTCCTTCCGTCAGAGATCTCCTAGACACCGCCTCAGCTCTGTATCGAGAAGCCTTAGAGTCTCCTGAGCATTGCTCACCTCACCA

Genotype D isolate #1

GGACTCTTGGACTCTCTGCAATGTCAACGACCGACCTTGAGGCATACTTCAAAGACTGTTTGTTTAAAGACTGGGAGGAGTTGGGGGGAGGAGATTAGATTAA
AGGTCTTTGTACTAGGAGGCTGTAGGCATAAATTGGTCTGCGCACCAGCACCCTGCAACTTTTTCACCTCTGCCTAATCATCTCTTGTTCATGTCCTACTGTTCAA
GCCTCCAAGCTGTGCCTTGGGTGGCTTTGGGGCATGGACATTGACCCTTATAAAGAATTTGGAGCTACCGTGGAGTTACTCTCGTTTTTGCCTTCTGACTTCTT
TCCTTCAGTACGAGATCTTCTAGATACCGCCTCAGCTCTGTATCGGGATGCCTTAGAGTCTCCTGAACATTGTTCACCTCACCA

Genotype D isolate #2

GGACTCTTGGACTCTCTGTAATGTCAACGACCGACCTTGAGGCATACTTCAAAGACTGTTTGTTCAAAGACTGGGAGGAGTTGGGGGAGGAGATTAGATTAA
AGGTCTTTGTACTAGGAGGCTGTAGGCATAAATTGGTCTGCGCACCAGCACCCTGCAACTTTTTCACCTCTGCCTAATCATCTTTTGTTCATGTCCTACTGTTCAA
GCCTCCAAGCTGTGCCTTGGGTGGCTTTGGGGCATGGACATTGATCCTTATAAAGAATTTGGAGCTACTGTGGAGTTACTCTCGTTTTTGCCTTCTGACTTCTTT
CCTTCAGTACGTGATCTTCTAGATACCGCCTCAGCTCTGTATCGGGAAGCCTTAGAGTCTCCTGAGCATTGTTCACCTCACCA

Genotype D consensus

GGACTCTTGGACTCTCTGTAATGTCAACGACCGACCTTGAGGCATACTTCAAAGACTGTTTGTTTAAAGACTGGGAGGAGTTGGGGGAGGAGATTAGATTAA
AGGTCTTTGTACTAGGAGGCTGTAGGCATAAATTGGTCTGCGCACCAGCACCCTGCAACTTTTTCACCTCTGCCTAATCATCTCTTGTTCATGTCCTACTGTTCAA
GCCTCCAAGCTGTGCCTTGGGTGGCTTTGGGGCATGGACATTGACCCTTATAAAGAATTTGGAGCTTCTGTGGAGTTACTCTCGTTTTTGCCTTCTGACTTCTT
TCCTTCAGTACGAGATCTTCTAGATACCGCCTCAGCTCTGTATCGGGAAGCCTTAGAGTCTCCTGAGCATTGTTCACCTCACCA